

==== Università degli Studi di Napoli Federico II  
Facoltà di Ingegneria



*Giusy Terracciano*

YIELD AND ULTIMATE ROTATIONS  
OF BEAM-TO-COLUMN END-PLATE CONNECTIONS

*Tesi di Dottorato  
XXV ciclo  
Il Coordinatore  
Prof. Ing. Luciano Rosati*

*Tutor: Prof. Ing. Raffaele Landolfo*

*Co-tutors: Dr. Ing. Gaetano Della Corte, Dr. Ing. Gianmaria Di Lorenzo*

==== *Dottorato di Ricerca in Ingegneria delle Costruzioni* ====



# TABLE OF CONTENTS

LIST OF FIGURES .....	v
LIST OF TABLES.....	xi
ABSTRACT .....	xv
ACKNOWLEDGMENTS .....	xvii
ABOUT THE AUTHOR.....	xix
MOTIVATIONS AND OBJECTIVES .....	1
1 INTRODUCTION.....	3
1.1 Displacement based design for moment resisting frame steel structures.....	3
1.2 Joint Modelling: the component method.....	4
1.2.1 Basic principles and components of joints.....	4
1.2.2 Prediction of flexural resistance and initial rotational stiffness. ....	6
1.2.1 Implementation of Eurocode 3 component method within Mathcad .....	12
1.3 Moment – rotation curve representation .....	13
1.4 Definitions of limit state rotations .....	14
1.5 Analysis methodology .....	15
2 EXPERIMENTAL DATA COLLECTION.....	17
2.1 Extended end-plate connections .....	17
2.1.1 Tests by Ghobarah <i>et al.</i> (1990).....	17
2.1.1.1 Description of specimens and test setup .....	17
2.1.1.2 Experimental results .....	20
2.1.1.2.1 Specimen A-1 .....	20
2.1.1.2.2 Specimen A-2 .....	21
2.1.1.2.3 Specimen A-3 .....	22
2.1.1.2.4 Specimen A-4 .....	24
2.1.1.2.5 Specimen A-5 .....	25
2.1.2 Test by Sumner and Murray (2002).....	26
2.1.2.1 Description of specimen and test set up.....	26
2.1.2.2 Experimental results .....	27
2.1.3 Tests by Nogueiro <i>et al.</i> (2006).....	28

2.1.3.1	Description of specimens and test set up.....	28
2.1.3.2	Experimental results .....	31
2.1.3.2.1	Specimens J-1 .....	31
2.1.3.2.2	Specimens J-3 .....	33
2.1.4	Tests by Shi <i>et al.</i> (2007 a) .....	35
2.1.4.1	Description of specimens and test set up.....	35
2.1.4.2	Experimental results .....	38
2.1.4.2.1	Specimen EPC-1 .....	38
2.1.4.2.2	Specimen EPC-2.....	39
2.1.4.2.3	Specimen EPC-3.....	41
2.1.4.2.4	Specimen EPC-4.....	43
2.1.4.2.5	Specimen EPC-5.....	45
2.1.5	Tests by Shi <i>et al.</i> (2007 b).....	47
2.1.5.1	Description of specimens and test set up.....	47
2.1.5.2	Experimental results .....	49
2.1.5.2.1	Specimen JD2.....	49
2.1.5.2.2	Specimen JD3.....	51
2.1.5.2.3	Specimen JD4.....	52
2.1.5.2.4	Specimen JD5.....	53
2.1.5.2.5	Specimen JD6.....	54
2.1.5.2.6	Specimen JD7.....	55
2.1.5.2.7	Specimen JD8.....	56
2.2	Flush end-plate connections .....	57
2.2.1	Tests by Broderick and Thomson (2002).....	57
2.2.1.1	Description of specimens and test setup.....	57
2.2.1.2	Experimental results .....	58
2.2.1.2.1	Specimen EP1 .....	58
2.2.1.2.2	Specimen EP2 .....	59
2.2.1.2.3	Specimens EP3 and EP4 .....	60
2.2.1.2.4	Specimen EP5 .....	61
2.2.1.2.5	Specimens EP6, EP7 and EP8 .....	61
2.2.2	Test by da Silva <i>et al.</i> (2004).....	63
2.2.2.1	Description of specimens and test setup.....	63
2.2.2.2	Experimental results .....	65
2.2.3	Tests by Broderick and Thomson (2005).....	66
2.2.3.1	Description of specimens and test setup.....	66
2.2.3.2	Experimental results .....	67
2.2.3.2.1	Specimens FP1 and FP2.....	67
2.2.3.2.2	Specimens FP3 and FP4.....	69



2.2.3.2.3	Specimens FP5 and FP6 .....	70
2.2.3.2.4	Specimens FP7 and FP8 .....	72
2.2.4	Test by Shi <i>et al.</i> (2007).....	73
2.2.4.1	Description of specimen and test setup.....	73
2.2.4.2	Experimental results .....	75
2.3	Digital database.....	76
3	THEORETICAL PREDICTIONS AND COMPARISON WITH EXPERIMENTAL RESULTS.....	79
3.1	Extended end-plate connections .....	79
3.1.1	Tests by Ghobarah <i>et al.</i> (1990).....	79
3.1.1.1	Specimen A-1.....	79
3.1.1.2	Specimen A-2.....	82
3.1.1.3	Specimen A-3.....	85
3.1.1.4	Specimen A-4.....	88
3.1.1.5	Specimen A-5.....	90
3.1.2	Test by Sumner and Murray (2002).....	93
3.1.3	Tests by Nogueiro <i>et al.</i> (2006).....	95
3.1.3.1	Specimens J1 .....	95
3.1.3.2	Specimens J3 .....	97
3.1.4	Tests by Shi <i>et al.</i> (2007 a) .....	99
3.1.4.1	Specimen EPC-1 .....	99
3.1.4.2	Specimen EPC-2 .....	102
3.1.4.3	Specimen EPC-3 .....	105
3.1.4.4	Specimen EPC-4 .....	107
3.1.4.5	Specimen EPC-5 .....	110
3.1.5	Tests by Shi <i>et al.</i> (2007 b).....	112
3.1.5.1	Specimen JD2 .....	112
3.1.5.2	Specimen JD3 .....	115
3.1.5.3	Specimen JD4 .....	118
3.1.5.4	Specimen JD5 .....	121
3.1.5.5	Specimen JD6 .....	123
3.1.5.6	Specimen JD7 .....	126
3.1.5.7	Specimen JD8 .....	128
3.2	Flush end-plate connections .....	131
3.2.1	Tests by Broderick and Thomson (2002).....	131
3.2.1.1	Specimen EP1 .....	131
3.2.1.2	Specimen EP2.....	133
3.2.1.3	Specimens EP3 and EP4.....	135
3.2.1.4	Specimen EP5.....	137

3.2.1.5 Specimen EP6, EP7 and EP8.....	139
3.2.2 Test by da Silva <i>et al.</i> (2004).....	141
3.2.3 Tests by Broderick and Thomson (2005).....	143
3.2.3.1 Specimens FP1 and FP2.....	143
3.2.3.2 Specimens FP3 and FP4.....	146
3.2.3.3 Specimens FP5 and FP6.....	148
3.2.3.4 Specimens FP7 and FP8.....	151
3.2.4 Test by Shi <i>et al.</i> (2007).....	153
3.3 Concluding remarks .....	155
4 ANALYTICAL STUDY OF YIELD ROTATIONS.....	161
4.1 Analytical equations.....	161
4.1.1 Basic assumptions .....	161
4.1.2 Bolt failure.....	164
4.1.3 End-plate failure.....	165
4.1.4 Column flange failure .....	166
4.1.5 Beam failure .....	167
4.1.6 Analytical equations accuracy.....	167
4.2 Parametric analyses and design tools.....	168
4.2.1 Basic assumptions .....	168
4.2.2 Design tools.....	170
4.2.3 Comparison of different joint configurations.....	175
5 ULTIMATE ROTATIONS .....	177
5.1 Analysis criteria .....	177
5.2 Plastic rotation capacity of extended end-plate connections .....	178
5.3 Concluding Remarks .....	182
6 CONCLUSIONS .....	185
REFERENCES.....	189
APPENDIX A .....	193
APPENDIX B.....	205

## LIST OF FIGURES

Figure 1.1: Components of end-plate beam-to-column joints .....	5
Figure 1.2: Eurocode 3 mechanical models.....	6
Figure 1.3: Yield line patterns and effective length of the end-plate T-stub for the first bolt row in tension.....	7
Figure 1.4: Yield line patterns and effective length of the column flange T-stub for the first bolt row in tension.....	7
Figure 1.5: T-Stub mechanisms and design resistance for each failure mode .....	8
Figure 1.6: Design resistance of column web in tension.....	8
Figure 1.7: Design resistance of beam web in tension.....	9
Figure 1.8: Design resistance of column web in compression .....	9
Figure 1.9: Design resistance of beam flange and web in compression..	10
Figure 1.10: Design resistance of unstiffened column web panel in shear .....	10
Figure 1.11: Additional resistance of the column web panel in shear for column web transverse stiffeners .....	10
Figure 1.12: Yield rotation of end-plate connections.....	14
Figure 1.13: Rotation capacity and ultimate rotation .....	15
Figure 2.1: Details of specimens .....	18
Figure 2.2: a) Test specimen, and b) test set-up.....	19
Figure 2.3: Loading protocol .....	20
Figure 2.4: a) Beam load versus beam tip displacement curve and b) failure mode for A-1 .....	21
Figure 2.5: Beam load versus beam tip displacement curve and failure mode for A-2 .....	22
Figure 2.6: Beam load versus beam tip displacement curve and failure mode for A-3 .....	23
Figure 2.7: Beam load versus beam tip displacement curve and failure mode for A-4 .....	24
Figure 2.8: a) Beam load versus beam tip displacement curve and b) failure mode for A-5.....	25
Figure 2.9: Test set up and loading protocol.....	27

Figure 2.10: a) Moment rotation curve and b) failure mode for 4E-1.25-1.5-24 .....	28
Figure 2.11: Details of the joint for Group 1 .....	29
Figure 2.12: Details of the joint for Group 3 .....	29
Figure 2.13: Test set-up .....	30
Figure 2.14: Results of the J-1.1 monotonic test .....	31
Figure 2.15: a) Final shear deformation of the column web panel and b) end-plate fracture .....	31
Figure 2.16: M- $\theta$ experimental curves for J-1.2 and J-1.3 tests .....	32
Figure 2.17: End-plate failure, column web panel and end-plate deformation for J-1.3 .....	32
Figure 2.18: Results of the J-3.1 monotonic test .....	33
Figure 2.19: Moment-rotation curves for a) J-3.2 and b) J-3.3 tests .....	34
Figure 2.20: Column web panel, end-plate and bolt failure for J-3.2 .....	35
Figure 2.21: Column web panel, beam flange failure and end-plate deformation for J-3.3 .....	35
Figure 2.22: Connection details .....	36
Figure 2.23: Test setup .....	37
Figure 2.24: Moment-rotation curve for EPC-1 .....	38
Figure 2.25: Failure mode for EPC-1 .....	38
Figure 2.26: a) Moment-shearing rotation and b) moment-gap rotation for EPC-1 .....	39
Figure 2.27: Moment-rotation curve for EPC-2 .....	40
Figure 2.28: Failure mode for EPC-2 .....	40
Figure 2.29: a) Moment-shearing rotation and b) moment-gap rotation for EPC-2 .....	41
Figure 2.30: Moment-rotation curve for EPC-3 .....	42
Figure 2.31: Failure mode for EPC-3 .....	42
Figure 2.32: a) Moment-shearing rotation and b) moment gap rotation for EPC-3 .....	42
Figure 2.33: Moment rotation curve for EPC-4 .....	43
Figure 2.34: Failure mode for EPC-4 .....	44
Figure 2.35: a) Moment--shearing rotation (b) and moment - gap rotation for EPC-4 .....	44
Figure 2.36: Moment-rotation curve for EPC-5 .....	45
Figure 2.37: Moment-rotation curve and failure mode for EPC-5 .....	45
Figure 2.38: a) Moment-shearing rotation and b) moment-gap rotation for EPC-5 .....	46
Figure 2.39: Connection details .....	47

Figure 2.40: Test setup and loading arrangement.....	49
Figure 2.41: a) Moment–rotation curve, b) moment–shearing rotation curve, c) moment–gap rotation curve and d) failure mode for JD2 .....	50
Figure 2.42: a) Moment–rotation curve, b) moment–shearing rotation curve, c) moment–gap rotation curve and d) failure mode for JD3 .....	51
Figure 2.43: a) Moment–rotation, b) Moment–shearing rotation curve, c) Moment–gap rotation curve and d) failure mode for JD4 ...	52
Figure 2.44: a) Moment–rotation curve, b) Moment–shearing rotation b) curve, c) Moment–gap rotation curve and d) failure mode for JD5 .....	53
Figure 2.45: a) Moment–rotation curve, b) Moment–shearing rotation curve, c) Moment–gap rotation curve and d) failure mode for JD6 .....	54
Figure 2.46:a) Moment–rotation curve b) Moment–shearing rotation curve, c) Moment–gap rotation curve and d) failure mode for JD7 .....	55
Figure 2.47: a) Moment–rotation curve, b) moment–shearing rotation curve, c) moment–gap rotation curve and d) failure mode for JD8 .....	56
Figure 2.48: a) Connection details and b) test setup .....	58
Figure 2.49: Moment rotation curve for EP2 .....	59
Figure 2.50: Moment rotation curve for EP3 .....	60
Figure 2.51: Moment rotation curve for EP4 .....	60
Figure 2.52: Moment rotation curve for EP6 .....	62
Figure 2.53: Moment rotation curve for EP7 .....	62
Figure 2.54: Moment rotation curve for EP8 .....	63
Figure 2.55: Layout of the joint.....	64
Figure 2.56: Experimental test setup .....	65
Figure 2.57: Moment - rotation curve for FE1 .....	65
Figure 2.58: a) Connection details and b) test setup .....	66
Figure 2.59: Moment rotation curve for FP1 .....	68
Figure 2.60: Moment rotation curve for FP2.....	68
Figure 2.61: Moment rotation curve for FP3.....	70
Figure 2.62: Moment rotation curve for FP4.....	70
Figure 2.63: Moment rotation curve for FP5.....	71
Figure 2.64: Moment rotation curve for FP6.....	71
Figure 2.65: Moment rotation curve for FP7.....	72

Figure 2.66: Moment rotation curve for FP8.....	73
Figure 2.67: Details of specimen JD1.....	74
Figure 2.68: Test setup .....	75
Figure 2.69: a) Moment–rotation curve, b) moment–shearing rotation curve, c) moment–gap rotation curve and d) failure mode for JD1 .....	76
Figure 2.70: The steel joints digital database .....	77
Figure 2.71: The digital database structure .....	77
Figure 3.1: Classification by strength and stiffness for A-1 .....	82
Figure 3.2: Classification by strength and stiffness for A-2 .....	85
Figure 3.3: Classification by strength and stiffness for A-3 .....	87
Figure 3.4: Classification by strength and stiffness for A-4 .....	90
Figure 3.5: Classification of specimen A-5 .....	92
Figure 3.6: Classification by strength and stiffness for 4E-1.25-1.5-24...95	95
Figure 3.7: Classification by strength and stiffness for EPC-1 .....	102
Figure 3.8: Classification by strength and stiffness EPC-2 .....	104
Figure 3.9: Classification by strength and stiffness EPC-3 .....	107
Figure 3.10: Classification by strength and stiffness EPC-4 .....	109
Figure 3.11: Classification by strength and stiffness EPC-5 .....	111
Figure 3.12: Classification by strength and stiffness for JD2.....	114
Figure 3.13: Classification by strength and stiffness for JD3.....	117
Figure 3.14: Classification by strength and stiffness for JD4.....	120
Figure 3.15: Classification by strength and stiffness for JD5.....	123
Figure 3.16: Classification by strength and stiffness for JD6.....	125
Figure 3.17: Classification by strength and stiffness for JD7.....	128
Figure 3.18: Classification by strength and stiffness for JD8.....	130
Figure 3.19: Classification by strength and stiffness for EP2.....	134
Figure 3.20: Classification by strength and stiffness for EP3.....	136
Figure 3.21: Classification by strength and stiffness for EP4.....	137
Figure 3.22: Classification by strength and stiffness for EP6.....	140
Figure 3.23: Classification by strength and stiffness for EP7 .....	141
Figure 3.24: Classification by strength and stiffness for EP8.....	141
Figure 3.25: Classification by strength and stiffness for FE1 .....	143
Figure 3.26: Classification by strength and stiffness for FP1 .....	145
Figure 3.27: Classification by strength and stiffness for FP2 .....	146
Figure 3.28: Classification by strength and stiffness for FP3 .....	148
Figure 3.29: Classification by strength and stiffness for FP4 .....	148
Figure 3.30: Classification by strength and stiffness for FP5 .....	150
Figure 3.31: Classification by strength and stiffness for FP6 .....	150

Figure 3.32: Classification by strength and stiffness for FP7 .....	152
Figure 3.33: Classification by strength and stiffness for FP8 .....	153
Figure 3.34: Classification by strength and stiffness for JD1.....	155
Figure 3.35: Theoretical to experimental ratios of the moment resistance for extended end-plate joints.....	157
Figure 3.36: Theoretical to experimental ratios of the initial stiffness for extended end-plate joints .....	157
Figure 3.37: Theoretical to experimental ratios of the yield rotation for extended end-plate joints .....	158
Figure 3.38: Theoretical to experimental ratios of the moment resistance for flush end-plate joints.....	159
Figure 3.39: Theoretical to experimental ratios of the initial stiffness for flush end-plate joints .....	159
Figure 3.40: Theoretical to experimental ratios of yield rotation for flush end-plate joints .....	159
Figure 4.1: Joint mechanical modelling.....	162
Figure 4.2: Basic joint components and assumptions.....	163
Figure 4.3: Accuracy of the analytical equations.....	168
Figure 4.4: Analyzed joint configurations – a) Flush end-plate connections, b) Extended end-plate connections .....	169
Figure 4.5: Basic assumptions and arrangements for a) flush end-plate and b) extended end-plate connections .....	170
Figure 4.6: Normalized charts .....	171
Figure 4.7: Use of normalized charts.....	172
Figure 4.8: a) Normalized stiffness b) normalized resistance and c) yield rotation of extended end-plate connections (column shape: HEM 280; beam shape: IPE 550; steel grade S275; bolt grade 8.8).....	173
Figure 4.9: a) Normalized stiffness b) normalized resistance and c) yield rotation of extended end-plate connections (column shape: HEM 280; beam shape: IPE 550; steel grade S275; bolt grade 8.8).....	174
Figure 4.10: Failure modes for an extended end-plate joint (column shape: HEM 280; beam shape: IPE 550; steel grade S275; bolt grade 8.8).....	174
Figure 4.11: Comparison between different joint configurations .....	176
Figure 5.1: Analysis criteria for rotation capacity .....	178
Figure 5.2: Plastic rotation capacities for Ghobarah et al. (1990) specimens .....	179

Figure 5.3: Plastic rotation capacities for specimen 4E-1.25-1.5-24 tested by Sumner and Murray (2002) .....	180
Figure 5.4: Plastic rotation capacities for Shi et al. (2007a) specimens..	181
Figure 5.5: Plastic rotation capacities for Shi et al. (2007b) specimens.	182



## LIST OF TABLES

Table 2.1: Material properties .....	19
Table 2.2: Specimen details .....	26
Table 2.3: Coupon test results .....	26
Table 2.4: Details of the joint for the Group 1 and Group 3.....	29
Table 2.5: Types and details of specimens.....	36
Table 2.6: Material properties .....	37
Table 2.7: Details of specimens.....	48
Table 2.8:Material properties .....	48
Table 2.9: Specimen details .....	57
Table 2.10: Experimental moment-rotation characteristics of EP3 and EP4 .....	61
Table 2.11: Experimental moment-rotation characteristics .....	63
Table 2.12: Steel mechanical properties .....	64
Table 2.13: Details of specimens.....	66
Table 2.14: Experimental results of FP1 and FP2.....	67
Table 2.15: Experimental results of FP3 and FP4.....	69
Table 2.16: Experimental results of FP5 and FP6.....	71
Table 2.17: Experimental results of FP7 and FP8.....	73
Table 2.18: Material properties.....	74
Table 3.1: Resistance and stiffness coefficients of the joint components for A-1 .....	80
Table 3.2: Resistance and stiffness coefficients of the joint components for A-2.....	83
Table 3.3: Resistance and stiffness coefficients of the joint components for A-3.....	86
Table 3.4: Resistance and stiffness coefficients of the joint components for A-4.....	88
Table 3.5: Resistance and stiffness coefficients of the joint components for A-5.....	91
Table 3.6: Resistance and stiffness coefficients of the joint components .....	93
Table 3.7: Resistance and stiffness coefficients of the joint components for J-1 .....	96

Table 3.8: Resistance and stiffness coefficients of the joint components for J-3 .....	98
Table 3.9: Resistance and stiffness coefficients of the joint components for EPC-1 .....	100
Table 3.10: Resistance and stiffness coefficients of the joint components for EPC-2 .....	103
Table 3.11: Resistance and stiffness coefficients of the joint components for EPC-3 .....	106
Table 3.12: Resistance and stiffness coefficients of the joint components for EPC-4 .....	108
Table 3.13: Resistance and stiffness coefficients of the joint components for EPC-5 .....	110
Table 3.14: Resistance and stiffness coefficients of the joint components for JD2 .....	113
Table 3.15: Resistance and stiffness coefficients of the joint components for JD3 .....	116
Table 3.16: Resistance and stiffness coefficients of the joint components for JD4 .....	118
Table 3.17: Resistance and stiffness coefficients of the joint components for JD5 .....	121
Table 3.18: Resistance and stiffness coefficients of the joint components for JD6 .....	124
Table 3.19: Resistance and stiffness coefficients of the joint components for JD7 .....	127
Table 3.20: Resistance and stiffness coefficients of the joint components for JD8 .....	129
Table 3.21: Resistance and stiffness coefficients of the joint components for EP1 .....	132
Table 3.22: Resistance and stiffness coefficients of the joint components for EP2 .....	134
Table 3.23: Resistance and stiffness coefficients of the joint components for EP3 and EP4 .....	135
Table 3.24: Resistance and stiffness coefficients of the joint components for EP5 .....	138
Table 3.25: Resistance and stiffness coefficients of the joint components for EP6, EP7 and EP8 .....	139
Table 3.26: Resistance and stiffness coefficients of the joint components for FE1 .....	142

Table 3.27: Resistance and stiffness coefficients of the joint components for FP1and FP2 .....	144
Table 3.28: Resistance and stiffness coefficients of the joint components for FP3and FP4 .....	147
Table 3.29: Resistance and stiffness coefficients of the joint components for FP5and FP6 .....	149
Table 3.30: Resistance and stiffness coefficients of the joint components for FP7and FP8 .....	151
Table 3.31: Resistance and stiffness coefficients of the joint components for JD1 .....	154



## ABSTRACT

The deficiencies of traditional force-based design approaches and the recognition of the key-role of displacements and deformations as reliable and direct index of structural damage caused by earthquakes recently produced a shift in seismic design and assessment philosophy. In fact, new performance-based design requirements have strongly emerged internationally in seismic design and analysis. One design concept that was developed in response to these needs is currently known as “displacement-based” design (DBD). A large amount of work has already been undertaken in the field of displacement-based design especially for reinforced concrete structures. Recommendations for steel moment resisting frame (MRF) structures are few and the available proposals have not been fully confirmed. In this context, a research project – named DiSTEEL (Displacement based seismic design of STEEL moment resisting frame structures) and aiming to develop performance-based design guidelines for moment resisting steel frame structures – has been funded by the European Community. The DiSTEEL Project was the framework of the study presented in this thesis. In case of moment resisting steel frames, beam-to-column joints are essential structural components that significantly affect the overall seismic response. Therefore, a first step towards the development of DBD rules for MRFs is the analysis of response of beam-to-column joints with a focus on limit-state deformations.

Within the context briefly outlined, the focus of this work is on the features of the inelastic response of beam-to-column end-plate joints. The efforts are addressed to the development of simple yet reliable design equations and tools to predict joint rotations associated with selected limit-states. After a review of some available experimental data, an assessment of existing analytical models for predicting joint rotational stiffness and strength is presented. Using these analytical models the geometrical and material parameters mostly affecting the joint yield rotations are highlighted. Analytical predictions of yield rotations of both flush and extended end-plate joints are subsequently evaluated by comparison with experimental data. Once validated by such a

comparison, the analytical tools are further developed for design purposes, in the form of design charts to be obtained by an automated application of the analysis tools. Finally, discussion and preliminary evaluation of the rotation capacity of extended end-plate joints are presented.

## **ACKNOWLEDGMENTS**

(Only in the printed version)





## ABOUT THE AUTHOR

**Giusy Terracciano** is a Structural Engineer graduated at the University of Naples Federico II in 2009. She attended the PhD course in Construction Engineering at the Department of Structures for Engineering and Architecture from 2010 through 2013. Giusy Terracciano has multiple research interests, including steel structures (connections, cold-formed thin-walled members) and seismic vulnerability and retrofitting of existing masonry and reinforced concrete buildings. She is currently involved in both national and international research projects. She is co-author of about 10 papers published in proceedings of both national and international conferences.



## MOTIVATIONS AND OBJECTIVES

The recognition of the key-role of displacements and deformations as direct index of structural damage caused by earthquakes produced in the last decades the development of explicit displacement-based design (DBD) methods. Although current seismic design provisions implement the "Performance-Based Design" (PBD) philosophy, according to a multilevel performance approach (e.g. SEAOC, 1995), the procedures for structural seismic design and assessment are force-based (Force-Based Design, FBD). The limits of this approach and the advantages of alternative displacement-based design methods have been highlighted by several Authors (e.g. Priestley, 1993; Moehle, 1996; Priestley, 1998). Many efforts have been addressed to the development of design guidelines for a number of building structures and bridges (Sullivan *et al.*, 2012), but recommendations for moment resisting frame structures are insufficient yet.

In this context, a research project – named DiSTEEL (Displacement based seismic design of STEEL moment resisting frame structures) and aiming to develop performance-based design guidelines for moment resisting steel frame structures – has been funded by the European Community (Research Fund for Coal and Steel (RFCS), grant agreement n. RFSR-CT-2010-00029). Within the DiSTEEL project the University of Naples Federico II (UNINA-WP3) has been involved in the study of flexible full strength joints. It is well known that in the DBD methodology, the original multi degree of freedom (MDOF) structure is substituted with an equivalent single degree of freedom (SDOF) system (Shibata and Sozen, 1976), whose structural properties are estimated using design displacement profiles corresponding to certain drift limit and equivalent viscous damping, the latter accounting for the energy dissipated by the structure. Both maximum displacement profile and equivalent viscous damping are influenced by connection details, especially in case of partial strength connections. On the other hand, beam-to-column joints are essential structural components that significantly affect the overall seismic response (Della Corte *et al.*, 2002).

The analysis of response of beam-to-column joints is essential in order to develop DBD rules for moment resisting frame structures.

Therefore, the main objective of this work is to characterize the behaviour of beam-to-column joints in steel moment resisting frames, in terms of rotations associated to significant limit states. The focus is on end plate connections, a type widely used in steel frame structures because of the simplicity and economy associated to their fabrication and erection.

In the following, after a brief introduction on the DBD procedure and the method of joint modelling, the limit state rotations considered in this study are identified and the analysis methodology is presented (Chapter 1). Then a review of some available experimental data (Chapter 2) and an assessment of existing analytical models for predicting joint rotational stiffness and strength (Chapter 3) are given. Subsequently, a theoretical study on the yield rotation is described and design tools are developed (Chapter 4). Observations on the rotation capacity of extended end-plate joints are finally provided (Chapter 5). Finally, conclusions on the behaviour of beam-to-column end-plate joints are derived (Chapter 6).

# 1 INTRODUCTION

This Chapter contains a brief description of both the Displacement-based Design procedure and the component method. Subsequently the definitions of the limit state rotations considered in this study are given. Finally, the analysis methodology is presented.

## 1.1 DISPLACEMENT BASED DESIGN FOR MOMENT RESISTING FRAME STEEL STRUCTURES

The DBD procedure is based on the substitute structure analysis procedure developed by Shibata and Sozen (1976). The initial MDOF system is replaced by an equivalent SDOF (Figure 1.1 a) characterized by secant stiffness,  $K_e$ , at maximum displacement (Figure 1.1 b),  $\Delta_d$ , and a level of equivalent viscous damping appropriate to the energy dissipated by the structure. The design displacement  $\Delta_d$  is expressed as a function of the masses and displacements of the MDOF structure. By means  $\Delta_d$ , the damping is estimated from the expected ductility demand (Figure 1.1 c). The effective period  $T_e$  at maximum displacement response can be read from a set of design displacement spectra (Figure 1.1 d). Representing the structure (Figure 1.1 a)) as an equivalent SDOF oscillator, the effective stiffness  $K_e$  at maximum response displacement can be found by inverting the equation for natural period of a SDOF oscillator. Finally the design base shear  $V_b$  of the MDOF structure is obtained as the product of the effective stiffness  $K_e$  times the maximum displacement  $\Delta_d$  (Priestley M. J. N., 1998).

Implementing DBD methodology requires the definitions of the design displacement profiles corresponding to certain drift limit and equivalent viscous damping accounting the energy dissipated by the structure. Both maximum displacement profile and equivalent viscous damping are influenced by connection details, therefore, a first step towards the development of DBD rules for MRFs is the analysis of response of beam-to-column joints.

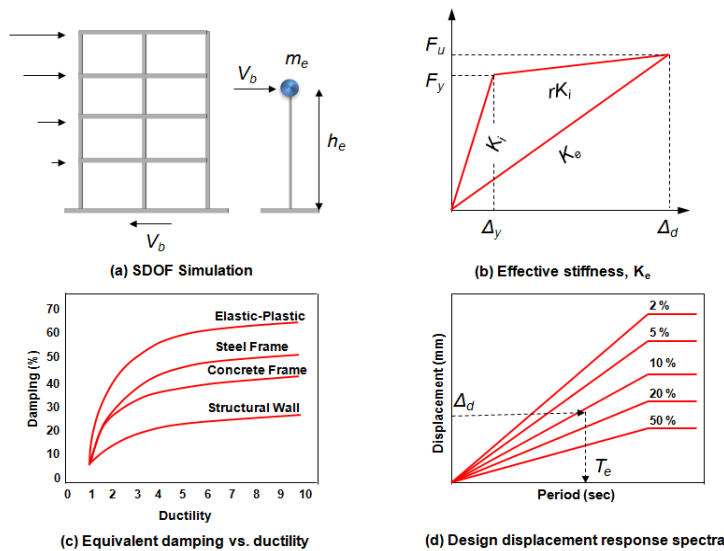


Figure 1.1 Fundamentals of “Direct Displacement-Based Design” (Prestley, 1998)

## 1.2 JOINT MODELLING: THE COMPONENT METHOD

### 1.2.1 Basic principles and components of joints

The experimental test is the most accurate knowledge of joint behaviour, but this technique is too expensive for everyday design practice and it is usually reserved for research purposes (Faella *et al.*, 2000). Literature provides several alternatives models which can be used to predict the mechanical behaviour of joints. Classifications of different methods are provided by several authors: Nethercot and Zandonini (1989), Faella *et al.* (2000) Jaspert (2000), Diaz *et al.* (2011) Chen *et al.* (2000, 2011). Among these, the mechanical approach, known as the component method, slowly became the reference by most of the researchers. The originality of the method lies in considering any joints as set of individual basic components. Each component is characterised by an own level of stiffness and force is tension compression and shear (Jaspert, 2000).

Nowadays it is the Eurocode 3 recommended procedure to evaluate the initial stiffness and flexural resistance of a great number of joint typology

subjected to pure bending. The application of the component method requires the following steps:

- a) Identification of relevant components;
- b) Evaluation of the force-deformation response of each component (initial stiffness design strength);
- c) Assemblage of the components to evaluate the mechanical characteristics of the whole joint (initial stiffness, design resistance).

This procedure can be applied to a great variety of joints, bolted or welded, provided that force-deformation response of each component is available (Faella *et al.*, 2000). The behaviour of active components has been deeply studied and recommendations for their characterization are given in Eurocode 3 part 1.8. In general, each component is characterized by a non-linear force-displacement curve; however simpler idealizations are possible, such as that proposed by Eurocode 3. The code approximates the complex nonlinear component behaviour by means of the elastic-perfectly plastic response, characterized by a plastic resistance and initial stiffness. Concerning the component ductility, Eurocode 3 provides only some qualitative principles.

The relevant components of an end-plate beam-to-column joint are: (*cws*) column web panel in shear, (*cwc*) column web in compression, (*cwt*) column web in tension, (*cfb*) column flange in bending, (*epb*) end-plate in bending, (*bfc*) beam flange and web in compression, (*bwt*) beam web in tension and (*bt*) bolts in tension (Figure 1.1).

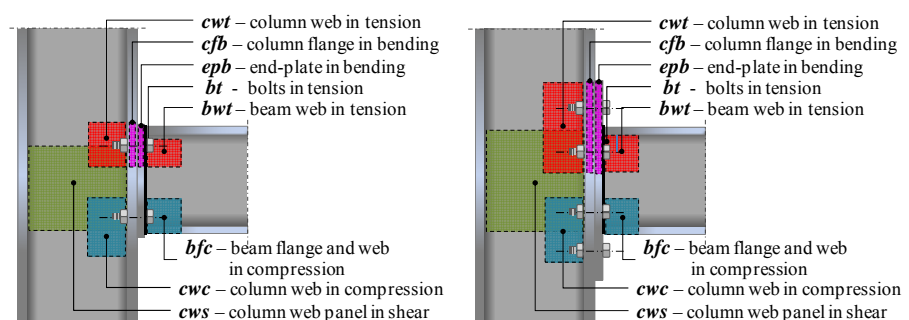


Figure 1.1: Components of end-plate beam-to-column joints

These components are assembled into a mechanical model in order to evaluate the plastic moment resistance and the initial rotational stiffness of the whole joint. The Eurocode 3 mechanical models for flush end-plate connections and extended end-plate connections are presented in Figure 1.2.

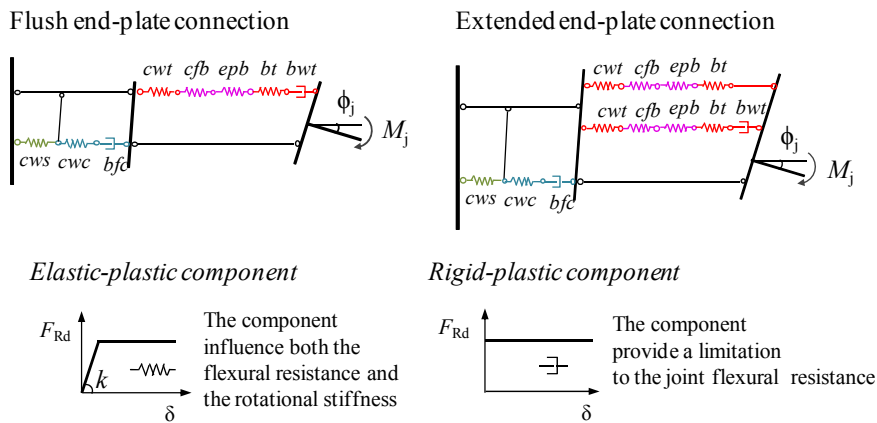


Figure 1.2: Eurocode 3 mechanical models

### 1.2.2 Prediction of flexural resistance and initial rotational stiffness

According to the component method, the flexural resistance of beam-to-column joints with bolted connections is evaluated as follows:

$$M_{j,Rd} = \sum_r h_r F_{tr,Rd} \quad (1.1)$$

where  $F_{tr,Rd}$  is the effective design resistance of bolt row  $r$ ;  $h_r$  is the distance of bolt row  $r$  from the centre of compression, assumed located at the level of the column flange,  $r$  is the bolt row number. The values of  $F_{tr,Rd}$  are calculated starting at the top row and working down. Bolt rows below the current row are ignored.

The effective tensile resistance of each bolt row is the smallest value of the tension resistance of the components, reduced if the total tensile resistance is greater than the design resistance of the column web panel in shear or if the compression strength is exceeded.



The resistance of the tension zone is governed by the following components: column flange in bending, end-plate in bending, column web in tension, beam web in tension, bolts in tension. Traditionally the tension components, column flange in bending and bolt in tension, end-plate in bending and bolts in tension, are represented as a T-stub of a equivalent width calculated using yield line patterns specified by Zoetemeijer (1990). Examples of the yield line patterns for extended and end-plate connections are in Figure 1.3 and Figure 1.4.

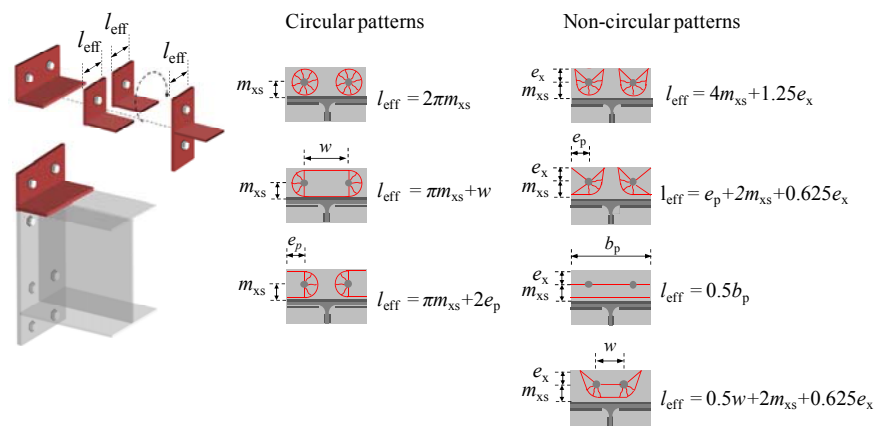


Figure 1.3: Yield line patterns and effective length of the end-plate T-stub for the first bolt row in tension

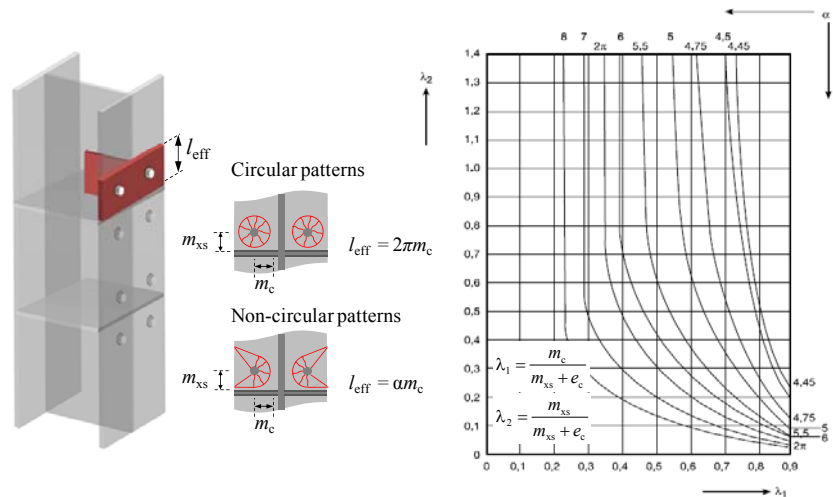


Figure 1.4: Yield line patterns and effective length of the column flange T-stub for the first bolt row in tension

In case of multiple bolt rows, on the basis of the vertical pitch of the bolt rows, yield lines can involve one or more bolt rows. In detail, if the distance between bolt rows is below a certain limit, and if the bolt rows are not separated by stiffeners, it is possible that two or more bolt rows fail together in a common yield line pattern.

The resistances of these components are equal to the resistances of the representative T-Stub, each evaluated as the minimum tensile resistance associated to the three different T-Stub failure mechanisms (Figure 1.5).

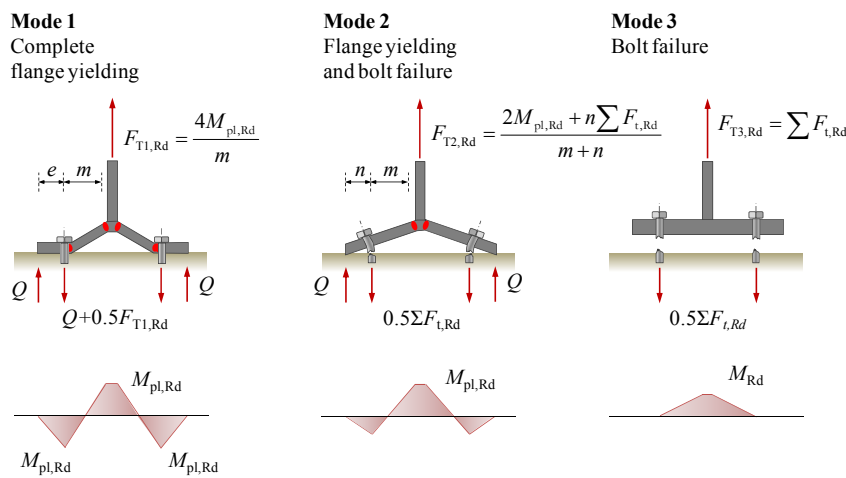


Figure 1.5: T-Stub mechanisms and design resistance for each failure mode

The column web in tension and the beam web in tension resistances are calculated on the basis of the effective T-Stub width of the column side and the beam side respectively (Figure 1.6, Figure 1.7).

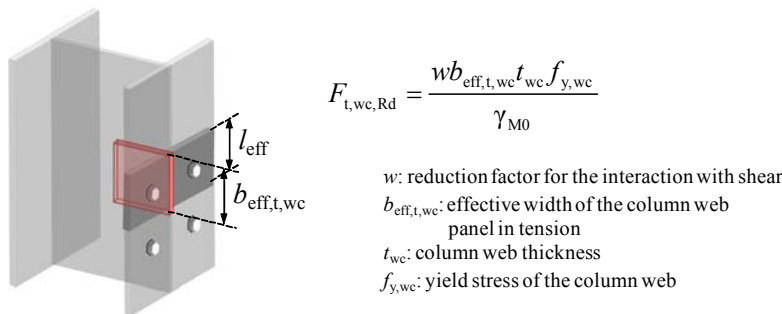
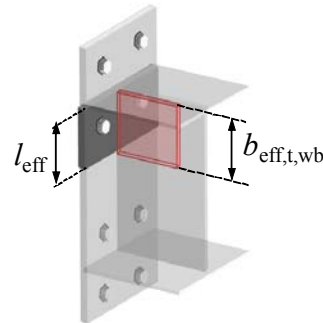


Figure 1.6: Design resistance of column web in tension

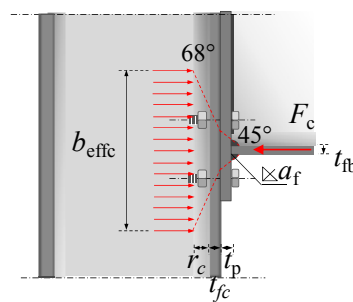


$$F_{t,wb,Rd} = \frac{b_{\text{eff},t,wb} t_{wb} f_{y,wb}}{\gamma_{M0}}$$

$w$ : reduction factor for the interaction with shear  
 $b_{\text{eff},t,wb}$ : effective width of the beam web in tension  
 $t_{wb}$ : beam web thickness  
 $f_{y,wb}$ : yield stress of the beam web

Figure 1.7: Design resistance of beam web in tension

At the compression side, the resistance is offered by the column web and the beam web and flange. The concentrated forces transmitted by the beam flanges produce normal stresses in the column web (Figure 1.8). The latter is also subjected to shear stresses and normal stresses due the axial load. This interaction of local stresses can decrease the strength of the basic component (Jaspart, 2000) and can produce the failure of column web panel in compression for crushing or buckling. The component method, as implemented in Eurocode 3, considers the moment-rotation behavior of the whole joint-beam system. The design resistance of joint is limited by the design plastic moment of the connected beam (Figure 1.9).



$$F_{c,wc,Rd} = \frac{w k_{wc} b_{\text{eff},c,wc} t_{wc} f_{y,wc}}{\gamma_{M0}}$$

$$F_{c,wc,Rd} \leq \frac{w k_{wc} \rho b_{\text{eff},c,wc} t_{wc} f_{y,wc}}{\gamma_{M0}}$$

$w$ : reduction factor for the interaction with shear  
 $k_{wc}$ : reduction factor for the longitudinal compressive stress  
 $\rho$ : reduction factor for plate buckling  
 $b_{\text{eff},c,wc}$ : effective width of the column web panel in compression  
 $b_{\text{eff},c,wc} = t_{fb} + 2\sqrt{2} a_p + 5(t_{fc} + r_c) + t_p$   
 $t_{wc}$ : column web thickness  
 $f_{y,wc}$ : yield stress of the column web

Figure 1.8: Design resistance of column web in compression

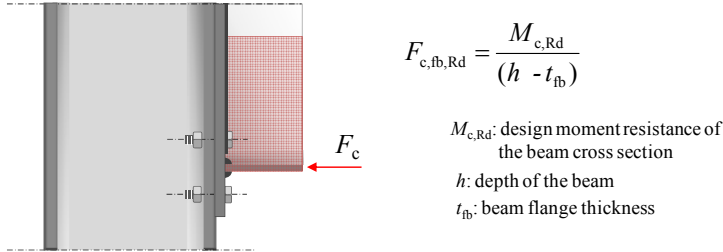


Figure 1.9: Design resistance of beam flange and web in compression

The design shear resistance of column web panel is given in Figure 1.10. It assumes a uniformly shear stress distribution in the column web panel and a limited column axial force in the column.

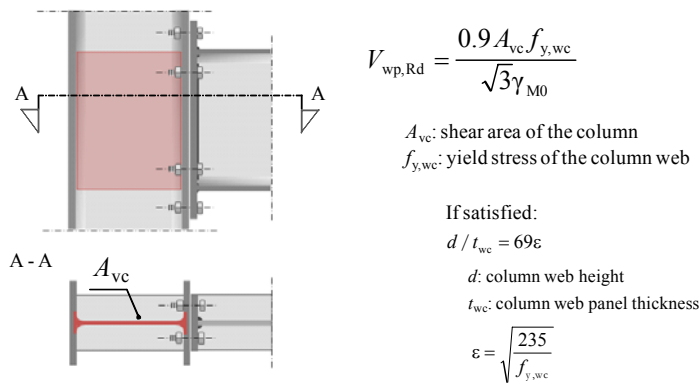


Figure 1.10: Design resistance of unstiffened column web panel in shear

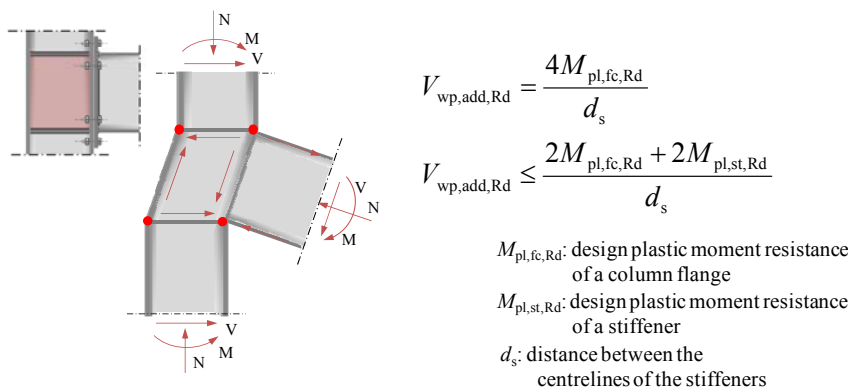


Figure 1.11: Additional resistance of the column web panel in shear for column web transverse stiffeners

The column web transverse stiffeners increase the shear resistance of the column web panel (Figure 1.11).

The component method is based on a plastic distribution of bolt forces, which is reasonable if the deformation of the column flange or end-plate can take place. This is ensured by placing a limit on the distribution of bolt row forces if the critical mode is no ductile one. This limit is applied if the resistance of a bolt row is greater than  $1.9 F_{t,Rd}$ . The effect of this limitation is to apply a triangular distribution of forces.

The initial rotational stiffness of joints is given by the following equation:

$$S_{j,ini} = \frac{E \cdot b^2}{\sum_i \frac{1}{k_i}} \quad (1.2)$$

where  $E$  is the Young modulus,  $b$  is the lever arm and  $k_i$  is the stiffness coefficient for the  $i$ -th basic joint component, which for end-plate connections are: ( $k_1$ ) column web panel in shear, ( $k_2$ ) column web in compression, ( $k_3$ ) column web in tension, ( $k_4$ ) column flange in bending, ( $k_5$ ) end-plate in bending and ( $k_{10}$ ) bolts in tension.

In case of two or more bolt rows, the stiffness coefficients of the bolt rows in tension are represented by an equivalent spring  $k_{eq}$  evaluated as follows (Eq. 1.3):

$$k_{eq} = \frac{\sum_r k_{eff,r} b_r}{z_{eq}} \quad (1.3)$$

where  $k_{eff,r}$  is the effective stiffness of bolt row  $r$ , determined by Eq. (1.4),  $b_r$  is the distance of the bolt row from the compression centre,  $z_{eq}$  is the equivalent lever evaluated by Eq. (1.5).

$$k_{eff,r} = \frac{1}{\sum_i k_{i,r}} \quad (1.4)$$

where  $k_{i,r}$  is the stiffness coefficient of the  $i$ -th component of bolt-row  $r$ .

$$\chi_{eq} = \frac{\sum_r k_{eff,r} b_r^2}{\sum_r k_{eff,r} b_r} \quad (1.5)$$

The model assumes that the compressive spring and the shear spring are located at the centre of compression which is the centerline of the beam flange, while the tensile springs are at bolt row level (Figure 1.2). The deformations of tensile springs are proportional to their distance from to the compression centre. According to the procedure, the assembly of tension springs in series and in parallel is replaced by an equivalent spring.

### 1.2.1 Implementation of Eurocode 3 component method within Mathcad

The Eurocode 3 calculation rules have been implemented into a Mathcad worksheet. This permits the automatic calculation of joint stiffness and strength with associated joint classification.

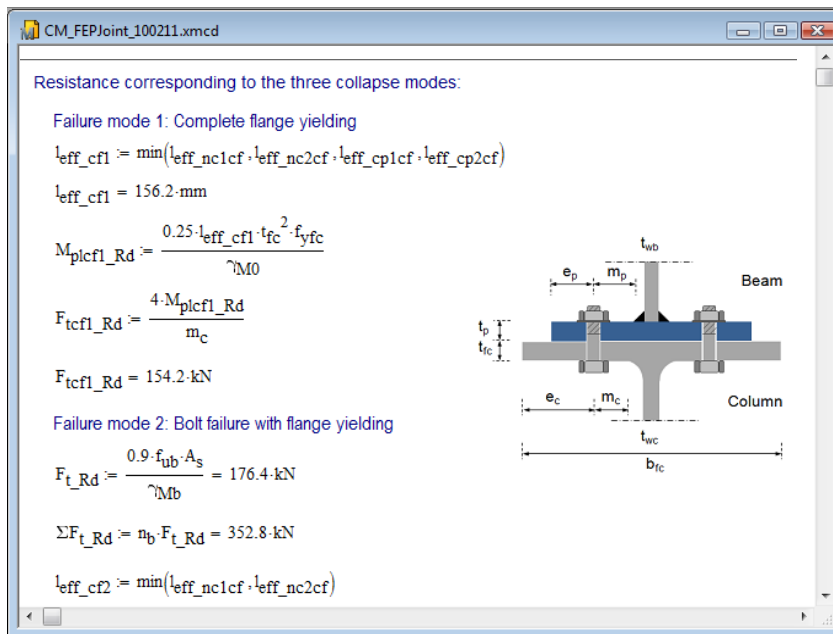


Figure 1.2 Example of the Mathcad worksheet

The procedure has been implemented for both the flush end-plate and extended end-plate joints. Together with the digital database (presented in the following Chapter), the automated calculation procedure allows the evaluation of the influence that different joint parameters may have on the moment-rotation response.

### 1.3 MOMENT – ROTATION CURVE REPRESENTATION

Structural joints, particularly bolted connections exhibit a nonlinear behaviour due, for example, to material discontinuity of the subassembly, yielding of some component parts and local buckling of plates. This complex behaviour is usually approximate introducing drastic simplifications.

In general, beam-to-column joints in steel frame structures can transmit axial and shear forces, bending and torsion moments. The bending actions are predominant compared with the axial and shear forces, while the torsion moments are negligible in planar frames. Therefore, the behaviour of beam-to-column joints is represented by a moment-rotation curve ( $M-\phi$ ) that describes the relationship between the applied bending moment ( $M$ ) and the corresponding rotation between the members ( $\phi$ ).

The mathematical representation of the moment–rotation curve can be performed by means of different relationships and levels of precision. The different mathematical representations of the moment–rotation curve are: a) linear; b) bilinear; c) multilinear; d) nonlinear. The most accurate representation of the beam-to-column behaviour is obtained using continuous nonlinear functions (Faella *et al.*, 2000; Diaz *et al.*, 2011).

Eurocode 3 suggests two possible idealizations of the  $M-\phi$  curve, bilinear (elastic-plastic curve) and nonlinear. The stiffness ratio  $\mu$ , used to define the nonlinear part of the  $M-\phi$  curve is defined as follows (Eq. (1.6)):

$$\mu = \left( 1.5 M_{j,Ed} \frac{1.5 M_{j,Ed}}{M_{j,Rd}} \right)^{\psi} \quad (1.6)$$

$\Psi$  is a coefficient which depends on the type of connection. For bolted end plate connections, it is equal to 2.7.

The theoretical study of the yield rotation and the calculation of the plastic rotation capacity of end-plate connection are based on bilinear and elastic-plastic representation of the moment-rotation curve.

### 1.4 DEFINITIONS OF LIMIT STATE ROTATIONS

Two limit state rotations have been considered in this study: the yield rotation and the ultimate rotation. The first is intended the rotation corresponding to initiation of significant plastic deformations within the joint. Conventionally it has been herein defined, according to the component method (Figure 1.12), as the ratio of the moment resistance ( $M_{j,R}$ ) and the initial rotational stiffness ( $S_{j,ini}$ ) (Eq. (1.7)).

$$\phi_{j,y} = \frac{M_{j,R}}{S_{j,ini}} \tag{1.7}$$

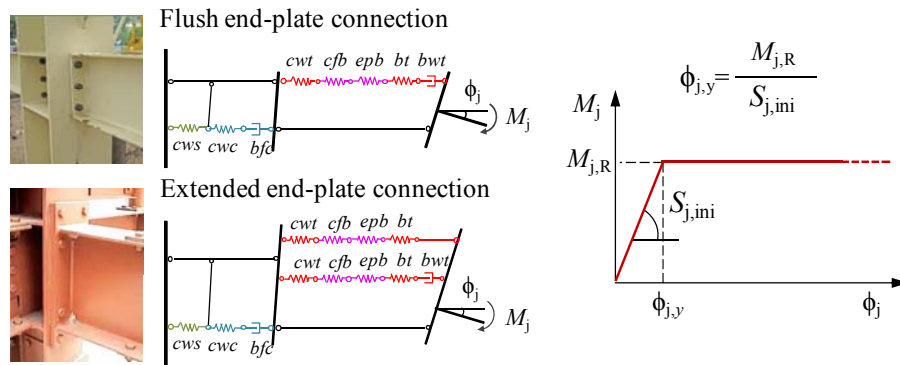


Figure 1.12: Yield rotation of end-plate connections

To establish limits of validity of the perfectly plastic joint mechanical model, the joint rotation capacity and the joint ultimate rotation have been identified.

The joint rotation capacity ( $\phi_{j,c}$ ) has been conventionally defined as the maximum rotation corresponding to a measured resistance never less than the theoretical resistance (Figure 1.13). The ultimate rotation ( $\phi_{j,u}$ )



has been considered as the rotation associated to some form of joint failure, e.g. rupture of bolts, fracture of plates, very large loss of strength.

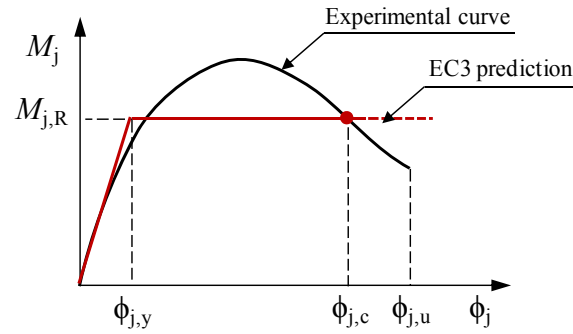


**Figure 1.13: Rotation capacity and ultimate rotation**

Consequently the plastic rotation capacity ( $\phi_{j,pc}$ ) and the ultimate plastic rotation ( $\phi_{j,pu}$ ) have been defined as follows (Eq. (1.8) Eq. (1.9)):

$$\phi_{j,pc} = \phi_{j,c} - \phi_{j,y} \quad (1.8)$$

$$\phi_{j,pu} = \phi_{j,u} - \phi_{j,y} \quad (1.9)$$

where  $\phi_{j,y}$  is the yield rotation given by the component method defined by Eq. (1.7).

The ultimate rotation can be larger than the defined rotation capacity, when the system exhibit gradual and smooth loss of strength, e.g. when degradation is due to local inelastic buckling. In such a case the ultimate rotation could be defined as that corresponding to a predefined maximum loss of system strength. When a sudden failure occurs, e.g. a bolt rupture or a plate fracture, the ultimate rotation coincides with the above defined rotation capacity.

## 1.5 ANALYSIS METHODOLOGY

The analytical study of the yield rotation was carried out by means the component method and parametric analyses. First the accuracy of the mechanical approach was evaluated. At this aim the theoretical

prediction were compared with experimental results. Therefore, experimental tests on end-plate connections were collected and analyzed in term of yield rotation. From experimental point of view, conventional moment resistance and initial stiffness were considered. The first was assumed equal to the plastic flexural strength of the connected beam for full strength joints, while for partial strength joints the moment resistance was fixed equal to the flexural strength corresponding to a secant stiffness of  $1/3$  times the initial stiffness. Generally the experimental initial rotational stiffness is provided by Authors. If not available it was determined graphically as the slope of the tangent to the curve in the elastic range. By means the mechanical approach, the theoretical structural properties and the yield rotation of each specimen were evaluated. Once assessed the accuracy of the method, through the mechanical approach, analytical closed-form equations to calculate yield rotation of flush end-plate connections were derived. Starting from the conventional definition of the yield rotation, analytical manipulations of the joint moment resistance and initial stiffness led to the identification of yield rotation equations associated to the different possible failure mode of the connection. The analytical expressions allowed the recognition of the non-dimensional geometrical and material parameters mostly affecting the end-plate joint rotations, relevant for the subsequent parametric study aimed to the identification of the influence of connections detail on the response of beam-to-column joints. Concerning the study on the ultimate rotations, once defined the conventional plastic rotation and the ultimate rotations, the experimental data on extended end-plate connections were analyzed and divided in two different classes depending on the difference noted between the plastic mechanism and the ultimate failure mode. The results were analyzed in order to associate a rotation capacity to a plastic mechanism.

## 2 EXPERIMENTAL DATA COLLECTION

A large amount of experimental tests were performed by several Authors to investigate the behaviour of end-plate connections. The analysis methodology adopted in this study requires an accurate knowledge of the geometrical and material properties of all specimens, which is not always available. In this study the experimental works carried out by Ghobarah *et al.* (1990), Sumner and Murray (2002), Nogueiro *et al.* (2006) Shi *et al.* (2007), da Silva *et al.* (2004) and Broderick and Thomson (2002, 2005) are considered. The Chapter contains a detailed description of the experimental programs and the corresponding test results.

### 2.1 EXTENDED END-PLATE CONNECTIONS

#### 2.1.1 Tests by Ghobarah *et al.* (1990)

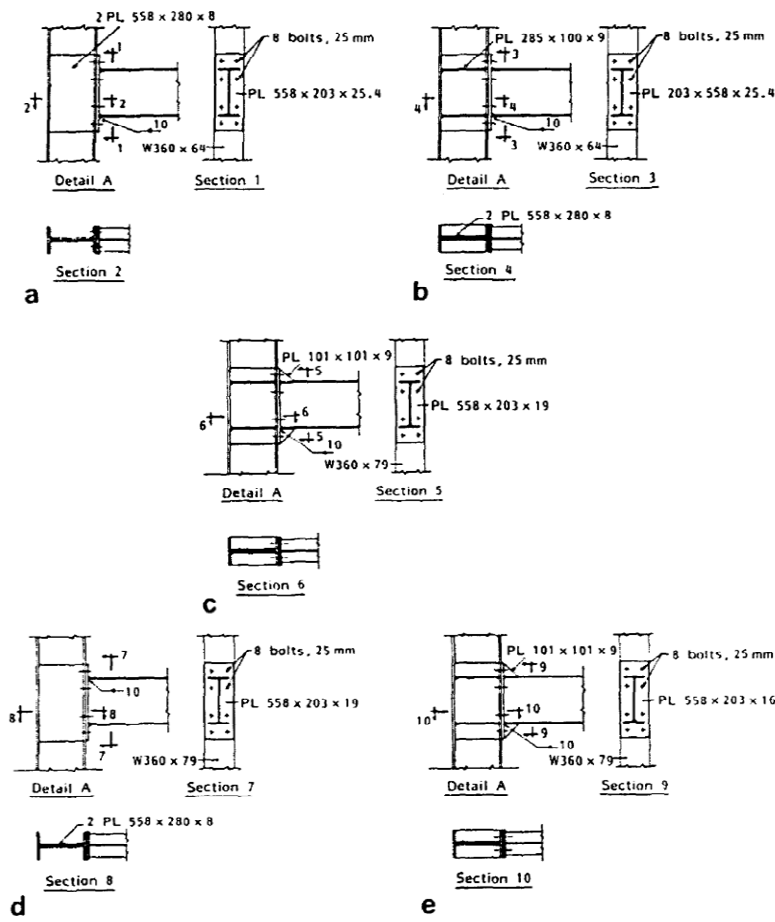
##### 2.1.1.1 *Description of specimens and test setup*

Five bolted end-plate beam-to-column connections were tested under cyclic loading. The experimental campaign was carried out to investigate the behaviour of this type of connection and to evaluate the effect of design parameters such as end-plate thickness, column flange stiffeners and bolt properties on the overall joint behaviour.

A W360×170×45 section was used for beams and a W360×200×79 or W360×200×64 section for the column stubs. The column web was reinforced by 8 mm thick doubler plates. All beams were welded to the end-plates by 10 mm and 7 mm fillet welds for the flange and web, respectively. The geometrical details and the joint arrangement of each specimen are given in Figure 2.1.

The material used for all five test specimens, including members, stiffeners and end-plates, was G40.21-M300W steel (minimum yield stress  $f_y=300$  MPa). High-strength tensile bolts were used in the

connection. The bolt diameter was equal to 25 mm and the grade was ASTM A490M (minimum tensile strength  $f_u=1040$  MPa). Coupons from the beam sections were extracted to evaluate the actual properties of members. The results are given in Table 2.1.



(a) Specimen A-1; (b) specimen A-2; (c) specimen A-3; (d) specimen A-4; (e) specimen A-5

Figure 2.1: Details of specimens

A cantilever scheme was chosen for the study. The column stub length was fixed equal to 1220 mm, while the cantilever length was varied depending on the beam section (Figure 2.2 a)). Figure 2.2 b) shows that

the column stub was rigidly clamped to a rigid fixture frame, while a hydraulic actuator was used to apply the load to the beam tip. The specimens were provided by lateral supports at the end of the beam to prevent lateral buckling. A guide at the mid-span of the cantilever to prevented lateral displacement of the top flange.

**Table 2.1: Material properties**

Specimen	Coupon location	Yield stress (MPa)	Tensile strength (MPa)
A-1	Flange	310.9	500.0
	Web	315.7	480.7
A-2	Flange	316.1	503.3
	Web	322.1	480.6
A-3	Flange	310.9	500.0
	Web	315.7	480.7
A-4	Flange	310.9	500.0
	Web	315.7	480.7
A-5	Flange	316.1	503.3
	Web	322.1	480.6

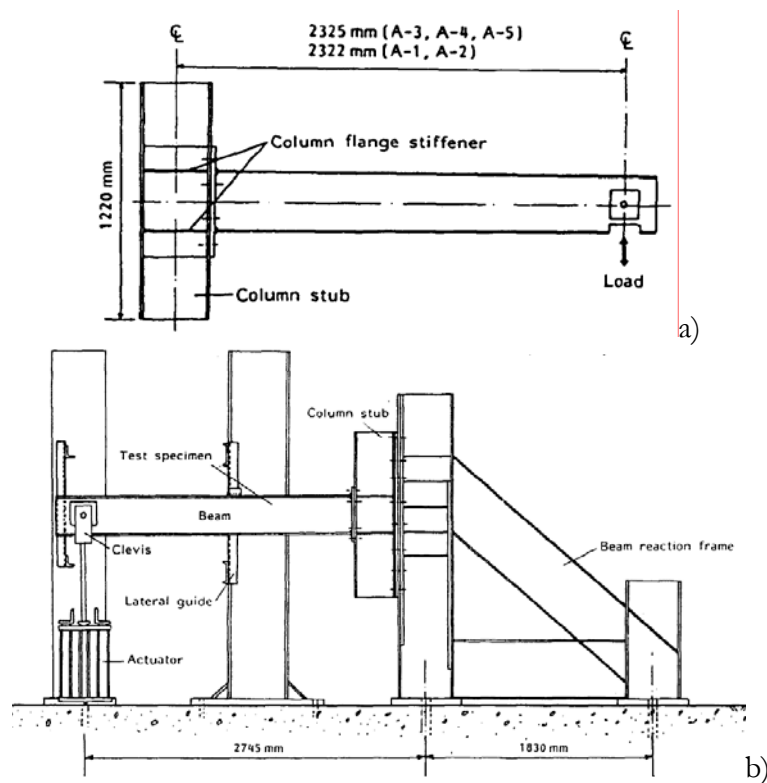


**Figure 2.2: a) Test specimen, and b) test set-up**

The adopted loading protocol is presented in Figure 2.3. Before reaching the yield point, each specimen was subjected to four load cycles of half the expected yield value. Then the load was increased until the beam yielding and two cycles were applied. Subsequently, the beam tip displacement was increased by half the yield displacement up to partial ductility of four (partial ductility is defined as the ratio of beam-tip displacement to the beam-tip displacement at the first yield). If no failure was detected two additional cycles were applied.

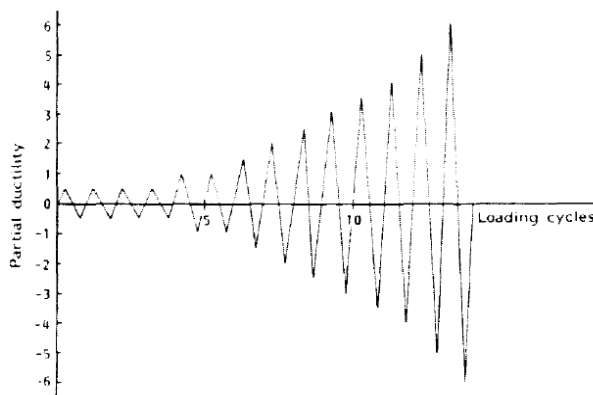


Figure 2.3: Loading protocol

### 2.1.1.2 Experimental results

#### 2.1.1.2.1 Specimen A-1

Specimen A-1 consisted of a W360×45 (W14×30) beam and a W360×64 (W14×43) column. The length of the column stub and the beam were 1220 mm and 2322 mm respectively. The end plate was 25 mm thick. Eight 25 mm diameter bolts were employed in the connection. The column web was reinforced by 8 mm doubler plate. No continuity plates were used to stiffen the column flange (Figure 2.1).

The experimental behaviour was represented by the beam-tip deflection versus beam-tip load curve (Figure 2.4). Since the column stub was rigidly fixed to the fixture frame, the end-beam deflection was due to elastic and inelastic deformations of the beam, column flanges, end-plate and bolts. Separation between the column flange and the end-plate was

noted up to the end of the test. Consequently, failure of A-1 was attributed to excessive deformations of the column flanges. The maximum load attained during the test was equal to 147 kN. The most of the energy was dissipated by the column flange with a minor amount dissipated by the beam flange.

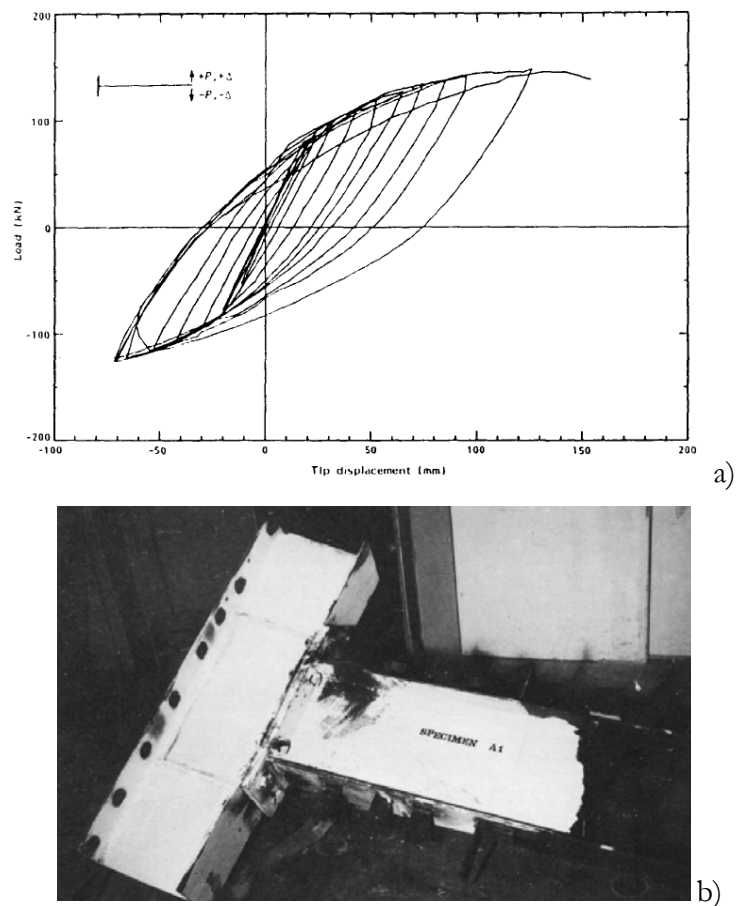


Figure 2.4: a) Beam load versus beam tip displacement curve and b) failure mode for A-1

#### 2.1.1.2.2 Specimen A-2

A-2 had the same geometrical properties of A-1, but differently from it, the column web was reinforced by 9 mm thick transverse stiffeners. During the test was observed the buckling of the beam flanges and the

web. The introduction of the continuity plates produced overstrength connection to enable the development of the beam plastic hinge. As in the previous case the beam-to-column behaviour was represented by the beam load versus beam-tip displacement curve. The hysteretic loops (Figure 2.5) show that the maximum load of 154.5 kN was reached during the test.

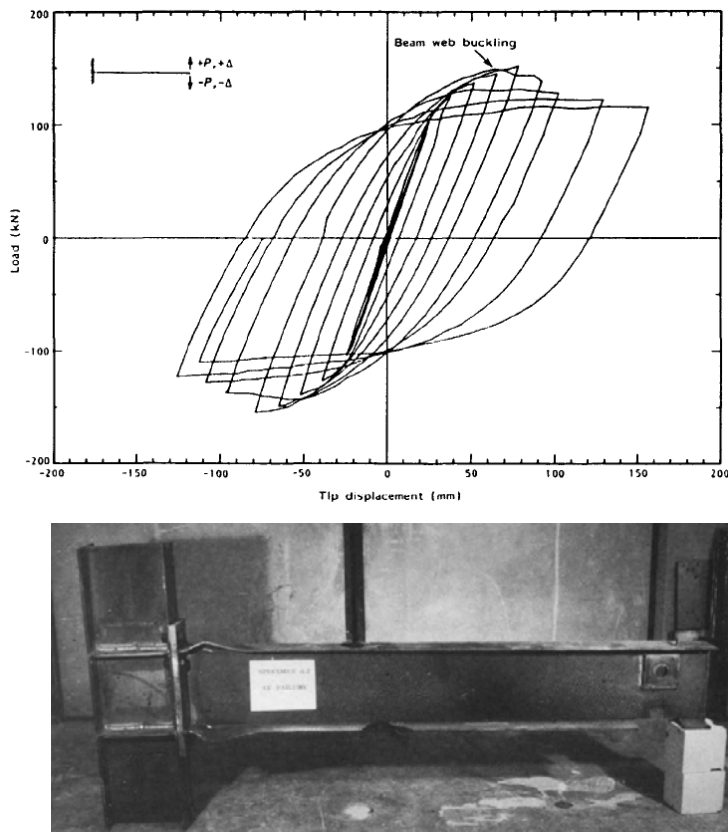


Figure 2.5: Beam load versus beam tip displacement curve and failure mode for A-2

### 2.1.1.2.3 Specimen A-3

Specimen A-3, differently from the above cases, had a thicker column flange and a thinner and stiffened end-plate. In detail, a W360×200×79 column and was used for this specimen. The beam was connected to the column by a 19mm thick end-plate. The latter was reinforced by a 9 mm



rib stiffener. The column stub and the cantilever length were 1220mm and 2325mm respectively. The column web was reinforced by 8mm thick doubler plate and 9 mm thick continuity plates (Figure 2.1).

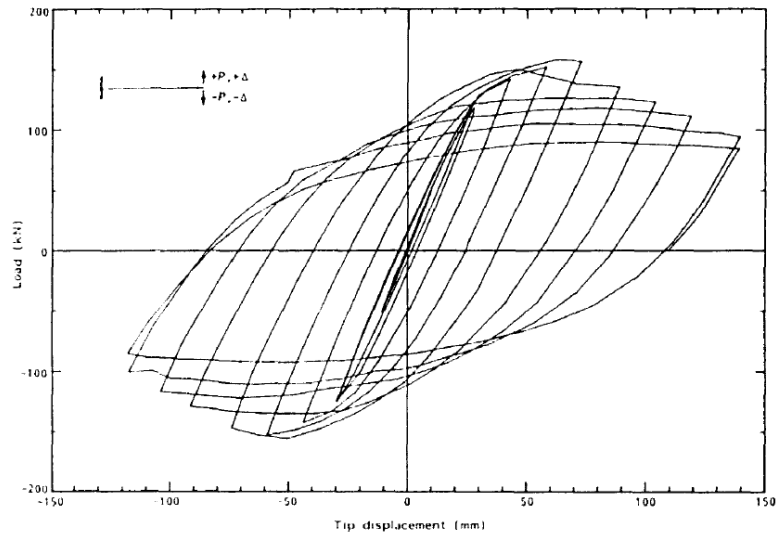


**Figure 2.6: Beam load versus beam tip displacement curve and failure mode for A-3**

The beam load versus beam-tip displacement curve is presented in Figure 2.6. The loops exhibited stable characteristics up to the buckling of the beam flanges and web. The maximum load attained during the test was equal to 156.4 kN.

#### 2.1.1.2.4 Specimen A-4

Specimen A-4 was obtained from A-3 removing the column and the end-plate stiffeners. The absence of the rib stiffeners made the end-plate the weakest component, which fractured in the extended part (Figure 2.7).

The maximum beam-tip load reached during the test was equal to 134.6 kN. However, this failure did not produce the complete collapse of the connection, since the inside bolts could still sustain a significant load. Severe damage was observed in the column flange.

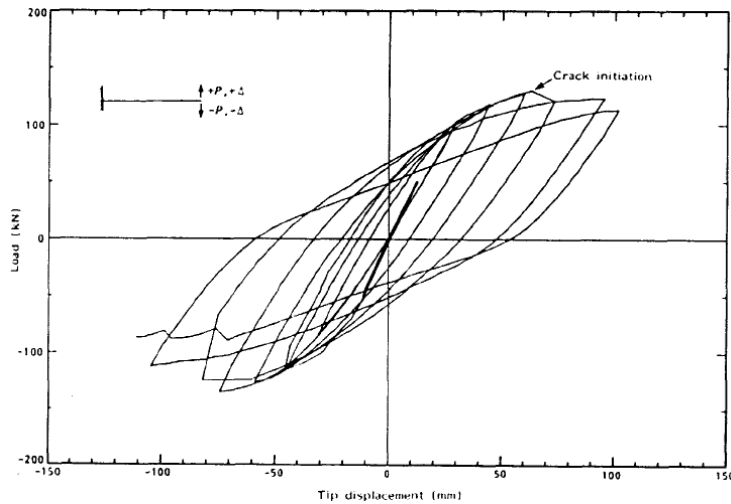


Figure 2.7: Beam load versus beam tip displacement curve and failure mode for A-4

### 2.1.1.2.5 Specimen A-5

Specimen A-5 was similar to A-3, but differently from it, the end-plate thickness was reduced to 16 mm.

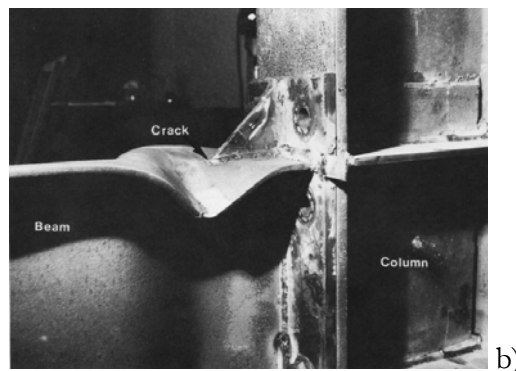
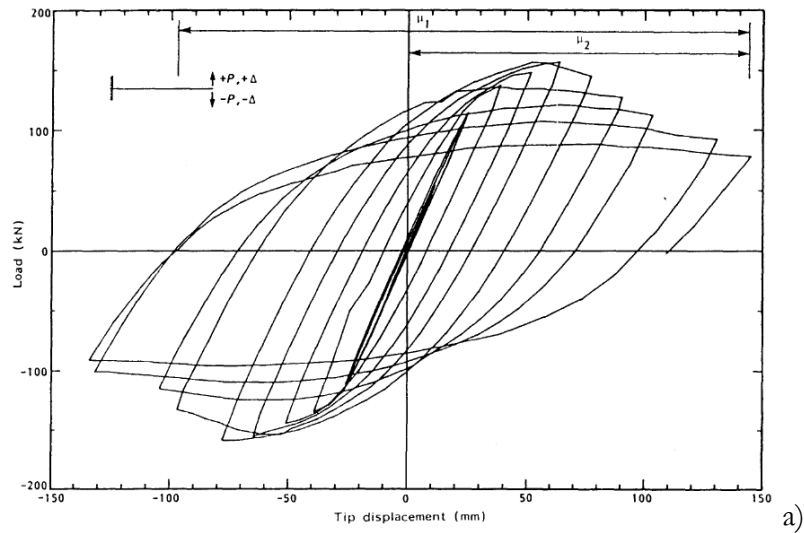


Figure 2.8: a) Beam load versus beam tip displacement curve and b) failure mode for A-5

Specimen A-5 behaved as A-3. The beam flange and web buckling were responsible for the deterioration of the loops (Figure 2.8). For specimen A-5 the maximum load applied was 158.9 kN.

## 2.1.2 Test by Sumner and Murray (2002)

### 2.1.2.1 Description of specimen and test set up

An extended end-plate beam-to-column connection was tested under cyclic loading. A W610×230×101 beam was connected to the flange of a W360×370×179 column. The end plate was welded to the beam using complete joint penetration groove welds for the flanges and fillet welds for the web (8 mm fillet welds on both sides of the web). The column had continuity plates in line with both connecting beam flanges and a web doubler plate, 9.5 mm thick, attached to one side of the web.

The main geometrical details of the specimen are summarised in Table 2.2.

**Table 2.2: Specimen details**

Specimen	Beam	Column	Bolt diameter	End-plate thickness
4E-1.25-1.5-24	W610×230×101	W360×370×179	32 mm (1 1/4 in.)	38 mm (1 1/2 in.)

The beam and column were ASTM A572 Grade 50 steel (nominal yielding stress  $f_y = 50$  ksi), while the end plate, continuity plates, and web doubler plates were ASTM A36 steel (nominal yielding stress  $f_y = 36$  ksi). The bolts used are ASTM A490 (minimum tensile strength  $f_u = 150$  ksi). Coupon tests results are given in Table 2.3.

**Table 2.3: Coupon test results**

Material	Measured yield strength (ksi)	Measured tensile strength (ksi)
Beam	53.6	70.7
Column	52.0	70.6
Column web doubler plate	42.1	64.95
End-plate	38.1	68.8

Figure 2.9 shows the test setup details and the loading protocol. The boundary conditions for the column ends were considered partially restrained. The load was applied by a loading jack, at a distance approximately of 900 mm from the beam tip, according to the SAC loading protocol (SAC Joint Venture 1997). A beam web stiffener was

used at the point of load application and lateral supports were provided to prevent lateral torsional buckling of the beam.

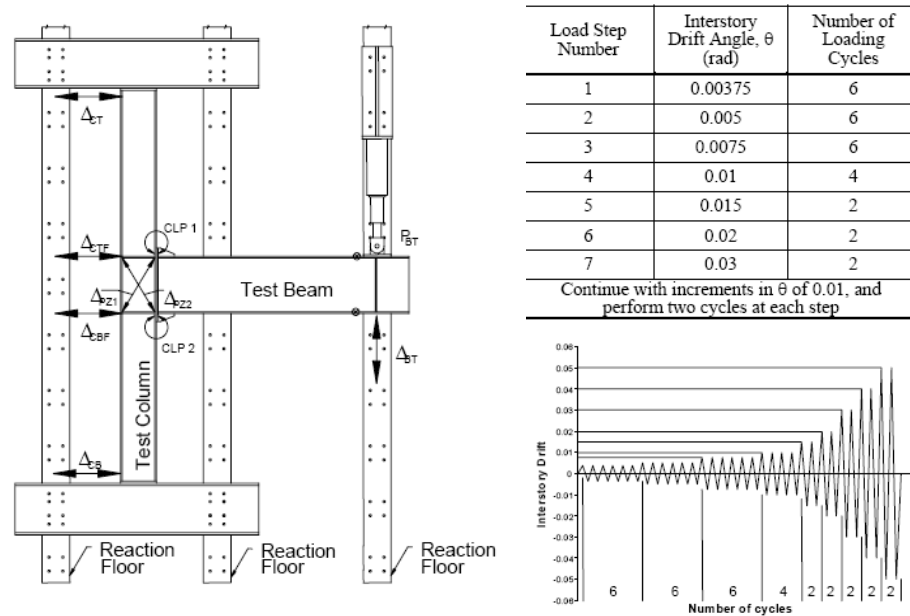
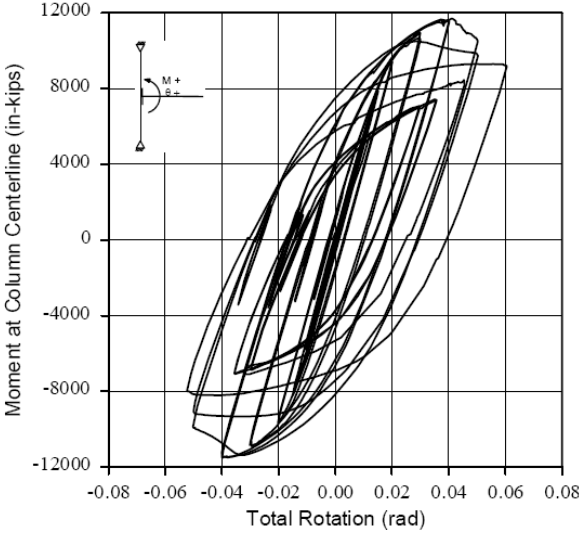


Figure 2.9: Test set up and loading protocol

Instrumentations of the test specimen measured the applied beam tip load, beam and column rotation, panel zone rotation, rigid body rotation of the test assembly, beam flange strains, column flange strains, panel zone shear strains, bolt strains, and end-plate separations.

### 2.1.2.2 Experimental results

The performance parameters used to evaluate the test results were the maximum applied moment, and the total inter-story drift angle. Both parameters were evaluated at the column centreline. The total rotation was free of any rigid body rotations of the column end supports.



a)



b)

Figure 2.10: a) Moment rotation curve and b) failure mode for 4E-1.25-1.5-24

The specimen behaved as expected with beam failure exhibiting large ductility, rotation capacity, and energy dissipation. The beam failure involved a combination of flange and web local buckling (Figure 2.10).

2.1.3 Tests by Nogueiro *et al.* (2006)

2.1.3.1 Description of specimens and test set up

Six end-plate beam-to-column steel joints were tested under arbitrary cyclic loading. The experimental programme was divided into two

groups varying the column section size, as can be observed in Table 2.4, Figure 2.11 and Figure 2.12. End plates, 18 mm thick, were connected to the beam-ends by full strength continuous fillet welds. All the material is steel grade S355 (nominal yielding stress  $f_y=355$  MPa). Eight M24 bolts, class 10.9 (nominal ultimate stress  $f_u=1000$  MPa), were employed in each connection (Figure 2.11 and Figure 2.12).

**Table 2.4: Details of the joint for the Group 1 and Group 3**

Group 1 (J1)	Beam	Column	Loading type
Test J-1.1	IPE 360	HEA 320	Monotonic
Test J-1.2	IPE 360	HEA 320	Cyclic
Test J-1.3	IPE 360	HEA 320	Cyclic
Group 3 (J3)	Beam	Column	Loading type
Test J-3.1	IPE 360	HEB 320	Monotonic
Test J-3.2	IPE 360	HEB 320	Cyclic
Test J-3.3	IPE 360	HEB 320	Cyclic

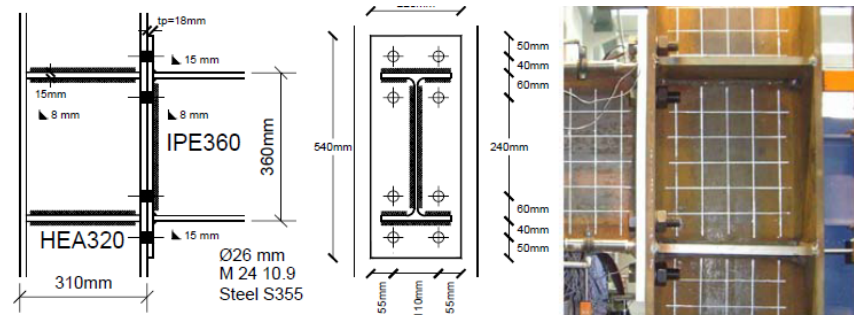


**Figure 2.11: Details of the joint for Group 1**

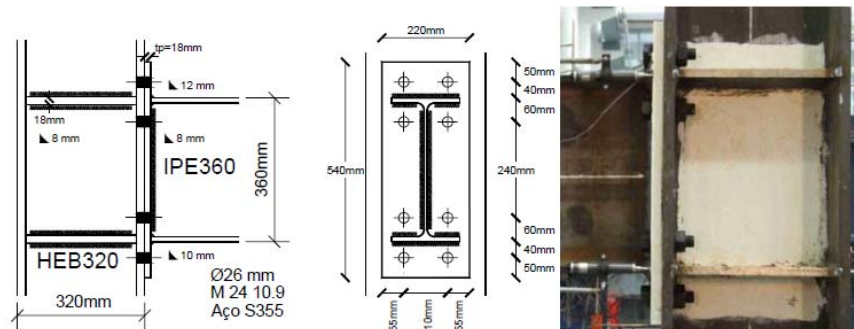


**Figure 2.12: Details of the joint for Group 3**

The cantilever scheme used for the experimental study (Figure 2.13) presented the columns 3.0 m high and beams approximately 1.2 meters long.

The load was applied at the beam tip by means of a hydraulic actuator. For each group, the first specimen was tested under monotonically increasing load, the remaining two specimens were tested under 2 distinct cyclic histories: (i) increasing cyclic amplitude in the elastic range and constant amplitude loading at approximately  $\varphi_y \times 3$ ; (ii) increasing cyclic amplitude in the elastic range and constant amplitude loading at approximately  $\varphi_y \times 6$ .

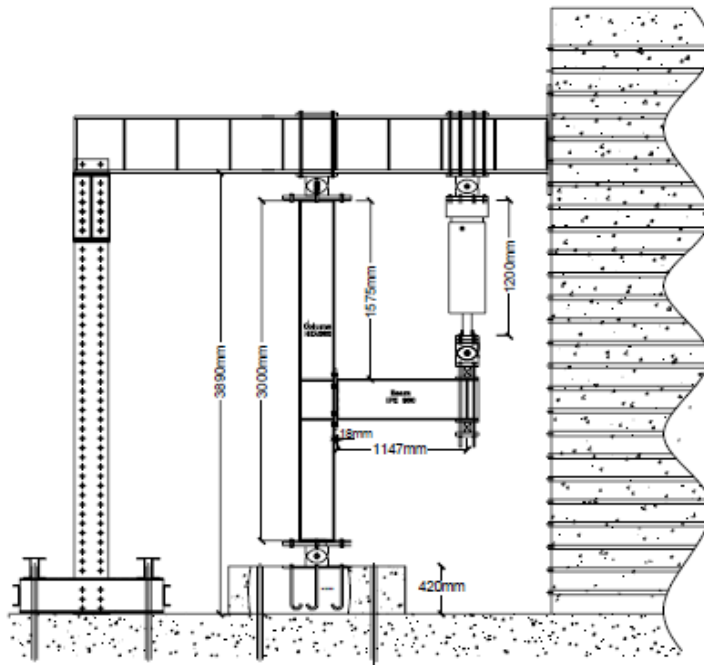


Figure 2.13: Test set-up

As described above, all the specimens belonging to one group have the same geometrical and material properties. They differ only for the loading type. Consequently, the experimental results are presented for each group of specimens.



### 2.1.3.2 Experimental results

#### 2.1.3.2.1 Specimens J-1

As explained in the previous Section, all specimens of the first groups consisted of IPE360 beam section and HEA 320 column sections. The end-plate thickness is 18mm thick, and M24 bolts were used in the connection. Figure 2.14 presents the results of the monotonic test. The measured initial stiffness and the ultimate moment resistance of J-1.1 were approximately equal to 69500 kNm/rad and 419 kNm respectively. Failure of specimen J-1.1 was attributed to the excessive shear deformation of the column web panel, even if the model was further loaded up to the end-plate failure.

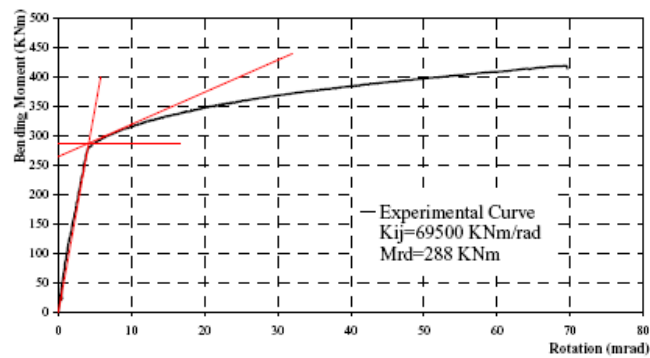


Figure 2.14: Results of the J-1.1 monotonic test

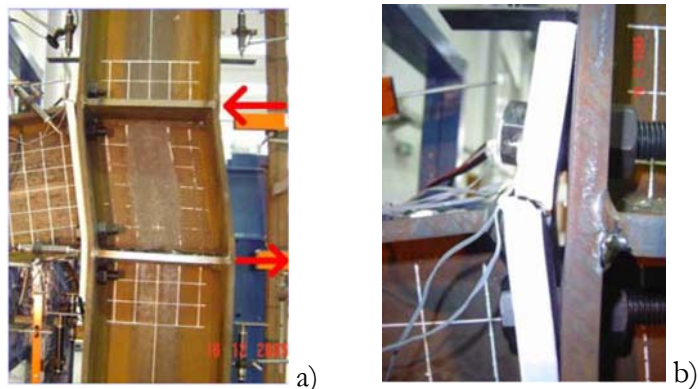


Figure 2.15: a) Final shear deformation of the column web panel and b) end-plate fracture

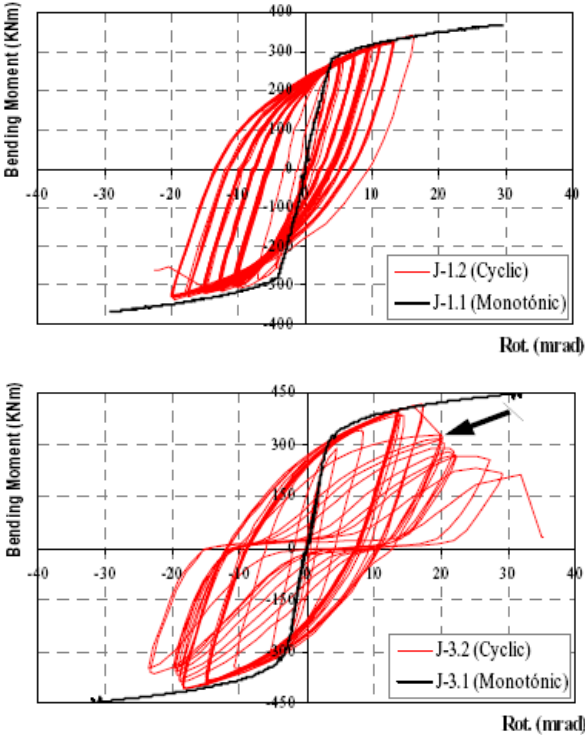


Figure 2.16: M- $\theta$  experimental curves for J-1.2 and J-1.3 tests

Figure 2.16 presents the hysteretic moment-rotation experimental curves, respectively for J-1.2 and J-1.3 tests. Both specimen J-1.2 and J-1.3 exhibited cracking in the extended end plate at the HAZ zone.



Figure 2.17: End-plate failure, column web panel and end-plate deformation for J-1.3

Although the mode of failure for these two tests was the same, J-1.2, tested with lower amplitudes, reached a greater number of cycles before failure. In detail, J-1-2 reached 82 cycles against 22 reached for J-1.3. A great part of the energy was dissipated by the column web panel (80%) and by the extended end-plate.

### 2.1.3.2.2 Specimens J-3

In specimens called J-3 was varied the column section. Differently from the previous group, HEB 320 sections were used as columns. The end-plate layout and thickness, the bolt diameter and the material properties were unchanged.

Figure 2.18 shows the experimental curve of J-3.1. The specimen presented the initial stiffness and the ultimate moment resistance approximately equal to 100000 kNm/rad and 477 kNm respectively. As the monotonic test of the previous group, failure was attributed to the excessive shear deformation of the column web panel. No bolt failure was observed during the test.

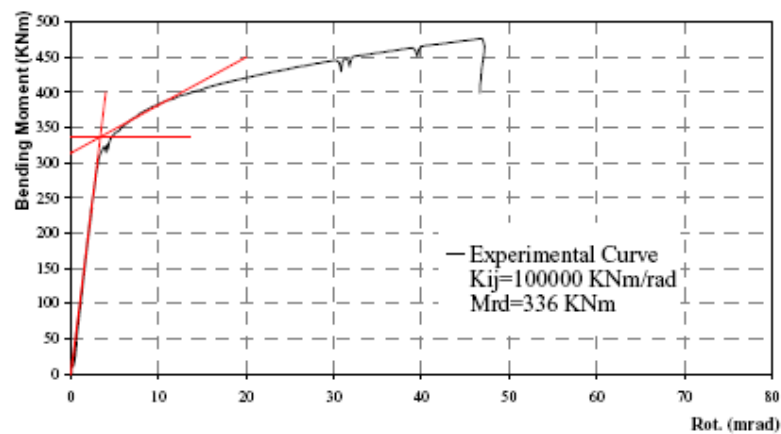


Figure 2.18: Results of the J-3.1 monotonic test

Concerning the cyclic tests, J-3.2 test reached failure after 26 cycles on the extended end-plate as can be seen in Figure 2.19. However the loading was maintained until the bolt below the beam flange ruptured (Figure 2.20). As observed for J-1.3, because of the larger amplitudes, J-3.3 only endured 13 cycles. The great part of the joint deformation

occurred in the column web panel between the transversal stiffeners. Final failure occurred at the HAZ zone on the beam side (Figure 2.21). The ultimate moment resistance was equal to 429.7 kNm. The cyclic tests of this group of specimens were characterized by lower number of cycles to failure than the models from group 1. This was due the stronger column which made the end-plate the component relatively weaker.

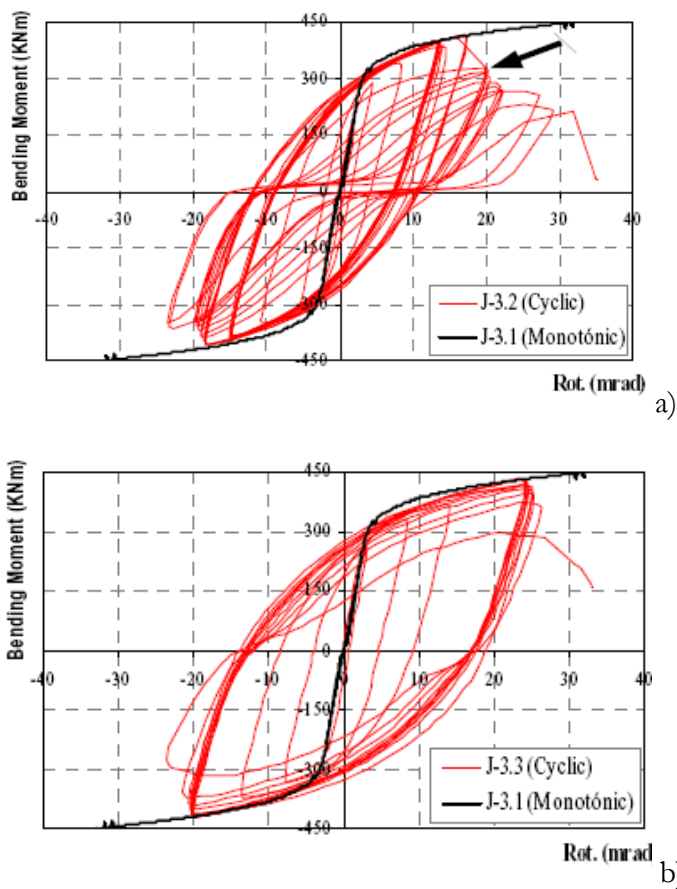


Figure 2.19: Moment-rotation curves for a) J-3.2 and b) J-3.3 tests



Figure 2.20: Column web panel, end-plate and bolt failure for J-3.2



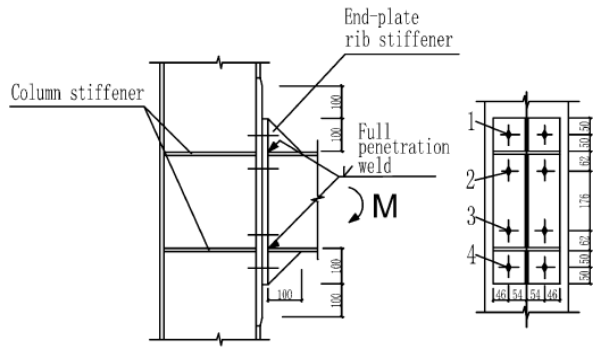
Figure 2.21: Column web panel, beam flange failure and end-plate deformation for J-3.3

#### 2.1.4 Tests by Shi *et al.* (2007 a)

##### 2.1.4.1 Description of specimens and test set up

Five specimens of stiffened and extended beam-to-column end-plate connections were tested under monotonic loads. Starting from a reference configuration (EPC-1), the end-plate thickness and/or the bolt diameter were varied to investigate the influence of these geometrical properties on the joint behaviour.

The beams and columns were built up I-shaped cross-sections and they were identical for all 5 specimens. Figure 2.22 and Table 2.5 show the details of the specimens.



Built-up sections	Column	Beam
Height (mm)	300	300
Flange width (mm)	250	200
Flange thickness (mm)	12	12
Web thickness (mm)	8	8

Figure 2.22: Connection details

Table 2.5: Types and details of specimens

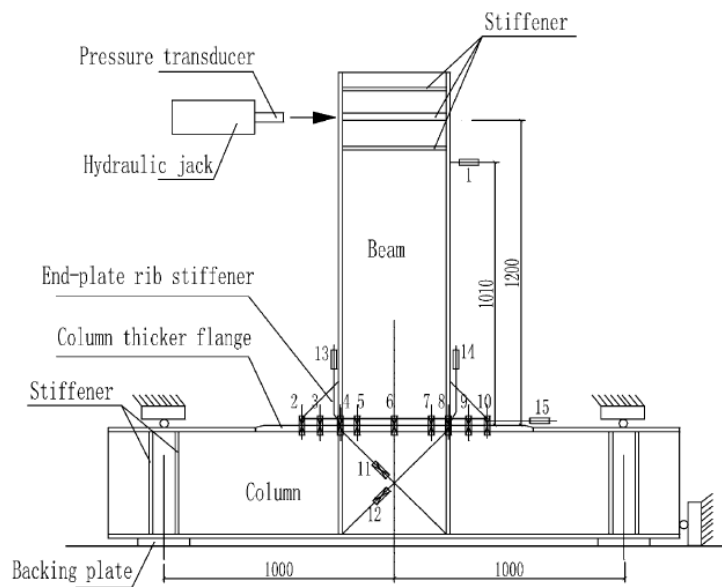
Specimen number	End-plate thickness (mm)	Bolt diameter (mm)
EPC-1	20	20
EPC-2	25	20
EPC-3	20	24
EPC-4	25	24
EPC-5	16	20

The thickness of the column flange was equal to that of the end-plate within the range of 100 mm above and below the extension edge of the end-plate. The column stiffener and end-plate rib stiffeners were 12 mm and 10 mm thick, respectively. Full penetration welds were applied between the end-plate and beam flanges and fillet welds with 8 mm leg size were used to connect end-plates and beam webs.

The steel grade was Q345 (nominal yielding stress  $f_y = 345$  MPa), and the bolts were high strength bolts (Grade 10.9). The material properties are given Table 2.6. They were obtained from tensile tests on coupons and from the bolt certificate of quality.

**Table 2.6: Material properties**

Material	Measured yield strength (MPa)	Measured tensile strength (MPa)
Steel (thickness $\leq 16$ mm)	391	559
Steel (thickness $> 16$ mm)	363	537
Bolts (M20)	995	1160
Bolts (M24)	975	1188

**Figure 2.23: Test setup**

A typical test setup is presented in Figure 2.23. The load was applied by a hydraulic jack at beam tip, at the distance of 1.2 m from the column flange. The out-of-plane deformation of specimens was restrained during tests. Displacements transducers were installed to measure the displacement at the loading point, the relative deformation and the slippage between the end-plate and the column flange and the shearing deformation of the panel zone.

### 2.1.4.2 Experimental results

#### 2.1.4.2.1 Specimen EPC-1

EPC-1 was the reference specimen. As described in the previous section, the end-plate thickness was 20 mm as well as the diameter of the bolts (Table 2.5).

The moment resistance and the initial stiffness of EPC-1 were 343.7 kNm and 52276 kNm/rad respectively. During the test bolt fracture occurred. The moment-rotation curve and the failure mode are given in Figure 2.24 and Figure 2.25 respectively. The joint rotation  $\phi$  includes the shearing rotation  $\phi_s$ , contributed by the panel zone of the column, and the gap rotation  $\phi_{ep}$  which includes the bending deformation of the end-plate and column flange as well as the extension of the bolts.

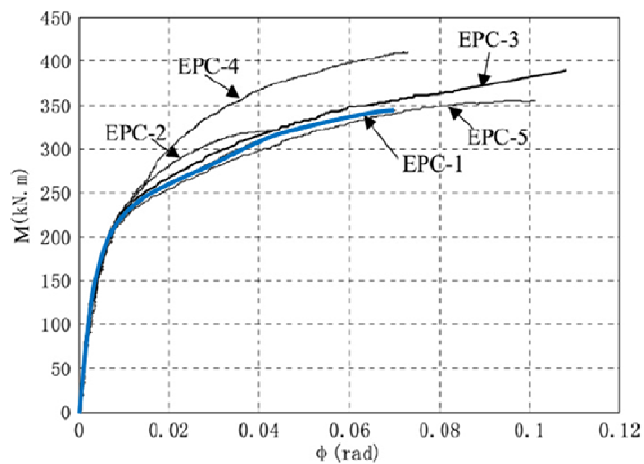


Figure 2.24: Moment-rotation curve for EPC-1



Figure 2.25: Failure mode for EPC-1



The moment-shear rotation and moment-gap rotation curves are given in Figure 2.26 a) and b).

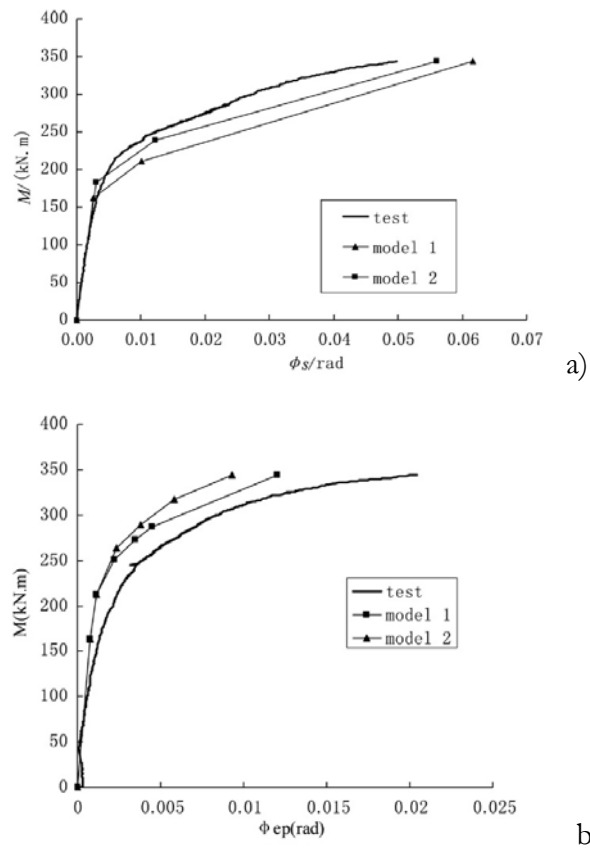


Figure 2.26: a) Moment-shearing rotation and b) moment-gap rotation for EPC-1

As shown, the column web panel was the component which first yielded. The end-plate provided a smaller contribution to the deformation of the joint. The ductility of both the column web panel and the end-plate produced bolt rupture.

#### 2.1.4.2.2 Specimen EPC-2

The specimen EPC-2 had increased the end-plate thickness compared with EPC-1. The end-plate was 25 mm thick while the bolt diameter, as in the previous case, was equal to 20 mm (Table 2.5).

EPC-2 presented a moment resistance and the initial rotational stiffness equal to 322.1 kN and 46094.0 kNm/rad respectively. During the experimental analysis the bolt rupture occurred. The moment-rotation curve, the failure mode, the moment-shear rotation and moment-gap rotation curves are presented in Figure 2.27, Figure 2.28, and Figure 2.29 respectively. As before, the column web panel was the joint component which first yielded (Figure 2.29). The strain hardening which characterized this component produced the connection failure. Because of the thicker end-plate, bolts were the weakest components. The brittle failure was the responsible of the smallest moment resistance and joint rotations measured during this test.

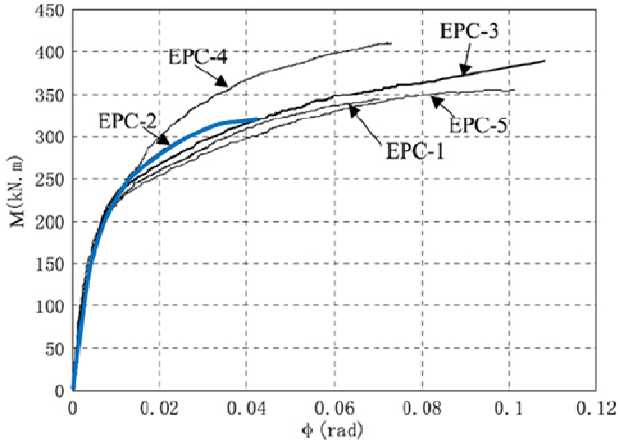


Figure 2.27: Moment-rotation curve for EPC-2



Figure 2.28: Failure mode for EPC-2

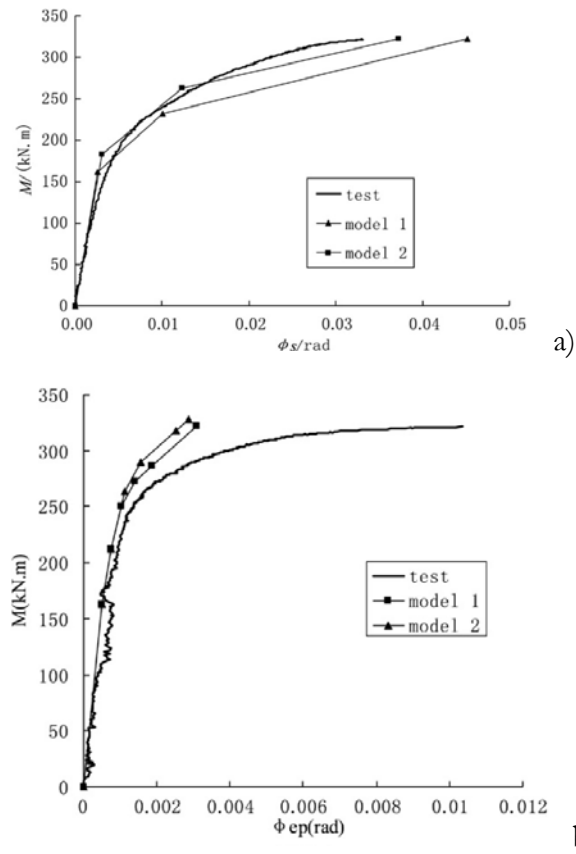


Figure 2.29: a) Moment-shearing rotation and b) moment-gap rotation for EPC-2

### 2.1.4.2.3 Specimen EPC-3

The specimen EPC-3 has increased the bolt diameter compared with EPC-1 (Table 2.5). The measured moment resistance and the initial rotational stiffness were equal to 390.3 kNm and 46066.0 kNm/rad respectively. The specimen was loaded up to the buckling of beam flange and web in compression. Also in this test, the plastic deformations first appeared in the column web panel for shear, but the strain hardening of this component shifted away failure. Stronger bolts permitted great deformation of the end-plate and the development of the beam plastic hinge. The moment-rotation curve, the failure mode, the moment-shear rotation and moment-gap rotation curves are given in Figure 2.30, Figure 2.31 and Figure 2.32 respectively.

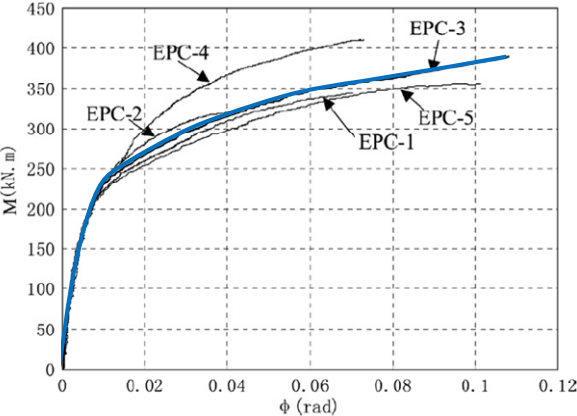


Figure 2.30: Moment-rotation curve for EPC-3



Figure 2.31: Failure mode for EPC-3

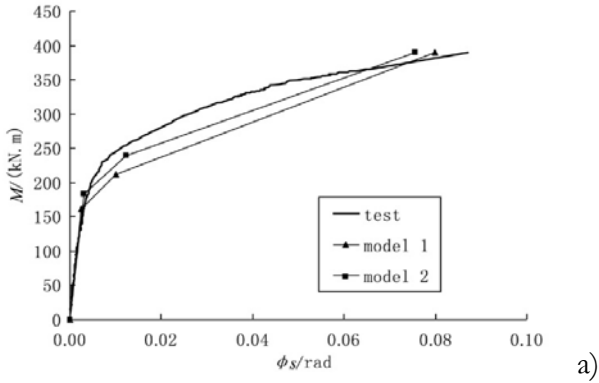
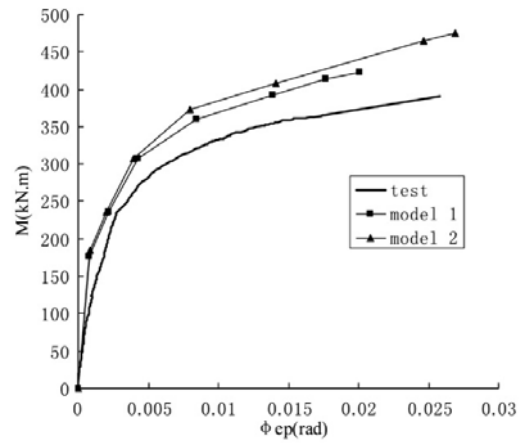


Figure 2.32: a) Moment-shearing rotation and b) moment gap rotation for EPC-3



b)

Figure 2.32: a) Moment-shearing rotation and b) moment gap rotation for EPC-3 (continued)

#### 2.1.4.2.4 Specimen EPC-4

The specimen EPC-4 has increased the end-plate thickness and bolt diameter compared with EPC-1. The end-plate thickness and the bolt diameter were 25 mm and 24 mm respectively.

The moment resistance and the initial stiffness were 410.8 kNm and 47469 kNm/rad, respectively. The moment-rotation curve and the failure mode in Figure 2.33 and Figure 2.34 are shown.

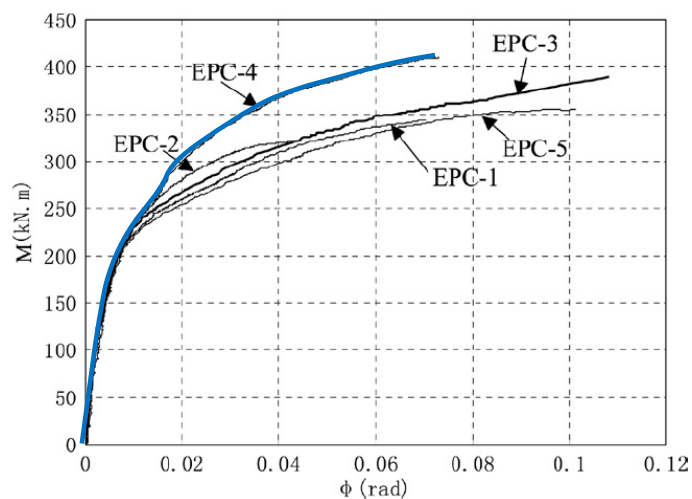


Figure 2.33: Moment rotation curve for EPC-4



Figure 2.34: Failure mode for EPC-4

In Figure 2.35 a) and b) are depicted the moment-shear rotation and moment-gap rotation curves.

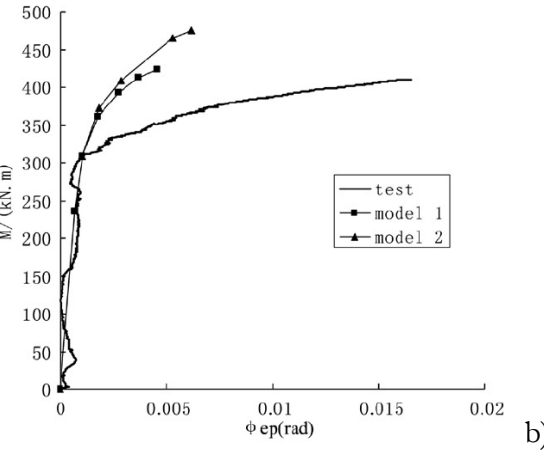
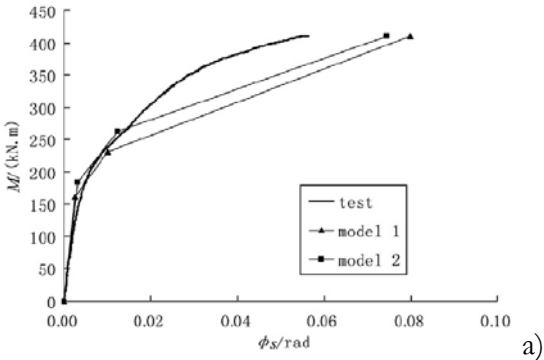


Figure 2.35: a) Moment--shearing rotation (b) and moment – gap rotation for EPC-4

### 2.1.4.2.5 Specimen EPC-5

EPC-5 was created reducing the end-plate thickness up to 16mm. The moment resistance and the measured initial rotational stiffness were equal to 355.4 kNm and 41634 kNm/rad respectively. In case of EPC-5 the failure was due to the bolt rupture and buckling of end-plate rib stiffener in compression. The joint moment-rotation curve and the failure mode are in Figure 2.37 and Figure 2.37 respectively.

During this test, after the yielding of the column web panel for shear, the strain hardening of the panel zone enabled plastic deformation in the connection. The moment resistance increased, and its rotational stiffness

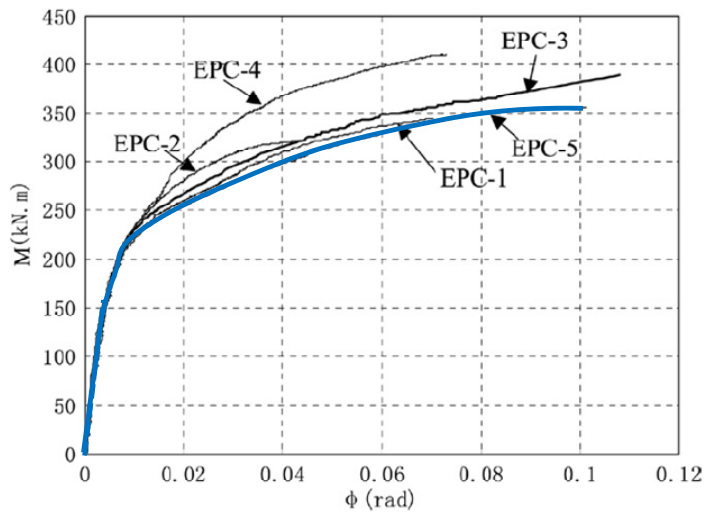


Figure 2.36: Moment-rotation curve for EPC-5



Figure 2.37: Moment-rotation curve and failure mode for EPC-5

was smaller. On the other hand, the specimen showed great ductility and rotation capacity. Moment-shearing rotation and moment-gap rotation are provided in Figure 2.38

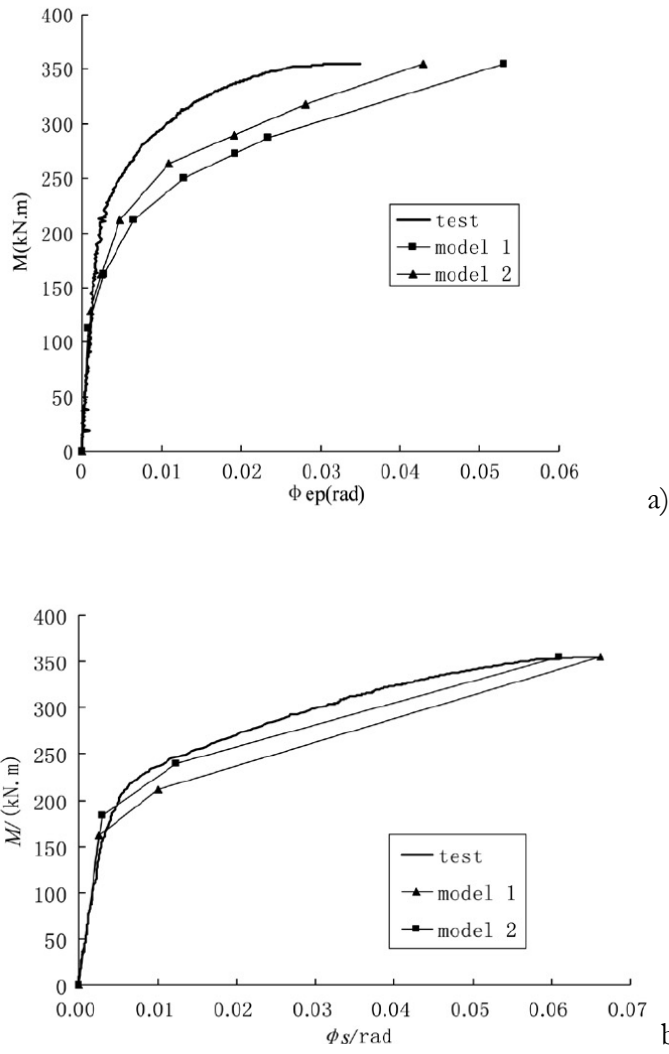


Figure 2.38: a) Moment-shearing rotation and b) moment-gap rotation for EPC-5

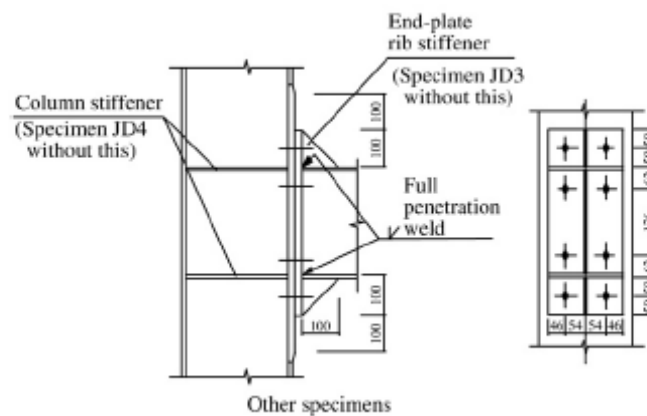


## 2.1.5 Tests by Shi *et al.* (2007 b)

### 2.1.5.1 Description of specimens and test set up

Beam-to-column end-plate connections were tested under cyclic loads, to investigating the influence of end-plate stiffener, column flange stiffener, size of bolts and end-plate thickness on the connection strength and stiffness.

A typical extended end-plate connection is shown in Figure 2.39. The beam and column cross-sections were unchanged for all these specimens. They were built-up I-shaped sections, whose geometrical details are specified in Figure 2.39. The thickness of the column flange was taken as the same as the end-plate within the range of 100 mm above and below the extension edge of the end-plate. The thickness of the column stiffener and end-plate extended stiffener was 12 mm and 10 mm respectively. Full penetration welds were applied between the end-plate and beam flanges and fillet welds with 8 mm leg size were used to connect end-plates and beam webs.



Built-up sections	Column	Beam
Height (mm)	300	300
Flange width (mm)	250	200
Flange thickness (mm)	12	12
Web thickness (mm)	8	8

Figure 2.39: Connection details

In Table 2.7 are the list of specimens and the corresponding geometrical details.

**Table 2.7: Details of specimens**

Specimen	End-plate thickness (mm)	Bolt diameter (mm)	Column stiffener	End-plate stiffener
JD2	20	20	Yes	Yes
JD3	20	20	Yes	No
JD4	20	20	No	Yes
JD5	25	20	Yes	Yes
JD6	20	24	Yes	Yes
JD7	25	24	Yes	Yes
JD8	16	20	Yes	Yes

The steel was grade Q345 (nominal yielding strength  $f_y = 345$  MPa) and the bolts were high strength friction-grip bolts of grade 10.9 (nominal tensile strength  $f_u = 1000$  MPa). The actual material properties of the steel and bolts obtained from tensile tests on coupons and from the bolt certificate of quality are given in Table 2.8.

**Table 2.8: Material properties**

Material	Measured yield strength (MPa)	Measured tensile strength (MPa)
Steel (thickness $\leq 16$ mm)	409.0	536.6
Steel (thickness $> 16$ mm)	372.6	537
Bolts (M20)	995	1160
Bolts (M24)	975	1188

Figure 2.40 shows the test set up. The cyclic loads were applied by the hydraulic jack at the end of the beam at a distance from the end-plate equal to 1200 mm, according to a load/displacement control method.

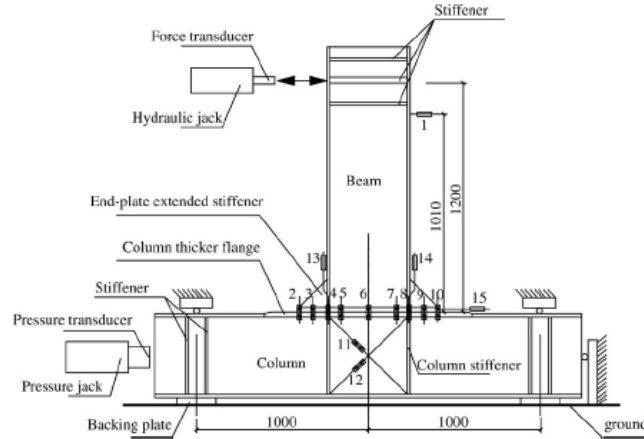


Figure 2.40: Test setup and loading arrangement

Before the specimen yields, load control was adopted and the yielding load was applied by three incremental steps, and for each incremental load step the number of cycles was only one. After yielding appeared, the load was applied by controlling the displacement at the end of the beam. Each displacement incremental step was 10 mm, and for each displacement incremental step the number of cycles were two. The out-of-plane deformation of the specimens was restrained during tests.

### 2.1.5.2 Experimental results

#### 2.1.5.2.1 Specimen JD2

The specimen JD2 has a 20 mm thick end-plate. It is reinforced by a 10 mm rib stiffener. Eight bolts, 20 mm diameter are used in the connection (Table 2.7). In the previous section are the geometrical details of the beam and column.

The experimental results are presented in terms of moment capacity, rotational stiffness, and hysteretic curve. The joint rotation  $\phi$  is defined as the relative rotation of the centrelines of the beam flanges at the beam end, it includes the shearing rotation  $\phi_s$  contributed by the panel zone of the column, and the gap rotation  $\phi_{ep}$ , caused by the relative deformation between the end-plate and the column flange including the bending deformation of the end-plate and column flange as well as the extension of the bolts. The moment–rotation hysteretic curves and the failure mode of JD2 are in Figure 2.41.

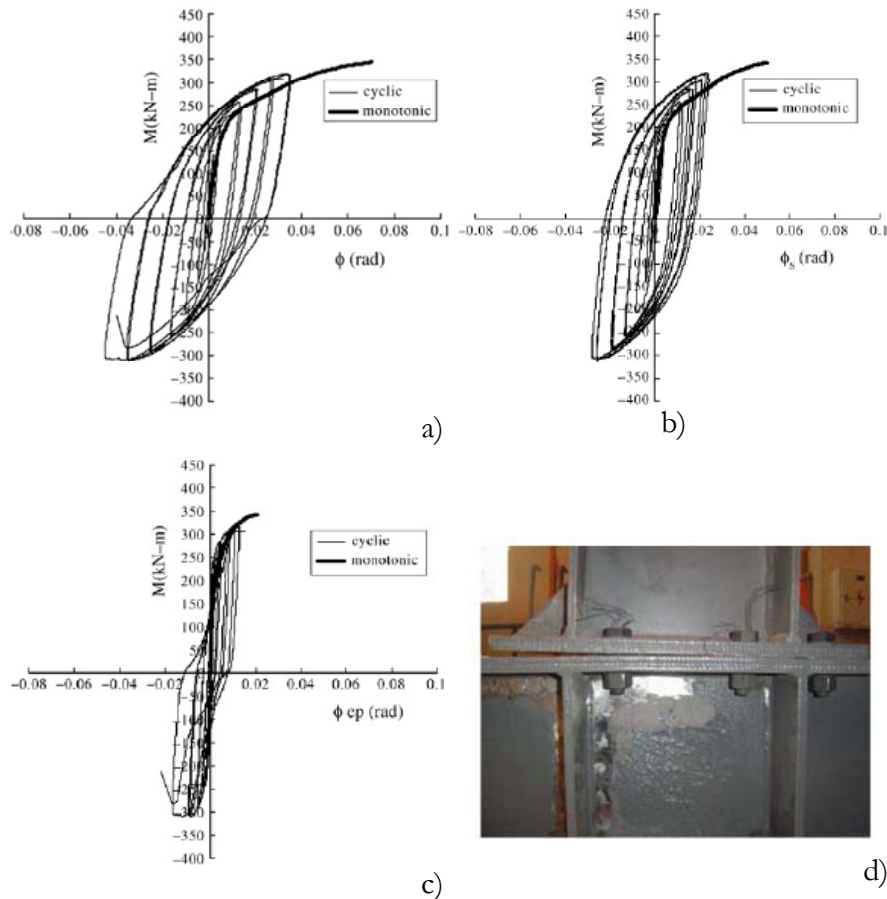


Figure 2.41: a) Moment–rotation curve, b) moment–shearing rotation curve, c) moment–gap rotation curve and d) failure mode for JD2

The maximum moment and initial rotational stiffness of JD2 are 320.1 kNm and 28011 kNm/rad respectively.

The column web panel was the component which first yielded. The end-plate provided a smaller contribution to the deformation of the joint. In fact, because of the end-plate stiffener, the gap rotation did not develop very much; therefore the joint rotation mainly came from the shearing rotation. The great ductility of the column web panel produced bolt rupture.

### 2.1.5.2.2 Specimen JD3

The specimen JD3 had the same geometrical details of JD2, but differently from it, the end-plate was not reinforced by the rib stiffener (Table 2.7).

According to the test results the maximum bending moment was 288 kNm and the initial stiffness was 32547 kNm/rad. Failure was attributed to bolt rupture and end-plate yielding. In Figure 2.42 are the hysteretic curves and the failure mechanism of JD3.

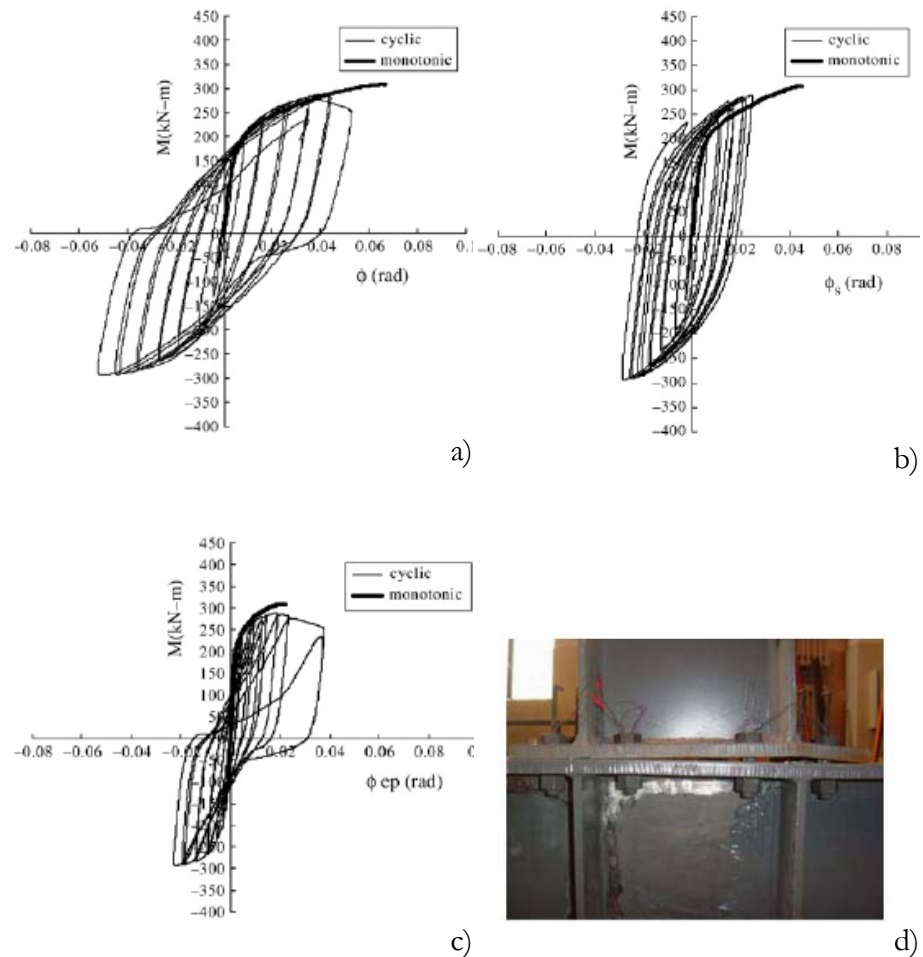


Figure 2.42: a) Moment-rotation curve, b) moment-shearing rotation curve, c) moment-gap rotation curve and d) failure mode for JD3

Because of the deformation of the un-stiffened end-plate, the gap rotation developed. However the joint rotation mainly came from both the column web panel shearing deformations.

### 2.1.5.2.3 Specimen JD4

The specimen JD4 is free of the column web transversal stiffeners. The end-plate thickness and the diameter of bolts the end-plate reinforcing were the same of the reference specimen. The experimental results are presented in Figure 2.43. The moment capacity and the initial stiffness of JD4 were 289.40 kNm and 3535810 kNm/rad respectively.

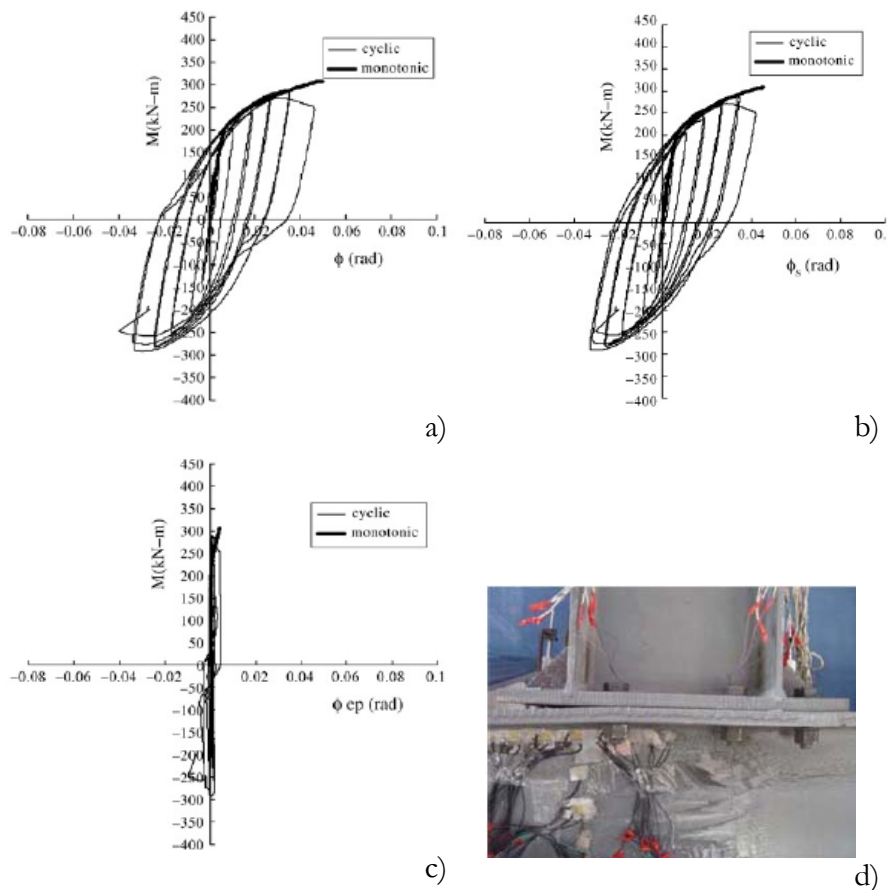


Figure 2.43: a) Moment–rotation, b) Moment–shearing rotation curve, c) Moment–gap rotation curve and d) failure mode for JD4

During the experimental test, the buckling of the column web panel in compression and the bolt rupture were observed.

#### 2.1.5.2.4 Specimen JD5

In JD5 the end-plate thickness was increased up to 25mm. The other connection details are the same of JD2 (Table 2.7.). The moment capacity and the initial stiffness of JD5 were 331.4 kNm and 57248 kNm/rad respectively. During the experimental test, the bolt rupture was attained (Figure 2.44). Because of the thicker end-plate, bolts became the weakest components.

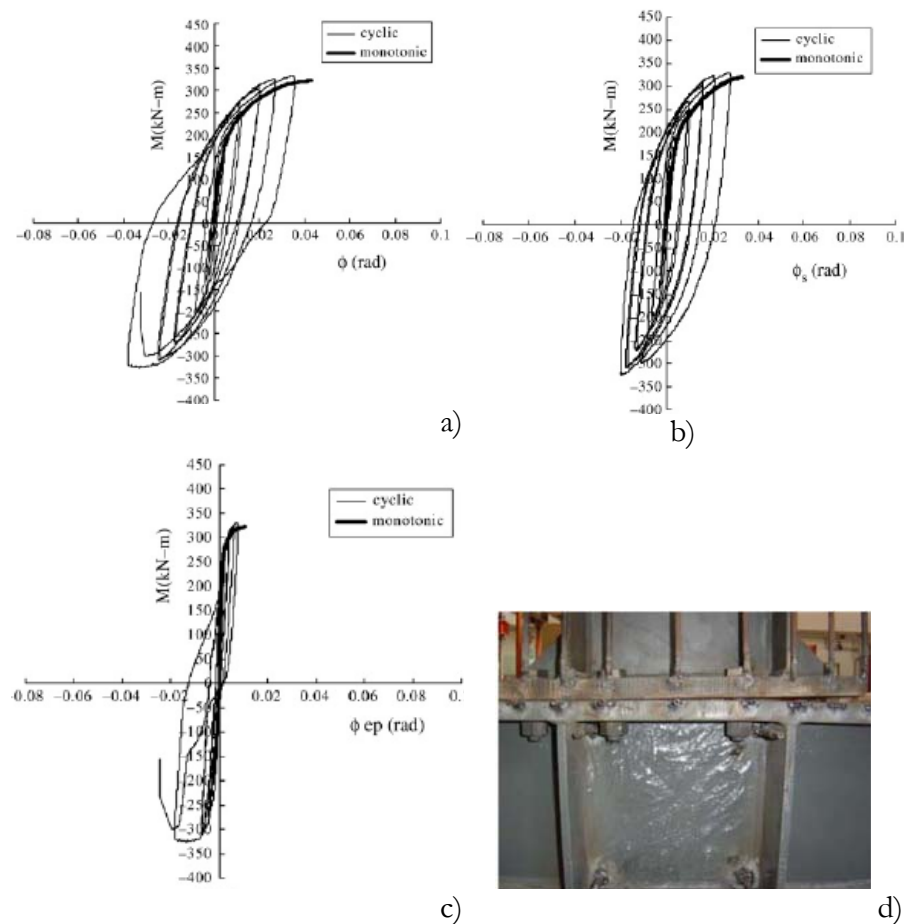


Figure 2.44: a) Moment–rotation curve, b) Moment–shearing rotation b) curve, c) Moment–gap rotation curve and d) failure mode for JD5

As shown in Figure 2.44, the column web panel is the first component which first yields. Thanks to the strain hardening of this component failure occurred in the connection.

### 2.1.5.2.5 Specimen JD6

In JD6 the bolt diameter was increased up to 24mm. The other geometrical properties were unchanged. The experimental results are presented in terms of moment capacity, rotational stiffness, and hysteretic curves in Figure 2.45. The moment resistance and the initial stiffness were 336.2 kNm and 41310 kNm/rad respectively.

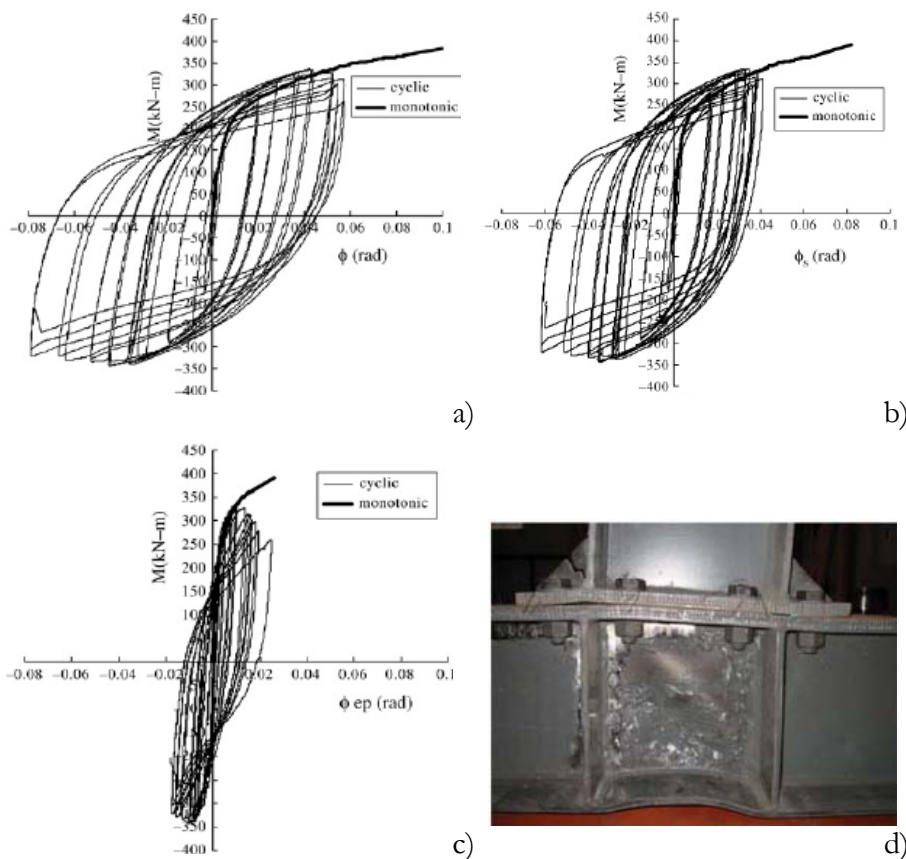


Figure 2.45: a) Moment–rotation curve, b) Moment–shearing rotation curve, c) Moment–gap rotation curve and d) failure mode for JD6



Stronger bolts permitted great deformations in the column web panel up to the shearing buckling of the panel zone. The large deformation lead to end-plate stiffener fracture, and beam flange weld crack.

#### 2.1.5.2.6 Specimen JD7

In case of JD7, both the end-plate thickness and the bolt diameter were increased. The end-plate thickness was chosen equal 25 mm, while the diameter of bolts was 24 mm.

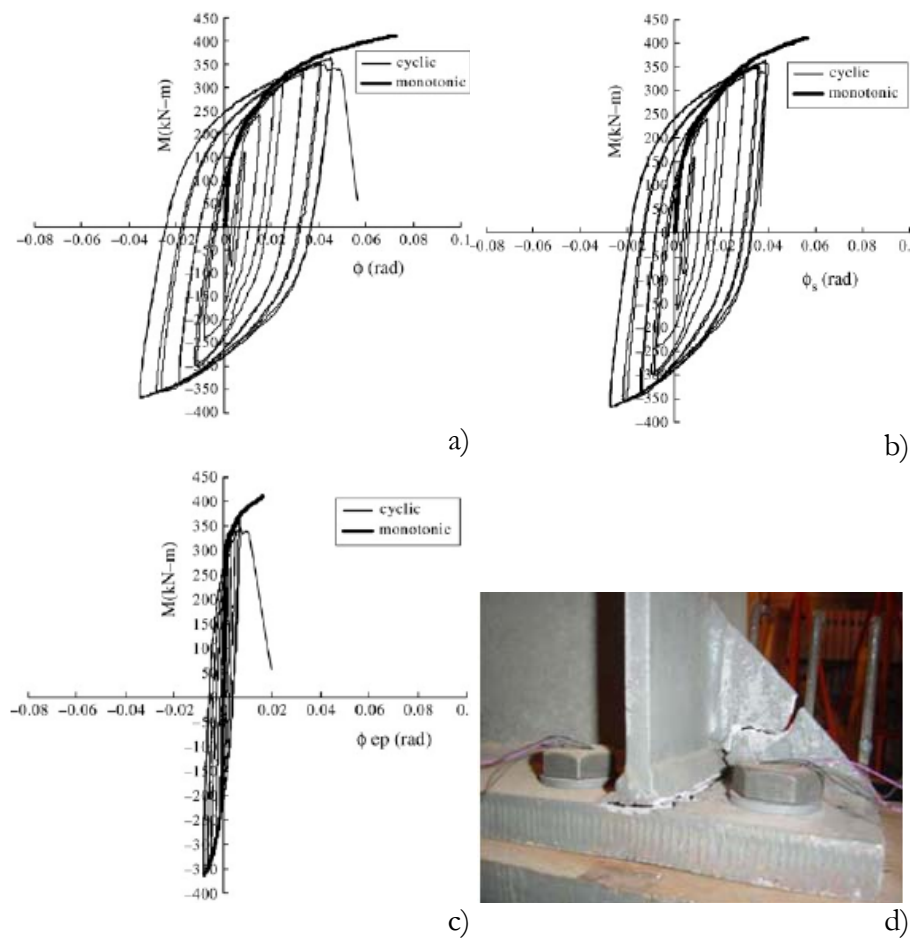


Figure 2.46: a) Moment-rotation curve b) Moment-shearing rotation curve, c) Moment-gap rotation curve and d) failure mode for JD7

The experimental results are presented in Figure 2.46. The configuration JD7 presented the moment capacity and the initial stiffness equal to 364.0 kNm and 52502 kNm/rad, respectively. As for previous cases, the great panel zone ductility shifted failure in the connection. Beam welds crack and the rib stiffener fracture were observed.

### 2.1.5.2.7 Specimen JD8

In JD8 was reduced the end-plate thickness compared to JD2 (Table 2.7). The experimental results of JD8 are presented in Figure 2.47.

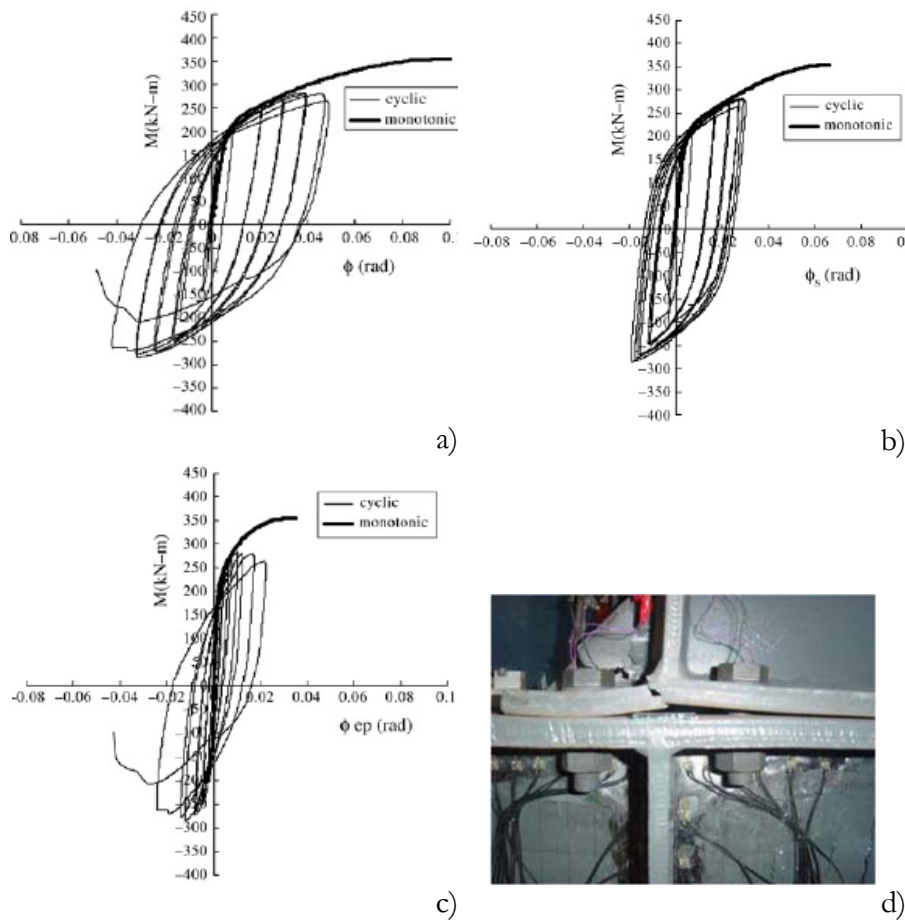


Figure 2.47: a) Moment-rotation curve, b) moment-shearing rotation curve, c) moment-gap rotation curve and d) failure mode for JD8

The specimen exhibited the maximum moment resistance of 331.4 kNm. Its initial rotational stiffness was 57248 kNm/rad. Because of the end-plate thickness, great deformations in the connection were measured. Also in this case, the column web offered great contribution to the joint rotation. Its rotation capacity shifted failure in the connection. The rib stiffener fracture, the end-plate rupture and the bolt failure were observed.

## 2.2 FLUSH END-PLATE CONNECTIONS

### 2.2.1 Tests by Broderick and Thomson (2002)

#### 2.2.1.1 Description of specimens and test setup

Eight flush end-plate connection specimens were tested under cyclic and monotonic loads. The specimens consisted of a 1 m length of universal beam section connected to a 1 m length of universal column section. The column section used was 203×203×86 kg/m UC, while two different beam sizes were employed. The end-plate was welded to the end of the beam with full strength continuous welds and bolted to the column flange. The details of the joints were varied to produce the three T-Stub failure modes: complete flange yielding (mode 1); flange yielding and bolt failure (mode 2); bolt failure (mode 3). Table 2.9 shows the details of each test specimen.

**Table 2.9: Specimen details**

Specimen	Beam size [kg/m UB]	End-plate thickness [mm]	Bolt grade	Bolt diameter [mm]	Loading type
EP1	254×102×22	8	8.8	20	Cyclic
EP2	254×102×22	12	8.8	20	Cyclic
EP3	254×146×37	12	8.8	20	Monotonic
EP4	254×146×37	12	8.8	20	Cyclic
EP5	254×146×37	12	10.9	20	Cyclic
EP6	254×146×37	20	8.8	16	Monotonic
EP7	254×146×37	20	8.8	16	Cyclic
EP8	254×146×37	20	8.8	16	Cyclic

Authors did not provide any information about the steel grade of beams columns and end-plate. The missing details were found in Authors' previous work (STESSA 2000), according to which the steel grade was S275 (nominal yielding stress  $f_y = 275$  MPa). Bolt class 8.8 (nominal tensile strength  $f_u = 800$  MPa) or 10.9 (nominal tensile strength  $f_u = 1000$  MPa) were employed in the connections. The full experimental set-up is presented in Figure 2.48. Six of the eight specimens were tested under cyclic loads, in accordance with the ECCS short testing procedure. The remaining two specimens were subjected to monotonic loads in which the displacement was increased until failure occurred, or the equipment limits were reached.

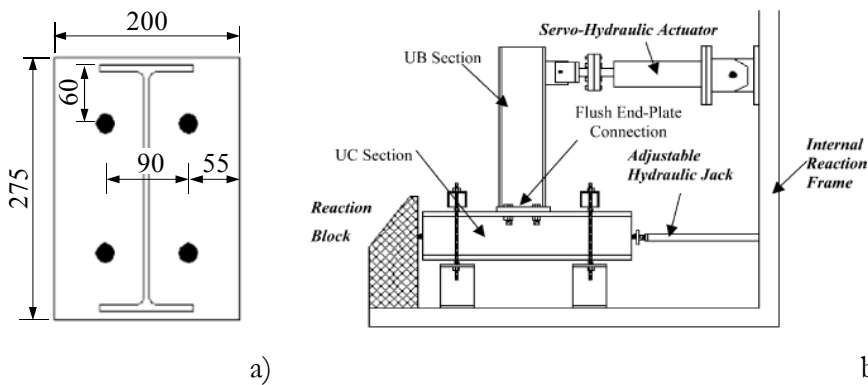


Figure 2.48: a) Connection details and b) test setup

As described in Table 2.9, EP3 and EP4 as well as EP6, EP7 and EP8 have the same geometrical and material properties. Consequently, the experimental results are presented for each group of specimens.

### 2.2.1.2 Experimental results

#### 2.2.1.2.1 Specimen EP1

EP1 consisted of 254×102×22 UB beam section and 203×203×86 kg/m UC column section. End-plate 8 mm thick and 20 mm bolt diameter were employed in the connection. Because of the experimental equipment limitations, the specimen did not reach the failure. However the post-experimental observation revealed the tearing of the

end-plate on the underside of the end-plate along the beam flange and web weld lines. Consequently failure mode 1 was reasonable for EP1. The moment capacity and the initial stiffness of EP were equal to 53.92 kNm and 8.50 kNm/mrad respectively. The moment was calculated multiplying the measured load at the actuator by the distance between the point of application of the load and the end-plate, which was about 750 mm (Figure 2.48).

### 2.2.1.2.2 Specimen EP2

EP2 compared with EP1 had a thicker end-plate. It was equal to 12 mm (Table 2.9). Figure 2.49 shows the specimen moment-rotations curve, where the moment was calculated, as in the previous case, multiplying the measured load at the actuator by the distance between the point of application of the load and the end-plate (750 mm). The joint rotation was determined removing the elastic displacement of the beam from the actuator displacement.

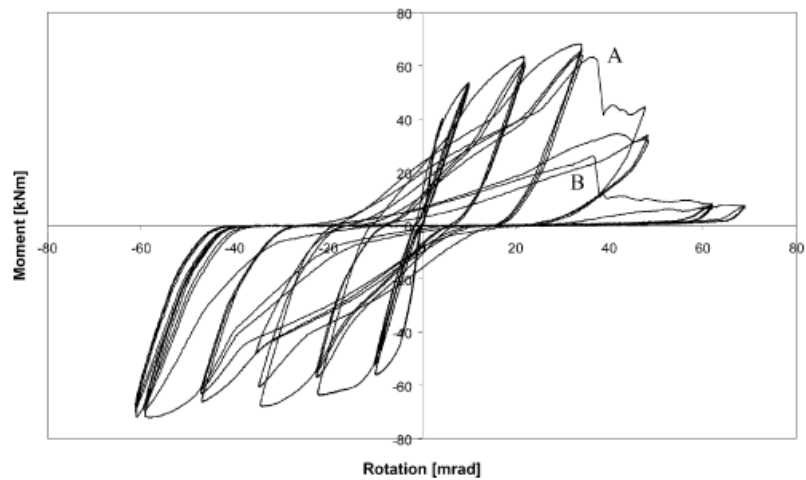


Figure 2.49: Moment rotation curve for EP2

According to the experimental test, the moment resistance and the initial stiffness were 67.70 kNm and 10.21 kNm/mrad respectively.

As shown in Figure 2.49, the specimen reached its full moment capacity only in one loading direction. During the test the threads of bolts in the tension stripped suddenly (A and B in Figure 2.49). This connection failed according to mode 2.

**2.2.1.2.3 Specimens EP3 and EP4**

EP3 and EP4 differed from EP1 for the beam section and the end-plate thickness. A 254×146×37 kg/m UB beam section and a 12 mm thick end-plate were used. EP3 was tested under monotonic load, while EP4 was examined under cyclic load (Table 2.9). Figure 2.50 and Figure 2.51 represent the moment rotation curve of EP3 and EP4 respectively, while

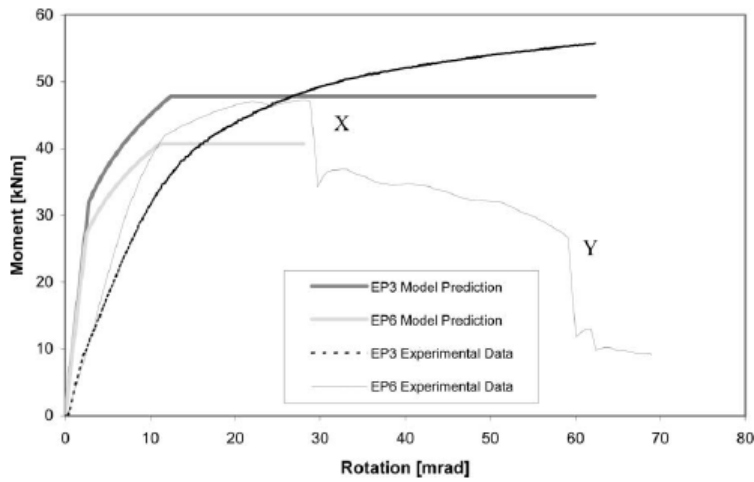


Figure 2.50: Moment rotation curve for EP3

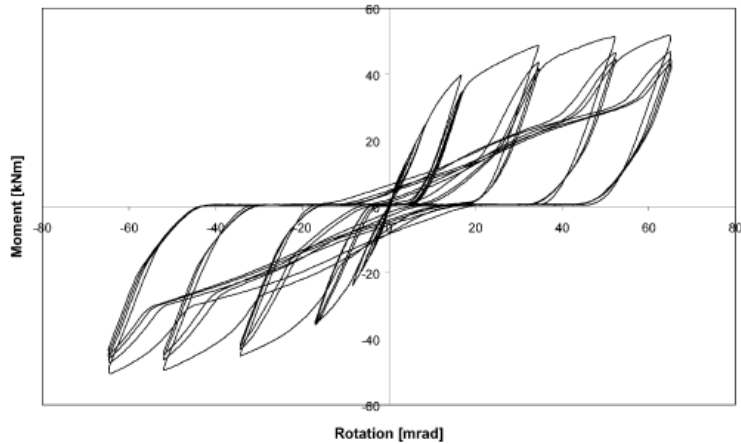


Figure 2.51: Moment rotation curve for EP4

Table 2.10 summarizes the experimental results of EP3 and EP4. As expected, the specimen tested monotonically exhibited a higher resistance. A great difference in the initial stiffness (about 50%) was measured. In both cases, the ultimate failure mechanisms were not observed because the experimental equipment limitations were reached. Anyway, post-experimental observation indicated for these specimens the failure mode 1.

**Table 2.10: Experimental moment-rotation characteristics of EP3 and EP4**

Specimen	Initial stiffness kNm/mrad)	Ultimate moment (kNm)	Ultimate failure mode
EP3	7.34	55.81	1
EP4	3.55	51.86	1

#### **2.2.1.2.4 Specimen EP5**

EP5 was identical to EP3 and EP4 except for the bolt grade which was 10.9 (nominal ultimate stress  $f_u=1000$  MPa) (Table 2.9). The details of specimen EP5 were selected to increase the ductility of the joint. Post-experimental examination of the connection showed that the improved bolt grade prevented the stripping of the bolt threads and the specimen could fail according to mode 1. The moment capacity and initial stiffness of EP5 were 41.21 kNm and 5.53 kNm/mrad, respectively. Unfortunately, due to problems that arose during the execution of this test, the recorded moment levels were not considered completely reliable.

#### **2.2.1.2.5 Specimens EP6, EP7 and EP8**

EP6, EP7 and EP8 consisted of 254×146×37 UB beam and 203×203×86 kg/m UC column. They were designed to fail in mode 3 manner. To this aim, an end-plate 20 mm thick and 16 mm bolt diameter were chosen for these specimens. EP6 was tested under monotonic load, while EP7 and EP8 were investigated under cyclic loads (Table 2.9).

The moment and rotation curve of EP6 is shown in Figure 2.52. During the test, the fracture of the two bolts in tension was observed (point X and Y). The same failure characterized EP7 whose moment–rotation relationship is shown in Figure 2.53. As shown, the moment–rotation curve appeared were nearly identical for both positive and negative

rotations. This symmetry was due to the large thickness of the end-plate which ensured that both pairs of bolts undergone very similar axial deformations. A similar behaviour was displayed by specimen EP8 as shown in Figure 2.54. The ultimate moment capacity of the connection was slightly higher. This difference was probably due to the material differences.

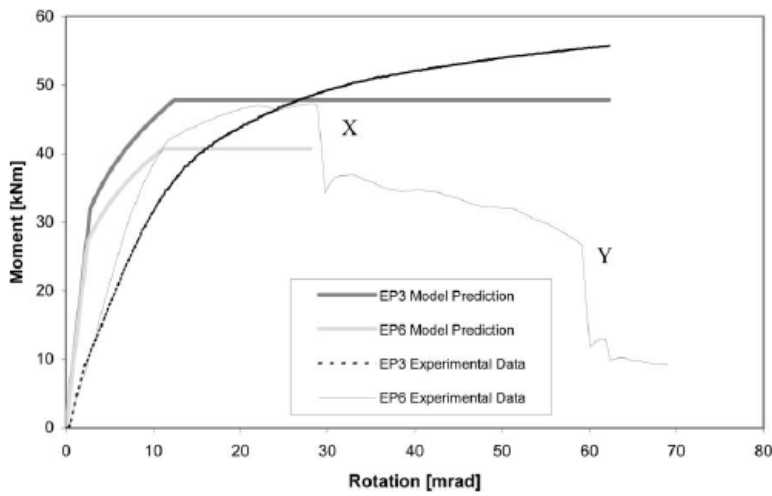


Figure 2.52: Moment rotation curve for EP6

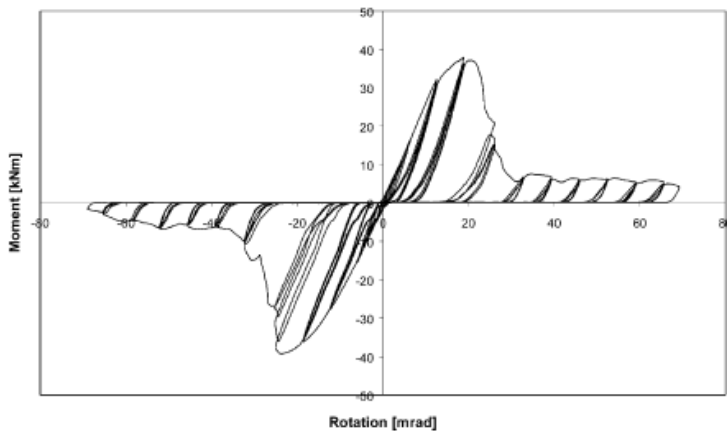


Figure 2.53: Moment rotation curve for EP7



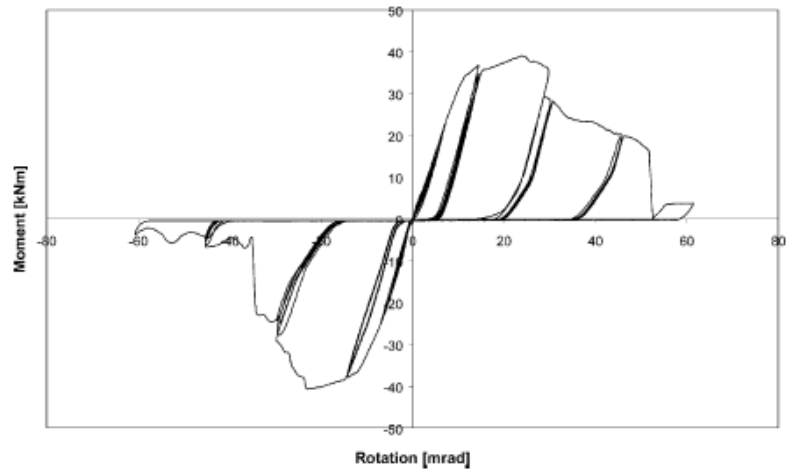


Figure 2.54: Moment rotation curve for EP8

The Authors noted a gradual stripping of the bolts in the cyclic loading tests (specimens EP7 and EP8) in contrast with the sudden fracture observed in the monotonic test (EP6). The experimental moment-rotation characteristics of EP6, EP7 and EP8 are summarized in Table 2.11.

Table 2.11: Experimental moment-rotation characteristics

Specimen	Initial stiffness kNm/mrad	Ultimate moment (kNm)	Observed failure mode
EP6	3.81	47.25	3
EP7	3.20	39.90	3
EP8	2.75	37.76	3

## 2.2.2 Test by da Silva *et al.* (2004)

### 2.2.2.1 Description of specimens and test setup

FE1 belonged to an experimental campaign aimed at studying the behaviour of beam-to-column joints subjected to a combination of bending moments and axial forces. FE1 consisted of an IPE240 beam section beam connected to a HEB240 column section by means 15 mm

end-plate and M20 bolts. The steel grade was S275 (nominal yielding stress  $f_y = 275$  MPa), while the bolt class was 10.9 (nominal ultimate stress  $f_u=1000$  MPa).

The joint arrangement is presented in Figure 2.55, while in Table 2.12 are the results of tensile tests on coupons extracted from the beams columns and end-plate.

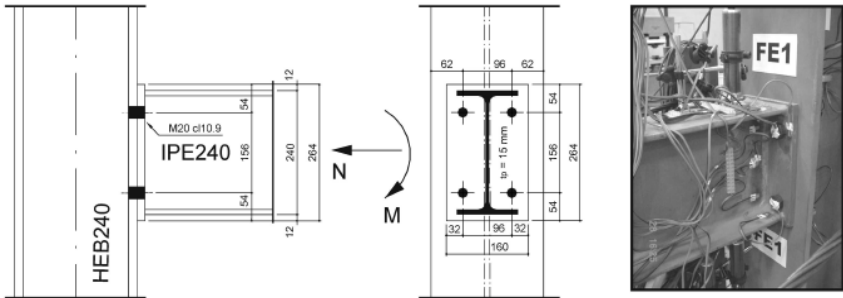


Figure 2.55: Layout of the joint

Table 2.12: Steel mechanical properties

Coupon location	Yield stress (MPa)	Tensile strength (MPa)
Beam web	366.45	460.36
Beam flange	365.83	444.52
Column web	392.63	491.82
Column flange	344.92	410.06
End-plate	365.39	504.45

FE1 was tested under monotonic loads. The test-set up is presented in Figure 2.56. The columns were simply-supported at both ends. The loads were applied by the hydraulic actuator at the end of the beam at a distance from the column flange equal to 1000 mm.

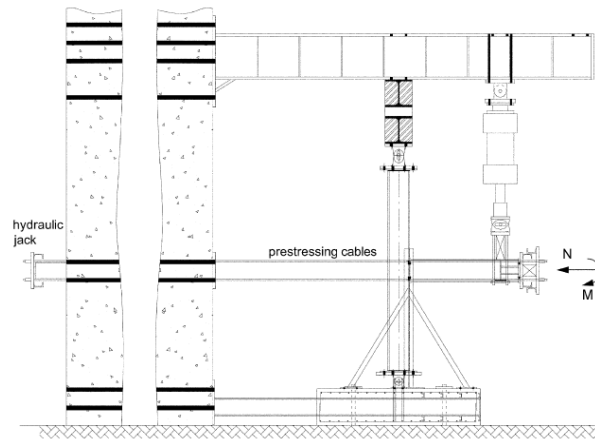


Figure 2.56: Experimental test setup

### 2.2.2.2 Experimental results

The experimental moment-rotation curve of FE1 is presented in Figure 2.57. The specimen exhibited great deformations in the end-plate. The bending moment resistance and the initial rotational stiffness were 68.4 kNm and 7244 kNm/rad respectively.

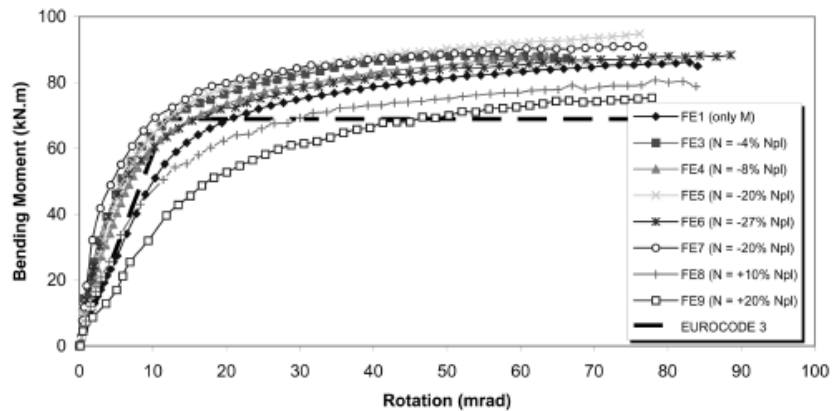


Figure 2.57: Moment - rotation curve for FE1

## 2.2.3 Tests by Broderick and Thomson (2005)

### 2.2.3.1 Description of specimens and test setup

Eight beam-to-column flush end-plate connection specimens were tested under monotonic and cyclic loading conditions. The specimens consisted of one meter length of universal column section attached to one meter length of universal beam section. A  $254 \times 146 \times 37$  kg/m UB section was used for all specimens, but the UC was varied. All beams were connected to the end-plate by full strength continuous fillet welds.

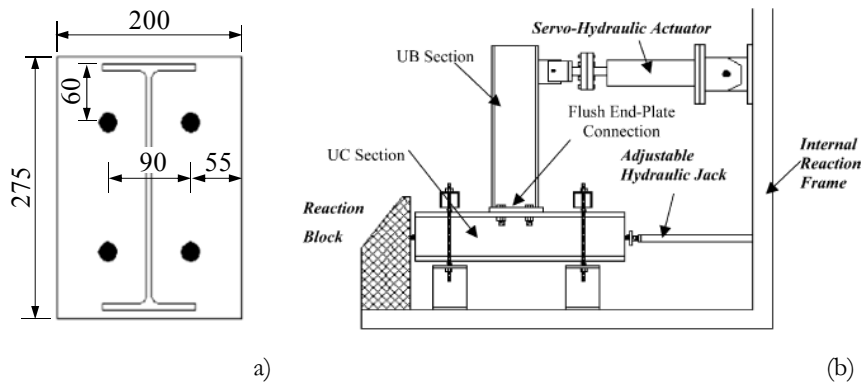


Figure 2.58: a) Connection details and b) test setup

Table 2.13: Details of specimens

Specimen	Column size (kg/m UC)	End-plate thickness (mm)	Bolt grade	Bolt diameter (mm)	Loading type
FP1	203×203×86	10	8.8	20	M/LAC
FP2	203×203×86	10	8.8	20	IAC
FP3	203×203×86	15	8.8	20	IAC
FP4	203×203×86	15	8.8	20	IAC
FP5	203×203×52	12	8.8	20	M/LAC
FP6	203×203×52	12	8.8	20	IAC
FP7	203×203×86	12	10.9	20	M/LAC
FP8	203×203×86	12	10.9	20	IAC

M/LAC: Monotonic/Large amplitude Cyclic  
IAC: Increasing Amplitude Cyclic

Specimen details are given in Figure 2.58 a) and Table 2.13. These were chosen to ensure failure according to mode 1 and mode 2 of the T-stub. Grade S275 steel (nominal yielding stress  $f_y = 275$  MPa) was used for all specimens, while the bolts used are either grade 8.8 (nominal tensile strength  $f_u = 800$  MPa) or 10.9 (nominal tensile strength  $f_u = 1000$  MPa). The experimental set-up is shown in Figure 2.58 b). Beam tip displacements were applied by a servo-hydraulic actuator with hinged bearings at both ends. Sliding and rigid body rotations of specimens were prevented during the test.

### 2.2.3.2 Experimental results

#### 2.2.3.2.1 Specimens FP1 and FP2

FP1 and FP2 consisted of a 254×146×37kg/m UB beam section and 203×203×86 kg/m UC column section. End-plate 10 mm thick and 20 mm bolt diameter of grade 8.8 were employed in the connection. Table 2.14 presents the observed experimental results in term of initial stiffness, moment capacities and failure mode. Specimens FP1 and FP2 were designed to ensure the complete yielding of the end-plate. They behaved as designed.

**Table 2.14: Experimental results of FP1 and FP2**

Specimen	Initial stiffness kN/mrad)	Ultimate moment (kNm)	Ultimate failure mode
FP1	2.21	49.78	1
FP2	3.48	44.02	1

Figure 2.59 presents the moment-rotation curve of FP1. Test FP1 consisted of large amplitude cyclic test. The monotonic moment-rotation relationship may be determined from the initial quarter cycle. Moments were calculated as the product of the measured actuator load and times the vertical distance between the actuator displacement and the end-plate. Joint rotations were determined from the actuator displacement, removing the elastic displacement of the beam.

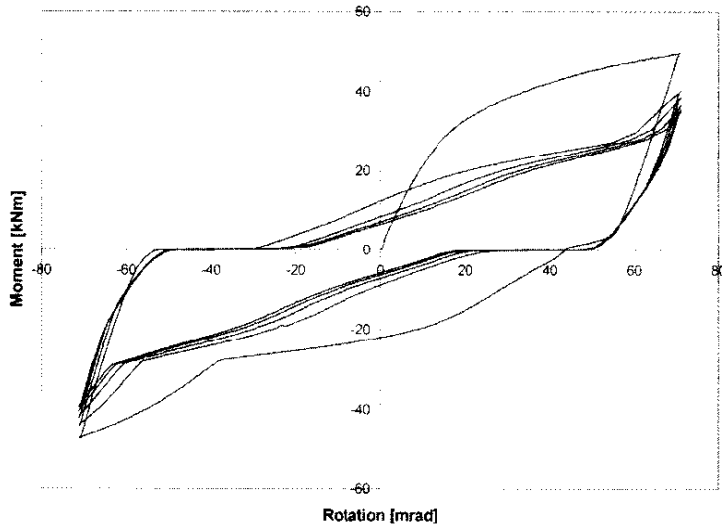


Figure 2.59: Moment rotation curve for FP1

Concerning FP2 (Figure 2.60), it was tested under an increasing cyclic amplitude. The hysteresis curve displayed a large degree of pinching. The ultimate resistance was 13% lower than FP1. This difference was due to the cyclic loading imposed. In contrast the initial stiffness was higher than that of FP1.

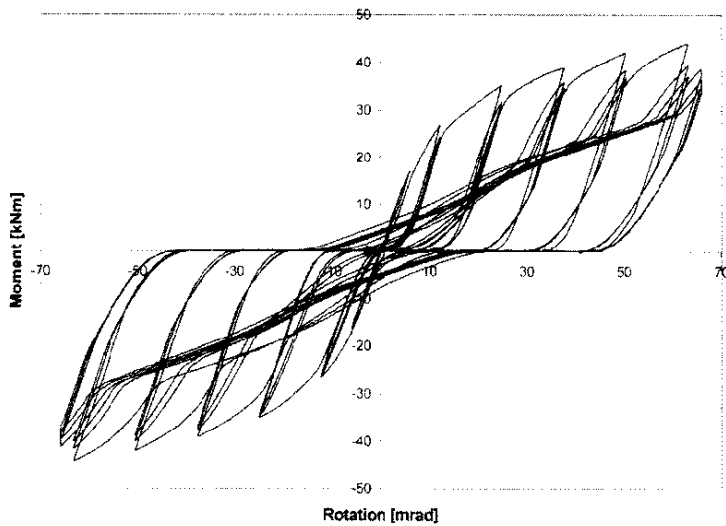


Figure 2.60: Moment rotation curve for FP2

### 2.2.3.2.2 Specimens FP3 and FP4

FP3 and FP4 differed from previous configuration for the end-plate thickness. As reported in Table 2.13, it was increased up to 15mm. Table 2.15 contains the observed experimental results. These specimens were designed to fail according mode 2, which was observed during the test. In both tests, yielding of the end-plate is followed by sudden stripping of the bolts.

**Table 2.15: Experimental results of FP3 and FP4**

Specimen	Initial stiffness kN/mrad	Ultimate moment (kNm)	Ultimate failure mode
FP3	3.13	59.06	2
FP4	3.55	59.36	2

FP3 and FP4 were tested under increasing cyclic loads, but the tests differ for the loading rate. FP3 was tested at higher loading rate (0.025 Hz), while specimen FP4 was tested at the same rate of the other specimens (0.01 Hz). The failure was not influenced by the increased rate, failing the specimens both according to mode 2.

Figure 2.61 presents the FP3 moment-rotation curve. As shown a sudden reduction of the resistance was noted. It was due the failure of one bolt in tension. The second bolt failed in the subsequent displacement increment. Post-test inspection identified yield circular pattern around the bolts and yield patterns extending along each side of the beam web line.

In case of the FP4 (Figure 2.62), the situation is very similar but both bolts in one row failed at the same displacement cycle. Post-experimental examination highlighted significant bolt elongations which justify the pinching of the hysteretic loops.

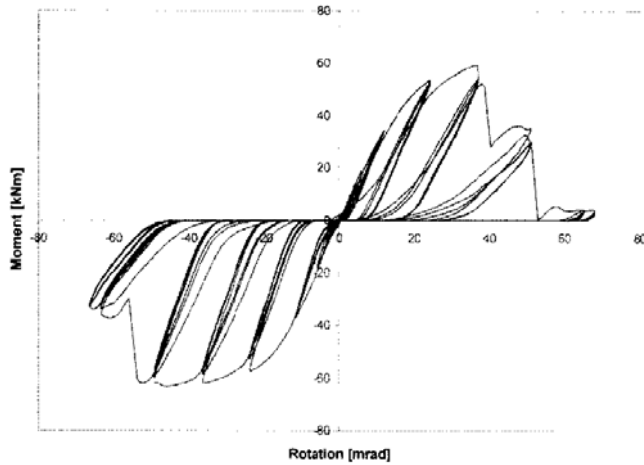


Figure 2.61: Moment rotation curve for FP3

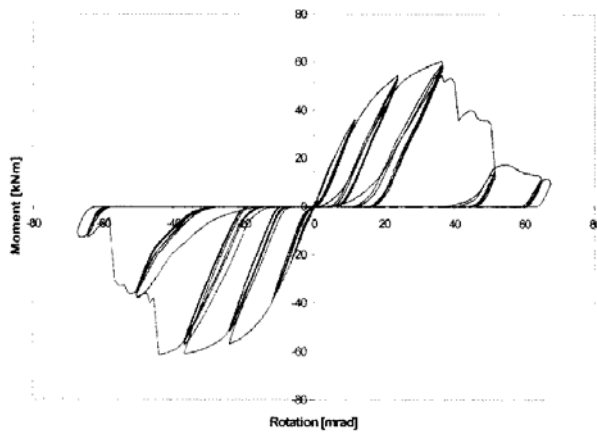


Figure 2.62: Moment rotation curve for FP4

### 2.2.3.2.3 Specimens FP5 and FP6

FP5 and FP6, compared with FP1 and FP2, presented a smaller column section and an increased end-plate thickness. As shown in Table 2.13, a  $203 \times 203 \times 52$  UC column and an end-plate, 15mm thick, were used. Table 2.16 contains the observed experimental results. FP5 and FP6 were designed to display yielding of the column flange and bolt failure. This failure mechanism was observed in both tests.



Table 2.16: Experimental results of FP5 and FP6

Specimen	Initial stiffness (kN/mrad)	Ultimate moment (kNm)	Ultimate failure mode
FP5	3.51	50.13	2
FP6	3.16	45.76	2

The moment-rotation relationship of FP5 is given in Figure 2.63. FP5 was subjected to large amplitude test cycle.

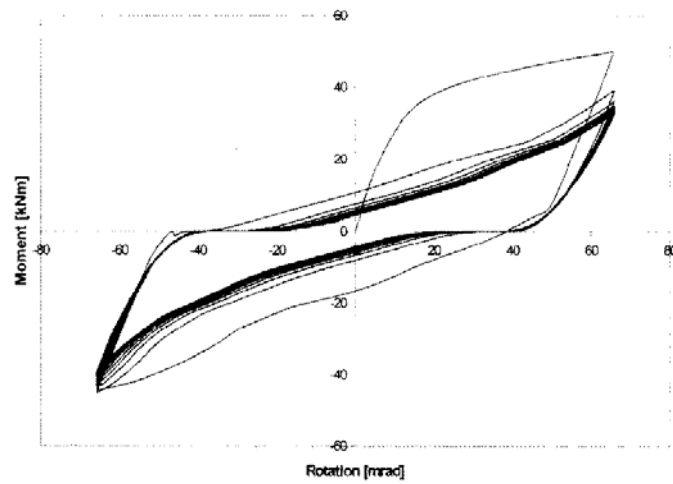


Figure 2.63: Moment rotation curve for FP5

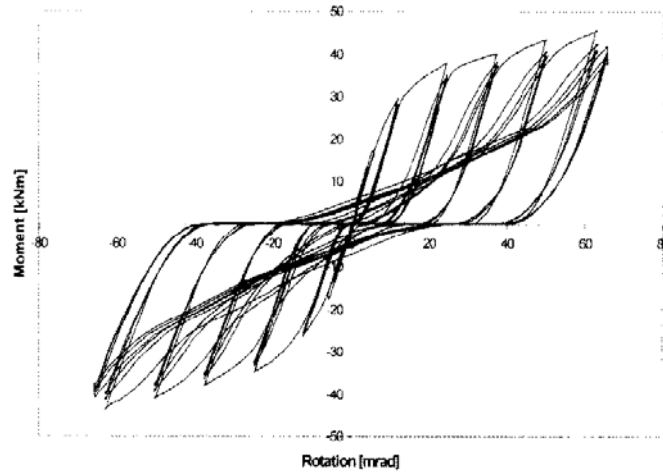


Figure 2.64: Moment rotation curve for FP6

Post-experimental examination of bolts did not identify significant yielding of bolts in contrast to mode 2 failure. Conversely, in case of specimen FP6 (Figure 2.64), subjected to increasing amplitude loading, post-experimental examination revealed significant elongation and thread stripping. The initial stiffness and ultimate moment resistance of FP6 were about 10% lower than those of specimen FP5.

#### 2.2.3.2.4 Specimens FP7 and FP8

FP7 and FP8 had increased end-plate thickness and bolt grade. The end-plate thickness was equal 12 mm, while the bolt grade was 10.9. They were designed to display mode 1 failures. Although neither specimen reached its ultimate rotation during the imposed loading, observation during the test and post-experimental examinations confirmed that the joint behaved in the mode for which they were designed.

The moment-rotation curves of FP7 and FP8 are given in Figure 2.65 and Figure 2.66 respectively. The initial stiffness of FP8 is slightly lower than that of FP7, while the ultimate moments are 10-15% lower (Table 2.17). As observed with the other tests on specimen pairs, the resistance in the monotonic first quarter-cycle of the constant amplitude tests is greater than that achieved during the increasing amplitude test.

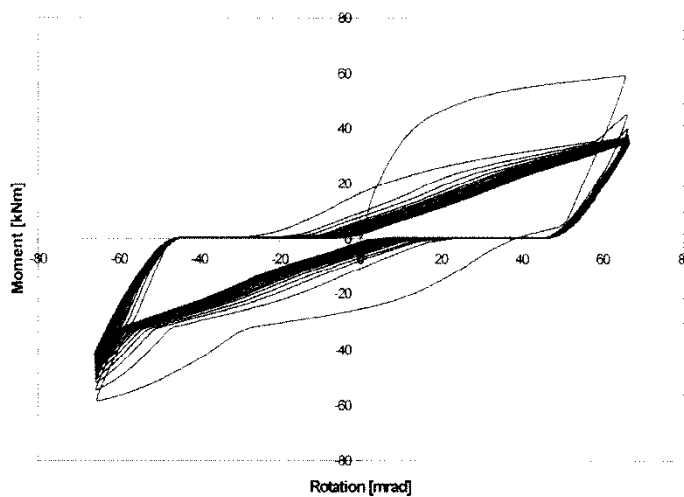


Figure 2.65: Moment rotation curve for FP7

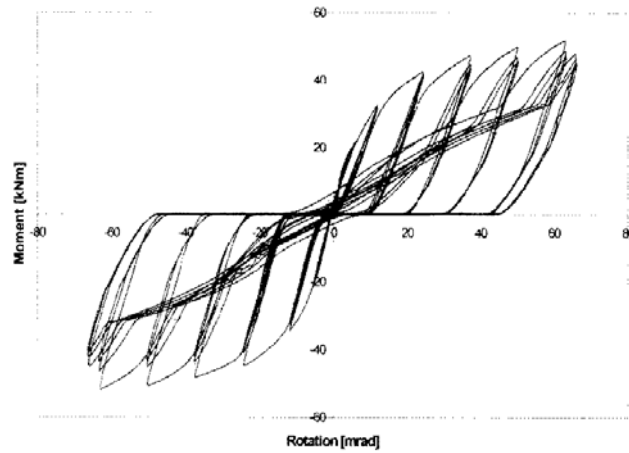


Figure 2.66: Moment rotation curve for FP8

Table 2.17: Experimental results of FP7 and FP8

Specimen	Initial stiffness kN/mrad)	Ultimate moment (kNm)	Ultimate failure mode
FP7	4.72	59.11	1
FP8	4.23	51.91	1

## 2.2.4 Test by Shi *et al.* (2007)

### 2.2.4.1 Description of specimen and test setup

The specimen JD1 consisted of a 2 m column length connected to approximately 1.5 m beam length. The beam and column cross-sections were built-up I-shaped sections. The beam was connected to the beam by 20 mm end-plate and bolt diameter. The details of the cross sections are shown in Figure 2.67.

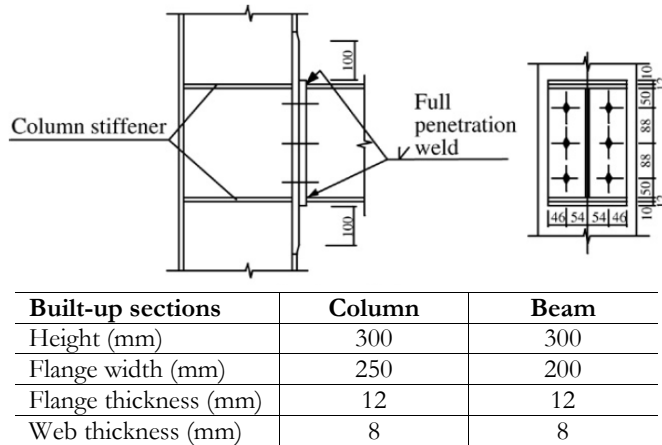


Figure 2.67: Details of specimen JD1

The steel was grade Q345 (nominal yielding strength  $f_y = 345$  MPa) and the bolts are high strength friction-grip bolts, grade 10.9 (ultimate tensile stress  $f_u = 1000$  MPa). The actual material properties of the steel and bolts obtained from tensile tests on coupons and from the bolt certificate of quality are provided in Table 2.18.

Table 2.18: Material properties

Material	Measured yield strength (MPa)	Measured tensile strength (MPa)
Steel (thickness $\leq 16$ mm)	409.0	536.6
Steel (thickness $> 16$ mm)	372.6	537
Bolts (M20)	995	1160
Bolts (M24)	975	1188

The specimen was tested under cyclic loads according to a load/displacement control method. Before the specimen yields, load control was adopted and the yielding load was applied by three incremental steps, and for each incremental load step the number of cycles was only one. After yielding appeared, the load was applied by controlling the displacement at the end of the beam. Each displacement incremental step was 10 mm, and for each displacement incremental step the number of cycles were two.

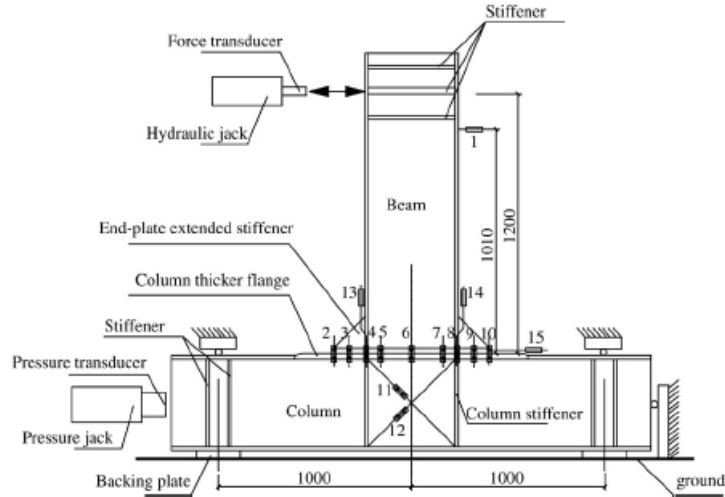


Figure 2.68: Test setup

#### 2.2.4.2 Experimental results

The experimental results are presented in terms of moment capacity, rotational stiffness, and hysteretic curve. The joint rotation  $\phi$  includes the shearing rotation  $\phi_s$  contributed by the panel zone of the column, and the gap rotation  $\phi_{ep}$ , caused by the relative deformation between the end-plate and the column flange including the bending deformation of the end-plate and column flange as well as the extension of the bolts.

During the test, the two bolts in tension ruptured suddenly at the same time. The maximum moment and the initial rotational stiffness were 164.5. kNm and 28011 kNm/rad respectively.

The moment–rotation, moment–shearing rotation and moment–gap rotation hysteretic curves of JD1 are given in Figure 2.69. As shown, the hysteretic loops of the joint and those of the connection presented a noticeable pinch (Figure 2.69 a) and c)) and the deformation of the column panel zone was not remarkable (Figure 2.69 b)).

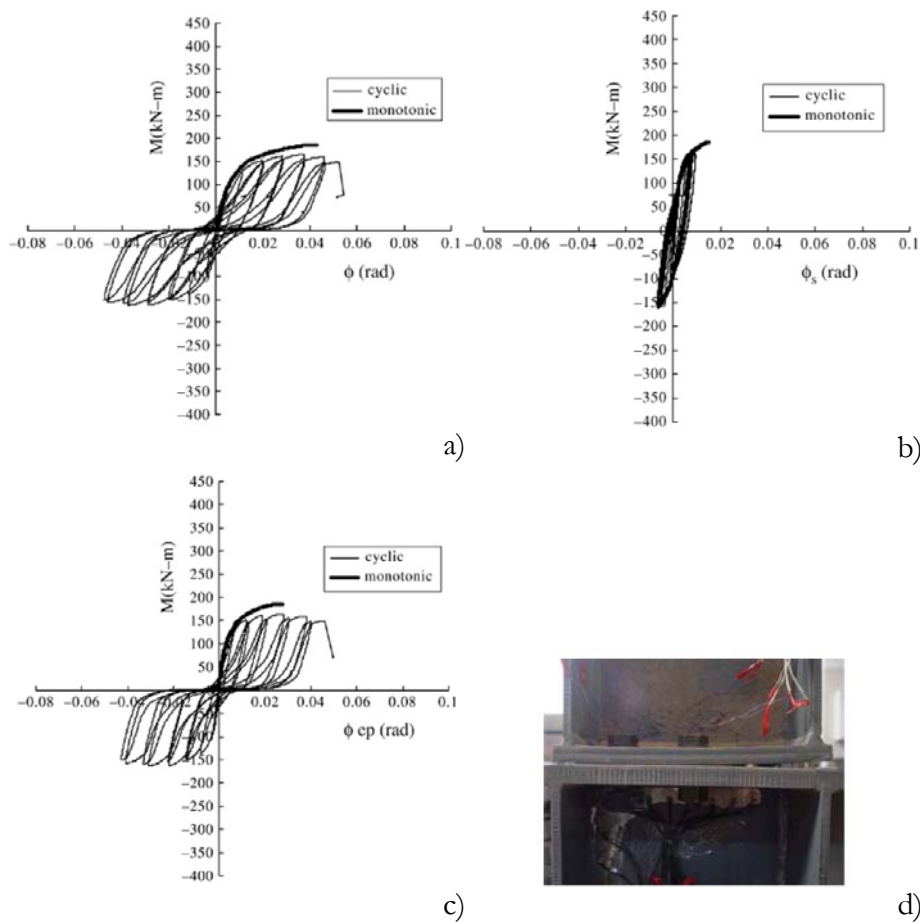


Figure 2.69: a) Moment–rotation curve, b) moment–shearing rotation curve, c) moment–gap rotation curve and d) failure mode for JD1

### 2.3 DIGITAL DATABASE

Using a digital data management system (Microsoft Access), the collected data have been stored in such a way to organize and manage in a flexible manner the data. The digital database shall permit to retrieve any desired information from the experimental data ensemble. Figure 2.70 shows a picture of the digital database system. It consists of three section called Input, Output and Report. The first section allows to add and to modify

data. The output section permits to view the collected data. Finally, by the last section report of collected data can be created.

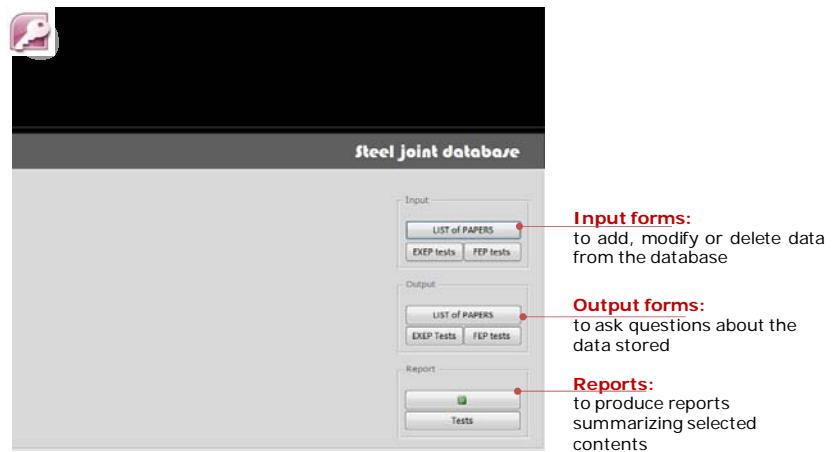


Figure 2.70: The steel joints digital database

As depicted in Figure 2.71, the database is composed by: tables, form reports and several facilities (queries and macros) to add, modify, delete and retrieve data.

All data are stored into a table, in which each row corresponds to one specific paper and contains all the relevant information.

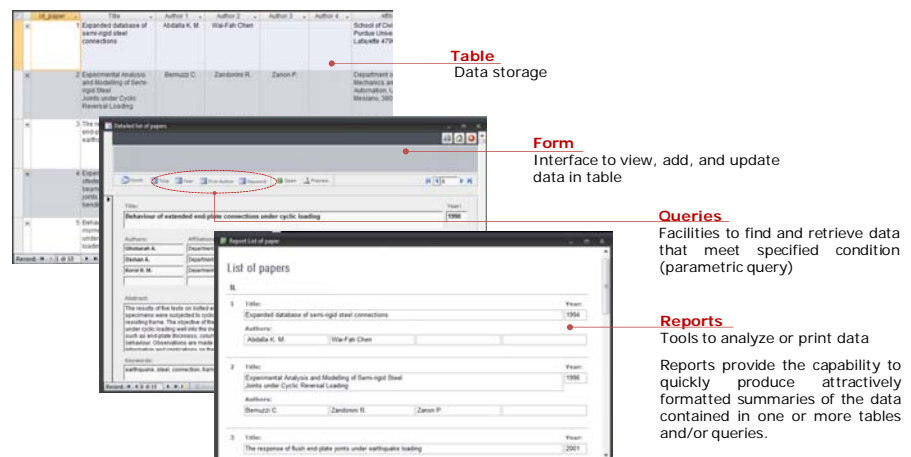


Figure 2.71: The digital database structure

The user-friendly interface allows users to enter or modify information in a graphical form. In addition queries allow users to find and retrieve data that meets specified condition (e.g. paper title, author, any keyword, etc.).

Thanks to reports, formatted summaries of the data contained in one or more tables and/or selected by queries could be created.

A simple summary of data (Figure 2.71), as well as a detailed description of each test can be produced. Example of the detailed report is in Appendix A. For each collected test the title of paper, the Authors and the source are specified. Geometrical details available as well as the material properties of systems are reported. Main experimental results are described. More specifically, information concerning the type of test, the loading protocol, the moment-rotation or force-displacement curves, the failure mode and joint capacities are included.



### 3 THEORETICAL PREDICTIONS AND COMPARISON WITH EXPERIMENTAL RESULTS

In this Chapter, the details of the component method applications are presented. Subsequently, the results of the comparison between the theoretical predictions and the experimental results are shown. Classification of each joint, in term of strength and stiffness, according to Eurocodes, is also provided. Finally, first observations about the influence of connection details on the joint structural properties are given.

#### 3.1 EXTENDED END-PLATE CONNECTIONS

##### 3.1.1 Tests by Ghobarah *et al.* (1990)

###### 3.1.1.1 Specimen A-1

Table 3.1 summarizes the results of calculations according to the Eurocode 3 component method. The components are grouped according to tension, compression and shear loading. For each component, the third and the fourth columns give the strength ( $F_R$ ) and the stiffness coefficient ( $k_i$ ), respectively. The last (fifth) column gives the resisting bending moment ( $M_R$ ) evaluated as the product of the weakest component strength ( $F_R$ ) times the internal lever arm, per each loading type (tension, compression, shear). The theoretical predictions consider nominal geometrical properties of the beam, column and end-plate. Since the details of the end-plate layout were not available, a likely configuration was assumed for it. About the material modelling, the expected value of the yield equal to 394.38 MPa was used for the column, end-plate and column reinforcing plates. It considers a material

overstrength factor of 1.3 (ANSI/AISC 341-10, 2010). The ultimate stress of 1000 MPa was used for the bolts. Actual values obtained from tensile test on coupon were considered for the beam. In detail the yield stresses equal to 310.9 MPa and 315.7 MPa were adopted for the beam flange and the column web respectively. It is noted that in accordance with Eurocode 3, Part 1.8 the contribution of any bolt row closer to the centre of compression is ignored.

The component method indicates that for both the first and the second bolt rows in tension (Table 3.1) the weakest component is the column flange in bending, which fails according to the complete flange yielding mechanism. The corresponding strengths of the first and second bolt rows are equal to 349.59 kN and 164.33 kN respectively. The resisting

**Table 3.1: Resistance and stiffness coefficients of the joint components for A-1**

Specimen	Component	$F_R$	$k_i$	$M_R$	
A-1		(kN)	(mm)	(kNm)	
Tension	Column web in tension	1389.15	9.16	175.86	
	Column flange in bending	-	4.20		
	First bolt row in tension	T-Stub complete flange yielding	349.59	-	
		T-Stub flange yielding and bolt failure	390.80	-	
		Bolt in tension	703.39	10.08	
		End-plate in bending	-	19.70	
		T-Stub complete flange yielding	600.16	-	
		T-Stub flange yielding and bolt failure	520.02	-	
		Column web in tension	691.19	4.30	
		Column flange in bending	-	1.97	
	Second bolt row in tension	T-Stub complete flange yielding	164.33	-	
		T-Stub flange yielding and bolt failure	384.61	-	
		Bolts in tension	703.39	10.08	
		End-plate in bending	-	24.29	
		T-Stub complete flange yielding	1294.06	-	
		T-Stub flange yielding and bolt failure	746.80	-	
		Beam web in tension	630.48	$\infty$	
	Compression	Column web in compression	780.32	7.64	241.92
		Beam flange and web in compression	706.96	$\infty$	
Shear	Column web in shear	1589.74	6.00	544.01	

bending moment due to tension failure of the connection is equal to 175.86 kNm, which is obtained as the product of the total tension resistance (the sum of the strength of the first and second bolt rows) times the internal lever arm.

As far as the compression side is concerned, the weakest component is the beam flange and web, whose strength is equal to 706.96 kN. The corresponding bending moment strength due to compression failure in the connection is equal to 241.92 kNm. Therefore, failure of the connection is expected to occur on the tension side because of column flange yielding and the corresponding flexural strength is equal to 175.86 kNm. Finally, the shear strength of the column web panel zone is equal to 1589.74 kN. The shear resistance is transformed into a bending strength of 544.01 kNm. The latter is larger than the flexural strength of the connection whose failure is therefore dominating the response of the joint. According to the component method the effective tensile resistances associated to the first and the second bolt row are 349.59 kN and 164.33 kN. Considering that the distances of each bolt row from the centre of compression are equal to 400 mm and 284 mm respectively, the bending moment resistance ( $M_{j,R}$ ) of A-1 was equal to 186.59 kNm. Failure is expected to occur in the column flange, for complete flange yielding of the representative T-Stub.

Concerning the initial rotational stiffness ( $S_{jini}$ ), Table 3.1 shows that the main source of deformability is the connection. The column flange in bending components with the stiffness coefficients equal to 4.20 mm and 1.97 mm respectively for the component belonging to the first bolt row and second bolt row are the more flexible components. According to the component method,  $S_{jini}$  is equal to 39486.30 kNm/rad. Consequently the theoretical yield rotation  $\phi_{i,y}$  is 4.73 mrad.

The theoretical predictions were compared with experimental results. At this aim, the experimental initial stiffness was assumed equal to the slope of the tangent of the curve in the elastic range, while the experimental conventional moment resistance was evaluated as the flexural resistance corresponding to joint secant stiffness equal to 1/3 times the initial rotational stiffness. The comparison shows that, in this case the component method underestimates the bending strength and the initial stiffness of 24% and 10% respectively, while the yield rotation prediction was similar to the experimental value. They differ about 5%. Concerning the failure mode, the predicted plastic mechanism coincides with the failure mode observed during the experimental test.

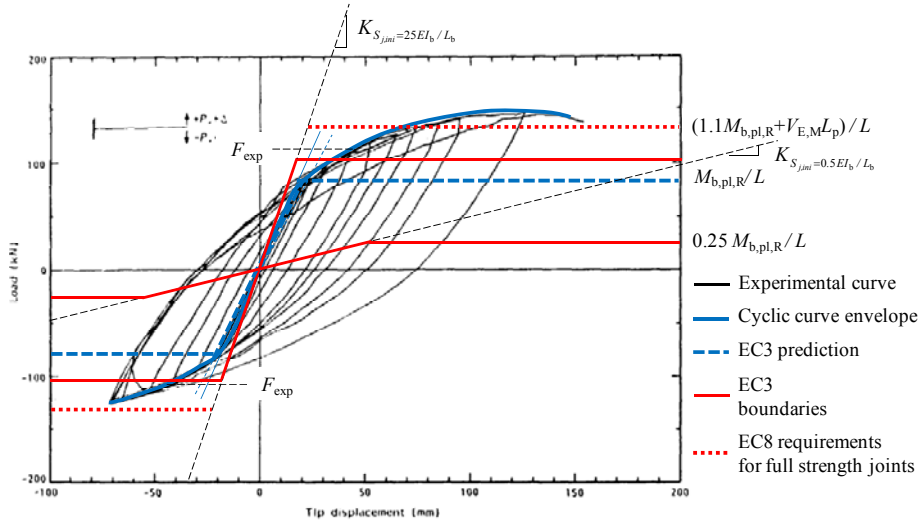


Figure 3.1: Classification by strength and stiffness for A-1

The classification by strength and stiffness of A-1 according to the Eurocode 3 is shown in Figure 3.1. The continuous red lines represent the boundaries for bending moment resistance and the initial stiffness, while the red dotted lines correspond to the bending moment strength limit for full strength joint according to Eurocode 8. This limit considers the beam plastic hinge at a distance from the end-plate equal to 1/3 times the beam height (FEMA 350, 2000). The blue lines, the continuous and the dashed one, represent the cyclic curve envelope and the component method prediction respectively. According to classification by strength the joint can be classified as partial strength. The difference between the experimental curve and the theoretical prediction is due to the strain hardening neglected by the component method. Assuming a beam span length equal to 2 times the cantilever length (4644 mm), the classification by stiffness indicates that A-1 is semi-rigid.

### 3.1.1.2 Specimen A-2

The details of the application of the component method are presented in Table 3.2. As in the previous case, the plastic moment resistance and the initial stiffness were determined considering the nominal geometrical properties of the beam and column sections. The end-plate layout was assumed the same of specimen A-1.

Concerning material properties, the expected yield stress of 394.38 MPa ( $1.3 \times 303.37$  MPa) was considered for the column, end-plate and column reinforcing plates. The nominal ultimate stress of 1000 MPa was used for the bolts. Actual values obtained from tensile test on coupon were considered for the beam. In particular the yield stresses equal to 316.1 MPa and 322.1 MPa were adopted for the beam flange and the column web respectively.

**Table 3.2: Resistance and stiffness coefficients of the joint components for A-2**

Specimen	Component	$F_R$ (kN)	$k_i$ (mm)	$M_R$ (kNm)	
A-2	Tension				
	Column web in tension	1494.54	9.98	260.72	
	Column flange in bending	-	4.57		
	First bolt row in tension	T-Stub complete flange yielding	380.94	-	
		T-Stub flange yielding and bolt failure	400.07	-	
		Bolt in tension	703.39	10.08	
		End-plate in bending	-	44.50	
		T-Stub complete flange yielding	600.16	-	
		T-Stub flange yielding and bolt failure	520.02	-	
		Column web in tension	1494.54	9.98	
		Column flange in bending	-	4.57	
	Second bolt row in tension	T-Stub complete flange yielding	380.94	-	
		T-Stub flange yielding and bolt failure	400.07	-	
		Bolts in tension	703.39	10.08	
		End-plate in bending	-	24.06	
		T-Stub complete flange yielding	1281.74	-	
		T-Stub flange yielding and bolt failure	746.80	-	
		Beam web in tension	636.94	$\infty$	
		Compression			
	Column web in compression	1595.17	$\infty$	245.97	
Beam flange and web in compression	718.78	$\infty$			
Shear	Column web in shear	1631.27	6.00	558.22	

Table 3.2 shows that for both the first and the second bolt rows in tension the weakest component was the column flange in bending which fails according to the complete flange yielding mechanism. The corresponding strengths are equal to 380.94 kN. The corresponding

resisting bending moment is 260.72 kNm. At the compression side, the weakest component is the beam web and flange, with the resistance equal to 718.78 kN. The bending moment resistance due to compression failure in the connection is equal to 245.97 kNm. Therefore, the failure of the connection is expected to occur on the compression side due to the beam failure. The shear strength of the column web panel zone is equal to 1631.27 kN. It is determined taking into account the increased column shear area as described above. The shear resistance produced a bending strength of 558.22 kNm. The latter being larger than the flexural strength, the response of the joint is governed by the connection behaviour. Finally, the effective tensile resistances are 380.94 kN, and 337.84 kN. These multiplied for the lever arm of each bolt row, 400 mm and 284 mm respectively, provide the bending moment resistance ( $M_{j,R}$ ) equal to 248.46 kNm.

Concerning the stiffness coefficients, Table 3.2 shows that the main contribution to stiffness is provided by the end-plate. The stiffness coefficients are 21.65 mm and 24.06 mm respectively for the component of the first bolt row and the second one. The more flexible component is the column flange in bending with the stiffness coefficients equal to 4.57 mm. Because of continuity plates, the stiffness coefficient of the column web in compression is assumed equal to infinity. Great deformability is expected in the column web panel for shear. The stiffness coefficient of the component is 6 mm. As a consequence joint rotational initial stiffness is 61805.65 kNm/rad. It is noted that the presence of the column stiffeners produce an increase of the joint mechanical properties. In case of A-2, the flexural resistance and the initial stiffness are greater than the previous configuration, free of column stiffeners. Finally, the theoretical yield rotation is 3.98 mrad.

The theoretical predictions were compared with experimental results. As explained above, the experimental initial stiffness was assumed as the slope of the tangent of the curve in the elastic range, while the experimental conventional moment resistance, for full strength joints was fixed equal to the beam plastic moment. The comparison shows that the component method overestimates the initial stiffness of 13%, while the yield rotation is underestimated of 24%. The predicted column flange failure was observed during the experimental test.

In Figure 3.2 the classification by strength and stiffness of A-2 according to the Eurocode 3 is given. As shown, the specimen is semi-rigid full strength joint. The classification by stiffness takes into account a beam

span length equal to 2 times the cantilever length (4644 mm). Theoretically the joint does not present sufficient overstrength to satisfy Eurocode 8 requirements for full strength joints, contrary to the experimental behaviour. The difference between the experimental curve and the theoretical prediction is due to the strain-hardening not taken into account by the component method.

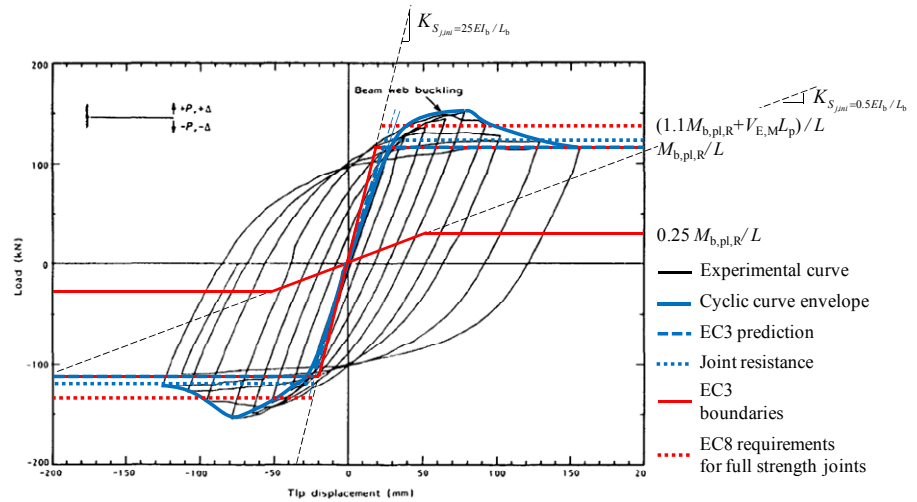


Figure 3.2: Classification by strength and stiffness for A-2

### 3.1.1.3 Specimen A-3

Table 3.3 summarizes the component method application. The calculations consider the nominal geometrical proprieties of the beam and the column sections. The end-plate layout was the same of specimen A-1. Concerning the material properties, the expected yield stress of 394.38 MPa ( $1.3 \times 303.37$  MPa) was considered for the column, end-plate and column reinforcing plates. The nominal ultimate stress of 1000 MPa was used for the bolts. Actual values of the steel yield stress were considered for the beam. In detail the yield stresses equal to 310.9 MPa and 315.7 MPa were adopted for the beam flange and the column web respectively. As shown in Table 3.3, at the tension zone the weakest component is again the column flange in bending, but differently from A-2, the failure mechanism is the flange yielding and bolt failure. In fact, the thicker column flange increased the flexural resistance of the

equivalent T-Stub flange produced a shift of the failure mode from a ductile mode to a brittle one. The corresponding tensile strengths are equal to 423.57 kN. The latter implies a resisting bending moment equal to 289.89 kNm. The beam web and flange component governs the resistance of the compression side with the resistance equal to 706.96 kN. The corresponding bending moment resistance due to compression failure in the connection is equal to 241.92 kNm.

**Table 3.3: Resistance and stiffness coefficients of the joint components for A-3**

Specimen	Component	$F_R$	$k_i$	$M_R$	
A-3		(kN)	(mm)	(kNm)	
Tension	Column web in tension	1775.54	11.96	317.25	
	Column flange in bending	-	9.12		
	First bolt row in tension	T-Stub complete flange yielding	589.94	-	
		T-Stub flange yielding and bolt failure	463.54	-	
	Bolt in tension	703.39	10.54		
	End-plate in bending	-	9.42		
		T-Stub complete flange yielding	635.10	-	
		T-Stub flange yielding and bolt failure	469.15	-	
	Second bolt row in tension	Column web in tension	1775.54	11.96	
		Column flange in bending	-	9.12	
		T-Stub complete flange yielding	589.94	-	
		T-Stub flange yielding and bolt failure	463.54	-	
		Bolts in tension	703.39	10.54	
		End-plate in bending	-	10.76	
		T-Stub complete flange yielding	754.57	-	
		T-Stub flange yielding and bolt failure	546.73	-	
	Beam web in tension	636.49	$\infty$		
Compression	Column web in compression	2119.08	$\infty$	241.92	
	Beam flange and web in compression	706.96	$\infty$		
Shear	Column web in shear	1854.89	6.78	634.74	

Therefore, connection failure is expected to occur on the compression side because of the beam web and flange failure. The shear strength of the column web panel zone is equal to 1426.84 kN. The related bending strength of 488.26 kNm is larger than the flexural strength of the connection; hence the resistance of the joint is governed by the



connection one. The effective tensile resistances are 463.54 kN and 243.41 kN and the corresponding distance from the centre of compression joint resistance are equal to 400mm and 284mm respectively. As a consequence the bending moment resistance of A-3 is 241.92 kNm. Failure is expected in the column flange and in the beam web and flange.

Concerning the stiffness coefficients, Table 3.3 shows that the main source of deformability is the panel zone in shear. Its stiffness coefficient is equal to 6.78 mm. The theoretical procedure returned the joint rotational initial stiffness of 70889.05 kNm/rad and consequently yield rotation of 3.41 mrad.

Although the analytical approach underestimates of 40% the initial rotational stiffness, it provides a good prediction of the flexural strength. The yield rotation is overestimated of 66%. For specimen A-3, the expected failure of the beam flange and web in compression is observed during the experimental test.

The classification of A-3 is shown in Figure 3.3. According to Eurocode 3, A-3 is classified as full strength joint. The specimen satisfies Eurocode 8 requirements for full strength joints too. Assuming a beam span length equal to 2 times the cantilever length (4650 mm), according to the classification by stiffness A-3 is semi-rigid.

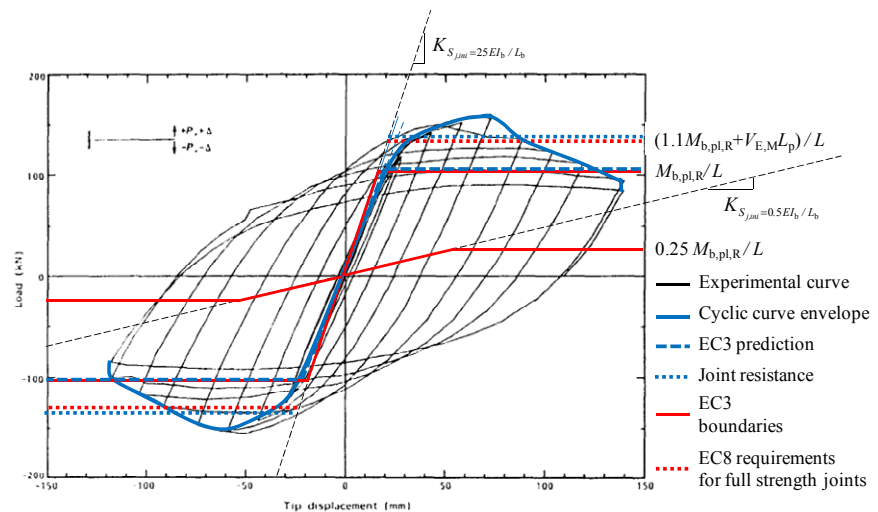


Figure 3.3: Classification by strength and stiffness for A-3

### 3.1.1.4 Specimen A-4

As previously, the theoretical moment resistance and initial stiffness were determined using the nominal geometrical proprieties for the beam and the column sections, while the end-plate layout was assumed the same of specimen A-1. The expected yield stress of 394.38 MPa ( $1.3 \times 303.37$  MPa) was considered for the column the end-plate and the column reinforcing plates. The nominal ultimate stress of 1000MPa was used for the bolts. A summary of the application of the analytical procedure is in Table 3.4.

**Table 3.4: Resistance and stiffness coefficients of the joint components for A-4**

Specimen	Component	$F_R$ (kN)	$k_i$ (mm)	$M_R$ (kNm)	
A-4	Tension	Column web in tension	1664.06	11.07	207.20
		Column flange in bending	-	8.44	
	First bolt row in tension	T-Stub complete flange yielding	545.82	-	
		T-Stub flange yielding and bolt failure	450.59	-	
		Bolt in tension	703.39	10.54	
		End-plate in bending	-	8.65	
		T-Stub complete flange yielding	346.65	-	
		T-Stub flange yielding and bolt failure	462.39	-	
		Column web in tension	841.37	5.25	
		Column flange in bending	-	4.00	
	Second bolt row in tension	T-Stub complete flange yielding	258.83	-	
		T-Stub flange yielding and bolt failure	442.32	-	
		Bolts in tension	703.39	10.54	
		End-plate in bending	-	10.66	
		T-Stub complete flange yielding	747.45	-	
		T-Stub flange yielding and bolt failure	546.73	-	
		Beam web in tension	630.48	$\infty$	
	Compression	Column web in compression	1133.10	9.79	241.92
		Beam flange and web in compression	706.96	$\infty$	
Shear	Column web in shear	1796.18	6.78	614.65	

Actual yield stresses equal to 310.9 MPa and 315.7 MPa were adopted respectively for the beam flange and the column web. As shown, for the first bolt row in tension the weakest component is the end-plate. The

failure mechanism is complete flange yielding of the equivalent T-Stub which represents the component. For the second bolt row, instead, the failure occurs in column flange for complete flange yielding mechanism. The corresponding strengths of the first and second bolt rows are equal to 346.65 kN and 258.83 kN respectively. The resisting bending moment due to tension failure of the connection is equal to 207.20 kNm. As far as the compression side is concerned, the weakest component is the beam flange and web, whose strength is equal to 706.96 kN. The corresponding bending moment strength due to compression failure in the connection is equal to 241.92 kNm. Therefore, failure of the connection is expected to occur on the tension side. Finally, the shear strength of the column web panel zone is equal to 1796.18 kN. It was determined taking into account the increased column shear area as described in the previous cases. The shear resistance is transformed into a bending strength of 614.65 kNm. The latter is larger than the flexural strength of the connection whose failure is therefore dominating the response of the joint. Consequently, for the first and the second bolt row, the effective tensile resistances are 346.65 kN and 258.83 kN, respectively. Being their lever arm equal to 400mm and 284mm, A-4 presents a moment resistance of 212.28 kNm.

About joint initial stiffness, the comparison of data in Table 3.4 displays that the main contribution to stiffness is provided by connection. In fact the column web in tension is the more rigid component of the joint. Its stiffness coefficient is 11.07 mm. A great role is also played by the end-plate of the second bolt row and the bolts in tension, since their stiffness coefficient are 10.66 mm and 10.54 mm respectively. Although the column web panel is stiffened by supplementary web plates, it presents a lower stiffness coefficient. It is equal to 6.78 mm. However the more flexible components of whole joint are the end-plate of the first bolt row and the column flange belonging to the second bolt row. In fact their stiffness coefficients are 4.21 mm and 4.00 mm respectively. Accordingly joint rotational initial stiffness is equal 48430.71 kNm/rad.

The yield rotation of A-4 is equal to 4.38 mrad.

From the theoretical point of view, failure is expected in the external part of the end-plate and in the column flange (Table 3.4). These provisions are in good agreement with the experimental results. In fact, as described in the previous Section, the fracture of the end-plate in the external part and severe damage of the column flange are observed. The component

method underestimates the bending strength while overestimates the initial stiffness of 19% and 15% respectively.

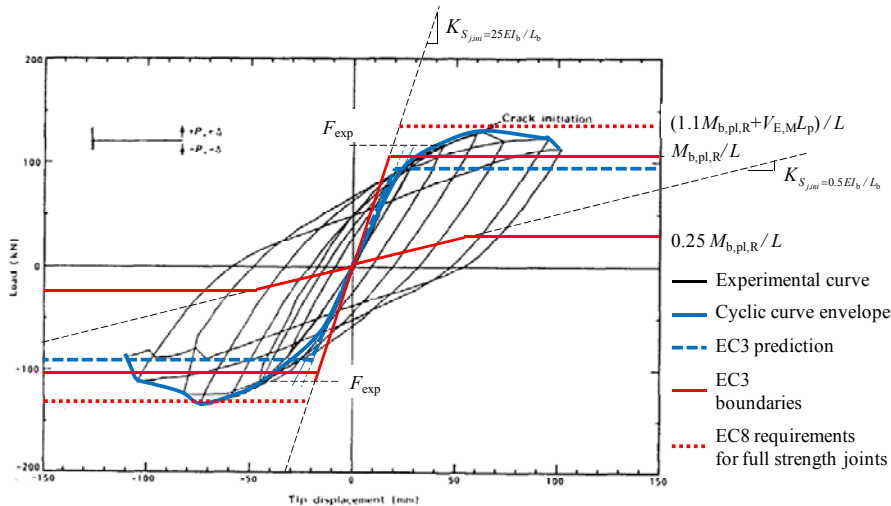


Figure 3.4: Classification by strength and stiffness for A-4

The classification of A-4 is shown in Figure 3.4. The moment resistance of the joint is smaller than beam plastic resistance. The latter is equal to 241.92 kNm. Consequently, according to EC3, A-4 can be classified partial strength joint. Assuming a beam span length equal to 2 times the cantilever length (4650 mm), the classification by stiffness identifies A-4 as semi-rigid. The differences noted between the theoretical predictions and the experimental curve is due to the strain-hardening neglected by the component method.

### 3.1.1.5 Specimen A-5

The theoretical moment resistance and initial stiffness were determined using the nominal geometrical proprieties for the beam and column sections, while the end-plate layout was assumed the same of specimen A-1. The expected yield stress of 394.38 MPa ( $1.3 \times 303.37$  MPa) was considered for the column the end-plate and the column reinforcing plates. The nominal ultimate stress of 1000MPa was used for the bolts. Actual yield stresses equal to 316.1 MPa and 322.1 MPa were adopted respectively for the beam flange and the column web. A summary of the application of the analytical procedure is given in Table 3.5. As shown,

for the two bolt rows in tension the weakest component is the end-plate. The failure mechanism is flange yielding and bolt failure of the equivalent T-Stub which represents the component. The corresponding strengths of the first and second bolt rows are equal to 397.30 kN and 444.77 kN respectively. The resisting bending moment due to tension failure of the connection is equal to 287.74 kNm. As far as the compression side is concerned, the weakest component is the beam flange and web, whose strength is equal to 718.78 kN. The corresponding bending moment strength due to compression failure in the connection is equal to 245.97 kNm. Therefore, failure of the connection is expected to occur on compression side.

**Table 3.5: Resistance and stiffness coefficients of the joint components for A-5**

Specimen	Component	$F_R$ (kN)	$k_i$ (mm)	$M_R$ (kNm)	
A-5	Tension	Column web in tension	1570.67	11.96	287.74
		Column flange in bending	-	9.12	
	First bolt row in tension	T-Stub complete flange yielding	521.87	-	
		T-Stub flange yielding and bolt failure	443.55	-	
		Bolt in tension	703.39	11.10	
		End-plate in bending	-	5.62	
		T-Stub complete flange yielding	398.41	-	
		T-Stub flange yielding and bolt failure	397.30	-	
		Column web in tension	1570.67	11.96	
		Column flange in bending	-	9.12	
	Second bolt row in tension	T-Stub complete flange yielding	521.87	-	
		T-Stub flange yielding and bolt failure	443.55	-	
		Bolts in tension	703.39	11.10	
		End-plate in bending	-	6.43	
T-Stub complete flange yielding		473.35	-		
T-Stub flange yielding and bolt failure		444.77	-		
Beam web in tension	649.39	$\infty$			
Compression	Column web in compression	1916.84	$\infty$	245.97	
	Beam flange and web in compression	718.78	$\infty$		
Shear	Column web in shear	1640.86	6.78	561.50	

Finally, the shear strength of the column web panel zone is equal to 1640.86 kN. As described above, it was determined taking into account the increased column shear area for the supplementary web plates. The shear resistance is transformed into a bending strength of 561.50 kNm. The latter is larger than the flexural strength of the connection whose failure is therefore dominating the response of the joint. In conclusion, A-5 presents a moment resistance of 245.97 kNm. Failure is expected in the external part of the end-plate and in the beam flange and web.

About joint initial stiffness, as shown in Table 3.5 the main contribution to stiffness is provided by bolts in tension. Their stiffness coefficients are 11.10 mm. A great role is also played by the column flange with stiffness coefficient equal to 9.12 mm. Although the column web panel is stiffened by supplementary web plates, it presents a lower the stiffness coefficient. It is equal to equal to 6.78 mm. However the more flexible component of whole joint is the end-plate of the first bolt row. Its stiffness coefficient is 5.62 mm. As a result, joint rotational initial stiffness is equal 73216.16 kNm/rad. A-5 yield rotation is equal to 3.40 mrad.

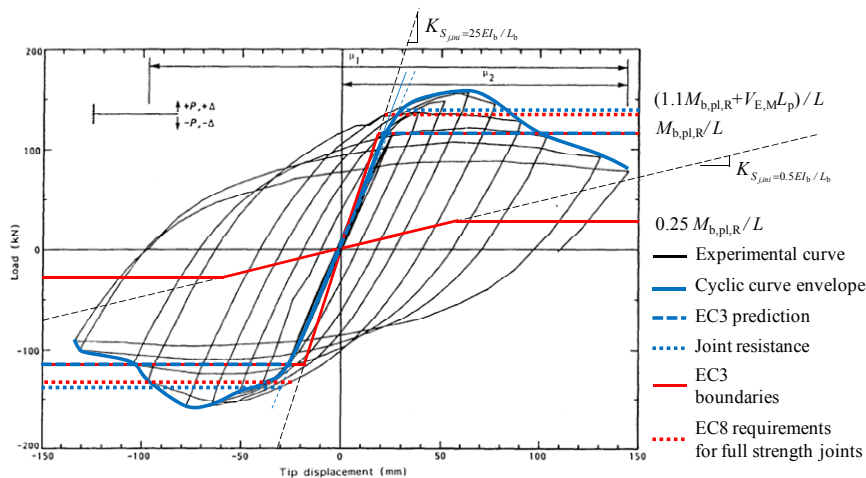


Figure 3.5: Classification of specimen A-5

Comparing the theoretical predictions with the experimental results, a good agreement between the two procedures is observed. The expected beam plastic hinge is observed during the test. The initial stiffness is underestimated of 8%. The classification of A-5 is shown in Figure 3.4.

According to Eurocode 3, A-5 can be classified full strength joint. Eurocode 8 requirements for full strength joints are also satisfied. Assuming a beam span length equal to 2 times the cantilever length (4650 mm), according to the classification by stiffness A-5 is semi-rigid.

### 3.1.2 Test by Sumner and Murray (2002)

Table 3.6 contains a summary of the application of the analytical procedure. The strength and the stiffness coefficients of each component were determined using the nominal geometrical properties presented in Table 2.2. Actual material properties were considered for the column, beam, end-plate, column reinforcing plates and bolts, whereas the nominal properties were fixed for the continuity plates.

**Table 3.6: Resistance and stiffness coefficients of the joint components**

Specimen	Component	$F_R$ (kN)	$k_i$ (mm)	$M_R$ (kNm)	
4E-1.25-1.5-24	Tension				
	Column web in tension	2358.04	19.27	1110.94	
	Column flange in bending	-	24.18		
	First bolt row in tension	T-Stub complete flange yielding	1286.76	-	
		T-Stub flange yielding and bolt failure	982.67	-	
		Bolt in tension	1163.79	12.60	
		End-plate in bending	-	82.94	
		T-Stub complete flange yielding	1169.20	-	
		T-Stub flange yielding and bolt failure	906.37	-	
		Column web in tension	2358.04	19.27	
		Column flange in bending	-	24.18	
	Second bolt row in tension	T-Stub complete flange yielding	1286.76	-	
		T-Stub flange yielding and bolt failure	982.67	-	
		Bolts in tension	1163.79	12.60	
		End-plate in bending	-	81.20	
		T-Stub complete flange yielding	2313.41	-	
		T-Stub flange yielding and bolt failure	1213.85	-	
		Beam web in tension	1386.21	$\infty$	
	Compression	Column web in compression	-	$\infty$	1072.28
		Beam flange and web in compression	1823.30	$\infty$	
Shear	Column web in shear	1827.85	5.69	1074.96	

In detail the yield stresses of 358.53 MPa, 369.56 MPa, 262.69 MPa, 290.27 MPa were used respectively for the column, the beam, the end-plate and column web doubler plate. A bolt ultimate stress of 779.11 MPa was considered. An expected yield stress of 322.67 MPa was used for continuity plates. The latter consider a material overstrength factor of 1.3 (ANSI/AISC 341-10, 2010). Table 3.6 shows that for the first bolt row in tension the weakest component is the end-plate in bending. The failure mechanism is the flange yielding and the bolt failure of the equivalent T-Stub which represents the component. The corresponding strength is equal to 906.37 kN. The column flange is the weakest component of the second bolt row. It fails also for flange yielding and bolt failure of the corresponding T-Stub. The column flange strength is equal to 982.67 kN. The resisting bending moment due to tension failure of the connection is equal to 1110.94 kNm, which is obtained as the product of the total tension resistance (the sum of the strength of the first and second bolt rows) times the internal lever arm. As far as the compression side is concerned, the weakest component is the beam flange and web, whose strength is equal to 1823.30 kN. The corresponding bending moment strength due to compression failure in the connection is equal to 1072.28 kNm. Therefore, failure of the connection is expected to occur on the compression side. Finally, the shear strength and the bending strength of the column web panel zone are equal to 1827.85 kN and 1074.96 kNm. Being the latter higher than the flexural strength of the connection the last governs the response of the joint. According to the component method the moment resistance of 4E-1.25-1.5-24 is equal to 1072.28 kNm. Failure is expected in the external part of the end-plate and in the beam web and flange.

Concerning the theoretical initial stiffness, Table 3.6 shows that the main contribution to joint stiffness is provided by the connection. The end-plate is the more rigid component. The stiffness coefficient of the component belonging to the first bolt row is equal to 82.94 mm. The same component of the second bolt row has the stiffness coefficient of 81.20 mm. The more flexible components of the connection are the bolts. Their stiffness coefficients are equal to 12.60 mm. However the column web in shear is the more flexible component of the whole joint. Its stiffness coefficient is 5.69 mm. As a result the initial rotational stiffness is equal to 270241.99 kNm/rad. Finally the yield rotation is equal to 3.97 mrad.



Concerning the failure mode, the theoretical prediction is in agreement with the experimental results since the beam web and flange buckling was observed during the test. The component method overestimates the initial stiffness of 20%.

Classification of 4E-1.25-1.5-24 according to Eurocode 3 is given in Figure 3.6. As shown, the specimen can be classified as semi-rigid full strength. The specimen does not satisfy the requirements for full strength joints recommended by Eurocode 8. The classification by stiffness considers a beam span length equal to 8623mm.

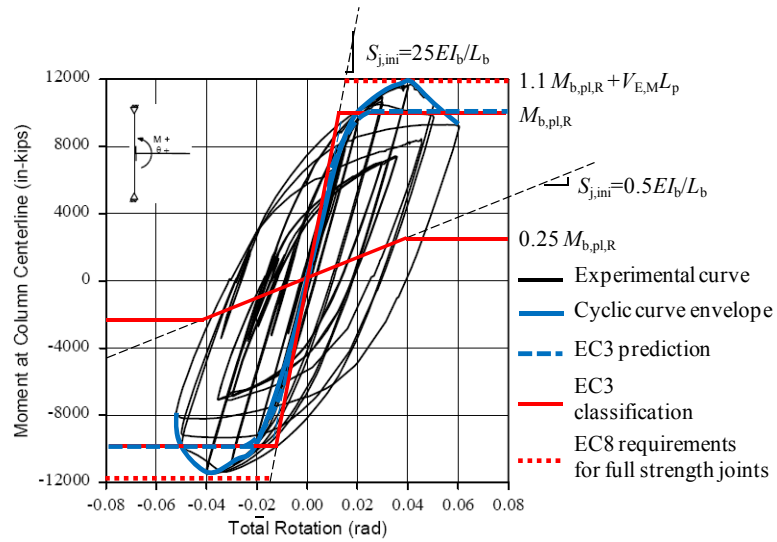


Figure 3.6: Classification by strength and stiffness for 4E-1.25-1.5-24

### 3.1.3 Tests by Nogueiro *et al.* (2006)

#### 3.1.3.1 Specimens J1

Table 3.7 contains a summary of the application of the component method. The strengths and the stiffness coefficients of each component are determined assuming the nominal values of the geometrical properties and material ones. Concerning the material proprieties, the expected yield stress of 390.50 MPa is used for the members, the end-plate and the continuity plates. The material overstrength factor was assumed equal to 1.1. The ultimate stress of 1000 MPa was assumed for bolts. Table 3.7 shows that for the first bolt row in tension the weakest

component is the end-plate in bending. The failure mechanism is the flange yielding and the bolt failure of the equivalent T-Stub which represents the component. The corresponding strength is equal to 487.30 kN. The second bolt row in tension the column flange fails according to the same mechanism. The related strength is 519.79 kN. The resisting bending moment due to tension failure of the connection is equal to 349.76 kNm, which is obtained as the product of the total tension resistance (the sum of the strength of the first and second bolt rows) times the internal lever arm.

**Table 3.7: Resistance and stiffness coefficients of the joint components for J-1**

Specimen	Component	$F_R$	$k_i$	$M_R$	
J-1		(kN)	(mm)	(kNm)	
Tension	Column web in tension	581.39	5.08	349.76	
	Column flange in bending	-	25.21		
	First bolt row in tension	T-Stub complete flange yielding	589.47	-	
		T-Stub flange yielding and bolt failure	519.79	-	
		Bolt in tension	635.40	10.36	
		End-plate in bending	-	47.27	
		T-Stub complete flange yielding	604.33	-	
		T-Stub flange yielding and bolt failure	487.30	-	
		Column web in tension	581.39	5.08	
	Column flange in bending	-	25.21		
	Second bolt row in tension	T-Stub complete flange yielding	589.47	-	
		T-Stub flange yielding and bolt failure	519.79	-	
		Bolts in tension	635.40	10.36	
		End-plate in bending	-	18.74	
		T-Stub complete flange yielding	794.96	-	
		T-Stub flange yielding and bolt failure	529.66	-	
		Beam web in tension	823.40	$\infty$	
	Compression	Column web in compression	-	$\infty$	397.98
		Beam flange and web in compression	1145.92	$\infty$	
Shear	Column web in shear	1025.11	4.50	356.02	

As far as the compression side is concerned, the weakest component is the beam flange and web, whose strength is equal to 1145.92 kN. The bending moment strength due to compression failure in the connection

is equal to 397.98 kNm. As a consequence, failure of the connection is expected to occur on the tension side. Finally, the shear strength of the column web panel zone is equal to 1025.11 kN. The shear resistance is transformed into a bending strength of 356.02 kNm. The latter is greater than the flexural strength of the connection therefore the connection governs the response of the joint. According to the component method the effective tensile resistances associated to the first and the second bolt row are 487.30 kN and 519.79 kN respectively. Considering that the distances of each bolt row from the centre of compression are approximately equal to 394 mm and 301 mm respectively, the bending moment resistance of J-1 is equal to 348.25 kNm. Failure is expected in the end-plate and in the column flange for the mixed mechanism of the T-Stub.

Referring to the rotational stiffness, Table 3.7 shows that the main contribution to stiffness is provided by the connection. The column flange, with the stiffness coefficient equal to 25.21 mm, is the more rigid component. The end-plate belonging to the first bolt row is the more rigid component. Its stiffness coefficient is 47.27 mm. The column web in shear is the more flexible component of the joint with the stiffness coefficient of 4.50 mm. As a result J-1 initial rotational stiffness is equal to 61785.12 kNm/rad. Therefore, the yield rotation is equal to 5.60 mrad.

The theoretical predictions cannot be compared with experimental results since the expected plastic mechanism is not the same observed during the experimental test. The difference is due to an approximate material modelling not based to actual material properties but on expected yield strength. This approximation does not permit to identify the real hierarchy of the components to yielding.

### ***3.1.3.2 Specimens J3***

A summary of the application of the analytical procedure is given in Table 3.8. The strengths and the stiffness coefficients of each component were determined assuming the nominal values of the geometrical properties and material ones. Concerning the material properties, the expected yield stress of 390.50 MPa ( $1.1 \times 355$  MPa) was used for the members, end-plate and continuity plates. The ultimate stress of 1000 MPa was assumed for bolts. Table 3.8 shows that for the two bolt rows in tension the weakest component is the end-plate in

bending. The failure mechanism is flange yielding and bolt failure of the equivalent T-Stub which represents the component.

**Table 3.8: Resistance and stiffness coefficients of the joint components for J-3**

Specimen	Component	$F_R$	$k_{\xi}$	$M_R$	
J-3		(kN)	(mm)	(kNm)	
Tension	Column web in tension	714.01	6.22	343.99	
	Column flange in bending	-	63.72		
	First bolt row in tension	T-Stub complete flange yielding	1031.12	-	
		T-Stub flange yielding and bolt failure	644.75	-	
		Bolt in tension	635.40	9.49	
		End-plate in bending	-	24.46	
		T-Stub complete flange yielding	485.16	-	
		T-Stub flange yielding and bolt failure	460.81	-	
		Column web in tension	714.01	6.22	
	Column flange in bending	-	63.72		
	Second bolt row in tension	T-Stub complete flange yielding	1031.12	-	
		T-Stub flange yielding and bolt failure	644.75	-	
		Bolts in tension	635.40	9.49	
		End-plate in bending	-	18.74	
T-Stub complete flange yielding		794.96	-		
T-Stub flange yielding and bolt failure		529.66	-		
Beam web in tension	823.40	$\infty$			
Compression	Column web in compression	-	$\infty$	397.98	
	Beam flange and web in compression	1145.92	$\infty$		
Shear	Column web in shear	1324.01	5.66	459.83	

The corresponding strengths are equal to 460.81 kN and 529.66 kN respectively. The resisting bending moment due to tension failure of the connection is equal to 343.99 kNm, which is obtained as the product of the total tension resistance (the sum of the strength of the first and second bolt rows) times the internal lever arm. Concerning the compression side, the weakest component is the beam flange and web, whose strength is equal to 1145.92 kN. The bending moment strength due to compression failure in the connection is equal to 397.98 kNm. As a consequence, failure of the connection is expected to occur on the tension side. Finally, the shear strength of the column web panel zone is

equal to 1324.01 kN. The shear resistance is transformed into a bending strength of 459.83 kNm. The flexural strength of the connection is smaller than that of the column web panel, therefore the response of the joint is governed by the connection. The effective tensile resistances associated to the first and the second bolt rows are 460.81 kN and 529.66 kN respectively. Considering that the distances of each bolt row from the centre of compression are approximately equal to 394 mm and 301 mm respectively, the bending moment resistance of J-3 is 340.80 kNm. Failure is expected in the end-plate for complete flange yielding and for flange yielding and bolt failure of the T-Stubs representative of the component of each bolt row.

Table 3.8 shows that the main contribution to stiffness is provided by the connection. The column flange, with the stiffness coefficient equal to 63.72 mm, is the more rigid component. The stiffness coefficient of the end-plate component belonging to the first bolt row is 24.46 mm. The column web in shear is the more flexible component of the joint with the stiffness coefficient of 5.66 mm. As a result J-1 initial rotational stiffness,  $S_{j,ini}$ , is equal to 73619.34 kNm/rad. Finally the yield rotation is equal to 4.60 mrad.

As in case of J-1 specimens, the theoretical predictions cannot be compared with experimental results since the expected plastic mechanism is not the same observed during the experimental test. Also in this case the approximate material modelling does not permit to identify the real hierarchy of the components to yielding.

### 3.1.4 Tests by Shi *et al.* (2007 a)

#### 3.1.4.1 Specimen EPC-1

Table 3.9 contains a summary of the application of the mechanical approach. The strength and the stiffness coefficients were determined assuming the nominal values of the geometrical properties of the beam, column, end-plate and bolts. Actual values of the material properties were considered, instead. In particular, the yield stress of 363.37 MPa was considered for the column flange and the end-plate, while 391 MPa for the column web, the beam and the continuity plates. The ultimate stress of 1160 MPa was used for the bolts. Table 3.9 shows that for both the first and the second bolt row the weakest component is the end-plate in bending. The failure mechanism is the flange yielding and the bolt

failure of the equivalent T-Stub which represents the component. The corresponding strengths are equal to 462.54 kN and 485.47 kN respectively. The resisting bending moment due to tension failure of the connection is equal to 273.03 kNm, which is obtained as the product of the total tension resistance (the sum of the strength of the first and second bolt rows) times the internal lever arm. As far as the compression side is concerned, the weakest component is the beam flange and web, whose strength is equal to 1145.24 kN. The corresponding bending moment strength due to compression failure in the connection is equal to 329.83 kNm.

**Table 3.9: Resistance and stiffness coefficients of the joint components for EPC-1**

Specimen	Component	$F_R$	$k_i$	$M_R$
EPC-1		(kN)	(mm)	(kNm)
Tension	Column web in tension	648.98	5.22	273.03
	Column flange in bending	-	26.98	
	First bolt row in tension	T-Stub complete flange yielding	912.32	-
		T-Stub flange yielding and bolt failure	496.64	-
		Bolt in tension	511.56	6.70
		End-plate in bending	-	25.24
		T-Stub complete flange yielding	812.18	-
		T-Stub flange yielding and bolt failure	462.54	-
	Second bolt row in tension	Column web in tension	648.98	5.22
		Column flange in bending	-	26.98
		T-Stub complete flange yielding	912.32	-
		T-Stub flange yielding and bolt failure	496.64	-
		Bolts in tension	511.56	6.70
		End-plate in bending	-	24.69
		T-Stub complete flange yielding	834.90	-
		T-Stub flange yielding and bolt failure	485.47	-
	Beam web in tension	736.51	$\infty$	
Compression	Column web in compression	1291.11	$\infty$	329.83
	Beam flange and web in compression	1145.24	$\infty$	
Shear	Column web in shear	873.43	4.22	251.55

Therefore, failure of the connection is expected to occur on the tension side. Finally, the shear strength of the column web panel zone is equal to 962.19 kN. The shear resistance is transformed into a bending strength of 251.55 kNm. The latter is smaller than the flexural strength of the connection therefore the column web panel in shear governs the response of the joint. According to the component method the effective tensile resistances associated to the first and the second bolt row are 462.54 kN and 410.89 kN respectively. Considering that the distances of each bolt row from the centre of compression are equal to 344 mm and 232 mm respectively, the bending moment resistance of EPC-1 is equal to 254.44 kNm. Failure is expected in the end-plate for the flange yielding and bolt failure of the T-Stub and in the column web for shear.

About the rotational stiffness, Table 3.9 shows that the main contribution to stiffness is provided by the column flange and the end-plate. The column flange, with the stiffness coefficient equal to 26.98 mm, is the more rigid component. A great role is played by the end-plate too, in fact the stiffness coefficients are 25.24 mm and 24.69 mm, for the first and the second bolt row respectively. The column web in shear and the bolts in tension is the more flexible component. Their stiffness coefficients are 4.22 mm and 6.70 mm respectively. Because of continuity plates, the stiffness coefficient of the column web in compression is assumed equal to infinity. As a result EPC-1 initial rotational stiffness is equal to 38391.50 kNm/rad. Finally the yield rotation is equal to 6.63 mrad.

These results compared with the corresponding experimental values indicate that the analytical procedure overestimates the experimental moment resistance and yield rotation of 4%, while it underestimates the experimental initial rotational stiffness of 27%. Concerning the failure mode, rupture is expected in the external part of the end-plate, according to the T-Stub failure mode 2, and in the column web panel for shear. These provisions agree with the experimental results, since the available moment-gap rotation and moment-shear rotation curves demonstrate that both the end-plate and the column web panel in shear yield. The observed bolt failure was the ultimate failure mechanism.

The classification by strength and stiffness of EPC-1 according to the Eurocode 3 is given in Figure 3.7. As shown, EPC-1 according to EC3 can be classified as semi-rigid partial strength. The classification by stiffness considers a beam span length of 2740 mm.

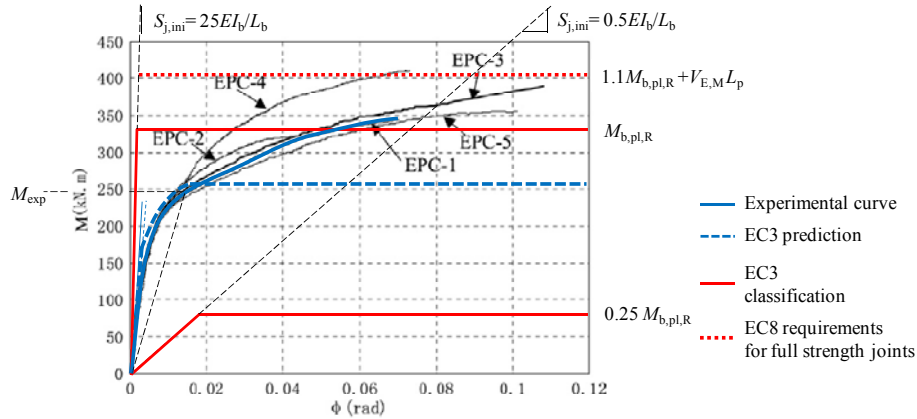


Figure 3.7: Classification by strength and stiffness for EPC-1

### 3.1.4.2 Specimen EPC-2

Table 3.9 contains a summary of the application of the application of the component method. The theoretical predictions are based on the nominal values of the geometrical properties and actual values of the material properties. In particular, the yield stress of 363.37 MPa was considered for the column flange and the end-plate, while 391MPa for the column web, beam and continuity plates. The ultimate stress of 1160MPa was used for the bolts. Table 3.10 shows that according to the mechanical approach the weakest components are the bolts in tension for both the first and the second bolt row. The corresponding strengths are equal to 511.56 kN. The resisting bending moment due to tension failure of the connection is equal to 294.66 kNm, which is obtained as the product of the total tension resistance (the sum of the strength of the first and second bolt rows) times the internal lever arm. The compression side, instead, is governed by the beam flange and web, whose strength is equal to 1145.24 kN. The corresponding bending moment strength due to compression failure in the connection is equal to 329.83 kNm. Therefore, failure of the connection is expected to occur on the tension side. Finally, the shear strength of the column web panel zone is equal to 953.31 kN, which correspond a bending strength of 274.55 kNm. The latter is smaller than the flexural strength of the connection therefore the column web panel in shear governs the response of the joint.



**Table 3.10: Resistance and stiffness coefficients of the joint components for EPC-2**

Specimen	Component	$F_R$ (kN)	$k_i$ (mm)	$M_R$ (kNm)	
EPC-2	Tension	Column web in tension	659.47	5.22	294.66
		Column flange in bending	-	52.69	
	First bolt row in tension	T-Stub complete flange yielding	1425.50	-	
		T-Stub flange yielding and bolt failure	623.77	-	
		Bolt in tension	511.56	5.72	
		End-plate in bending	-	49.29	
		T-Stub complete flange yielding	1269.03	-	
		T-Stub flange yielding and bolt failure	568.71	-	
		Column web in tension	659.47	5.22	
		Column flange in bending	-	52.69	
	Second bolt row in tension	T-Stub complete flange yielding	1425.50	-	
		T-Stub flange yielding and bolt failure	623.77	-	
		Bolts in tension	511.56	5.72	
		End-plate in bending	-	48.22	
		T-Stub complete flange yielding	1304.53	-	
		T-Stub flange yielding and bolt failure	606.31	-	
		Beam web in tension	736.51	$\infty$	
	Compression	Column web in compression	1342.26	$\infty$	329.83
		Beam flange and web in compression	1145.24	$\infty$	
Shear	Column web in shear	953.31	4.43	274.55	

The effective tensile resistances are consequently equal to 511.56 kN and 441.75 kN. Considering that the distances of each bolt row from the centre of compression are equal to 344mm and 232mm respectively, the bending moment resistance of EPC-2 is equal to 278.46 kNm. According to the component method, the bolt rupture as well as the column web for shear one are expected.

Concerning the stiffness coefficients, Table 3.10 shows that the more flexible components are the column web panel in shear and the bolts in tension with the stiffness coefficients equal to 4.43 mm and 5.89 respectively. The column flange and the end plate in bending are the more rigid components. Because of the continuity plates, the stiffness coefficients corresponding to the column web in compression is

assumed equal to infinity. Finally the joint initial rotational stiffness and the yield rotation are estimated equal to 39907.44 kNm/rad and 6.98 mrad.

The component method, in this case, provides a good prediction of the resistance but overestimates the initial rotational stiffness of 13%. The yield rotation is underestimated of 16%. Concerning failure mode, as described in the previous section the bolt rupture is expected together with the column web in shear failure. These provisions are in agreement with the experimental results. In fact, the moment - gap rotation and moment-shear rotation curves demonstrate that both the end-plate and the column web panel in shear reach the yielding. The bolt failure is the ultimate mechanism.

The classification by strength and stiffness of EPC-2 according to the Eurocode 3 is given in Figure 3.8. The limit for full strength joint according to EC8 is also provided. As depicted, both the experimental and the theoretical bending moment are greater than 0,25 times the beam plastic moment but less than the beam plastic resistance, therefore EPC-2 according to EC3 is classified as partial strength. Therefore the moment resistance cannot satisfy the EC8 requirements for full strength joints too. Assuming a beam span length of 2740 mm, according to the classification by stiffness the joint is semi-rigid.

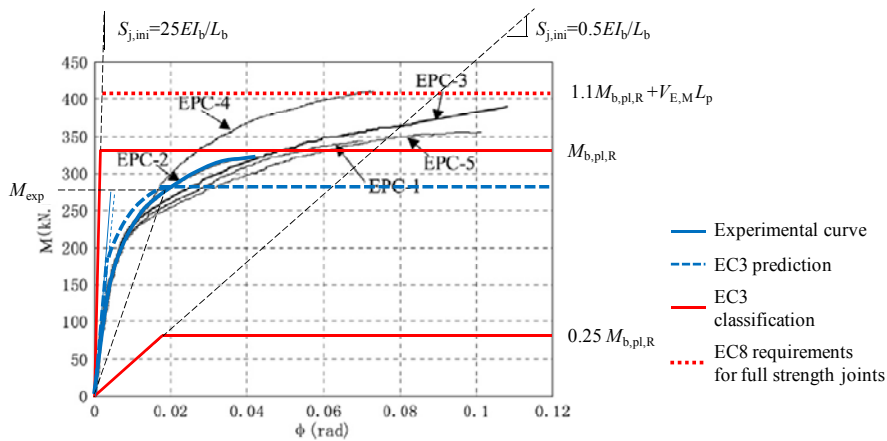


Figure 3.8: Classification by strength and stiffness EPC-2

### ***3.1.4.3 Specimen EPC-3***

The details of the analytical procedure in Table 3.11 are shown. The properties of each component were determined assuming nominal values for geometrical properties of the beam, column, end-plate and bolts and actual values of the material properties. In particular the yield stress of 363.37 MPa was taken into account for the column flange and the end-plate, while 391MPa for the column web, beam and continuity plates. The ultimate stress of 1188 MPa was used for the bolts. Table 3.11 displays that the component which governs the tension resistance of the two bolt rows is the end-plate with strengths of 592.75 kN and 614.18 kN, due to the flange yielding and bolt failure of the T-Subs representing the components. The resisting bending moment due to tension failure of the connection is equal to 347.60 kNm, which is obtained as the product of the total tension resistance (the sum of the strength of the first and second bolt rows) times the internal lever arm. The compression side, instead, is governed by the beam flange and web, whose strength is equal to 1145.24 kN. The corresponding bending moment strength due to compression failure in the connection is equal to 329.83 kNm. Therefore, failure of the connection is expected to occur on the compression side. Finally, the shear strength of the column web panel zone is equal to 873.43 kN, which correspond a bending strength of 251.55 kNm. The latter is smaller than the flexural strength of the connection therefore the column web panel in shear governs the response of the joint. According to the component method the effective tensile resistances associated to the first and the second bolt row are 592.75 kN and 280.70 kN respectively. Since the distances of each bolt row from the centre of compression are equal to 344mm and 232mm respectively, the bending moment resistance of EPC-3 is equal to 269.02 kNm. According to the component method, the end-plate failure as well as the column web for shear one are expected.

Concerning the stiffness coefficients, Table 3.11 shows that the more flexible components are the column web panel in shear and the bolts in tension with the stiffness coefficients equal to 4.22 mm and 9.26 respectively. The column flange and the end plate in bending are the more rigid components. Combining the axial stiffness the joint initial rotational stiffness is equal to 40291.55 kNm/rad. Finally the yield rotation is 6.68 mrad.

**Table 3.11: Resistance and stiffness coefficients of the joint components for EPC-3**

Specimen	Component	$F_R$ (kN)	$k_i$ (mm)	$M_R$ (kNm)	
EPC-3	Tension	Column web in tension	648.98	5.22	347.60
		Column flange in bending	-	26.98	
	First bolt row in tension	T-Stub complete flange yielding	912.32	-	
		T-Stub flange yielding and bolt failure	625.36	-	
		Bolt in tension	754.86	9.26	
		End-plate in bending	-	25.24	
		T-Stub complete flange yielding	812.18	-	
		T-Stub flange yielding and bolt failure	592.75	-	
		Second bolt row in tension	Column web in tension	648.98	5.22
	Column flange in bending		-	26.98	
	T-Stub complete flange yielding		912.32	-	
	T-Stub flange yielding and bolt failure		625.36	-	
	Bolts in tension		754.86	9.26	
	End-plate in bending		-	24.69	
	T-Stub complete flange yielding		834.90	-	
T-Stub flange yielding and bolt failure	614.18	-			
	Beam web in tension	736.51	$\infty$		
Compression	Column web in compression	1291.11	$\infty$	329.83	
	Beam flange and web in compression	1145.24	$\infty$		
Shear	Column web in shear	873.43	4.22	251.55	

According to the component method, failure is expected in the end-plate and in the column web panel for shear, differently from the buckling of the beam flange and web in compression observed during the experimental test. The apparent inconsistency is due to the simplifications included in the mechanical approach. In fact, the component method provides an estimate of the resistance of the first component which first yield, without taking into account of the strain hardening, which can be the responsible of the fact that the component which first yields is not the same that fails. However, the moment - gap rotation and moment-shear rotation curves demonstrate that both the end-plate and the column web panel in shear reach the yielding. Comparing the theoretical predictions with the experimental results, a

good estimation of the joint resistance is noted, whereas an underestimation of the initial stiffness of 13% is obtained. The classification of EPC3 is given in Figure 3.9. As shown, EPC-3 is classified as semi-rigid partial strength. The classification by stiffness assumes a beam span length of 2740 mm.

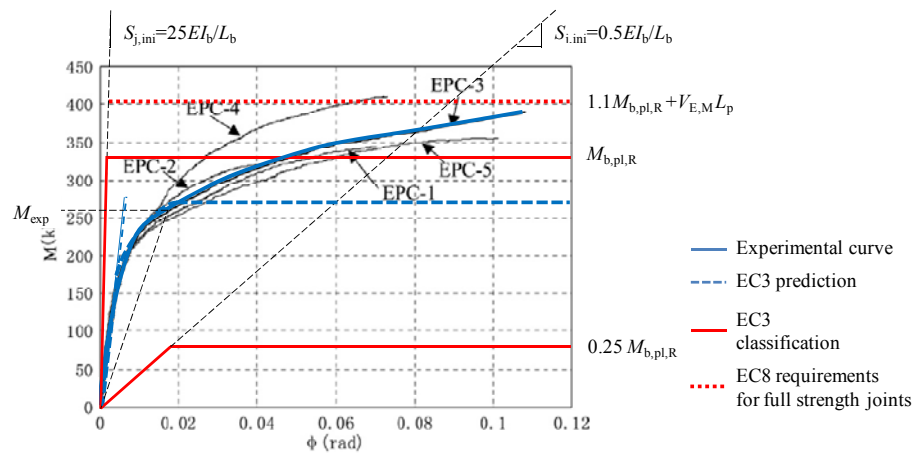


Figure 3.9: Classification by strength and stiffness EPC-3

#### 3.1.4.4 Specimen EPC-4

The strengths and the stiffness coefficients of EPC 4 were determined assuming the nominal values of the geometrical properties of the beam, column, end-plate and bolts. Actual values of the material were considered. In particular, the yield stress of 363.37 MPa was considered for the column flange and the end-plate, while 391 MPa for the column web, the beam and the continuity plates. The ultimate stress of 1188 MPa was used for the bolts. Table 3.12 shows that for both the first and the second bolt row the weakest component is the column web in tension, whose strength is equal to 659.47 kN. The resisting bending moment due to tension failure of the connection is equal to 379.86 kNm, which is obtained as the product of the total tension resistance (the sum of the strength of the first and second bolt rows) times the internal lever arm. In the compression side, the weakest component is the beam flange and web, whose strength is equal to 1145.24 kN. The corresponding bending moment strength due to compression failure in the connection is equal to 329.83 kNm. Therefore, failure of the connection is expected

to occur on the compression side. Finally, the shear strength of the column web panel zone is equal to 953.31 kN, which correspond to a bending strength of 274.55 kNm. The latter is smaller than the flexural strength of the connection therefore the column web panel in shear governs the response of the joint.

**Table 3.12: Resistance and stiffness coefficients of the joint components for EPC-4**

Specimen	Component	$F_R$ (kN)	$k_i$ (mm)	$M_R$ (kNm)	
EPC-4	Tension	Column web in tension	659.47	5.22	379.86
		Column flange in bending	-	52.69	
	First bolt row in tension	T-Stub complete flange yielding	1425.50	-	
		T-Stub flange yielding and bolt failure	752.48	-	
		Bolt in tension	754.86	7.95	
		End-plate in bending	-	49.29	
		T-Stub complete flange yielding	1269.03	-	
		T-Stub flange yielding and bolt failure	698.92	-	
		Second bolt row in tension	Column web in tension	659.47	5.22
	Column flange in bending		-	52.69	
	T-Stub complete flange yielding		1425.50	-	
	T-Stub flange yielding and bolt failure		752.48	-	
	Bolts in tension		754.86	7.95	
	End-plate in bending		-	48.22	
	T-Stub complete flange yielding		1304.53	-	
T-Stub flange yielding and bolt failure	735.03	-			
	Beam web in tension	736.51	$\infty$		
Compression	Column web in compression	1342.26	$\infty$	329.83	
	Beam flange and web in compression	1145.24	$\infty$		
Shear	Column web in shear	953.31	4.43	274.55	

The effective tensile resistances are 659.47kN and 293.83 kN. The sum of the effective tensile resistances multiplied for the corresponding distance from the centre of compression joint resistance, equal to 344 mm and 232 mm respectively, the bending moment resistance of 295.03 kNm provides. Failure is expected in column web panel for tension and shear.

About the stiffness coefficients, Table 3.12 shows that the main sources of deformability are the column web panel in shear and the bolt in tension, with stiffness coefficients equal to 4.43 mm and 7.95 mm respectively. The stiffness coefficient of the column web in compression is assumed equal to infinity to take account of the transversal column stiffeners. The joint rotational initial stiffness is equal to 42378.02 kNm/rad. Finally the yield rotation is equal to 6.96 mrad.

According to the component method, failure is expected to occur in the column web panel for tension and shear, differently from the buckling of the beam flange and web in compression observed as ultimate failure mode. As explained above the apparent contradiction is due to the strain hardening of the components, neglected in the mechanical approach, which is responsible of the fact that the component that first yields is not necessarily the same which fails. However the available moment-gap rotation and moment-shear rotation curves demonstrate that both the connection and the column web panel in shear yield.

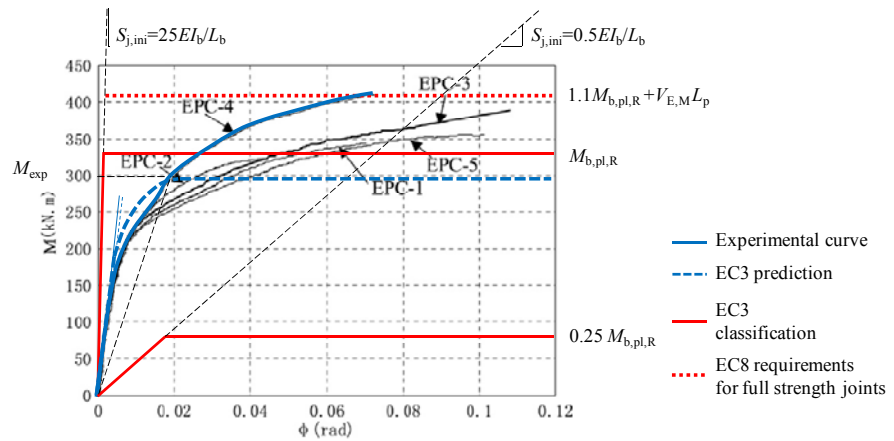


Figure 3.10: Classification by strength and stiffness EPC-4

The classification of EPC-4 according to EC3 is given in Figure 3.10. The joint can be classified as semi-rigid partial strength. As previously classification by stiffness assumes a beam span length of 2740 mm.

### 3.1.4.5 Specimen EPC-5

The strengths and the stiffness coefficients were determined assuming the nominal values of the geometrical properties of the beam, column, end-plate and bolts. Actual values of the material were considered. In particular, the yield stress of 363.37 MPa was considered for the column flange and the end-plate, while 391 MPa for the column web, the beam and the continuity plates. The ultimate stress of 1188 MPa was used for the bolts.

**Table 3.13: Resistance and stiffness coefficients of the joint components for EPC-5**

Specimen	Component	$F_R$	$k_i$	$M_R$	
EPC-5		(kN)	(mm)	(kNm)	
Tension	Column web in tension	659.47	5.22	379.86	
	Column flange in bending	-	52.69		
	First bolt row in tension	T-Stub complete flange yielding	1425.50	-	
		T-Stub flange yielding and bolt failure	752.48	-	
		Bolt in tension	754.86	7.95	
		End-plate in bending	-	49.29	
		T-Stub complete flange yielding	1269.03	-	
		T-Stub flange yielding and bolt failure	698.92	-	
	Column web in tension	659.47	5.22		
	Column flange in bending	-	52.69		
	Second bolt row in tension	T-Stub complete flange yielding	1425.50	-	
		T-Stub flange yielding and bolt failure	752.48	-	
		Bolts in tension	754.86	7.95	
		End-plate in bending	-	48.22	
		T-Stub complete flange yielding	1304.53	-	
		T-Stub flange yielding and bolt failure	735.03	-	
	Beam web in tension	736.51	$\infty$		
	Compression	Column web in compression	1342.26	$\infty$	329.83
Beam flange and web in compression		1145.24	$\infty$		
Shear	Column web in shear	953.31	4.43	274.55	

Table 3.13 shows that for both the first and the second bolt row the weakest component is the column web in tension, whose strength is equal to 659.47 kN. The resisting bending moment due to tension failure



of the connection is equal to 379.86 kNm, which is obtained as the product of the total tension resistance (the sum of the strength of the first and second bolt rows) times the internal lever arm. In the compression side, the weakest component is the beam flange and web, whose strength is equal to 1145.24 kN. The corresponding bending moment strength due to compression failure in the connection is equal to 329.83 kNm. Therefore, failure of the connection is expected to occur on the compression side. Finally, the shear strength of the column web panel zone is equal to 953.31 kN, which correspond to a bending strength of 274.55 kNm. The latter is smaller than the flexural strength of the connection therefore the column web panel in shear governs the response of the joint. The effective tensile resistances are 659.47kN and 293.83 kN. The sum of the effective tensile resistances multiplied for the corresponding distance from the centre of compression joint resistance, equal to 344 mm and 232 mm respectively, the bending moment resistance of 295.03 kNm provides. Failure is expected in column web panel for tension and shear.

About the stiffness coefficients, Table 3.13 shows that the main sources of deformability are the column web panel in shear and the bolt in tension, with stiffness coefficients equal to 4.43 mm and 7.95 mm respectively. The column web in compression stiffness coefficient is assumed equal to infinity to take account of the transversal column stiffeners. The joint rotational initial stiffness is equal to 35489.34 kNm/rad. Finally the yield rotation is equal to 6.64 mrad.

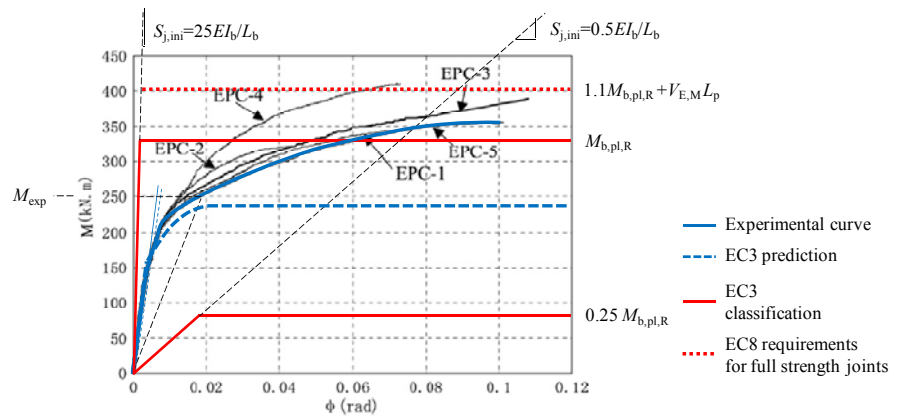


Figure 3.11: Classification by strength and stiffness EPC-5

Also in this case, comparing the theoretical prediction with the experimental results, a difference between the expected plastic mechanism and the ultimate failure mode is noted. This is due to the simplifications included in the mechanical approach. However the available moment-gap rotation and moment-shear rotation curves demonstrate that both the connection and the column web panel in shear yield. The classification of EPC-5 according to EC3 is given in Figure 3.11. As shown it can be classified as semi-rigid partial strength. As previous cases, the classification by stiffness considers a beam span length of 2740 mm.

### **3.1.5 Tests by Shi *et al.* (2007 b)**

#### ***3.1.5.1 Specimen JD2***

Table 3.14 contains a synthesis of the application of the component method. The theoretical bending moment strength and initial stiffness of specimen JD2 were determined assuming the nominal values for geometrical properties of the beam, column end-plate and bolts. Actual values of the material properties were instead supposed. In detail, the yield stress of 372.6MPa was considered for the column flange and the end-plate, while the yield stress of 409MPa was used for the column web, the beam and the continuity plates. The ultimate stress of 1160MPa was employed for the bolts. Table 3.14 shows that for both the first and the second bolt row the component which first yields is the end-plate. The failure mechanism is the flange yielding and the bolt failure of the equivalent T-Stub which represents the component. The corresponding strengths are equal to 467.53 kN and 491.15 kN respectively. The resisting bending moment due to tension failure of the connection is equal to 276.10 kNm, which is obtained as the product of the total tension resistance (the sum of the strength of the first and second bolt rows) times the internal lever arm. The compression side is governed by the beam flange and web, whose strength is equal to 1197.96 kN. The corresponding bending moment strength due to compression failure in the connection is equal to 345.01 kNm. Therefore, failure of the connection is expected to occur on the tension side. Finally, the shear strength of the column web panel zone is equal to 912.16 kN. The shear resistance is transformed into a bending strength of 262.70 kNm. The

latter is smaller than the flexural strength of the connection therefore the column web panel in shear governs the response of the joint.

**Table 3.14: Resistance and stiffness coefficients of the joint components for JD2**

Specimen JD2	Component	$F_R$ (kN)	$k_i$ (mm)	$M_R$ (kNm)	
Tension	Column web in tension	678.86	5.22	276.10	
	Column flange in bending	-	26.98		
	First bolt row in tension	T-Stub complete flange yielding	936.45	-	
		T-Stub flange yielding and bolt failure	502.62	-	
		Bolt in tension	511.56	6.70	
		End-plate in bending	-	25.24	
		T-Stub complete flange yielding	833.66	-	
		T-Stub flange yielding and bolt failure	467.53	-	
		Column web in tension	678.86	5.22	
	Column flange in bending	-	26.98		
	Second bolt row in tension	T-Stub complete flange yielding	936.45	-	
		T-Stub flange yielding and bolt failure	502.62	-	
		Bolts in tension	511.56	6.70	
		End-plate in bending	-	24.69	
T-Stub complete flange yielding		856.98	-		
T-Stub flange yielding and bolt failure		491.15	-		
Beam web in tension		770.42	$\infty$		
Compression	Column web in compression	-	$\infty$	345.01	
	Beam flange and web in compression	1197.96	$\infty$		
Shear	Column web in shear	912.16	4.22	262.70	

Thereby, according to the component method the effective tensile resistances associated to the first and the second bolt row are 467.53 kN and 444.63 kN respectively. Considering that the distances of each bolt row from the centre of compression are equal to 344 mm and 232 mm respectively, the bending moment resistance of JD2 is equal to 263.98 kNm. The failure is expected in the end-plate, for flange yielding and bolt failure of the T-Stub, and in the column web for shear.

Referring to the rotational stiffness, Table 3.14 shows that the main contribution to stiffness is provided by the column flange and the end-plate. The column flange, with the stiffness coefficient equal to 26.98

mm, is the more rigid component. A great role is played by the end-plate too, in fact the stiffness coefficients are 25.24 mm and 24.69 mm, for the first and the second bolt row respectively. The column web in shear together with the bolts in tension is the more flexible component. Their stiffness coefficients are 4.22 mm and 6.70 mm respectively. Because of continuity plates, the stiffness coefficients of the column web in compression and in tension are assumed equal to infinity. As a result JD2 initial rotational stiffness is equal to 38391.50 kNm/rad. Finally the yield rotation is equal to 6.88 mrad.

The theoretical bending moment resistance was compared with the conventional bending moment identified as the flexural resistance corresponding to a joint secant stiffness of 1/3 times the joint initial rotational stiffness, while the initial rotational stiffness is compared with the slope of the tangent to the moment-rotation curve. The method, in this case, overestimates the resistance of 10% and underestimates the initial rotational stiffness of 44%. The yield rotation is about twice the experimental value. Concerning the failure mode, the rupture is expected in the external part of the end-plate, according to the T-Stub failure mode 2, and in the column web panel for shear.

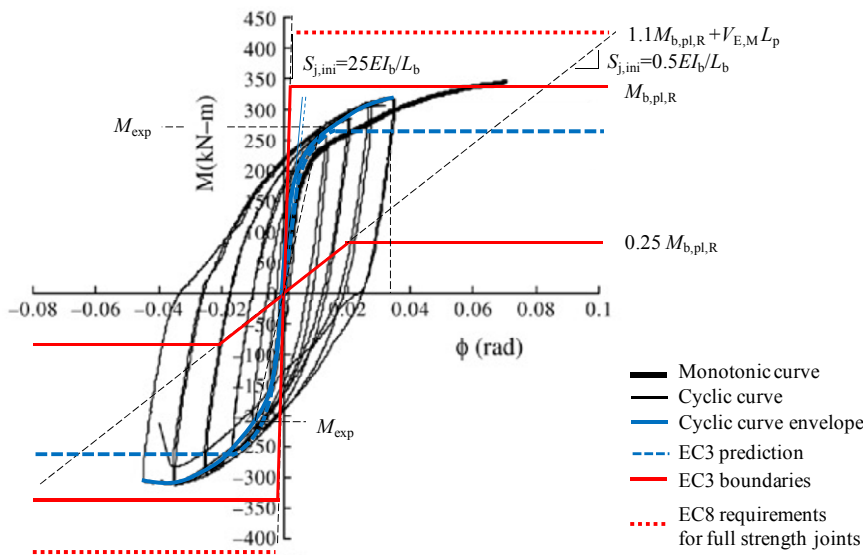


Figure 3.12: Classification by strength and stiffness for JD2

These provisions agree with the experimental results. In fact, the bolt rupture was observed and the available moment-gap rotation and moment-shear rotation curves demonstrate that both the end-plate and the column web panel in shear yield.

The classification by strength and stiffness of JD2 according to the Eurocode 3 is given Figure 3.12. The limit of the bending moment strength which satisfies the recommendations for full strength joint in seismic area according to EC8 is highlighted. As shown, JD2 is classified as semi-rigid partial strength. The classification by stiffness is based on a beam span evaluated as 2 times the specimen beam length (2700mm).

### **3.1.5.2 Specimen JD3**

JD3 components, divided according to their type of loading (tension, compression or shear), are listed in Table 3.15. The same table contains the details of the analytical procedure. For each component the resistance and the stiffened coefficient are specified. The calculations are based on nominal geometrical properties of the beam, column, end-plate and bolts and actual values of the steel yield and ultimate bolt strength. The yield stress of 372.6MPa was considered for the column flange and end-plate, while for the column web, beam and continuity plates the actual yield stress was 409 MPa. The ultimate stress of 1160MP was used for bolts. Comparing data (Table 3.15), on the tension side the minimum resistance is offered by end-plate. For both bolt row, the failure mechanism is flange yielding and bolt failure of the representative T-Stub. The tensile strengths are 330.30 kN and 491.15 kN respectively. At the compression side, the beam web and flange is the component which first yields. Its resistance is equal to 1197.96 kN. The bending strength of the tension side the compression one are 227.30 kNm and 345.01 kNm respectively. Therefore the failure occurs at the tension side of the connection. Concerning the shear strength, it is equal to 912.16 kN, which correspond to the bending strength of 262.70 kNm. The latter is greater than the connection one therefore the tension zone of the connection governs the joint behaviour. As above, the effective tensile resistance of each bolt row are 298.08 kN and 491.15 kN respectively. Since distance of each bolt row from the centre of compression are equal to 344mm and 232mm respectively, the flexural strength of JD3 is 216.49 kNm. Failure is expected to occur in the end-plate for flange yielding and bolt failure.

Concerning the initial rotational stiffness, Table 3.15 shows that the main contribution to stiffness is provided by the connection. In fact the column flange is the more rigid component with the stiffness coefficient equal to 26.98 mm. A great role is played by the end-plate component belonging to the second bolt row with the stiffness coefficients equal to 24.69 mm.

**Table 3.15: Resistance and stiffness coefficients of the joint components for JD3**

Specimen	Component	$F_R$	$k_i$	$M_R$	
JD3		(kN)	(mm)	(kNm)	
Tension	Column web in tension	678.86	5.22	227.30	
	Column flange in bending	-	26.98		
	First bolt row in tension	T-Stub complete flange yielding	936.45	-	
		T-Stub flange yielding and bolt failure	502.62	-	
		Bolt in tension	511.56	6.70	
		End-plate in bending	-	5.76	
		T-Stub complete flange yielding	298.08	-	
		T-Stub flange yielding and bolt failure	330.30	-	
		Column web in tension	678.86	5.22	
		Column flange in bending	-	26.98	
	Second bolt row in tension	T-Stub complete flange yielding	936.45	-	
		T-Stub flange yielding and bolt failure	502.62	-	
		Bolts in tension	511.56	6.70	
		End-plate in bending	-	24.69	
T-Stub complete flange yielding		856.98	-		
T-Stub flange yielding and bolt failure		491.15	-		
Beam web in tension	770.42	$\infty$			
Compression	Column web in compression	1350.55	$\infty$	345.01	
	Beam flange and web in compression	1197.96	$\infty$		
Shear	Column web in shear	912.16	4.22	262.70	

The external part of the end-plate and bolts in tension are the more flexible component of the connection. The column web in shear and the bolts in tension are the more flexible component. Their stiffness coefficients are 4.22 mm and 6.94 mm respectively. Because of continuity plates, the stiffness coefficients of the column web in compression and in tension are assumed equal to infinity. As a result JD3

initial rotational stiffness is 35984.57 kNm/rad and the yield rotation is equal to 6.02 mrad.

The comparison between the component results with the experimental ones indicates that, in case of JD3, the analytical procedure underestimates the experimental value of the moment resistance and yield rotation of 16% and 22% respectively. The component method overestimates the initial stiffness of about 11% (Figure 3.13).

Concerning the failure mode, as described above, the failure is expected in the end-plate, according to the T-Stub failure mode 2. These provisions agree with the experimental results. In fact, the available moment-gap rotation and moment-shear rotation curves demonstrate that both the end-plate and the column web panel in shear reach the yielding.

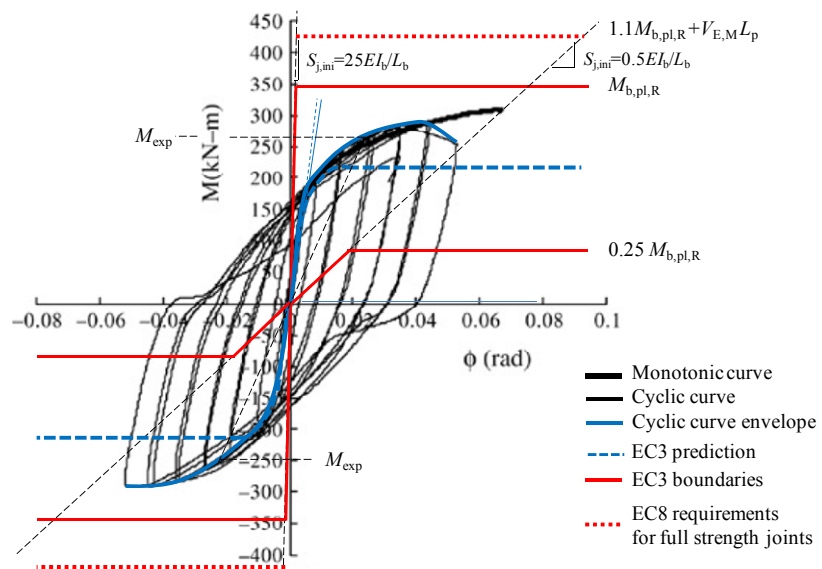


Figure 3.13: Classification by strength and stiffness for JD3

The classification by strength and stiffness of JD3 according to the Eurocode 3 is given in Figure 3.13. JD3 can be classified as semi-rigid partial strength. Classification by stiffness considers a beam span length equal to 2700 mm.

### 3.1.5.3 Specimen JD4

The theoretical prediction of the flexural strength and the initial rotational stiffness of JD4 are based on following assumptions. The geometrical properties of JD4 are supposed equal to the nominal ones. Whereas the material properties, yield stress of steel and the ultimate strength of bolts are assumed equal to the actual values determined by tensile tests on coupons. In particular, the yield stress of 372.6MPa is considered for the column flange and the end-plate, while the yield strength of 409 MPa is assumed for the column web, the beam and continuity plates. The ultimate stress of 1160MPa is taken for bolts.

**Table 3.16: Resistance and stiffness coefficients of the joint components for JD4**

Specimen	Component	$F_R$ (kN)	$k_i$ (mm)	$M_R$ (kNm)	
JD4	Tension	Column web in tension	670.64	5.12	235.19
		Column flange in bending	-	26.48	
	First bolt row in tension	T-Stub complete flange yielding	919.18	-	
		T-Stub flange yielding and bolt failure	487.08	-	
		Bolt in tension	511.56	6.70	
		End-plate in bending	-	25.24	
		T-Stub complete flange yielding	833.66	-	
		T-Stub flange yielding and bolt failure	467.53	-	
		Column web in tension	349.11	2.27	
		Column flange in bending	-	11.74	
	Second bolt row in tension	T-Stub complete flange yielding	407.64	-	
		T-Stub flange yielding and bolt failure	462.62	-	
		Bolts in tension	511.56	6.70	
		End-plate in bending	-	24.69	
		T-Stub complete flange yielding	856.98	-	
		T-Stub flange yielding and bolt failure	491.15	-	
	Beam web in tension	770.42	-		
	Compression	Column web in compression	327.97	2.68	94.46
		Beam flange and web in compression	1197.96	-	
	Shear	Column web in shear	811.54	4.22	233.72

Table 3.16 contains a synthesis of the application of the component method. As above, the joint components are grouped on the basis of the



loading type (tension, compression and shear loading). For each component, the strength and the stiffness coefficient are specified. The resisting bending moment evaluated as the product of the weakest component strength times the internal lever arm, per each loading type (tension, compression, shear) is also provided.

Table 3.16 shows that for the first bolt row the component which first yields is the end-plate. The failure mechanism is the flange yielding and the bolt failure of the equivalent T-Stub which represents the component. The corresponding strength is equal to 467.53 kN. The weakest component of second bolt row is the column web in tension, whose strength is equal to 407.64 kN. The resisting bending moment due to tension failure of the connection is equal to 235.19 kNm, which is obtained as the product of the total tension resistance (the sum of the strength of the first and second bolt rows) times the internal lever arm. The compression side is governed by the column web, whose strength is equal to 327.97 kN. The corresponding bending moment strength due to compression failure in the connection is equal to 94.46 kNm. Therefore, failure of the connection is expected to occur on the compression side. Finally, the shear strength of the column web panel zone is equal to 811.44 kN. The latter corresponds to a bending strength of 233.72 kNm. The flexural strength of the connection is smaller than those the column web panel one, hence the connection governs the response of the joint.

As a result the effective tensile resistances associated to the first and the second bolt row are 327.97 kN and 0 kN respectively. Being the distances of each bolt row from the centre of compression equal to 344 mm and 232 mm respectively, the bending moment resistance of JD4 is equal to 112.82 kNm. The failure is expected in the column web for compression.

About the initial rotational stiffness, Table 3.16 shows that the main contribution to stiffness is provided by the connection. In fact the stiffness coefficients of the column flange are equal to 26.98 mm and 11.74 mm respectively for the component belonging to the first and the second bolt row. A great role is played also by the end-plate components. The stiffness coefficients are equal to 25.24 mm and 24.69 mm respectively for the first and the second bolt row. In the connection the more flexible component is the column web in tension, belonging to the second bolt row, with the stiffness coefficient equal to 2.27. It is absolutely the more flexible component of the joint. As shown in Table 3.16, low stiffness coefficients are associated also to the column web

panel in compression and shear and the bolts in tension column. They are 4.22 mm, 2.68 mm and 6.70 respectively. As a consequence the initial rotational stiffness of JD4 is 19704.19 kNm/rad. Finally the yield rotation is equal to 5.73 mrad.

Comparing the theoretical predictions with the experimental results, an underestimation of the structural properties by the component method is noted. The moment resistance, the rotational stiffness and the yield rotation are underestimated of 58% 45% and 25% respectively. Concerning the failure mode, as described in the previous section, the rupture is expected for the buckling of the column web panel in compression. It is observed during the experimental test, but the bolt rupture is also occurred. The latter theoretically is not expected.

The classification by strength and stiffness of JD4 according to the Eurocode 3 is presented in Figure 3.14. The limit of the bending moment strength for full strength joint according to EC8 is shown. As depicted, the moment resistance is less than the beam plastic resistance; therefore JD4 is classified as partial strength joint. Assuming for JD4 the beam span length equal to 2700 mm, the configuration is semi-rigid.

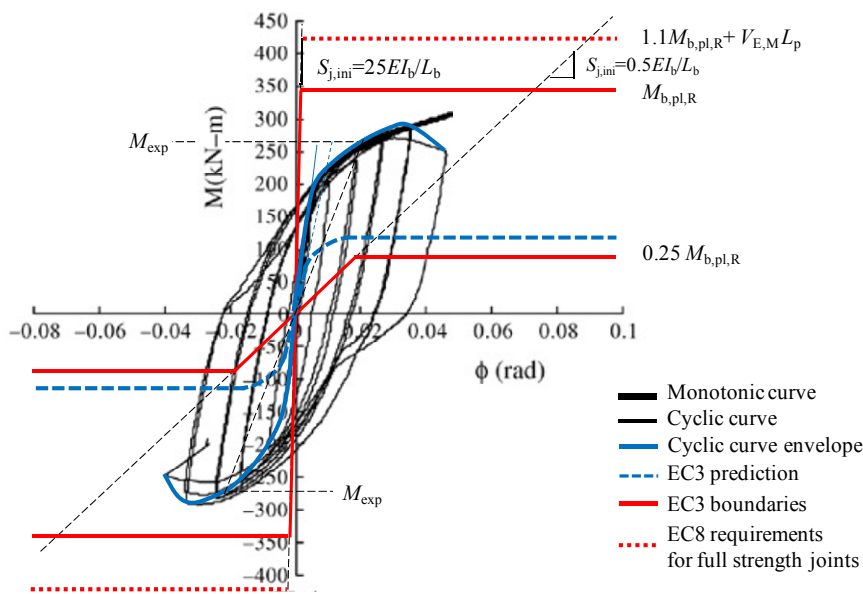


Figure 3.14: Classification by strength and stiffness for JD4

### 3.1.5.4 Specimen JD5

Table 3.17 contains a synthesis of the application of the component method. The theoretical predictions are based on following assumptions. The geometrical properties of JD5 were supposed equal to the nominal ones. Whereas the material properties, yield stress of steel and the ultimate strength of bolts were assumed equal to the actual values determined by tensile tests on coupons. In particular, the yield stress of 372.6 MPa was considered for the column flange and the end-plate, while the yield strength of 409 MPa was assumed for the column web, the beam and continuity plates. The ultimate stress of 1160MPa was taken for bolts.

**Table 3.17: Resistance and stiffness coefficients of the joint components for JD5**

Specimen	Component	$F_R$ (kN)	$k_i$ (mm)	$M_R$ (kNm)	
JD5	Tension	Column web in tension	689.83	5.22	294.66
		Column flange in bending	-	52.69	
	First bolt row in tension	T-Stub complete flange yielding	1463.20	-	
		T-Stub flange yielding and bolt failure	633.11	-	
		Bolt in tension	511.56	5.72	
		End-plate in bending	-	49.29	
		T-Stub complete flange yielding	1302.59	-	
		T-Stub flange yielding and bolt failure	576.51	-	
		Column web in tension	689.83	5.22	
		Column flange in bending	-	52.69	
	Second bolt row in tension	T-Stub complete flange yielding	1463.20	-	
		T-Stub flange yielding and bolt failure	633.11	-	
		Bolts in tension	511.56	5.72	
		End-plate in bending	-	48.22	
T-Stub complete flange yielding		1339.03	-		
T-Stub flange yielding and bolt failure		615.19	-		
Beam web in tension	770.42	$\infty$			
Compression	Column web in compression	1383.89	$\infty$	345.01	
	Beam flange and web in compression	1197.96	$\infty$		
Shear	Column web in shear	994.89	4.43	286.53	

Table 3.17 shows that for both the first and the second bolt row the weakest components are the bolts in tension. The increased thickness of both the end-plate and the column flange makes bolts the feeble components. The corresponding strengths are equal to 511.56 kN. The resisting bending moment due to tension failure of the connection is equal to 294.66 kNm, which is obtained as the product of the total tension resistance (the sum of the strength of the first and second bolt rows) times the internal lever arm. The compression side is governed by the beam flange and web, whose strength is equal to 1197.96 kN. The corresponding bending moment strength due to compression failure in the connection is equal to 345.01 kNm. Therefore, failure of the connection is expected to occur in the tension side. Finally, the shear strength of the column web panel zone is equal to 994.89 kN. The latter corresponds to a bending strength of 288.11 kNm. The shear bending moment strength of the column web panel latter is smaller than the flexural strength of the connection therefore the column web panel in shear governs the response of the joint. As a result the effective tensile resistances associated to the first and the second bolt rows are 511.56 kN and 483.33 kN respectively. Being the distances of each bolt row from the centre of compression are equal to 344 mm and 232 mm respectively, the bending moment resistance of JD5 is equal to 288.11 kNm. The bolt yielding is expected as well as the failure of the column web panel for shear.

About the initial rotational stiffness, Table 3.17 shows that the main contribution to stiffness is provided by the connection. In fact the stiffness coefficients of the column flange are equal to 52.69 mm. A great role is played also by the end-plate components. The stiffness coefficients are equal to 49.29 mm and 48.22 mm respectively for the first and the second bolt row. In the connection the more flexible components are the bolts in tension with the stiffness coefficient equal to 5.72. As shown in Table 3.17, the more flexible component of the joint is the column web panel in shear. The stiffness coefficient is equal to 4.43 mm. Finally the initial rotational stiffness of JD5 is 39907.44 kNm/rad. The corresponding yield rotation is equal to 7.22 mrad.

The comparison between the theoretical predictions and the experimental results indicates that, in case of JD5, the analytical procedure underestimates the moment resistance and the initial stiffness of 13 % and 30% respectively (Figure 3.15) and consequently the yield rotation is overestimated of 25%. Concerning the failure mode, the

provisions agree with the experimental results, since the bolt failure was observed and the moment-shear rotation curve demonstrates that web panel in shear yields.

In Figure 3.15 the classification of JD5 according to the Eurocode 3 is presented. As depicted, both the experimental and the theoretical bending moment resistance are less than the beam plastic resistance, therefore JD5 is classified as partial strength. Assuming the beam length equal to 2700 mm, the joint is classified semi-rigid.

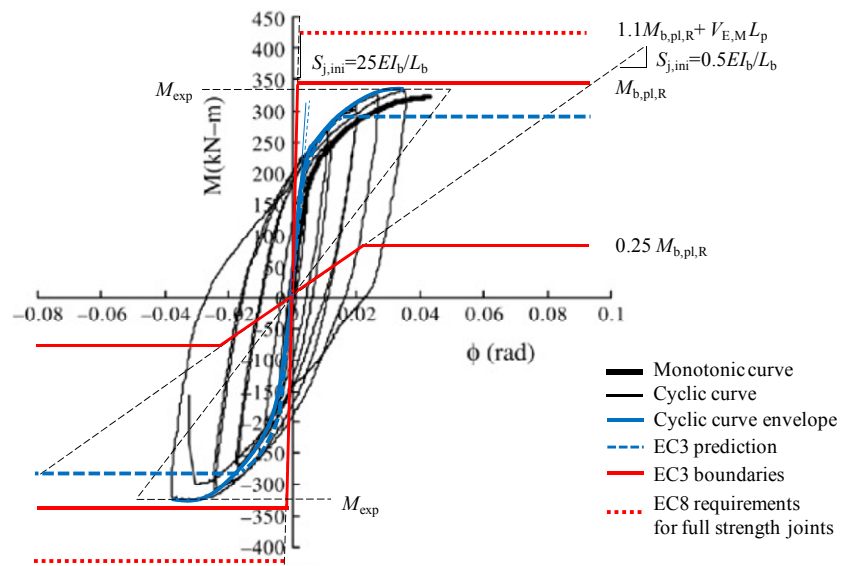


Figure 3.15: Classification by strength and stiffness for JD5

### 3.1.5.5 Specimen JD6

In Table 3.18 is a summary of the application of the analytical procedure. As before the component strengths and the stiffness coefficients were determined assuming the nominal values of the geometrical properties of the beam, the column, the end-plate and bolts. Actual values of the material properties were considered. In particular, the yield stress of 372.6MPa was counted for the column flange and the end-plate, while 409MPa for the column web, the beam and the continuity plates. The ultimate stress of 1188 MPa was used for the bolts. The nominal Young modulus was considered.

**Table 3.18: Resistance and stiffness coefficients of the joint components for JD6**

Specimen	Component	$F_R$	$k_i$	$M_R$	
JD6		(kN)	(mm)	(kNm)	
Tension	Column web in tension	678.86	5.22	350.67	
	Column flange in bending	-	26.98		
	First bolt row in tension	T-Stub complete flange yielding	936.45	-	
		T-Stub flange yielding and bolt failure	631.33	-	
	Bolt in tension	754.86	9.26		
	End-plate in bending	-	25.24		
	T-Stub complete flange yielding	833.66	-		
	T-Stub flange yielding and bolt failure	597.74	-		
	Second bolt row in tension	Column web in tension	678.86	5.22	
		Column flange in bending	-	26.98	
		T-Stub complete flange yielding	936.45	-	
		T-Stub flange yielding and bolt failure	631.33	-	
		Bolts in tension	754.86	9.26	
		End-plate in bending	-	24.69	
		T-Stub complete flange yielding	856.98	-	
		T-Stub flange yielding and bolt failure	619.86	-	
	Beam web in tension	770.42	$\infty$		
	Compression	Column web in compression	1350.55	$\infty$	345.01
Beam flange and web in compression		1197.96	$\infty$		
Shear	Column web in shear	912.16	4.22	262.70	

Table 3.18 shows that for both the first and the second bolt row the weakest component is the end-plate in bending. The failure mechanism is the flange yielding and the bolt failure of the equivalent T-Stub which represents the component. The corresponding strengths are equal to 597.74 kN and 619.86 kN respectively. The resisting bending moment due to tension failure of the connection is equal to 350.67 kNm. As far as the compression side is concerned, the weakest component is the beam flange and web, whose strength is equal to 1197.96 kN. The corresponding bending moment strength due to compression failure in the connection is equal to 345.01 kNm. Therefore, failure of the connection is expected to occur in the compression side. Finally, the shear strength of the column web panel zone is equal to 912.16 kN. The

shear resistance is transformed into a bending strength of 262.70 kNm. The latter is smaller than the flexural strength of the connection therefore the column web panel in shear governs the response of the joint. As a result the effective tensile resistances associated to the first and the second bolt rows are 597.74 kN and 314.42 kN respectively. Being the distances of each bolt row from the centre of compression are equal to 344 mm and 232 mm respectively, the bending moment resistance of JD6 is equal to 278.57 kNm. The failure is expected in the end-plate and in the column web for shear.

About the initial rotational stiffness, Table 3.18 shows that the main contribution to stiffness is provided by the connection. In fact the stiffness coefficients of the column flange are equal to 26.98 mm. A great role is played also by the end-plate components. The stiffness coefficients are equal to 25.24 mm and 24.69 mm respectively for the first and the second bolt row. In the connection the more flexible component are the bolts in tension with the stiffness coefficient equal to 9.26. As shown in Table 3.16, the more flexible component is the column web panel in shear. The stiffness coefficient is equal to 4.22 mm.

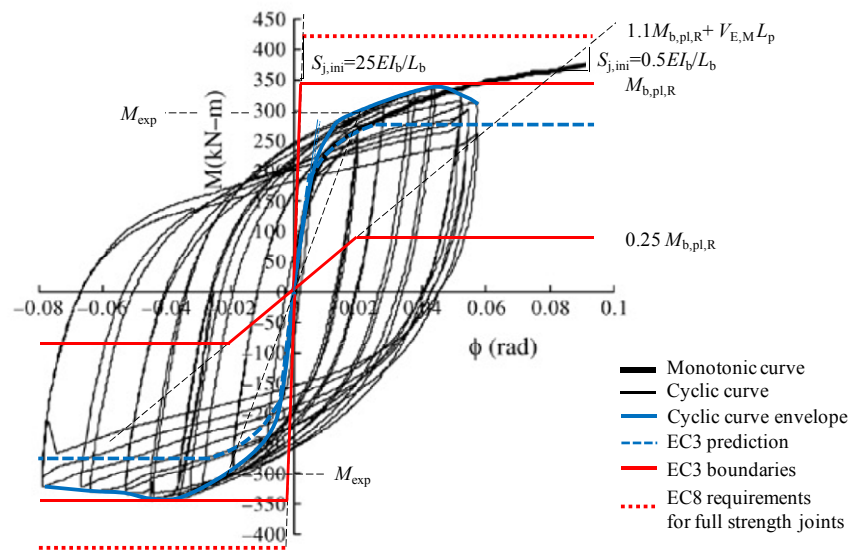


Figure 3.16: Classification by strength and stiffness for JD6

As a consequence the initial rotational stiffness of JD6 is equal to 40291.55 kNm/rad. Therefore the yield rotation is equal to 6.91 mrad.

The theoretical predictions are in accordance with the experimental results. The moment resistance, the initial stiffness and the yield rotation are underestimated of 7%, 2% and 5% respectively.

The classification by strength and stiffness of JD6 according to the Eurocode 3 is presented in Figure 3.16. As depicted, bending moment resistance is less than the beam plastic resistance; therefore JD6 according to EC3 is classified as partial strength. Assuming the beam span length equal to 2700 mm, the joint is semi-rigid.

#### **3.1.5.6 Specimen JD7**

The component method application is briefly summarized in Table 3.19. The prediction of the structural properties is based on some assumptions. The geometrical properties of the beam, the column, the end-plate and bolts are supposed equal to the geometrical values. The material properties are assumed equal to the actual values. In particular, the yield stress of 372.6MPa is considered for the column flange and the end-plate, while 409MPa for the column web, the beam and the continuity plates. The ultimate stress of 1188 MPa is used for the bolts. Finally, the elastic modulus is supposed equal to the nominal value.

As shown in Table 3.19, according the component method, the weakest component of both the first and the second bolt row in tension is the column web in tension. The corresponding strengths are equal to 689.83 kN. The resisting bending moment due to tension failure of the connection is equal to 397.34 kNm. Concerning the compression side, the weakest component is the beam flange and web, whose strength is equal to 1197.96 kN. The corresponding bending moment strength due to compression failure in the connection is equal to 345.01 kNm. Therefore, failure of the connection is expected to occur in the compression side. Finally, the shear strength of the column web panel zone is equal to 286.53kN. The shear resistance is transformed into a bending strength of 262.70 kNm. The latter is smaller than the flexural strength of the connection therefore the column web panel in shear governs the response of the joint. As a result the effective tensile resistances associated to the first and the second bolt row are 689.83 kN and 305.06 kN respectively. Being the distances of each bolt row from the centre of compression are equal to 344 mm and 232 mm respectively, the bending moment resistance of JD7 is equal to 308.08 kNm. The failure is expected in the column web for tension and shear.



**Table 3.19: Resistance and stiffness coefficients of the joint components for JD7**

Specimen	Component	$F_R$ (kN)	$k_i$ (mm)	$M_R$ (kNm)			
JD7	Tension	Column web in tension	689.83	5.22	397.34		
		Column flange in bending	-	52.69			
		First bolt row in tension	T-Stub complete flange yielding	1463.20		-	
			T-Stub flange yielding and bolt failure	761.82		-	
			Bolt in tension	754.86		49.29	
			End-plate in bending	-		7.95	
			T-Stub complete flange yielding	1302.59		-	
			T-Stub flange yielding and bolt failure	706.72		-	
			Second bolt row in tension	Column web in tension		689.83	5.22
				Column flange in bending		-	52.69
		T-Stub complete flange yielding		1463.20		-	
		T-Stub flange yielding and bolt failure		761.82		-	
		Bolts in tension		754.86		7.95	
		End-plate in bending		-		48.22	
		T-Stub complete flange yielding		1339.03		-	
T-Stub flange yielding and bolt failure	743.90	-					
Beam web in tension	770.42	$\infty$					
Compression	Column web in compression	1383.89	$\infty$	345.01			
	Beam flange and web in compression	1197.96	$\infty$				
Shear	Column web in shear	994.89	4.43	286.53			

About the initial rotational stiffness, Table 3.19 shows that the main contribution to stiffness is provided by the connection. In fact the stiffness coefficients of the column flange are equal to 52.69 mm. A great role is played also by the end-plate components. The stiffness coefficients are equal to 49.29 mm and 48.22 mm respectively for the first and the second bolt row. In the connection the more flexible component are the bolts in tension with the stiffness coefficient equal to 7.95. As shown in Table 3.19, the more flexible component is the column web panel in shear. The stiffness coefficient is equal to 4.43 mm. As a consequence the initial rotational stiffness of JD7 is equal to 42378.02 kNm/rad. Finally the yield rotation is equal to 7.27 mrad. As described in the previous Chapter, the rupture involves the end-plate stiffener and the welds between the beam and the end-plate, contrary to

the column web predicted by the theoretical procedure. This apparent contradiction is due to the simplifications included in the mechanical approach. In fact, the component method provides an estimate of the resistance of first yield strength of the weakest component without taking into account of the hardening, which can be the responsible of the fact that the component which first yields is not necessary the same that fails. However the available moment-gap rotation and moment-shear rotation curves demonstrate that both the connection and the column web panel in shear yield. In Figure 3.17 is the classification by strength and by stiffness of JD7. According to Eurocode 3, JD7 is classified as partial strength. Assuming the beam span length equal to 2700 mm, from the stiffness point of view the joint is semi-rigid.

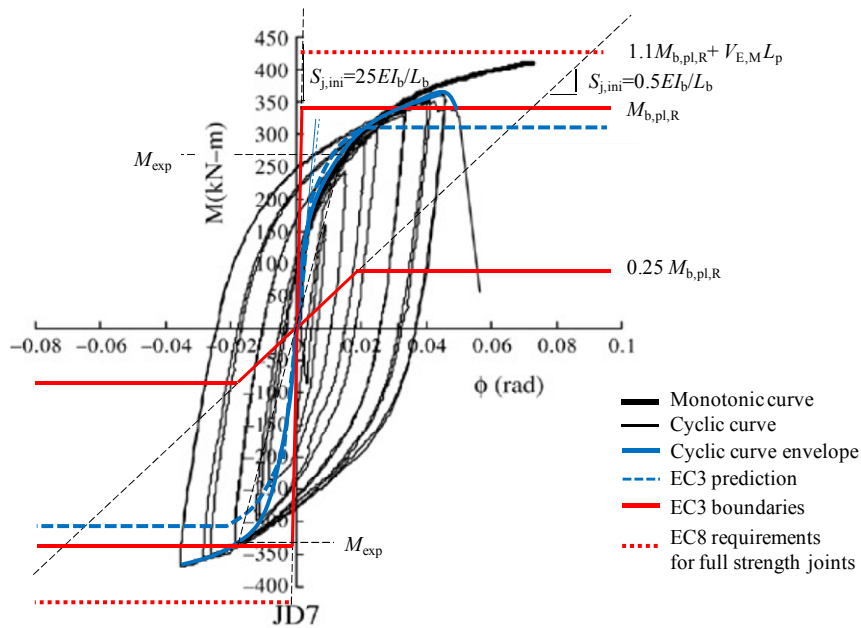


Figure 3.17: Classification by strength and stiffness for JD7

### 3.1.5.7 Specimen JD8

The summary of the application of the component method to the specimen JD8 is in Table 3.20. The theoretical predictions are based on nominal geometrical properties of the beam, column, end-plate and

bolts. Actual values of the material properties are instead supposed. In detail, the yield stress of 409 MPa is considered for the column, beam and end-plate, while the ultimate stress of 1160MPa is used for bolts. expected end-plate yielding and bolt failure is observed during the experimental test.

**Table 3.20: Resistance and stiffness coefficients of the joint components for JD8**

Specimen	Component	$F_R$ (kN)	$k_i$ (mm)	$M_R$ (kNm)	
JD8	Tension	Column web in tension	669.30	5.22	240.61
		Column flange in bending	-	13.81	
	First bolt row in tension	T-Stub complete flange yielding	657.87	-	
		T-Stub flange yielding and bolt failure	433.61	-	
		Bolt in tension	511.56	7.76	
		End-plate in bending	-	12.92	
		T-Stub complete flange yielding	585.66	-	
		T-Stub flange yielding and bolt failure	409.90	-	
		Column web in tension	669.30	5.22	
		Column flange in bending	-	13.81	
	Second bolt row in tension	T-Stub complete flange yielding	657.87	-	
		T-Stub flange yielding and bolt failure	433.61	-	
		Bolts in tension	511.56	7.76	
		End-plate in bending	-	12.64	
		T-Stub complete flange yielding	602.05	-	
		T-Stub flange yielding and bolt failure	425.55	-	
	Beam web in tension	770.42	$\infty$		
Compression	Column web in compression	1279.41	$\infty$	345.01	
	Beam flange and web in compression	1197.96	$\infty$		
Shear	Column web in shear	857.75	4.06	247.03	

Table 3.20 shows that for both the first and the second bolt row the component which first yields is the end-plate. The failure mechanism is the flange yielding and the bolt failure of the equivalent T-Stub which represents the component. The corresponding strengths are equal to 409.90 kN and 425.55 kN respectively. The resisting bending moment due to tension failure of the connection is equal to 240.61 kNm, which is obtained as the product of the total tension resistance (the sum of the

strength of the first and second bolt rows) times the internal lever arm. The compression side is governed by the beam flange and web, whose strength is equal to 1197.96 kN. The corresponding bending moment strength due to compression failure in the connection is equal to 345.01 kNm. Therefore, failure of the connection is expected to occur on the tension side. Finally, the shear strength of the column web panel zone is equal to 857.75 kN. The shear resistance is transformed into a bending strength of 247.03 kNm. The latter is greater than the flexural strength of the connection therefore the connection governs the response of the joint. Thereby, according to the component method the effective tensile resistances associated to the first and the second bolt row are 409.90 kN and 425.55 kN respectively. Considering that the distances of each bolt row from the centre of compression are equal to 344 mm and 232 mm respectively, the bending moment resistance of JD8 is equal to 239.73 kNm. The failure is expected in the end-plate for the flange yielding and bolt failure of the T-Stub representative of the component.

Referring to the rotational stiffness, Table 3.20 shows that the main contribution to stiffness is provided by the column flange and the end-plate. The column flange, with the stiffness coefficient equal to 13.81 mm, is the more rigid component. A great role is played by the end-plate too, in fact the stiffness coefficients are 12.92 mm and 12.64 mm, for the first and the second bolt row respectively.

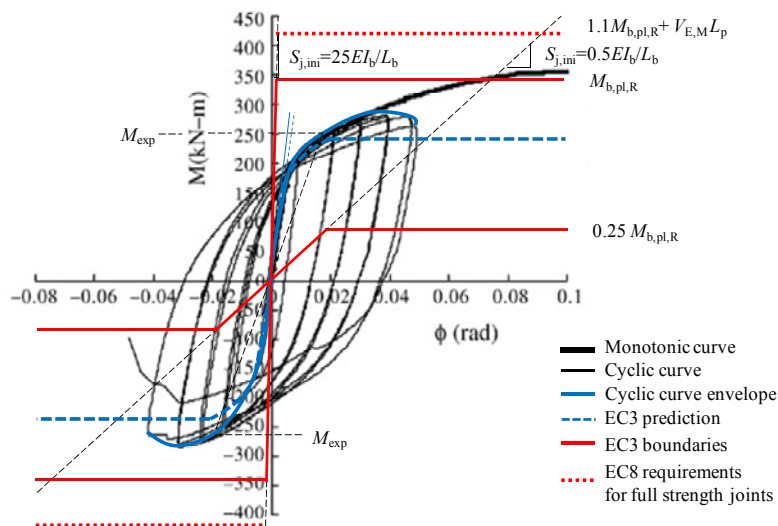


Figure 3.18: Classification by strength and stiffness for JD8

The column web in shear and the bolts in tension are the more flexible component. Their stiffness coefficients are 4.06 mm and 7.76 mm respectively. As a result JD8 initial rotational stiffness is equal to 35489.34 kNm/rad. Finally the yield rotation is equal to 6.75 mrad.

The theoretical predictions are in agreement with the experimental results. The difference between the experimental values and the theoretical ones do not exceed 5%. The classification by strength and stiffness of JD8 according to the Eurocode 3 is given in Figure 3.18. The bending moment resistance is less than the beam plastic resistance therefore JD8 can be classified as partial strength. Assuming for JD8 the beam span length equal to 2700 mm, according to classification by stiffness, the joint is semi-rigid.

## 3.2 FLUSH END-PLATE CONNECTIONS

### 3.2.1 Tests by Broderick and Thomson (2002)

#### 3.2.1.1 Specimen EP1

Table 3.21 contains a synthesis of the application of the component method. Similarly to the end-plate connections, the joint components are grouped on the basis of the loading type (tension, compression and shear loading). For each component, the third and the fourth columns give the strength ( $F_R$ ) and the stiffness coefficient ( $k_i$ ), respectively. The last (fifth) column gives, for each component, the moment resistance ( $M_R$ ) evaluated as the product of the component strength ( $F_R$ ) times the internal lever arm. The calculations are based on the nominal geometrical properties of the specimen (Chapter 2). The resistance of each component considers the expected value of the steel yield stress and nominal ultimate strength of bolts. The expected value of the steel yield stress, equal to 316.25 MPa, takes into account of a material overstrength factor of 1.15. Table 3.21 shows that for the bolt row in tension the component which first yields is the end-plate. The failure mechanism is complete flange yielding of the equivalent T-Stub. The corresponding strength is equal to 121.44 kN. The moment resistance corresponding to tension failure of the connection is equal to 23.15 kNm. The beam flange and web governs the compression side, whose strength is equal to

331.37 kN. The corresponding bending moment strength due to compression failure in the connection is equal to 63.16 kNm. Therefore, failure occurs on the tension side of the connection. Finally, the shear strength of the column web panel zone is equal to 644.86 kN. The bending strength corresponding to the shear resistance is equal to 122.91 kNm. The latter is greater than the flexural strength of the connection which, therefore, governs the response of the joint. As a result, according to the component method the moment resistance of EP1 is 23.15 kNm and the failure mode is complete flange yielding of the end-plate T-Stub.

**Table 3.21: Resistance and stiffness coefficients of the joint components for EP1**

Specimen	Component	$F_R$	$k_i$	$M_R$
EP1		(kN)	(mm)	(kNm)
Tension	Column web in tension	570.51	10.59	108.74
	Column flange in bending	-	52.40	-
	T-Stub complete flange yielding	835.06	-	159.16
	T-Stub flange yielding and bolt failure	386.24	-	73.62
	Bolt in tension	352.80	8.34	67.24
	End-plate in bending	-	1.56	-
	T-Stub complete flange yielding	121.44	-	23.15
	T-Stub flange yielding and bolt failure	224.26	-	42.74
	Beam web in tension	455.88	$\infty$	86.89
Compression	Column web in compression	529.12	9.30	100.85
	Beam flange and web in compression	331.37	$\infty$	63.16
Shear	Column web in shear	644.86	6.11	122.91

Concerning the rotational stiffness, Table 3.21 shows that the column flange is the more rigid component, in fact, the stiffness coefficient equal to 52.40 mm. The end-plate is the more flexible component instead. Its stiffness coefficient is equal to 1.56 mm. The other connection components, the column web panel in tension, compression and bolts present the stiffness coefficient equal to 10.59 mm, 9.30 mm and 8.34 mm respectively. Finally, a stiffness coefficient of 6.11 mm characterises the column web panel in shear. The rotational stiffness of the assemblage is equal to 6650.77 kNm/rad. Consequently the yield rotation is equal to 3.48 mrad.

As described in the previous Chapter, the Authors did not provide the moment rotation curve of EP1, therefore only the comparison with the experimental stiffness was possible. The comparison showed that, in case of EP1, the mechanical approach underestimates of 22% the initial rotational stiffness. In accordance with classification by strength, the configuration is partial strength; in fact the joint moment resistance is less than the beam plastic resistance. Assuming for EP1 a beam span twice the cantilever length (1722 mm), EP1, from the stiffness point of view, is semirigid.

### **3.2.1.2 Specimen EP2**

Table 3.22 contains the summary of the component method application. Similarly to the previous case, the calculations consider the following assumptions: the geometrical properties of the specimen are equal to the nominal values, the steel yield stress is equal to the expected value of 316.25 MPa evaluated assuming a material overstrength of 1.15; the ultimate strength of bolts is equal to the nominal value of 800 MPa. As shown (Table 3.22), at the tension side of the connection the weakest component is the end-plate again. Because of the thicker end-plate, the failure mechanism changed to flange yielding and bolt failure T-Stub. The strength and the resisting bending moment due to tension failure of the connection are equal to 259.59 kN and 49.48 kNm respectively. At the compression side, the weakest component is the beam flange and web, whose strength is equal to 331.37 kN. The corresponding bending moment strength is equal to 63.16 kNm. Therefore, failure occurs on the tension side of the connection. Concerning the shear strength, it is the same calculated for of EP1 since the column section is unchanged. The shear strength and the related bending strength are equal to 644.86 kN and 122.91 kNm respectively. The latter is greater than the flexural strength of the connection which, therefore, governs the response of the joint. As a result, according to the component method the moment resistance of EP2 is 49.48 kNm. The failure mechanism is flange yielding and bolt failure.

About the rotational stiffness, Table 3.22 shows that the column flange, with the stiffness coefficient equal to 52.40 mm, is the more rigid component. As the previous case, the more flexible component is the end-plate. Its stiffness coefficient is equal to 5.25 mm. The increased end-plate thickness produces higher end-plate stiffness coefficient. Changes are noted also for bolts in tension and column web panel in

compression stiffness coefficients. The first is slightly smaller than that of the previous case; in fact the bolt length is larger because of the increased end-plate thickness. Concerning the column web panel in compression contribution, it is greater than that determined for EP1. This is due to the proportional increase of the effective width. As a result, the initial rotational stiffness is equal to 10858.21kNm/rad. Consequently the yield rotation is equal to 4.56 mrad.

**Table 3.22: Resistance and stiffness coefficients of the joint components for EP2**

Specimen	Component	$F_R$	$k_i$	$M_R$
EP2		(kN)	(mm)	(kNm)
Tension	Column web in tension	570.51	10.59	108.74
	Column flange in bending	-	52.40	-
	T-Stub complete flange yielding	835.06	-	159.16
	T-Stub flange yielding and bolt failure	386.24	-	73.62
	Bolt in tension	352.80	7.69	67.24
	End-plate in bending	-	5.25	-
	T-Stub complete flange yielding	273.24	-	52.08
	T-Stub flange yielding and bolt failure	259.59	-	49.48
	Beam web in tension	455.88	$\infty$	86.89
Compression	Column web in compression	536.72	9.53	102.30
	Beam flange and web in compression	331.37	$\infty$	63.16
Shear	Column web in shear	644.86	6.11	122.91

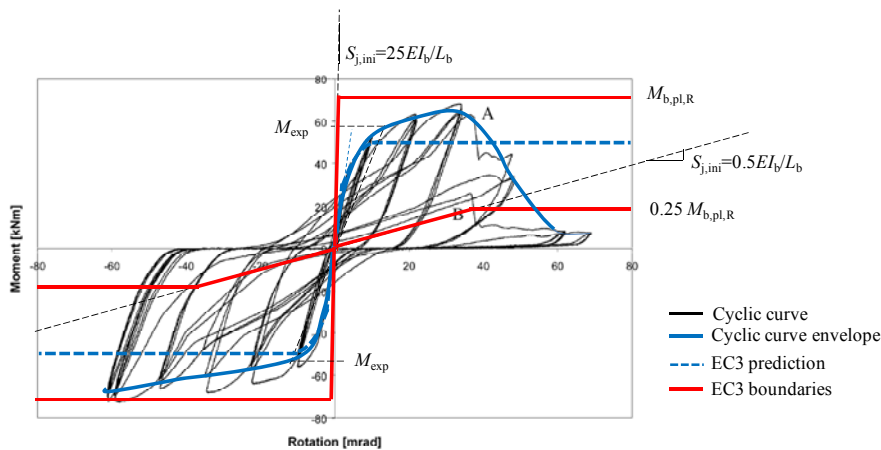


**Figure 3.19: Classification by strength and stiffness for EP2**



The comparison with the experimental results shows a great accordance between the theoretical predictions and the effective behaviour of the joint since the moment resistance is overestimated of 10% and the initial stiffness is overestimation of about 7%. The yield rotation is overestimated of 6%.

Figure 3.19 shows the classification by strength and stiffness of EP2 in accordance with Eurocode 3. As shown, the joint can be classified as semirigid partial strength. The classification by stiffness considers that the beam span is twice the cantilever length (1722 mm).

### 3.2.1.3 Specimens EP3 and EP4

The details of the application of the component method are given in Table 3.23. As for the previous two cases, they consider that the geometrical properties of the specimen are equal to the nominal values, the steel yield stress is equal to the expected value of 316.25 MPa ( $=275\text{MPa}\times 1.15$ ) evaluated assuming a material overstrength of 1.15; the ultimate strength of bolts is equal to the nominal value of 800 MPa.

**Table 3.23: Resistance and stiffness coefficients of the joint components for EP3 and EP4**

Specimen	Component	$F_R$	$k_i$	$M_R$
EP3, EP4		(kN)	(mm)	(kNm)
Tension	Column web in tension	570.51	10.59	106.37
	Column flange in bending	-	52.40	-
	T-Stub complete flange yielding	835.06	-	155.70
	T-Stub flange yielding and bolt failure	386.24	-	72.01
	Bolt in tension	352.80	7.69	65.78
	End-plate in bending	-	5.33	-
	T-Stub complete flange yielding	273.24	-	50.95
	T-Stub flange yielding and bolt failure	259.59	-	48.40
	Beam web in tension	500.29	$\infty$	93.28
Compression	Column web in compression	544.30	9.75	101.48
	Beam flange and web in compression	623.51	$\infty$	116.25
Shear	Column web in shear	640.95	6.25	119.50

The results are similar to those obtained for EP2, since the specimens differ only for the beam section. Therefore, as for EP2, on the tension

side the weakest component is the end-plate which fails according to the flange yielding and bolt failure. The corresponding strength and the moment resistance are equal to 259.59 kN and 48.40 kNm respectively. The column web, whose strength is equal to 544.30 kN, governs the compression side of the connection. The corresponding bending moment strength due to compression failure in the connection is equal to 101.48 kNm. Therefore, failure involves the tension side of the connection. Finally, the shear strength of the column web panel zone is equal to 640.95 kN. The shear resistance is transformed into a bending strength of 119.50 kNm. The latter is greater than the flexural strength of the connection which, therefore, governs the response of the joint. As a result, according to the component method the moment resistance of the specimens is 48.40 kNm. The failure mechanism is flange yielding and bolt failure of the end-plate equivalent T-Stub. Concerning the rotational stiffness, Table 3.23 shows that the main contribution to stiffness is provided by the connection. The column flange is again the more rigid component. Its stiffness coefficient is equal to 52.40 mm. The end-plate remains the more flexible component even if its stiffness coefficient is larger than the previous case (5.33 mm). A comparable stiffness coefficient is that of the column web panel in shear, which is equal to 6.25 mm. Consequently, the initial rotational stiffness of EP3 and EP4 is equal to 10520.84 kNm/rad. Finally, according to the component method the yield rotation is equal to 4.60 mrad.

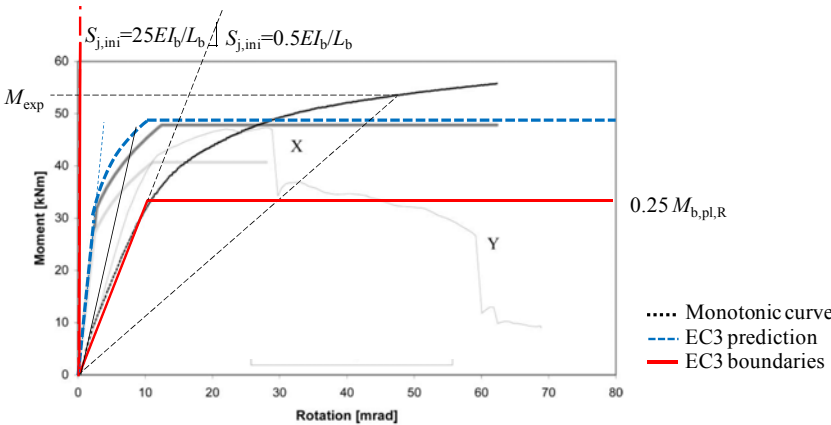


Figure 3.20: Classification by strength and stiffness for EP3

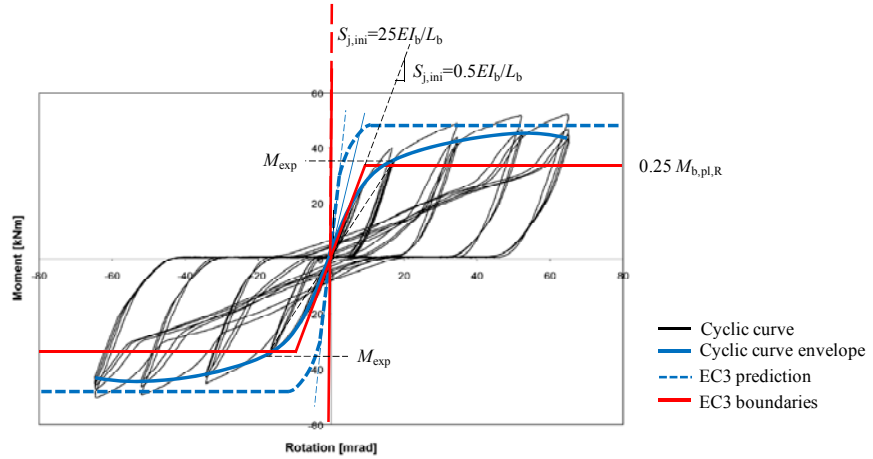


Figure 3.21: Classification by strength and stiffness for EP4

The comparison of the theoretical predictions with the experimental results is not possible because the expected plastic mechanism differs from that observed during the test. Mode 1 mechanism was observed instead of mode 2 mechanism. The discrepancy is probably due to the difference between the expected material properties, considered in this application, and the material actual values. Anyway, the classifications according to Eurocode 3 are in Figure 3.20 and Figure 3.21. As shown, both EP3 and EP4 are semi-rigid partial strength joints.

#### 3.2.1.4 Specimen EP5

Table 3.24 contains a summary of the application of the component method for EP5. The basic assumptions are the same adopted in the previous cases: the geometrical properties are the nominal ones, the steel yield stress is equal to the expected value (316.25 MPa) and the bolt strength is equal to the nominal value (1000 MPa). As displayed the weakest component of the tension side is the end-plate which fails for the complete flange yielding mechanism. The improvement of the bolt class (Table 2.9) prevents the bolt yielding and allows the end-plate failure according to mode 1. The strength of the end-plate is equal to 273.24 kN. The corresponding resisting bending moment is equal to 50.29 kNm. At the compression side the weakest component is the column web, whose strength is equal to 544.30 kN. The corresponding bending moment strength due to compression failure in the connection is equal to 101.48 kNm. Therefore, failure of the connection is expected

to occur on the tension side. Finally, the shear strength of the column web panel zone is equal to 640.95 kN. The shear resistance is transformed into a bending strength of 119.50 kNm. The latter is greater than the flexural strength of the connection which, therefore, governs the response of the joint. As a result, according to the component method the moment resistance of EP2 is 20.13 kNm. The failure is expected in the end-plate for complete flange yielding of the corresponding T-Stub.

**Table 3.24: Resistance and stiffness coefficients of the joint components for EP5**

Specimen	Component	$F_R$	$k_i$	$M_R$
EP5		(kN)	(mm)	(kNm)
Tension	Column web in tension	570.51	10.59	106.37
	Column flange in bending	-	52.40	-
	T-Stub complete flange yielding	835.06	-	155.70
	T-Stub flange yielding and bolt failure	435.24	-	81.15
	Bolt in tension	441.00	7.69	82.22
	End-plate in bending	-	5.33	-
	T-Stub complete flange yielding	273.24	-	50.29
	T-Stub flange yielding and bolt failure	308.59	-	57.54
	Beam web in tension	500.29	$\infty$	93.28
Compression	Column web in compression	544.30	9.75	101.48
	Beam flange and web in compression	623.51	$\infty$	116.25
Shear	Column web in shear	640.95	6.25	119.50

Concerning the rotational stiffness, Table 3.24 shows that the main contribution to stiffness is provided by the connection. The column flange, with the stiffness coefficient equal to 52.40 mm, is the more rigid component. On the other hand, the more flexible component is the end-plate. Its stiffness coefficient is equal to 5.33mm. Great deformability is also provided by the column web panel in tension, compression and bolts in tension. Their stiffness coefficients are 10.59 mm, 9.75 mm and 7.69 mm respectively. The stiffness coefficient of the column web panel in shear is 6.25mm. Consequently, the initial rotational stiffness is equal to 10520.84 kNm/rad. Finally, the yield rotation is equal to 4.84 mrad.

The moment rotation curve of EP5 is not provided; therefore the comparison with the experimental results is possible only from the

stiffness point of view. In case of EP5, the component method overestimates the initial stiffness of about 90%.

Concerning the joint classification, since the theoretical moment resistance is less than the beam plastic resistance, EP5 can be classified as partial strength. Assuming for EP5 the beam span equal to 1722 mm, the comparison of the joint rotational stiffness with the flexural stiffness of the connected beam, indicates that EP5 is semi-rigid.

### 3.2.1.5 Specimen EP6, EP7 and EP8

The details of the component method in case of EP6, EP7 and EP8 are in Table 3.25. As before, the calculations consider nominal geometrical properties of the specimen, the expected value of the steel yield stress (316.25 MPa) and the nominal bolt strength (800 MPa). Table 3.25 shows that for the bolt row in tension the weakest component is the bolt in tension. The thicker end-plate allows the mode 3 mechanism.

**Table 3.25: Resistance and stiffness coefficients of the joint components for EP6, EP7 and EP8**

Specimen	Component	$F_R$	$k_\xi$	$M_R$
EP6,EP7,EP8		(kN)	(mm)	(kNm)
Tension	Column web in tension	570.51	10.59	106.37
	Column flange in bending	-	52.40	-
	T-Stub complete flange yielding	835.06	-	155.70
	T-Stub flange yielding and bolt failure	315.84	-	58.89
	Bolt in tension	226.08	4.49	42.15
	End-plate in bending	-	24.67	-
	T-Stub complete flange yielding	759.00	-	141.52
	T-Stub flange yielding and bolt failure	302.23	-	56.35
	Beam web in tension	500.29	$\infty$	93.28
	Compression	Column web in compression	558.47	10.19
Beam flange and web in compression		623.51	$\infty$	116.25
Shear	Column web in shear	640.95	6.25	119.50

The strength and the resisting bending moment due tension failure are equal to 226.08 kN and 42.15 kNm respectively. The resistance of the compression side is equal to 558.47 kN. The corresponding bending

moment strength due to compression failure in the connection is equal to 104.13 kNm. Therefore, failure occurs in the connection.

Finally, the shear strength of the column web panel zone is equal to 640.95 kN. The corresponding bending strength is 119.50 kNm. The latter is greater than the flexural strength of the connection which, therefore, governs the response of the joint. As a result, according to the component method the moment resistance of EP6, EP7 and EP8 is equal to 42.15 kNm. Bolt failure is expected.

Concerning the rotational stiffness, Table 3.25 shows a great improvement of the end-plate stiffness (24.67 mm) even if the more rigid component is always the column flange (52.40 mm). In this configuration the bolt in tension is the more flexible component. In fact the stiffness coefficient is equal to 4.49 mm. The stiffness coefficients associated to the other components are almost unchanged. The initial rotational stiffness of EP6, EP7 and EP8 is equal to 11494.43 kNm/rad. Therefore the yield rotation is equal to 3.67 mrad.

Comparing the theoretical prediction with the experimental results, in case of EP6 the component method underestimates the moment resistance of 10% and overestimates of about 300% the initial stiffness. For EP7 and EP8 the procedure overestimates both the resistance and the stiffness instead. The resistance is overestimated of 14% (EP7) and 20% (EP8). Great overestimation of the stiffness are obtained in case of EP6 (359%) and EP7 (418%).

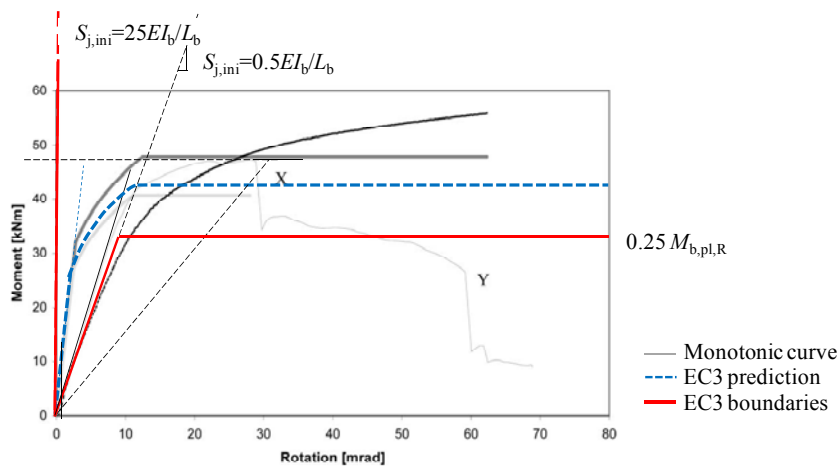


Figure 3.22: Classification by strength and stiffness for EP6

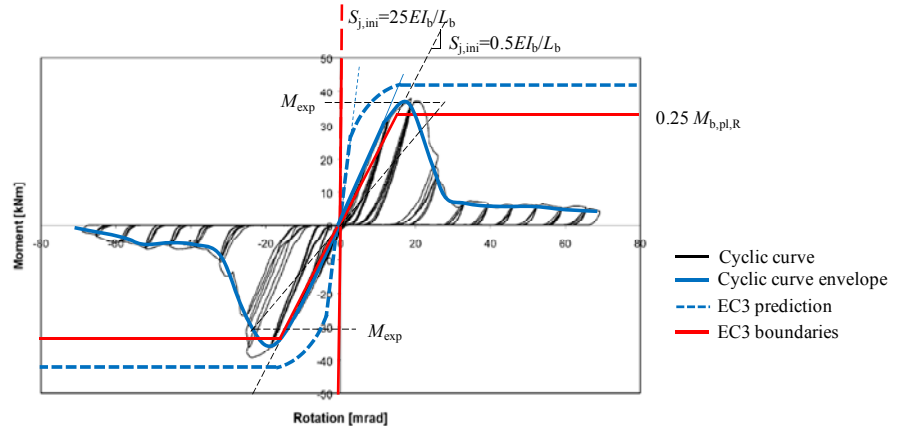


Figure 3.23: Classification by strength and stiffness for EP7

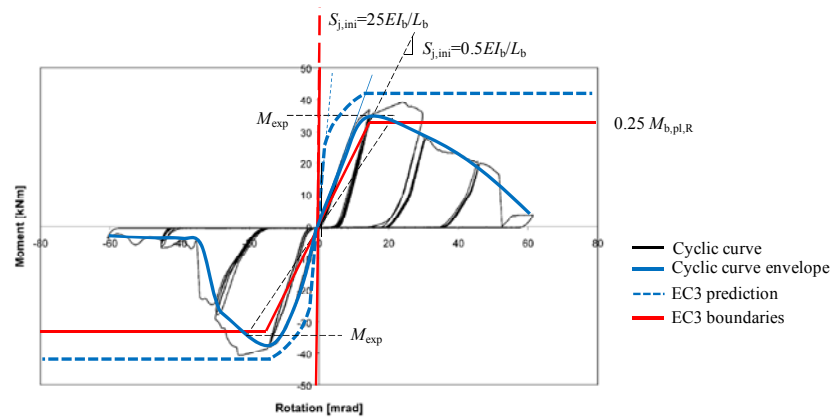


Figure 3.24: Classification by strength and stiffness for EP8

### 3.2.2 Test by da Silva *et al.* (2004)

The details of the analytical procedure are given in Table 3.26. The nominal geometrical properties of members, end-plate and bolts were used. Actual values of the steel yield stress were considered (Table 2.12). The yield stress of the column flange and web were equal to 344.92 MPa and 392.63 MPa respectively. For the beam web flange and they were 366.45 MPa and 365.83 MPa respectively. The yield strength of the end-plate was 365.39 MPa. The bolt ultimate stress was equal to the nominal value of 1000 MPa. Table 3.26 contains, similarly to the previous cases, a

list of components grouped on the basis of the loading type (tension, compression and shear loading). For each component the the strength, the stiffness coefficient and the resisting bending moment are specified. As shown, the weakest component of the tension side is the end-plate. The failure mechanism is the flange yielding and bolt failure of the equivalent T-Stub which represents the component. The corresponding strength is equal to 337.97 kN.

**Table 3.26: Resistance and stiffness coefficients of the joint components for FE1**

Specimen	Component	$F_R$	$k_i$	$M_R$
FE1		(kN)	(mm)	(kNm)
Tension	Column web in tension	562.82	7.03	108.83
	Column flange in bending	-	40.47	-
	T-Stub complete flange yielding	626.32	-	120.94
	T-Stub flange yielding and bolt failure	409.30	-	79.04
	Bolt in tension	441.00	7.76	85.16
	End-plate in bending	-	10.46	-
	T-Stub complete flange yielding	485.06	-	93.66
	T-Stub flange yielding and bolt failure	337.97	-	65.26
	Beam web in tension	554.86	$\infty$	107.14
Compression	Column web in compression	673.22	9.76	130.00
	Beam flange and web in compression	583.16	$\infty$	112.61
Shear	Column web in shear	760.37	6.54	146.83

The resisting bending moment due to tension failure of the connection is equal to 65.26 kNm. The compression side is governed by the beam flange and web, whose strength is equal to 583.16 kN. The corresponding bending moment strength due to compression failure in the connection is equal to 112.61 kNm.

Therefore, failure involves the tension side of the connection. Finally, the shear strength of the column web panel zone is equal to 760.37 kN. The shear resistance is transformed into a bending strength of 146.83 kNm. The latter is greater than the flexural strength of the connection which, therefore, governs the response of the joint. As a result, according to the component method the moment resistance of FE1 is



65.26 kNm. Flange yielding and bolt failure of the end-plate is the failure mechanism.

Concerning the rotational stiffness, Table 3.26 shows that the main contribution to stiffness is provided by the connection by the column flange, which is the more rigid component (40.47 mm). For FE1 the more flexible component is the column web panel in shear. Its stiffness coefficient is equal to 6.54 mm. Great deformability is also provided by the column web panel in tension and bolts in tension. Their stiffness coefficients are 7.03 mm and 7.76 mm respectively. Consequently the initial rotational stiffness is equal to 12106.46 kNm/rad. Finally the yield rotation is equal to 5.39 mrad.

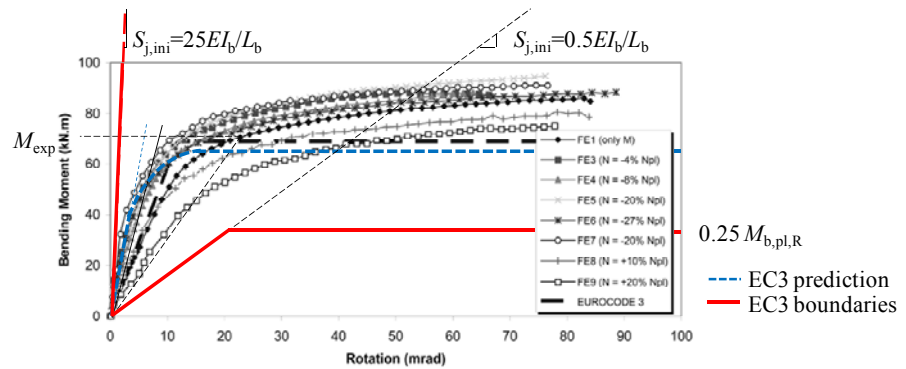


Figure 3.25: Classification by strength and stiffness for FE1

### 3.2.3 Tests by Broderick and Thomson (2005)

#### 3.2.3.1 Specimens FP1 and FP2

The bending strength and the initial stiffness of FP1 and FP2 were determined assuming the nominal geometrical properties of the beam, column, end-plate and bolts. These are described in detail in the previous Chapter. Concerning the material properties, Authors provided only the nominal values of the steel yield stress and the bolt ultimate tensile strength. For a better prediction, the expected value of the yield stress of the steel was considered. In accordance with Eurocodes the overstrength of 15% was supposed. The nominal Young modulus was considered.

Table 3.27 contains a synthesis of the application of the component method. The calculations are based on the nominal geometrical properties of the specimen (Chapter 2). The resistance of each

component consider expected value of the steel yield stress and nominal ultimate strength of bolts. The expected value of the steel yield stress (316.25 MPa) takes into account of a material overstrength factor of 1.15, while the ultimate bolt stress is equal to 800 MPa. As shown in the Table, the weakest component of the first bolt row in tension is the end-plate. The failure mechanism is complete flange yielding of the equivalent T-Stub. The corresponding strength is equal to 194.18 kN. The resisting bending moment due to tension failure of the connection is equal to 37.00 kNm. The column web is the weakest component of the compression side. Its strength is equal to 540.63 kN. The corresponding bending moment strength due to compression failure in the connection is equal to 103.02 kNm. Therefore, failure of the connection is expected to occur on the tension side. Finally, the shear strength of the column web panel zone is equal to 644.81 kN. The shear resistance is transformed into a bending strength of 122.87 kNm. The latter is greater than the flexural strength of the connection which, therefore, governs the response of the joint. As a result, according to the component method the moment resistance of FP1 and FP2 is 37.00 kNm.

**Table 3.27: Resistance and stiffness coefficients of the joint components for FP1 and FP2**

Specimen	Component	$F_R$	$k_i$	$M_R$
FP1, FP2		(kN)	(mm)	(kNm)
Tension	Column web in tension	570.51	10.59	108.71
	Column flange in bending	-	52.40	-
	T-Stub complete flange yielding	835.06	-	159.12
	T-Stub flange yielding and bolt failure	386.24	-	73.60
	Bolt in tension	352.80	8.00	67.23
	End-plate in bending	-	3.16	-
	T-Stub complete flange yielding	194.18	-	37.00
	T-Stub flange yielding and bolt failure	240.16	-	45.76
	Beam web in tension	511.96	$\infty$	97.55
Compression	Column web in compression	540.63	9.64	103.02
	Beam flange and web in compression	623.51	$\infty$	118.81
Shear	Column web in shear	644.81	6.11	122.87

Failure is expected in the end-plate for complete flange yielding of the corresponding T-Stub.

Concerning the rotational stiffness, Table 3.27 shows that the main contribution to stiffness is provided by the connection. The column flange, with the stiffness coefficient equal to 52.40 mm, is the more rigid component. The end-plate is the more flexible component. Its stiffness coefficient is equal to 3.16 mm. Great deformability is also provided by the column web panel in shear since its stiffness coefficient is 6.11 mm. Consequently the initial rotational stiffness is equal to 9267.81 kNm/rad. Finally the yield rotation is equal to 3.99 mrad.

Comparing the theoretical prediction with the experimental results, a slightly difference is noted in case of the moment resistance but significant differences are noted for the initial stiffness.

Figure 3.26 and Figure 3.27 show the classification by strength and stiffness of each specimen. Both FP1 and FP2 are partial strength joints. For a beam span twice the cantilever length (1722 mm), according to the classification by stiffness the joints are semi-rigid.

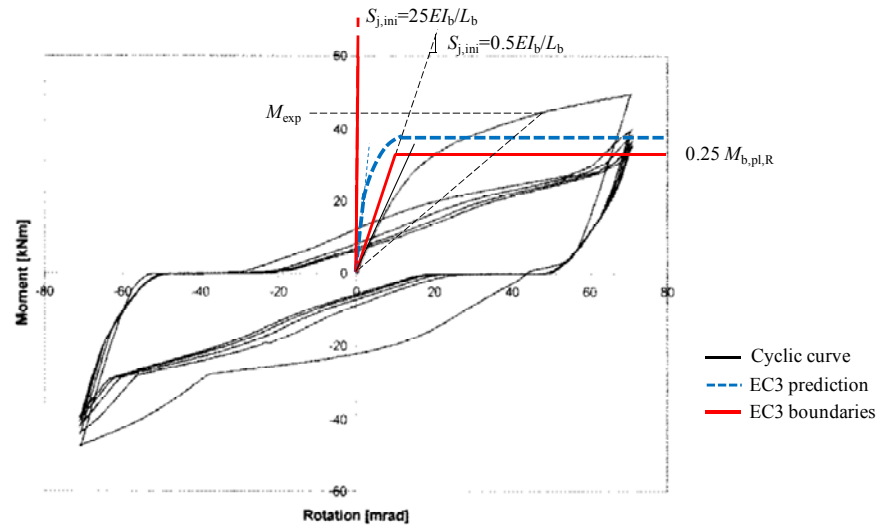


Figure 3.26: Classification by strength and stiffness for FP1

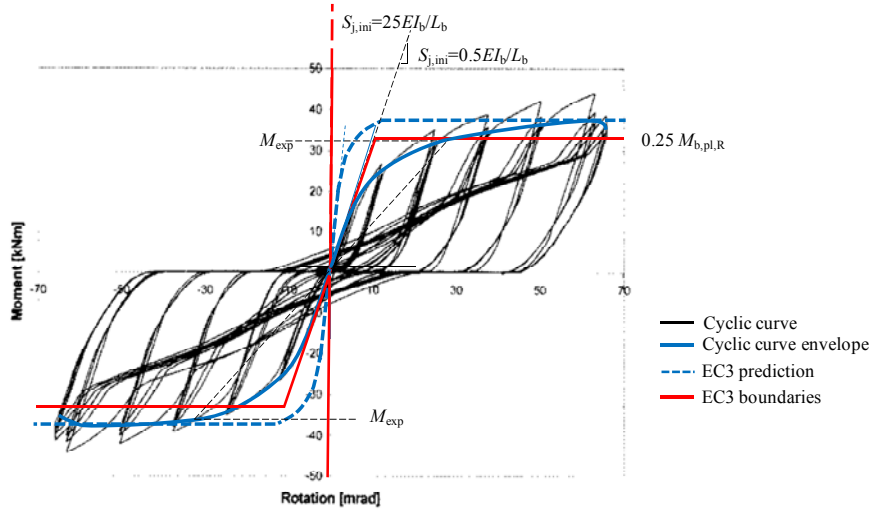


Figure 3.27: Classification by strength and stiffness for FP2

### 3.2.3.2 Specimens FP3 and FP4

The synthesis of the application of the component method is given in Table 3.28 contains a summary of the application in case of FP3 and FP4. As previously, the theoretical predictions are based on the nominal geometrical properties of the beam, column, end-plate and bolts, described in detail in Table 2.13. Expected value of the steel yield stress (316.25 MPa), and the nominal value of the ultimate stress (800 MPa) for bolts were considered. Table 3.28 shows that the weakest component of the bolt row in tension is the end-plate. The failure mechanism is the flange yielding and bolt failure of the equivalent T-Stub. The corresponding strength is equal to 295.35 kN. The resisting bending moment due to tension failure of the connection is equal to 56.28 kNm. The compression side is governed again by the column web, whose strength is equal to 542.18 kN. The corresponding bending moment strength due to compression failure in the connection is equal to 118.81 kNm. Therefore, failure of the connection is expected on the tension side. Finally, the shear strength of the column web panel zone is equal to 644.81 kN. The shear resistance is transformed into a bending strength of 122.87 kNm. The latter is greater than the flexural strength of the connection which, therefore, governs the response of the joint. As a result, according to the component method the moment resistance of

FP3 and FP4 is 56.28 kNm. Failure is expected in the end-plate for flange yielding and bolt failure of the equivalent T-Stub. Because of the thicker end-plate, the failure mechanism changed to flange yielding and bolt failure T-Stub. Concerning the rotational stiffness (Table 3.26), as before, the main contribution to stiffness is provided by the column flange (52.40 mm), which is the more rigid component. The end-plate stiffness (10.65 mm) is much higher than the previous configuration. Differently from the previous specimens, the more flexible component is the column web panel in shear. Its stiffness coefficient is equal to 6.11 mm. Great deformability is also provided by column web panel in tension compression and bolts in tension. Their stiffness coefficients are 10.59 mm, 9.92 mm and 7.26 mm respectively. As a result, the initial rotational stiffness is equal to 12508.82 kNm/rad. According to the component method, the yield rotation is equal to 4.50 mrad.

**Table 3.28: Resistance and stiffness coefficients of the joint components for FP3 and FP4**

Specimen	Component	$F_R$	$k_i$	$M_R$
FP3, FP4		(kN)	(mm)	(kNm)
Tension	Column web in tension	570.51	10.59	108.71
	Column flange in bending	-	52.40	-
	T-Stub complete flange yielding	835.06	-	159.12
	T-Stub flange yielding and bolt failure	386.24	-	73.60
	Bolt in tension	352.80	7.26	67.23
	End-plate in bending	-	10.65	-
	T-Stub complete flange yielding	436.90	-	83.25
	T-Stub flange yielding and bolt failure	295.35	-	56.28
	Beam web in tension	511.96	$\infty$	97.55
	Compression	Column web in compression	549.70	9.92
Beam flange and web in compression		542.18	$\infty$	118.81
Shear	Column web in shear	644.81	6.11	122.87

The comparison between the theoretical prediction and the experimental results shows that the component method provides a great prediction of the moment resistance, but it overestimates the initial stiffness of 350-400%. The classification of FP3 and FP4 is in Figure 3.28 and Figure 3.29 respectively.

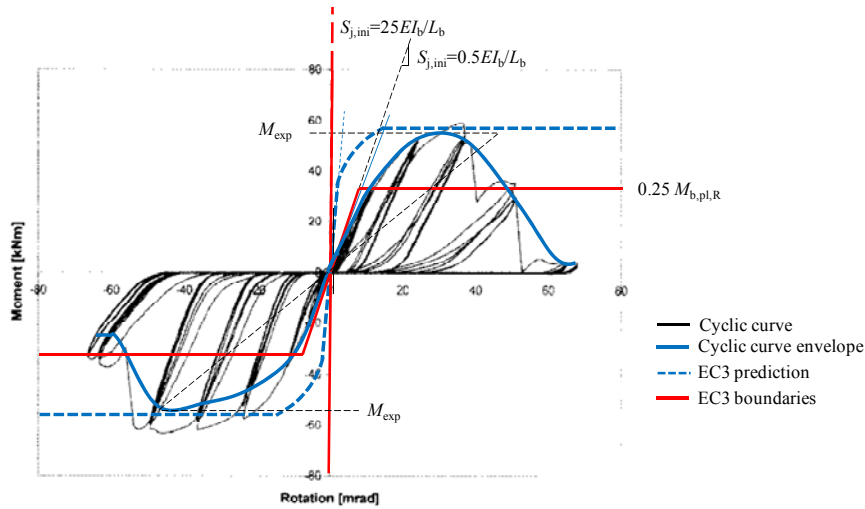


Figure 3.28: Classification by strength and stiffness for FP3

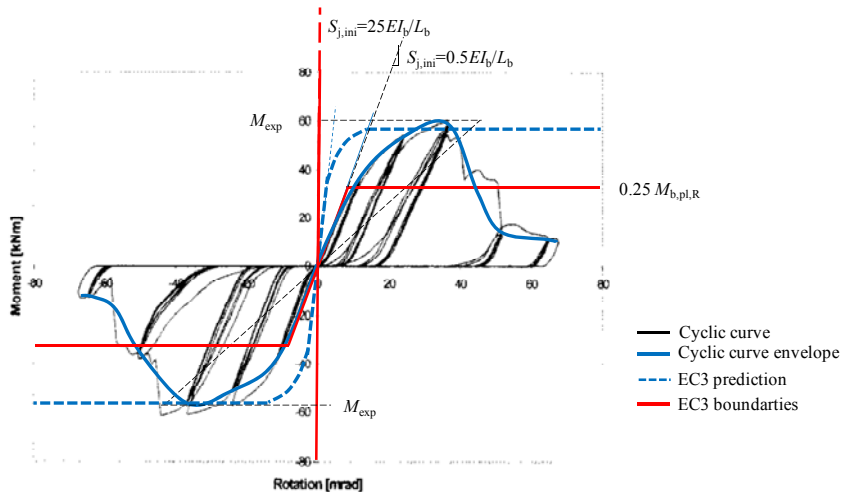


Figure 3.29: Classification by strength and stiffness for FP4

### 3.2.3.3 Specimens FP5 and FP6

Table 3.29 contains a synthesis of the application of the component method. The geometrical assumption and the material properties are the same of the previous pair of specimens. According to Table 3.29, the

weakest component of the bolt row in tension is the end-plate. The failure mechanism is flange yielding and bolt failure of the corresponding equivalent T-Stub. The related strength is equal to 259.59kN. The resisting bending moment due to tension failure of the connection is equal to 49.46 kNm. The compression side is governed by the column web, whose strength is equal to 285.00 kN. The corresponding bending moment strength due to compression failure in the connection is equal to 54.31 kNm. Therefore, failure of the connection is expected to occur on the tension side. Finally, the shear strength of the column web panel zone is equal to 393.25 kN. The shear resistance is transformed into a bending strength of 74.93 kNm. The latter is greater than the flexural strength of the connection which, therefore, governs the response of the joint. As a result, according to the component method the moment resistance of FP5 and FP6 is 49.46 kNm. Failure is expected in the end-plate for flange yielding and bolt failure

**Table 3.29: Resistance and stiffness coefficients of the joint components for FP5 and FP6**

Specimen	Component	$F_R$	$k_i$	$M_R$
FP5, FP6		(kN)	(mm)	(kNm)
Tension	Column web in tension	363.02	6.96	69.17
	Column flange in bending	-	10.03	-
	T-Stub complete flange yielding	304.98	-	58.11
	T-Stub flange yielding and bolt failure	263.77	-	50.26
	Bolt in tension	352.80	9.12	67.23
	End-plate in bending	-	5.45	-
	T-Stub complete flange yielding	279.62	-	53.28
	T-Stub flange yielding and bolt failure	259.59	-	49.46
	Beam web in tension	511.96	$\infty$	97.55
	Compression	Column web in compression	285.00	4.68
Beam flange and web in compression		623.51	$\infty$	118.81
Shear	Column web in shear	393.25	3.74	74.93

Concerning the rotational stiffness, Table 3.29 shows that the main contribution to stiffness is provided by the connection. The column flange in bending is the more rigid component even if its stiffness coefficient is much reduced compared the previous specimens. Its

stiffness coefficient is equal to 10.03 mm. The more flexible component is the column web panel in shear. Its stiffness coefficient is equal to 3.74 mm. Great deformability is also provided by the column web panel in tension, compression and the end-plate. Their stiffness coefficients are 6.96 mm, 4.68mm and 5.45 mm respectively. Consequently the initial rotational stiffness is equal to 7492.55 kNm/rad. Finally the yield rotation is equal to 6.60 mrad.

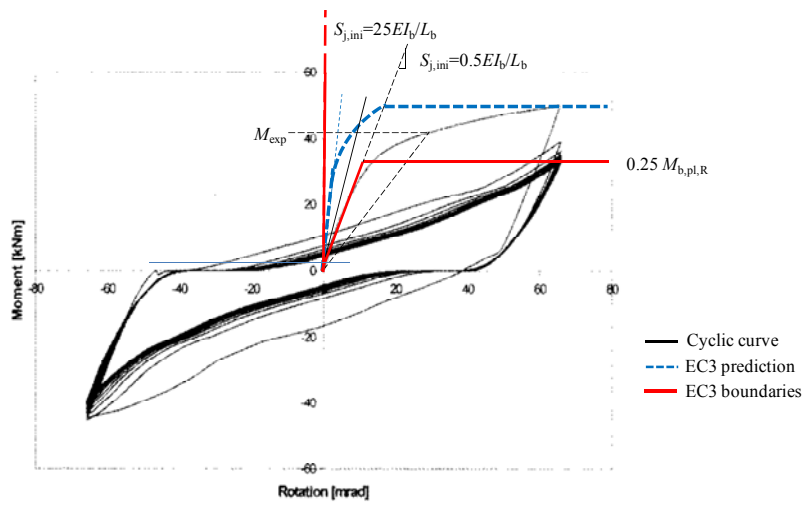


Figure 3.30: Classification by strength and stiffness for FP5

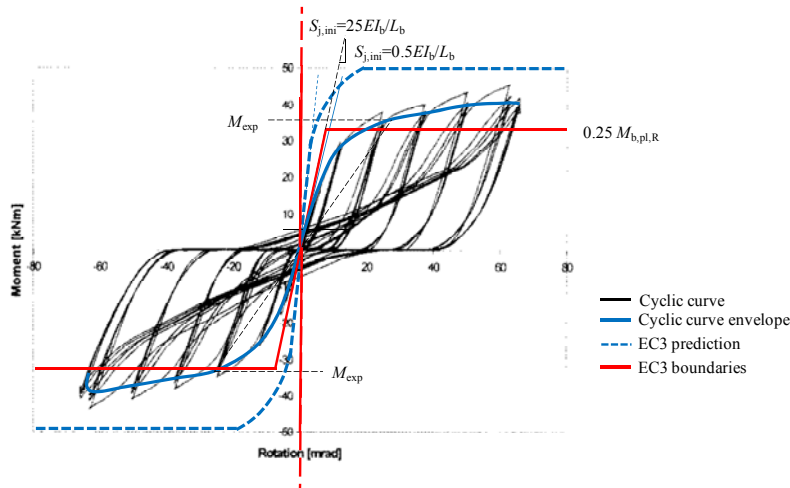


Figure 3.31: Classification by strength and stiffness for FP6



The comparison between the theoretical prediction and the experimental results shows again a great overestimation of the initial stiffness by the component method. In case of FP5 and FP6, the theoretical initial stiffness is about 2.13 and 2.37 times the experimental value.

The classification by strength and stiffness of both specimens are in Figure 3.30 and Figure 3.31.

#### 3.2.3.4 Specimens FP7 and FP8

Table 3.30 contains a synthesis of the application of the component method. The procedure assumes nominal geometrical properties, expected steel yield stress and ultimate strength of bolts as specified for the previous case. As shown the weakest component of the bolt row in tension is the end-plate. The failure mechanism is complete flange yielding of the equivalent T-Stub which represents the component. The corresponding strength is equal to 279.62 kN. The resisting bending moment due to tension failure of the connection is equal to 53.28 kNm.

**Table 3.30: Resistance and stiffness coefficients of the joint components for FP7 and FP8**

Specimen	Component	$F_R$	$k_i$	$M_R$
FP7, FP8		(kN)	(mm)	(kNm)
Tension	Column web in tension	570.51	10.59	108.71
	Column flange in bending	-	52.40	-
	T-Stub complete flange yielding	835.06	-	159.12
	T-Stub flange yielding and bolt failure	435.24	-	82.94
	Bolt in tension	441.00	7.69	84.03
	End-plate in bending	-	5.45	-
	T-Stub complete flange yielding	279.62	-	53.28
	T-Stub flange yielding and bolt failure	308.59	-	58.80
	Beam web in tension	511.96	$\infty$	97.55
Compression	Column web in compression	544.30	9.75	103.72
	Beam flange and web in compression	623.51	$\infty$	118.81
Shear	Column web in shear	644.81	6.11	122.87

The compression side is governed by the column web, whose strength is equal to 544.30 kN. The corresponding bending moment strength due to

compression failure in the connection is equal to 103.72 kNm. Therefore, failure of the connection is expected to occur on the tension side. Finally, the shear strength of the column web panel zone is equal to 644.81 kN. The shear resistance is transformed into a bending strength of 122.87 kNm. The latter is greater than the flexural strength of the connection which, therefore, governs the response of the joint. As a result, according to the component method the moment resistance of FP7 and FP8 is 53.28 kNm. Failure is expected in the end-plate for complete flange yielding of the corresponding T-Stub.

Concerning the rotational stiffness, Table 3.29 shows that the main contribution to stiffness is provided by the connection. The column flange is the more rigid component since the stiffness coefficient is equal to 52.40 mm. Great deformability is also provided by the column web panel. The more flexible component is the end-plate. Its stiffness coefficient is equal to 5.45 mm. Consequently the initial rotational stiffness is equal to 11000.68 kNm/rad. Finally the yield rotation, defined as the ratio between the moment resistance and the initial rotational stiffness, is equal to 4.84 mrad.

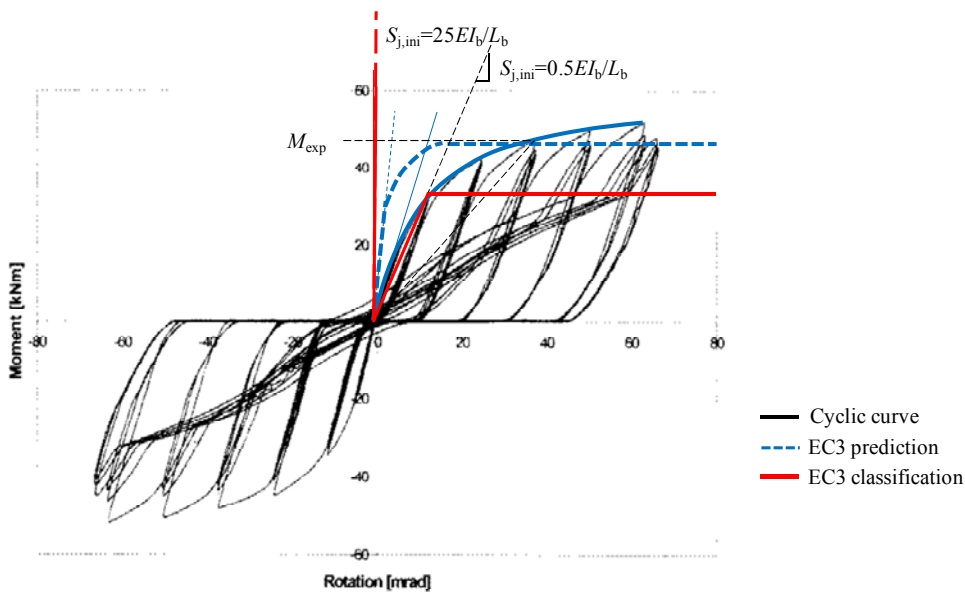


Figure 3.32: Classification by strength and stiffness for FP7

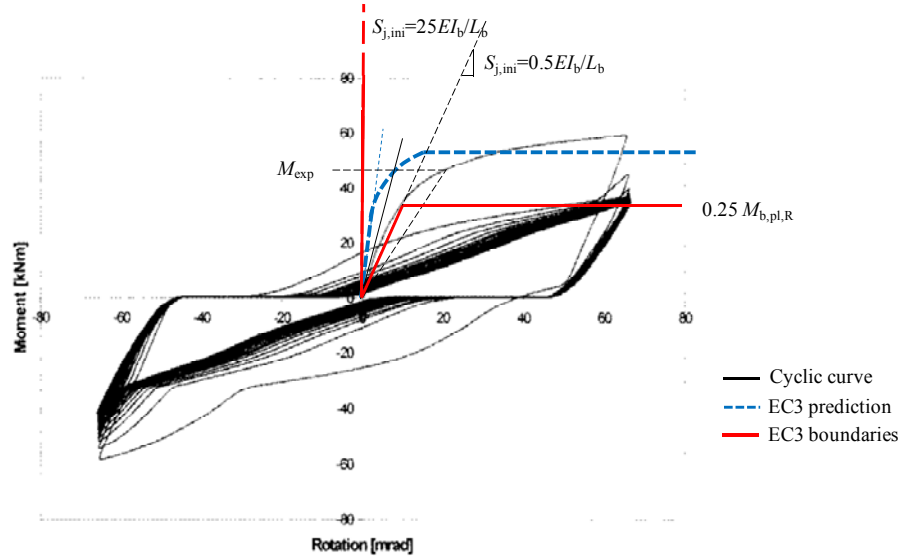


Figure 3.33: Classification by strength and stiffness for FP8

The classifications according to Eurocode 3 are in Figure 3.32 and Figure 3.33. As shown, both EP7 and EP8 are semi-rigid partial strength joints.

### 3.2.4 Test by Shi *et al.* (2007)

The theoretical bending moment strength and initial stiffness of specimen JD1 are determined assuming the nominal values for geometrical properties of the beam, the column and the end-plate and bolts. Actual values of the material properties are instead supposed. In detail, the yield stress of 372.6MPa was considered for the column flange, while the yield stress of 409MPa is used for the column web, the beam, the end-plate and the continuity plates. The ultimate stress of 1160MPa is employed for the bolts.

Table 3.31 contains a synthesis of the application of the component method. The joint components are grouped on the basis of the loading type (tension, compression and shear loading). For each component, the the strength ( $F_R$ ) and the stiffness coefficient ( $k_i$ ), the resisting bending moment ( $M_R$ ) are specified. The latter is evaluated as the product of the component strength ( $F_R$ ) times the internal lever arm.

**Table 3.31: Resistance and stiffness coefficients of the joint components for JD1**

Specimen	Component	$F_R$	$k_i$	$M_R$
JD1		(kN)	(mm)	(kNm)
Tension	Column web in tension	632.61	6.62	174.74
	Column flange in bending	-	18.44	-
	T-Stub complete flange yielding	924.05	-	214.38
	T-Stub flange yielding and bolt failure	485.96	-	112.74
	Bolt in tension	511.56	6.70	118.68
	End-plate in bending	-	15.84	-
	T-Stub complete flange yielding	819.72	-	190.18
	T-Stub flange yielding and bolt failure	488.99	-	113.45
	Beam web in tension	899.80	$\infty$	208.75
Compression	Column web in compression	1341.15	$\infty$	316.64
	Beam flange and web in compression	1198.13	$\infty$	277.97
Shear	Column web in shear	879.12	5.24	203.96

As shown the weakest component of the first bolt row in tension is the end-plate. The failure mechanism is the flange yielding and bolt failure of the equivalent T-Stub which represents the component. The corresponding strength is equal to 337.97 kN. The resisting bending moment due to tension failure of the connection is equal to 65.26 kNm. The compression side is governed by the beam flange and web, whose strength is equal to 583.16 kN. The corresponding bending moment strength due to compression failure in the connection is equal to 112.61 kNm. Therefore, failure of the connection is expected to occur on the tension side. Finally, the shear strength of the column web panel zone is equal to 557.35 kN. The corresponding bending strength is 103.92 kNm. The latter is greater than the flexural strength of the connection which, therefore, governs the response of the joint. As a result, according to the component method the moment resistance of EP6, EP7 and EP8 is 42.15 kNm. Column flange and bolt yielding are expected.

Concerning the rotational stiffness, Table 3.31 shows that the main contribution to stiffness is provided by the connection. The column flange is the more rigid component whose stiffness is 18.44 mm. A great role is also played by the end-plate, since its stiffness coefficient is equal to 15.84 mm. In this configuration the column web is the more flexible component. The stiffness coefficient is equal to 5.21 mm. Large

deformations are expected for bolts, since it is denoted by a stiffness coefficient of 6.70 mm. For the above, the initial rotational stiffness,  $S_{j,ini}$ , is equal to 18577.84 kNm/rad. The yield rotation is therefore equal to 6.07 mrad.

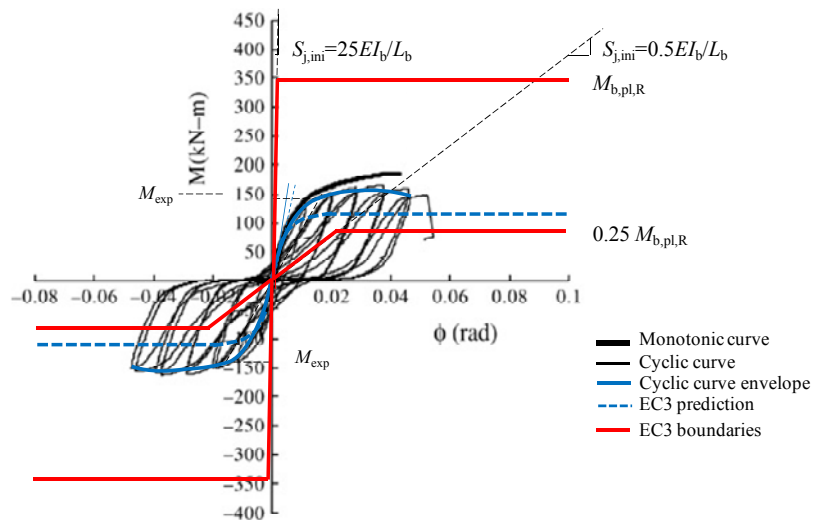


Figure 3.34: Classification by strength and stiffness for JD1

### 3.3 CONCLUDING REMARKS

Both extended end-plate joints and flush end-plate joints were analysed by the component method. By the comparison of the analytical results of specimens belonging to the same experimental campaign, the influence of connection details on the response can be analysed.

Analyzing the theoretical results obtained for Ghobarah *et al.* (1990) the following conclusions can be drawn. The extended end-plate connection without column web transverse stiffeners (A-1) is characterized by lower moment resistance and initial rotational stiffness compared with the stiffened one (A-2). Furthermore, if the column flange is thinner than the end-plate, it becomes the critical component in the connection (A-1 and A-2), while if the thicknesses are similar, the rupture can involve both the column flange and the end-plate (A-4). Beam failure, according to the theoretical calculations, can be observed in case of extended end-

plate connections with the continuity plates, with or without the end-plate rib stiffeners (A-2, A-3, A5).

Thanks to the theoretical predictions of the specimens tested by Shi *et al* (2007a), the influence of the connection details, e.g. the influence of the end-plate thickness, on the joint behaviour can be analysed. The specimens were extended end-plate connections with stiffened column web and end-plate. Starting from the reference configuration, one or two parameters were varied. All specimens presented the end-plate thickness equal to the column flange one. Comparing simultaneously two or more configurations, the following observation can be derived.

An increase of the end-plate (and column flange) thickness (EPC-2) leads on one hand (i) to the improvement of the flexural resistance of the T-Stubs representing both the end-plate and the column flange in bending and, on the other hand (ii) to failure of bolts in tension. Stronger bolts (EPC-3) produce a shift of the failure mechanism, with the failure involving the end-plate flange. Increasing both the bolt diameter and the end-plate thickness (EPC-4), failure moves from the connection to the column web panel. Reducing the end-plate thickness compared with the reference specimen, end-plate yielding and bolt failure, along with column web panel shear yielding, is obtained (EPC-5). The same observations are drawn analyzing the theoretical prediction of the specimens tested by Shi *et al* (2007 b). In fact, also in this case extended end-plate connections with stiffened column web and end-plate were analysed by varying the end-plate thickness and the bolt diameter. Differently from the previous study, the influence of both the continuity plates and end-plate rib stiffeners on the joint behaviour was investigated. Both the end-plate stiffeners (JD3) and the column flange stiffeners (JD4) contribute significantly to the behaviour of end-plate connections, since they produce higher moment resistance and initial stiffness.

Concerning flush end-plate connections, the experimental campaigns performed by Broderick and Thomson (2002, 2005) focused on the influence of geometrical details (end-plate thickness and bolt diameter) on the end-plate T-Stub mechanisms, highlighting the importance of the ratio between the end-plate thickness and bolt diameter.

The theoretical results were compared with the experimental results. From these comparisons the following observations can be drawn. All the theoretical predictions, except for Nogueiro *et al.* (2006) tests, are in accordance with the experimental results. The differences noted for

Nogueiro *et al.* (2006) specimens are probably due to the incorrect material modelling.

Concerning the accuracy of the component method, in the analyzed cases, it is noted that the procedure provides a great prediction of the structural properties of extended end-plate joints. In Figure 3.35, Figure 3.36 and Figure 3.37 are the ratios between the theoretical and the experimental values of the moment resistance and the initial stiffness respectively of extended end-plate joints.

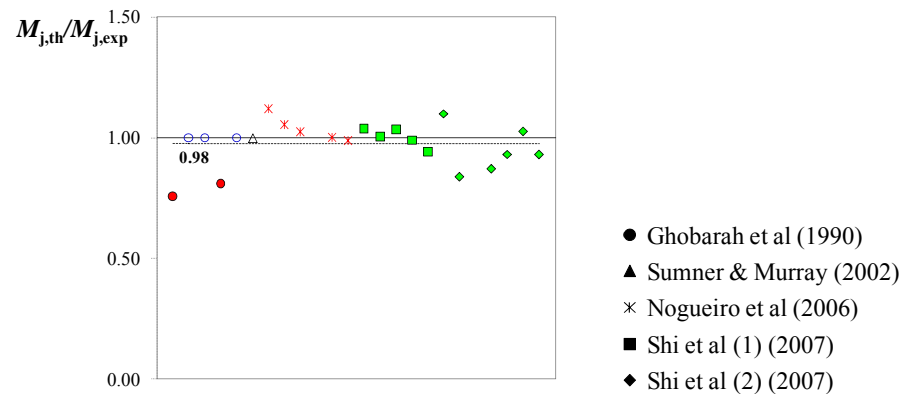


Figure 3.35: Theoretical to experimental ratios of the moment resistance for extended end-plate joints

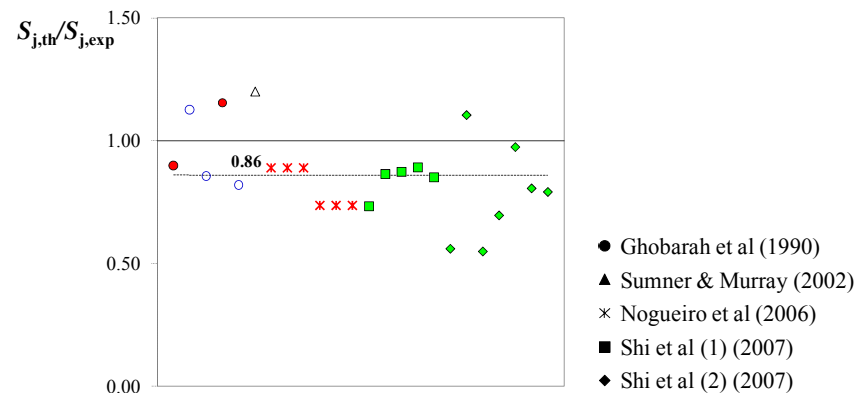
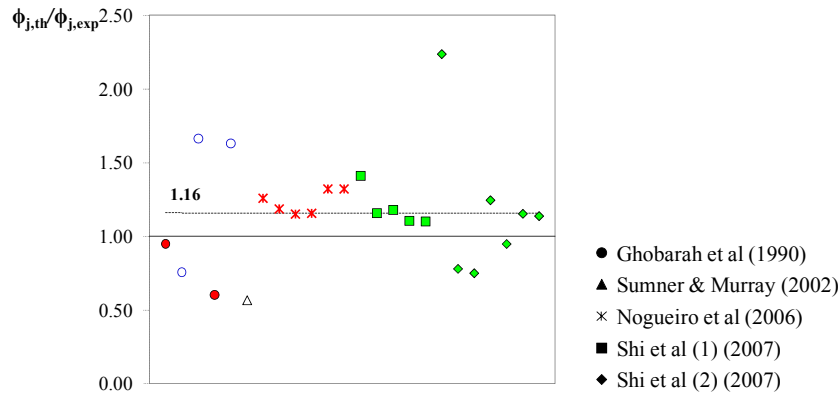


Figure 3.36: Theoretical to experimental ratios of the initial stiffness for extended end-plate joints



**Figure 3.37: Theoretical to experimental ratios of the yield rotation for extended end-plate joints**

As depicted  $M_{j,th}/M_{j,exp}$  ratio varies from 0.76 to 1.12; the average value is equal to 0.98. The  $S_{j,th}/S_{j,exp}$  ratio varies from 0.56 to 1.20, and its average value is 0.86. Consequently,  $\phi_{j,th}/\phi_{j,exp}$  ratio varies from 0.60 to 2.24 and the average value is equal to 1.16.

In all graphs the bold symbol indicates a partial strength configuration, while the empty symbol represents a full strength joint.

The red symbol indicates that the material properties of the components which failed were equal to the expected values. The blue symbol indicates that only for the beam was considered the actual material properties. Finally, the green symbol is used to highlight specimens in which the plastic mechanism differs from the ultimate failure mode.

In Figure 3.38, Figure 3.39 and Figure 3.40 are the theoretical to experimental ratios of the moment resistance, initial stiffness and yield rotation for flush end-plate joints. As shown, the component method provides a good prediction of the moment resistance but overestimates the initial rotational stiffness.

The ratio  $M_{j,th}/M_{j,exp}$  varies from 0.84 to 1.36; its average value is 1.05. The ratio  $S_{j,th}/S_{j,exp}$  ratio varies from 0.78 to 4.19; the corresponding average value is 2.62.



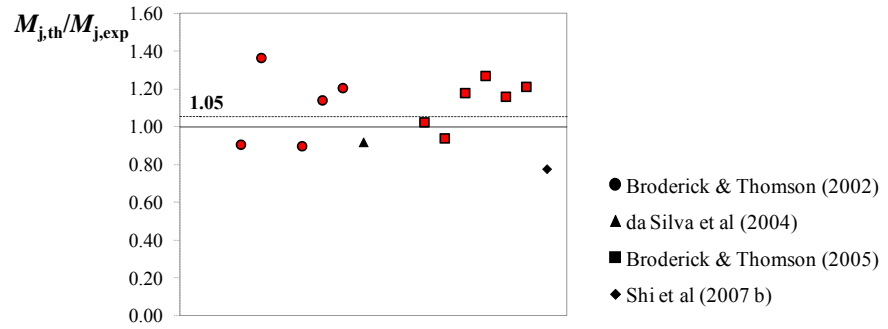


Figure 3.38: Theoretical to experimental ratios of the moment resistance for flush end-plate joints

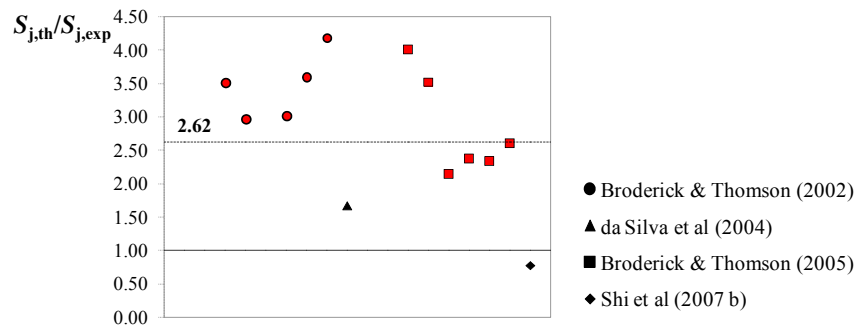


Figure 3.39: Theoretical to experimental ratios of the initial stiffness for flush end-plate joints

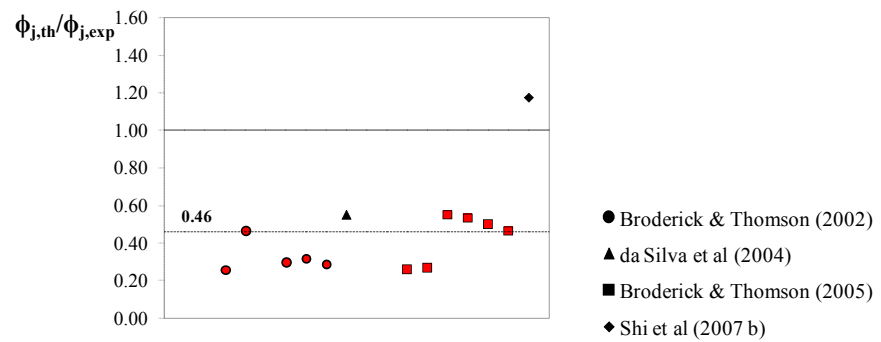


Figure 3.40: Theoretical to experimental ratios of yield rotation for flush end-plate joints

The great overestimation of the initial stiffness (about 3 times higher than the experimental value) is probably due to the end-plate width of the specimens which were not complying with the typical geometries considered as a reference in the Eurocode 3 method.

## 4 ANALYTICAL STUDY OF YIELD ROTATIONS

This Chapter contains a description of the theoretical study on the yield rotation. First, the work on the closed-form equations determined for the calculation of the yield rotation of flush end-plate connection is described. Subsequently, the description of the parametric analyses and the design tools on end-plate connections is given.

### 4.1 ANALYTICAL EQUATIONS

#### 4.1.1 Basic assumptions

The closed-form equations were determined by means the “component method”, as it is implemented into Eurocode 3. It is well known that the procedure provides the stiffness ( $S_{j,ini}$ ) and the strength ( $M_{j,R}$ ) of joints, starting from basic components. Conventionally the yield rotation is herein defined as the ratio of the moment resistance  $M_{j,R}$ , and the initial rotational stiffness  $S_{j,ini}$ .

As describe above, the basic components for the flush end-plate configuration are: column web in tension (*cwt*), column flange in bending (*cfb*), end-plate in bending (*epb*), bolt in tension (*bt*), beam web in tension (*bwt*), beam flange and web in compression (*bfc*), column web in compression (*cwc*), column web in shear (*cws*) (Figure 4.1 a).

Following the same method as implemented by Eurocode 3, the following steps of analysis have been identified:

- I. identification of components;
- II. evaluation of mechanical characteristics of each component;
- III. assembly of components and evaluation of the mechanical characteristics of the whole joint;

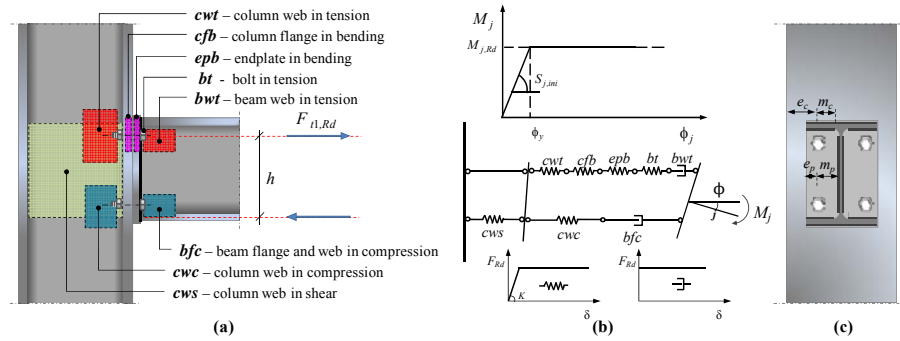


Figure 4.1: Joint mechanical modelling

According to the Eurocode 3 provisions, the basic components for the flush end-plate configuration are: column web in tension (*cwt*), column flange in bending (*cfb*), end-plate in bending (*epb*), bolt in tension (*bt*), beam web in tension (*bwt*), beam flange and web in compression (*bfc*), column web in compression (*cwc*), column web in shear (*cws*) (Figure 4.14 a).

Based on the identified components, the effective tensile resistance of a generic bolt row is provided by Eq. (4.1):

$$F_{t1,R} = \min(F_{Tfc,R}, F_{Tp,R}, V_{wp,R}, F_{twc,R}, F_{cwc,R}, F_{twb,R}, F_{twc,R}) \quad (4.1)$$

where the effective resistance of the bolt row ( $F_{t1,R}$ ) is the smallest value of the tension resistance of: column flange in bending ( $F_{Tfc,R}$ ), end-plate in bending ( $F_{Tp,R}$ ), column web in tension ( $F_{twc,R}$ ), beam web in tension ( $F_{twb,R}$ ), column web in compression ( $F_{cwc,R}$ ), beam flange and web in compression ( $F_{cb,R}$ ), column web panel in shear ( $V_{wp,R}$ ).

The moment resistance, the joint initial stiffness and the yield rotation are provided by Eq. (1.1), Eq. (1.2) and Eq. (1.7) respectively.

Eurocode 3 allows dealing with the web panel zone in shear in two alternative ways:

1. the column web panel zone contribution to strength and stiffness is assembled together with the other joint components in order to obtain mechanical properties of one single spring characterizing the joint moment-rotation response;

2. the column web panel zone in shear is considered as a separate component, originating an additional spring with relevant properties. Approach b) is followed in this study in order to identify the web panel zone contribution.

The study is carried out on the basis of simplifying assumptions to be subsequently verified:

- a) the contribution of the column web in tension or compression to the overall joint deformability is negligible ();
- b) the bolt tensile area is approximately assumed equal to 75% of the geometrical one;
- c) the horizontal pitch of bolts is fixed equal to the average value between the minimum and the maximum possible for a given column shape, taking into account the bolt distances from column round corner edges and weld roots;

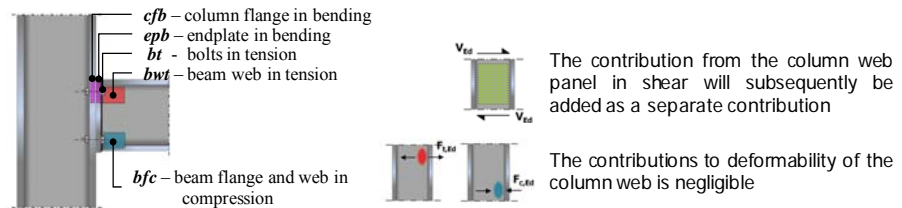


Figure 4.2: Basic joint components and assumptions

According to the hypothesis made at point a), the effective tensile resistance of the bolt row ( $F_{t1,R}$ ) is given by comparison of the resistance of column flange ( $F_{Tfc,R}$ ), end-plate ( $F_{Tp,R}$ ) and beam components (Eq.(4.2)):

$$F_{t1,R} = \min(F_{Tfc,Rd}, F_{Tp,Rd}, F_{twb,Rd}, F_{cwb}) \quad (4.2)$$

The initial rotational stiffness, generally provided by Eq. (1.2), can be written in the following form (Eq (4.6)):

$$S_{j,ini} = \frac{E \cdot b^2}{\frac{m_c^3}{0.9 \cdot l_{fc} \cdot t_{fc}^3} + \frac{m_p^3}{0.9 \cdot l_{ep} \cdot t_p^3} + \frac{L_p}{1.6 \cdot A_s}} \quad (4.3)$$

where:  $E$  is the Young modulus,  $b$  is the lever arm,  $m_c$  and  $m_p$  are the distances between the bolt axis and the expected location of the plastic hinge in the equivalent T-stub (Figure 4.1),  $L_p$  is the bolt length, and  $l_{ep}$   $l_{fc}$  are the effective lengths of the T-Stub representing column flange and end-plate in bending respectively;  $t_{fc}$  and  $t_p$  are column flange and end-plate thickness respectively,  $A_s$  is the bolt tensile area.

Since the yield rotation is the ratio of the joint strength and stiffness, the yield rotation equation will obviously depend on the type of failure mechanism. The following Sections provide some analytical details for each failure mode.

#### 4.1.2 Bolt failure

The effective tensile resistance of bolts and the corresponding moment resistance are given by Eq. (4.4) and Eq. (4.5):

$$F_{t,R} = 1.8 f_{ub} A_s \quad (4.4)$$

$$M_{j,R} = 1.8 f_{ub} A_s b \quad (4.5)$$

The initial joint stiffness is provided by Eq.(4.3).

Based on Eq. (4.3) and Eq. (4.5), it can be proved that the yield rotation corresponding to bolt failure can be expressed in the following form:

$$\phi_{y,Tb} = 1.17 \left( \frac{f_{ub}}{E} \right) \left[ \left( \frac{t_{fc} + t_p + d}{b} \right) + \left( \frac{d}{b} \right) \left( \left( \frac{d}{l_{fc}} \right) \xi^3 + \left( \frac{d}{l_{ep}} \right) \zeta^3 \right) \right] \quad (4.6)$$

$$\xi = \frac{m_c}{t_{fc}} \quad , \quad \zeta = \frac{m_p}{t_p} \quad (4.7)$$

where  $f_{ub}$  is the bolt tensile strength.

### 4.1.3 End-plate failure

In case of complete flange yielding, the effective tensile resistance and the design moment resistance are expressed by Eq. (4.8) and Eq. (4.9):

$$F_{t1,R} = \frac{4M_{pl,ep1}}{m_p} \quad (4.8)$$

$$M_{i,R} = \frac{4M_{pl,ep1}}{m_p} \cdot b = \frac{l_{ep1} t_p^2 f_{yp}}{m_p} \cdot b \quad (4.9)$$

where  $M_{pl,ep1}$  is the T-stub flange plastic moment for mode a) (Eurocode 3).  $M_{pl,ep1}$  is then given by  $(0.25l_{ep1}t_p^2f_{yp})$ , with  $l_{ep1}$  being the end-plate effective length, computed as  $l_{ep1} = \min(2\pi m_p; \alpha m_p)$  and  $f_{yp}$  is the plate yield strength. Consequently the yield rotation is given by Eq. (4.10):

$$\phi_{y,Tp1} = 5.5 \frac{f_{yp}}{E} \frac{t_p}{b} \left[ \left( \frac{(l_{fc} + t_p + d)t_p}{d^2} \right) + \left( \left( \frac{t_p}{l_{fc}} \right) \xi^3 + \left( \frac{t_p}{l_{ep}} \right) \zeta^3 \right) \right] \quad (4.10)$$

In case of a mixed failure mechanism (flange yielding and bolt failure), the effective tensile strength  $F_{t1,R}$  and the moment resistance are given by Eq. (4.11) and Eq. (4.12):

$$F_{t1R} = \frac{2M_{pl,ep2} + n_{ep} \sum F_{tR}}{m_p + n_{ep}} \quad (4.11)$$

$$M_{iR} = \frac{2M_{pl,ep2}}{m_p + n_{ep}} \cdot b + \frac{n_{ep} \sum F_{tR}}{m_p + n_{ep}} \cdot b \quad (4.12)$$

where  $M_{pl,ep2}$  is the T-stub flange flexural resistance according to a failure mode of type b). The latter results into a plastic flexural strength of the T-Stub flange given by  $(0.25l_{ep2}t_p^2f_{yp})$ , with  $l_{ep2}$  equal to  $(\alpha m_p)$ .

Based on Equations (4.12) and (4.3) after some algebraic manipulation, it can be easily shown that the yield rotation for the mixed mode of failure can be expressed in terms of the yield rotations associated to the bare bolt failure and complete flange yielding mechanisms, as shown by Equation (4.22).

$$\begin{aligned} \phi_{y, \text{Tp}2} = & \frac{1}{2} \frac{m_p}{(m_p + n_{\text{ep}})} \frac{5.5 f_{\text{yp}} t_p}{E b} \left[ \left( \frac{(t_{\text{fc}} + t_p + d) t_p}{d^2} \right) + \left( \left( \frac{t_p}{l_{\text{fc}}} \right) \xi^3 + \left( \frac{t_p}{l_{\text{ep}}} \right) \zeta^3 \right) \right] + \\ & + 1.17 \frac{n_{\text{ep}}}{(m_p + n_{\text{ep}})} \frac{f_{\text{ub}}}{E} \left[ \left( \frac{t_{\text{fc}} + t_p + d}{b} \right) + \left( \frac{d}{b} \right) \left( \left( \frac{d}{l_{\text{fc}}} \right) \xi^3 + \left( \frac{d}{l_{\text{ep}}} \right) \zeta^3 \right) \right] \end{aligned} \quad (4.13)$$

#### 4.1.4 Column flange failure

In case of complete column flange yielding, the effective tensile resistance and the moment resistance are given respectively by Eq. (4.26) and Eq. (4.27):

$$F_{\text{t}, \text{R}} = \frac{4M_{\text{pl}, \text{fc}1}}{m_c} \quad (4.14)$$

$$M_{\text{j}, \text{R}} = \frac{4M_{\text{pl}, \text{fc}1}}{m_c} \cdot b = \frac{l_{\text{fc}1} t_{\text{fc}}^2 f_{\text{yfc}}}{m_c} \cdot b \quad (4.15)$$

where  $M_{\text{pl}, \text{fc}1}$  is the T-stub flange plastic moment and  $l_{\text{fc}1}$  is the effective length for a failure mode of type a). The equivalent T-stub flange plastic moment is given by  $(0.25 l_{\text{fc}1} t_{\text{fc}}^2 f_{\text{yfc}})$ , with  $l_{\text{fc}1}$  obtained as  $\min(2\pi m_c; 4m_c + 1,25 m_c)$  ( $f_{\text{yfc}}$  is the column flange yield strength). Consequently, the yield rotation is given by Eq. (4.28).

$$\phi_{y, \text{Tfc}1} = 6.26 \frac{f_{\text{yfc}} t_{\text{fc}}}{E b} \left[ \left( \frac{(t_{\text{fc}} + t_p + d) t_{\text{fc}}}{d^2} \right) + \left( \frac{t_{\text{fc}}}{l_{\text{fc}}} \right) \xi^3 + \left( \frac{t_{\text{fc}}}{l_{\text{ep}}} \right) \zeta^3 \right] \quad (4.16)$$

Similar to the case of end-plate failure, also in the case of column flange failure, the yield rotation associated to the combined mechanism (flange yielding and bolts failure) is expressed in terms of yield rotations corresponding to the bare complete flange yielding and bolt failure mechanisms. The effective tensile resistance, the moment resistance and the joint are given by Eq. (4.17), Eq. (4.18) and (4.3) respectively. After some analytical manipulations, Eq. (4.33) is obtained.

$$F_{\text{t}, \text{R}} = \frac{2M_{\text{pl}, \text{fc}2} + n_{\text{ep}} \sum F_{\text{t}, \text{R}}}{m_p + n_{\text{ep}}} \quad (4.17)$$



$$M_{jR} = \frac{2M_{pl,fc2}}{m_p + n_p} \cdot b + \frac{n_{ep}}{m_p + n_{ep}} \sum F_{tR} \cdot b \quad (4.18)$$

$$\begin{aligned} \phi_{y,Tfc2} = & \frac{1.1}{2} \frac{l_{fc2}}{(m_c + n_c)} \frac{f_{yfc}}{E} \frac{t_{fc}}{b} \left[ \frac{(t_{fc} + t_p + d)t_{fc}}{d^2} + \left( \left( \frac{t_{fc}}{l_{fc}} \right) \xi^3 + \left( \frac{t_{fc}}{l_{ep}} \right) \zeta^3 \right) \right] + \\ & + 1.17 \frac{n_c}{(m_c + n_c)} \frac{f_{ub}}{E} \left[ \left( \frac{t_{fc} + t_p + d}{b} \right) + \left( \left( \frac{d}{l_{fc}} \right) \xi^3 + \left( \frac{d}{l_{ep}} \right) \zeta^3 \right) \frac{d}{b} \right] \end{aligned} \quad (4.19)$$

#### 4.1.5 Beam failure

The strength of the beam web in tension is given by Eq. (4.35):

$$F_{t1,R} = b_{eff,wb} t_{wb} f_{ywb} \quad (4.35)$$

where  $b_{eff,wb}$  is the effective width of the tensile zone, which is set by Eurocode 3 equal to the effective length of the equivalent T-stub representing the end-plate in bending, (i.e.  $b_{eff,wb} = \min(2\pi m_p; \alpha m_p)$ ),  $t_{wb}$  and  $f_{ywb}$  are the beam web thickness and yield strength respectively. The corresponding yield rotation can then be expressed in the following form:

$$\phi_{y,twb} = 1.1 \frac{f_{ywb}}{E} \frac{t_{wb}}{b} \left[ 2.17 \frac{p}{d} \left( \frac{t_{fc} + t_p + d}{d} \right) + \left( \left( \frac{l_{ep}}{l_{fc}} \right) \xi^3 + \zeta^3 \right) \right] \quad (4.36)$$

#### 4.1.6 Analytical equations accuracy

As discussed at the previous Sections, a number of approximations have been made to derive Equations for the yield rotation. The net effect of all the approximations can only be evaluated by comparing the yield rotations calculated by means of the approximate Equations and the Eurocode 3 method. Such a comparison is shown in Figure 4.3. The graph represents the theoretical prediction of the connection yield rotation of the experimental tests described in the previous Chapter. The bold circle indicates the yield rotation calculated via the Eurocode rules (components method, CM), while hollow circles are used for the results of the analytical equations (AE).

As shown in Figure 4.3, the predictions of the yield rotation by the analytical equations are almost identical to those obtained by the component method. Slightly differences are due to the simplifying assumptions of the analytical equations.

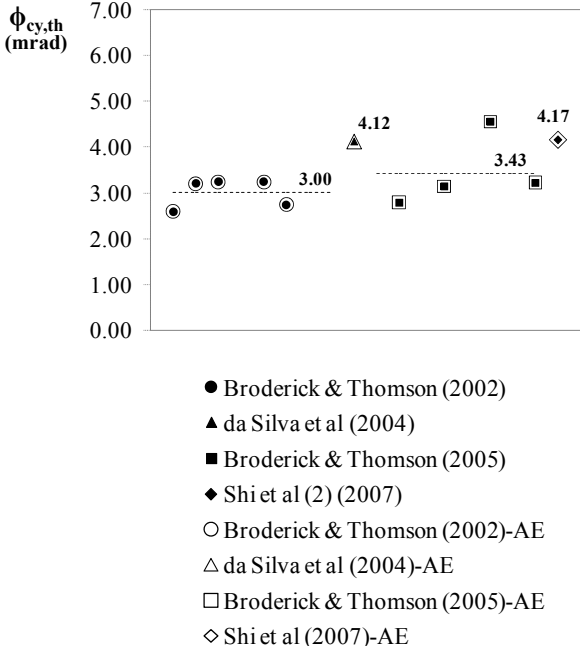


Figure 4.3: Accuracy of the analytical equations

## 4.2 PARAMETRIC ANALYSES AND DESIGN TOOLS

### 4.2.1 Basic assumptions

Parametric analyses were carried out to identify the structural properties of different end-plate joints. Material properties of members, plates and bolts, as well as their geometrical properties, are essential to define the moment resistance, initial rotational stiffness and yield rotation of joints. They can influence the hierarchy of components to yielding. To simplify the parametric analyses, the column and the beam sections are assumed to be preliminarily fixed, as well as the material properties of members,

plates and bolts. The end-plate thickness and the bolt diameter are then assumed to be the key parameters identifying the mechanical properties. Variation of the end-plate thickness and/or bolt diameter leads to rigid or semi-rigid, partial or full strength joint arrangements. Both flush and extended end-plate connections were analysed. A schematic picture showing the considered joint arrangements is given in Figure 4.4.

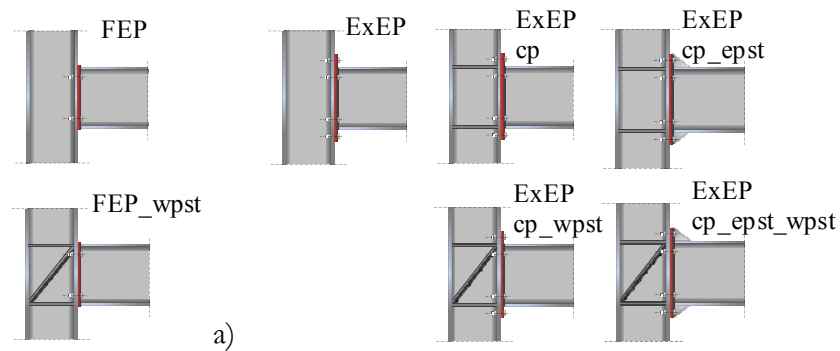


**Figure 4.4: Analyzed joint configurations – a) Flush end-plate connections, b) Extended end-plate connections**

The basic joint arrangements are flush end-plate (FEP) and extended end-plate (ExEP) connections. For the extended end-plate connections, the configuration with continuity plates (ExEP\_cp) and that end-plate rib stiffener (ExEP\_cp\_epst) were also considered. For both for flush end-plate and extended end-plate connections, the effect of the column web panel diagonal stiffener (configurations labelled as FEP\_wpst, ExEP\_cp\_wpst and ExEP\_cp\_epst\_wpst) was investigated.

The study was based on some geometrical assumptions, which are presented in Figure 3.2. As shown in the figure, for the flush end-plate connections (Figure 4.5 a)), the internal lever arm was assumed equal to 80% of the beam height. The horizontal bolt spacing was supposed being equal to the average value between the minimum and the maximum spacing possible for a given column shape. Concerning the extended end-plate joints, the vertical bolt spacing was fixed equal to the horizontal one, i.e. only square bolt arrangements were considered. Continuity plates were assumed to have a thickness equal to the beam flange thickness. The thickness of the end plate vertical stiffener was

supposed to be equal to beam web thickness. Finally, distances of bolts from edges satisfied the minimum Eurocode 3 requirements.

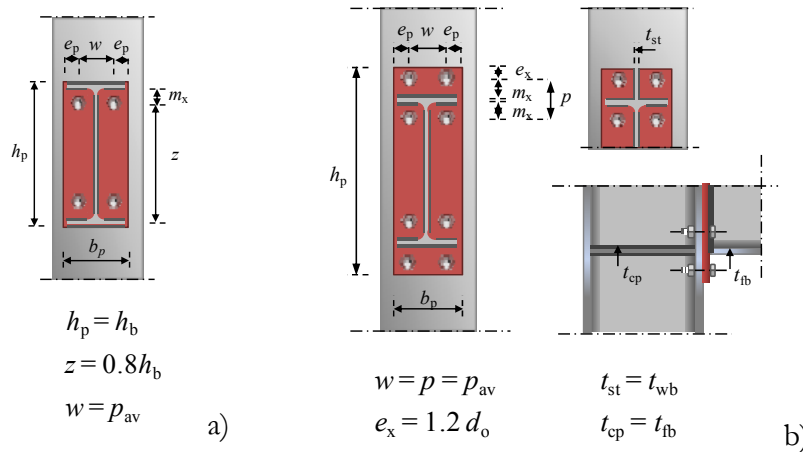
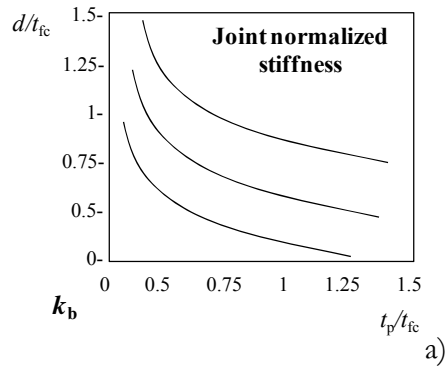


Figure 4.5: Basic assumptions and arrangements for a) flush end-plate and b) extended end-plate connections

#### 4.2.2 Design tools

The parametric analysis allowed developing non-dimensional graphs, providing the normalized stiffness, and strength of the beam-to-column joint for varying end plate thickness and bolt diameter. The yield rotation, defined as the ratio between the joint strength and its initial rotational stiffness, is consequently provided. The beam and column shapes are assumed to be known, as well as the basic joint properties as discussed in the preceding Section.

Figure 4.6 shows a schematic representation of such normalized graphs. In each graph, the x-axis is the ratio between the end plate thickness and the column flange thickness ( $t_p/t_{ic}$ ), while the y-axis is the ratio between the bolt diameter and the column flange thickness ( $d/t_{ic}$ ). Both parameters are assumed to vary from 0.5 to 1.5. Contour lines are associated to different values of the normalized stiffness ( $k_b$ ), strength ( $m_b$ ) and joint yield rotation ( $\phi_{jy}$ ).



$$k_b = \frac{S_{j,ini}}{EI_b/L_b}$$

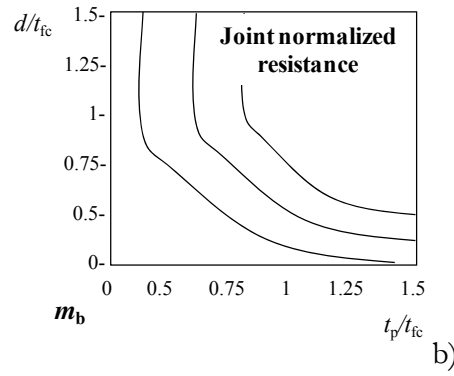
where:

$S_{j,ini}$  = Joint rotational stiffness;

$E$  = Young modulus;

$I_b$  = Beam second moment of area;

$L_b$  = beam length;

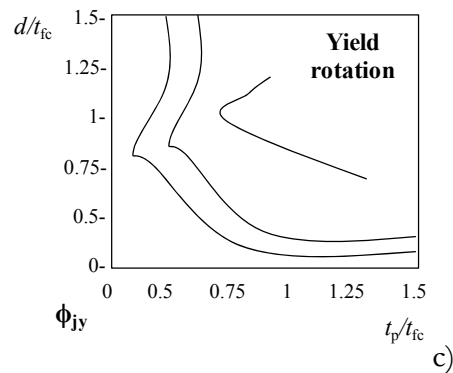


$$m_b = \frac{M_{j,Rd}}{M_{bpl,Rd}}$$

where:

$M_{j,Rd}$  = Joint design moment;

$M_{bpl,Rd}$  = Beam design plastic moment;



$$\phi_{j,y} = \frac{M_{j,Rd}}{S_{j,ini}}$$

where:

$M_{j,Rd}$  = Joint design moment;

$S_{j,ini}$  = Joint rotational stiffness;

Figure 4.6: Normalized charts

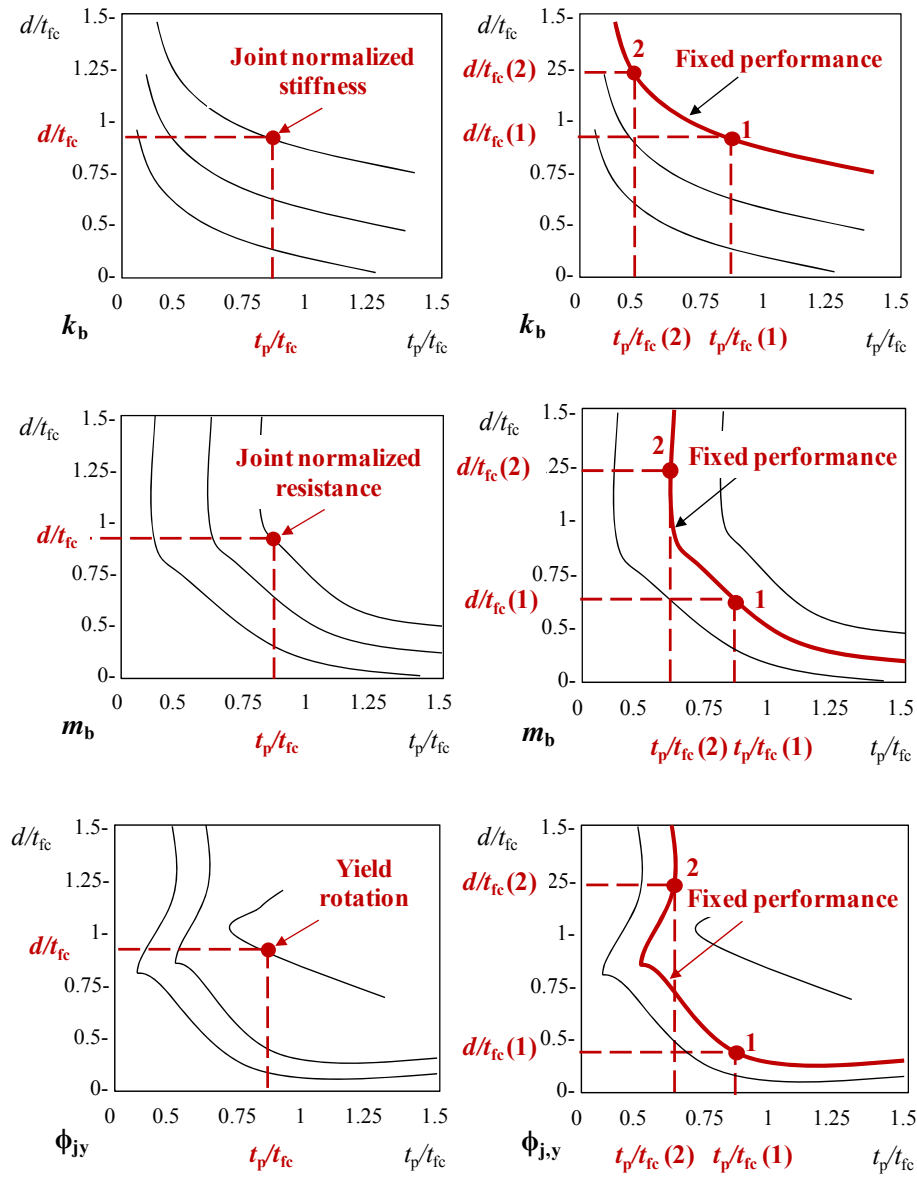


Figure 4.7: Use of normalized charts

For any selected end plate thickness and the bolt diameter, the left hand side panels of Figure 4.7 shows the way as to how the graphs simply and

quickly allows both the joint classification as per Eurocode 3 rules, as well as evaluation of the joint yield rotations, as required in order to apply displacement-based design methods. On the other hand, the right hand side panels of Figure 4.7 shows that – for any required joint performance in terms of normalized rotational stiffness, normalized moment resistance and yield rotation – the graphs allow identifying the combinations of geometrical parameters which guarantee a given joint performance.

The design charts are intended to be easy and quick tools to be used in the first phase of the design in order to identify joint configurations and geometrical properties satisfying specified joint structural performances.

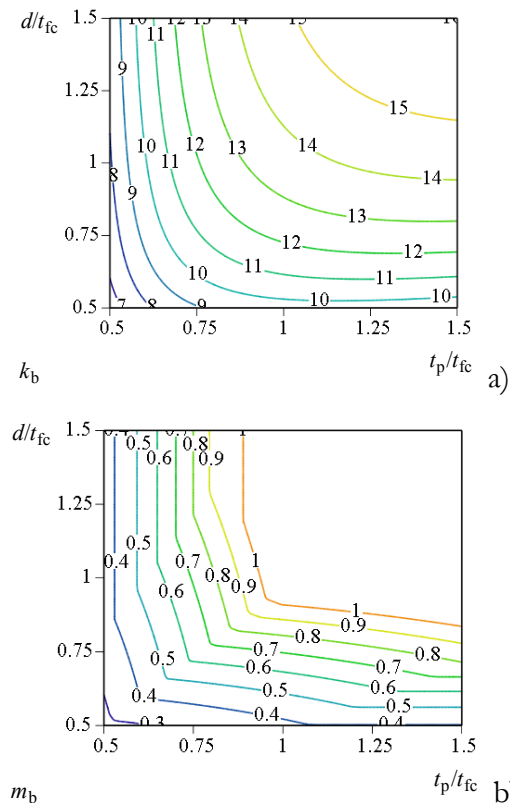


Figure 4.8: a) Normalized stiffness b) normalized resistance and c) yield rotation of extended end-plate connections (column shape: HEM 280; beam shape: IPE 550; steel grade S275; bolt grade 8.8)

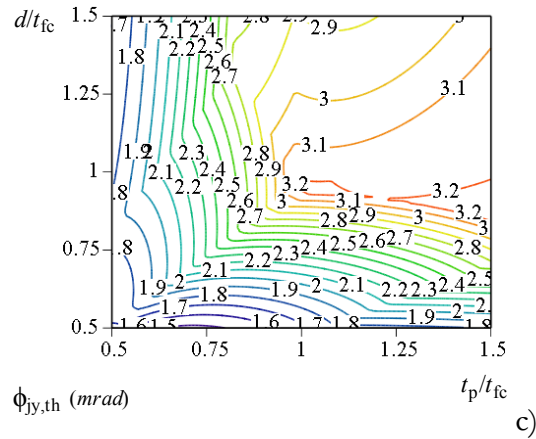


Figure 4.9: a) Normalized stiffness b) normalized resistance and c) yield rotation of extended end-plate connections (column shape: HEM 280; beam shape: IPE 550; steel grade S275; bolt grade 8.8)

Examples of the normalized graphs are given in Figure 4.9, assuming HEM 280 and IPE 550 beam and column shapes, an extended end plate connection, grade S275 steel and grade 8.8 bolts.

Figure 4.10 illustrates that the failure modes associated with each combination of design parameters can also be automatically identified, what could be usefulness when subsequently assigning a ductility capacity to a given beam to column joint.

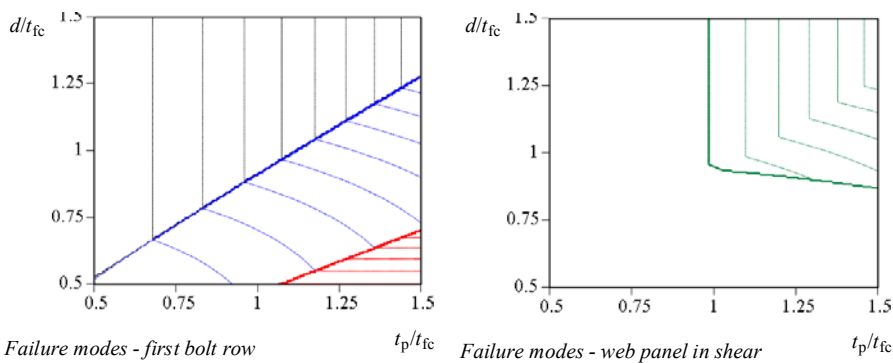
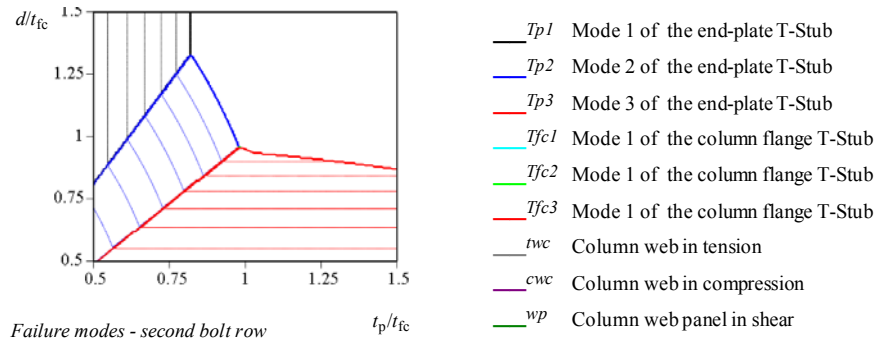


Figure 4.10: Failure modes for an extended end-plate joint (column shape: HEM 280; beam shape: IPE 550; steel grade S275; bolt grade 8.8)





**Figure 4.10: Failure modes for an extended end-plate joint (column shape: HEM 280; beam shape: IPE 550; steel grade S275; bolt grade 8.8)(continued)**

Appendix B contains the design charts for different joint configurations, assuming HEM 280 and IPE 550 beam and column shapes, grade S275 steel and grade 8.8 bolts.

### 4.2.3 Comparison of different joint configurations

For given beam and column shapes, different joint configurations were compared in terms of stiffness, resistance and yield rotation.

The comparison considers a ratio  $t_p/t_{fc}=1$ . Figure Figure 4.11 illustrates one example of such a comparison between the following configurations: FEP, ExEP, ExEP\_cp and ExEP\_cp\_epst.

As shown, FEP and ExEP configurations exhibit a similar behaviour, as well as ExEP\_cp and ExEP\_cp\_epst. In the case shown in the Figure, only extended end-plate joint configurations reinforced with continuity plates and optionally with end-plate rib stiffeners can be full strength joints. Introducing a column web panel diagonal stiffener in the extended end-plate joints, the yield rotation strongly reduces and becomes approximately constant (equal to 0.001 rad in the examined cases). This value is practically independent of the joint arrangement and geometrical details of the connection. Since the diagonal stiffener practically eliminates any source of flexibility in the panel zone in shear, the yield rotation computed on the latter case corresponds to the connection deformability only.

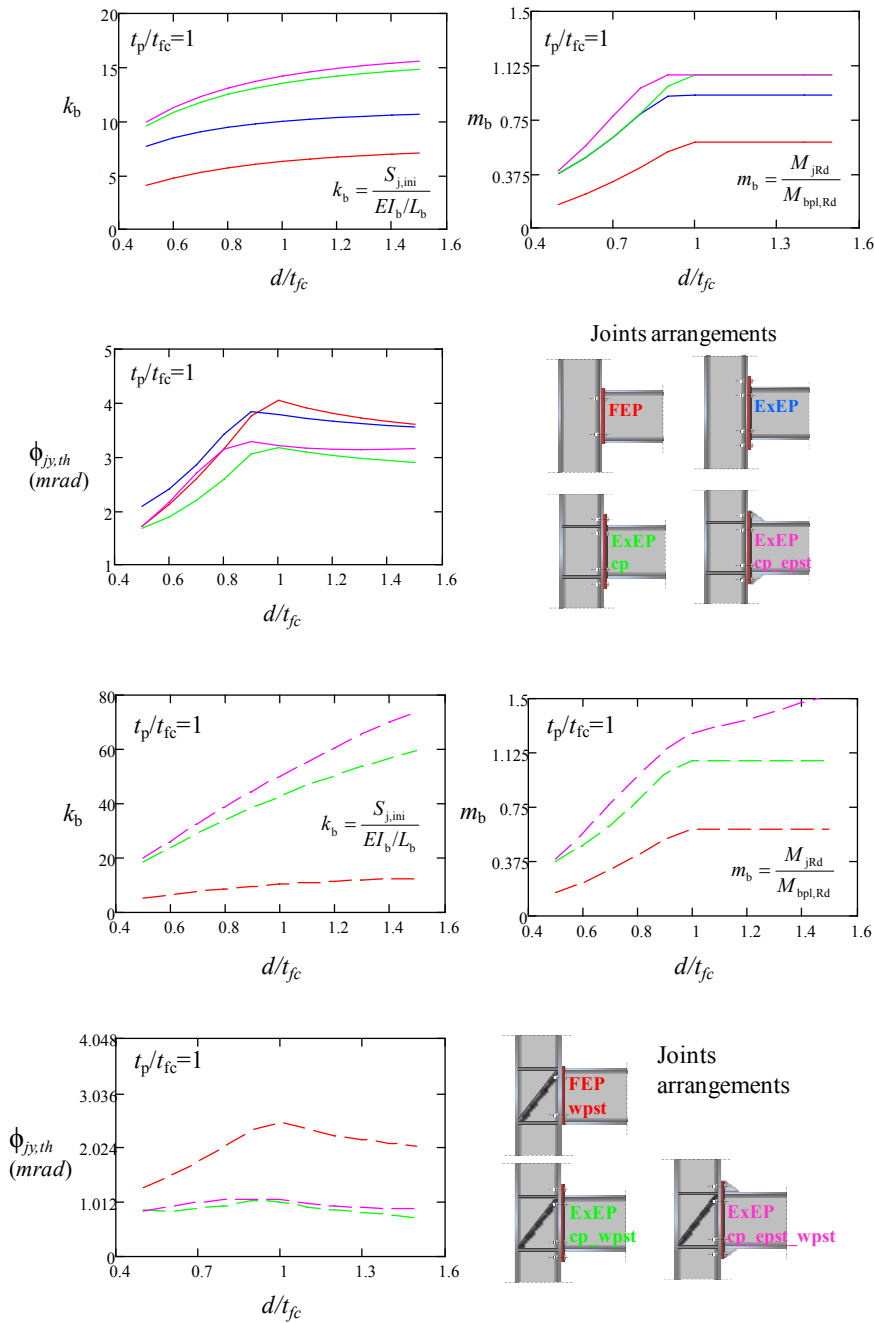


Figure 4.11: Comparison between different joint configurations

## 5 ULTIMATE ROTATIONS

This Chapter contains a description of the study on the plastic rotation capacity of extended end-plate connections.

### 5.1 ANALYSIS CRITERIA

The definition of the rotation capacity according to Figure 1.12 is intended to establish limits of validity of the perfectly plastic joint mechanical model. At rotations larger than the capacity, the joint resistance becomes smaller than the assumed and the trustworthiness of the model is lost. The ultimate rotation can be larger than the defined rotation capacity, when the system exhibit gradual and smooth loss of strength, e.g. when degradation is due to local inelastic buckling. In such a case the ultimate rotation could be defined as that corresponding to a predefined maximum loss of system strength. When a sudden failure occurs, e.g. a bolt rupture or a plate fracture, the ultimate rotation practically coincides with the above defined rotation capacity. The difference between the ultimate rotation and the rotation capacity, as introduced above, allows appreciating the consequences of joint failure in terms of exceedance of the rotation capacity, i.e. larger consequences could be associated with the case of an ultimate rotation being equal to the assumed capacity). On the other hand, economic consequences of exceeding a threshold of plastic rotation, in terms of the repairing costs, are not deal with in this study.

In general, joint failure may occur either in the component that first reaches the yield strength, or in a different component. In fact, due to the strain hardening the rupture can move from the weaker and more ductile component to a stronger and less ductile component. This happens, for example, when plastic deformations first appear in the column web panel in shear. The high ductility of the shear mode of deformations is associated with significant strain hardening of the panel zone, eventually leading to either connection failure or beam flexural yielding.

As a result of the above observations, Figure 5.1 shows the analysis criteria considered in the evaluation of the rotation capacity and the plastic rotation capacity based on experimental results.

The experimental tests were divided in two different classes, called A and B. The first class includes all those cases when the ultimate failure mode coincides with the plastic mechanism. Class B included the cases where differences are observed between the ultimate failure mode and the plastic mechanism. For each class, two subclasses were identified corresponding to  $\phi_{j,pc} = \phi_{j,pu}$  and  $\phi_{j,pc} < \phi_{j,pu}$  respectively.

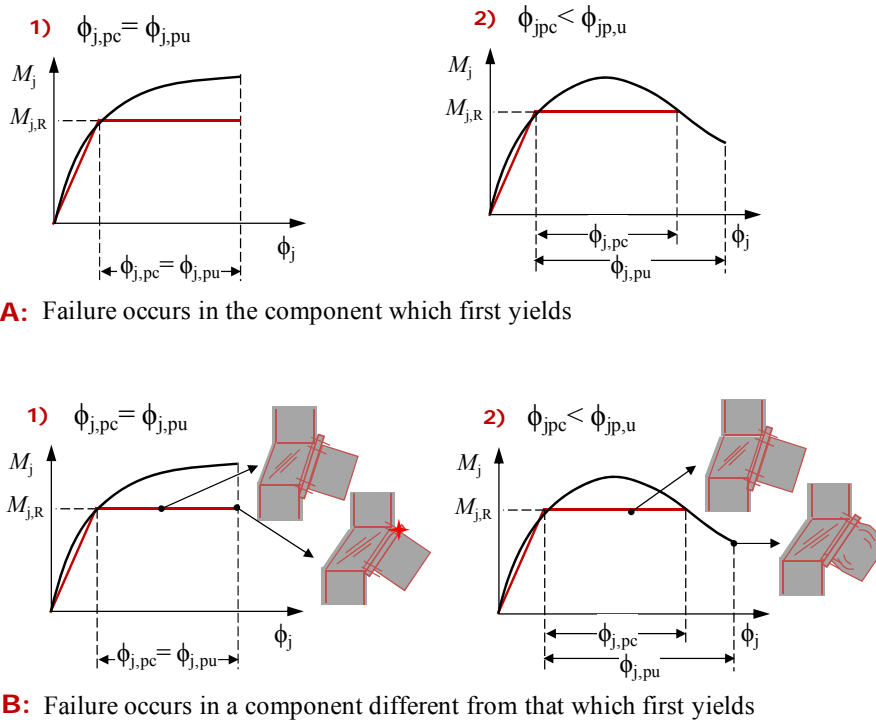


Figure 5.1: Analysis criteria for rotation capacity

## 5.2 PLASTIC ROTATION CAPACITY OF EXTENDED END-PLATE CONNECTIONS

The study on the plastic rotation capacity of extended end-plate connections is very briefly summarized in this Section, using the data

from some of the available experimental tests. The values obtained for the rotation capacity are grouped according to the experimental campaign. The values are shown in order of increasing plastic rotation capacity. Each specimen was classified according to the criteria presented in Figure 5.1. Figure 5.2 shows the plastic rotation capacity of specimens tested by Ghobarah *et al.* (1990). The tests were on extended end-plate connections with different arrangements. Specimens A-1 and A-4 were extended end-plate configurations free of column web and end-plate rib stiffeners, with different end-plate thickness. Both specimens behaved as partial strength joints. According to the analysis criteria, they belong to class A1 (Figure 5.1), since failure occurred in the component which first yielded (end plate in bending) and the plastic rotation capacity ( $\phi_{j,pc}$ ) was equal to the ultimate rotation capacity ( $\phi_{j,pu}$ ), because of fracture of the end plate. Specimens A-2, A-3 and A-5 were provided of beam flange continuity plates; in case of A-3 and A-5 end-plate stiffeners were also included. These three configurations were full strength joints with the formation of a beam plastic hinge. As for previous cases, in A-2, A-3, A-5 failure occurred in the component which first yielded, i.e. the beam end. The rotation capacity ( $\phi_{j,pc}$ ) is now smaller than the ultimate plastic rotation ( $\phi_{j,pu}$ ), because of the gradual strength deterioration associated with the flexural plastic hinge. It is worth to mention that this case is reported herein just for completeness as well as for comparison purposes, even if the rotation capacity is not strictly the one of the joint.

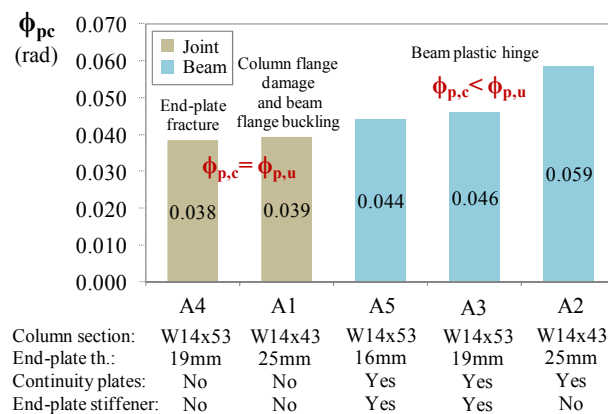
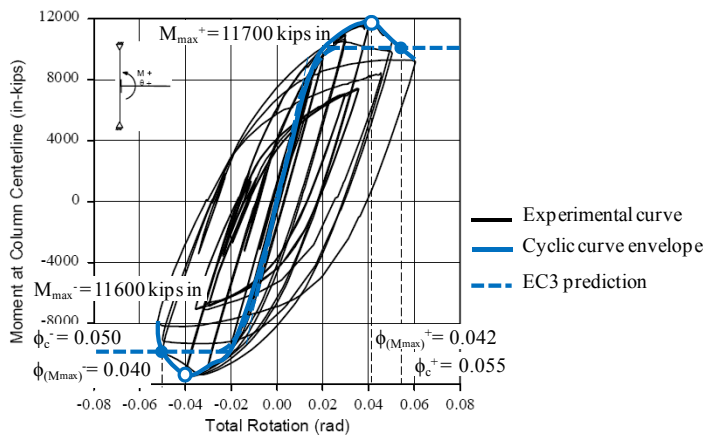


Figure 5.2: Plastic rotation capacities for Ghobarah *et al.* (1990) specimens

The specimen tested by Sumner and Murray (2002) was an extended end plate connection with beam continuity plates and a column web reinforcing plate. This is one more case where the joint exhibited full strength allowing the formation of a beam plastic hinge. This test is classified as A2 (Figure 5.1). In fact, the plastic mechanism coincides with the ultimate failure mode and the rotation capacity is smaller than the ultimate rotation of the joint (Figure 5.3). The plastic rotation capacity is comparable to the one exhibited in the tests by Ghobarah *et al.* (Figure 5.2).



**Figure 5.3: Plastic rotation capacities for specimen 4E-1.25-1.5-24 tested by Sumner and Murray (2002)**

Plastic rotation capacities of the specimens tested by Shi *et al.* (2007a and b) are given in Figure 5.4 and Figure 5.5. The two Figures are relevant to two different experimental investigations carried out by the Authors. In both cases extended end-plate connections with continuity plates and end-plate rib stiffeners were analyzed. Differences between the two sets of experimental tests were the loading protocols and the investigated joint parameters. In the first experimental activity, the specimens were tested under monotonic loads and the influence of the end-plate thickness and/or the bolt diameter on the joint behaviour was studied. The second experimental campaign considered cyclic loading protocols and, in addition to the geometrical parameters studied with the former

tests, the effect of continuity plates and end-plate stiffeners was also evaluated.

Figure 5.4 shows the rotation capacity evaluated for specimens belonging to the first experimental activity. The Authors provides the contribution to the whole joint response from both the connection and the column web panel in shear. As shown in the Figure, a large part of the plastic rotation capacity is due to the ductility of the column web panel in shear. The latter is the component predicted to yield first and to determine the joint moment plastic strength. However, because of the large deformation capacity and associated strain hardening, either connection failure (EPC-1, EPC2, EPC5) or the development of a beam plastic hinge (EPC3, EPC-4) was observed as the ultimate failure mode. All specimens were therefore classified as B1, according to the classification of Figure 5.1. Generally, a larger plastic rotation capacity was measured for the configuration with a weaker end-plate and strong bolts; an expected result in view of the larger ductility of the failure mode involving flexural deformations of the end plate.

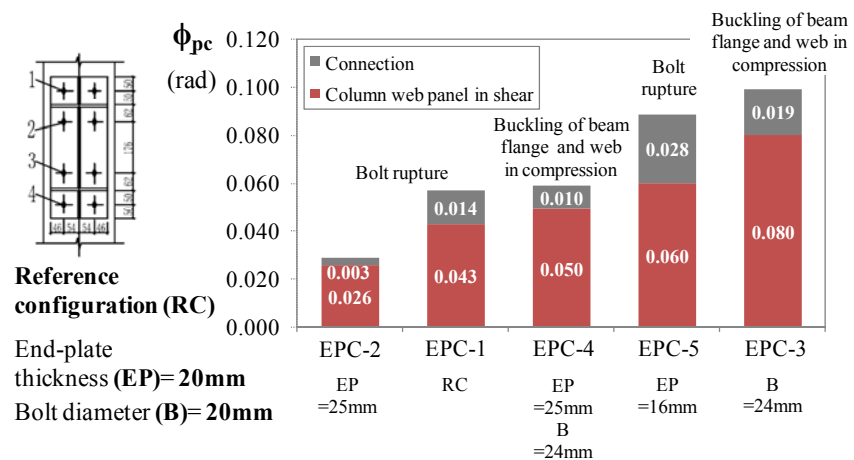


Figure 5.4: Plastic rotation capacities for Shi *et al.* (2007a) specimens

Similar observations are derived from the analysis of the results of the second experimental testing activity (Figure 5.5). In addition, observations on the influence of both the end-plate stiffener and the continuity plate can be derived. The removal of the end-plate stiffener produced the increase of the connection contribution to the plastic

rotation capacity because of the greater deformability of the end-plate. The opposite trend is observed when in case of removal of the continuity plates. The plastic rotation capacity is also in this case significantly contributed by the column web panel in shear, as much in percentage to the total rotation as more the connection is made full strength.

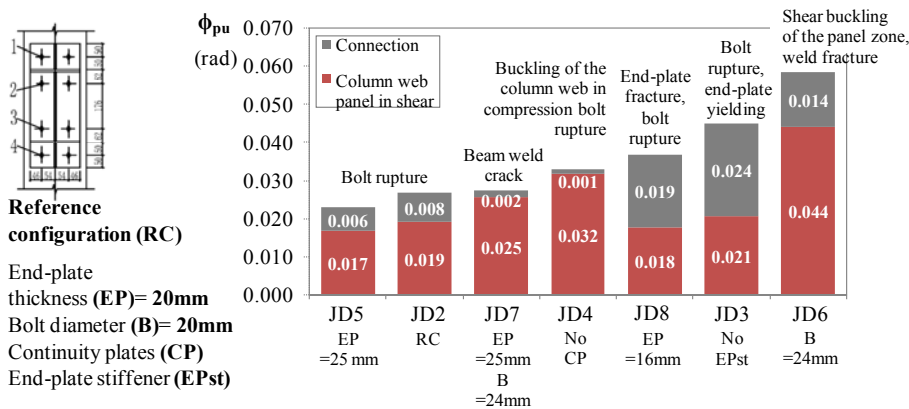


Figure 5.5: Plastic rotation capacities for Shi *et al.* (2007b) specimens

### 5.3 CONCLUDING REMARKS

The analyzed experimental data clearly show that the plastic rotation capacity is influenced by the ultimate failure mode. In general, full strength joints were characterized by larger values of the plastic rotation capacity compared with partial strength joints. Even if the column web panel provides large rotation capacity, sometimes comparable or even larger than that obtained in case of a beam plastic hinge, considerations regarding the consequences in terms of possibility to repair the damaged column should be taken into account. Besides, the large strain hardening of the column web panel in shear can lead to significantly larger requirements in terms of overstrength of the bolted end plate connection, in order to avoid relatively brittle ultimate failure (e.g. bolt rupture). The latter mode of failure corresponds to the easiest way to repair the joint but also to the largest consequences in terms of deterioration of the joint mechanical performance.



In addition to the above comments, it is noted that when strain hardening is responsible for the ultimate failure mode being different from the main (initial) plastic mechanism, then it is difficult to associate a plastic rotation capacity to the joint response, unless large variations of the real values are accepted as respect to the nominal one. This is because of the many different potential ultimate failure modes and the small quantity of available experimental data. Therefore, a characterization of the strain hardening of joint components is a necessary requisite in view of the development of rational methods to assess the joint rotation capacity.



## 6 CONCLUSIONS

The recognition of the key role of displacements and deformations as reliable and direct index of structural damage caused by earthquakes recently produced a shift in seismic design and assessment philosophy. Implementing displacement-based design methods for moment-resisting frame structures requires the characterization of limit-state rotations for beam-to-column joints. Within this general framework the study presented in this Thesis was focused on joints between I-shaped beams and columns and with end-plate connections.

Two limit-state rotations were considered: the yield rotation, the joint rotation capacity and the ultimate rotation. The yield rotation is intended as the rotation corresponding to initiation of significant plastic deformations within the joint. To establish limits of validity of the perfectly plastic joint mechanical model, the joint rotation capacity and the joint ultimate rotation were identified. The joint rotation capacity was defined as the maximum rotation corresponding to a measured resistance larger or equal than the theoretical resistance, while the ultimate rotation was considered as the rotation associated to some form of joint ultimate failure. When a sudden failure (i.e. an abrupt and large loss of strength) occurs, the ultimate rotation and the rotation capacity coincide. Conversely, if the system exhibit gradual and smooth loss of strength, the ultimate rotation can be larger than the defined rotation capacity. In this case the ultimate rotation could be defined as that corresponding to a predefined loss of system strength.

In Europe, with reference to steel structures, advanced methods are available for calculating the stiffness and strength of beam-to-column joints. Among these, the mechanical approach, known as the component method, slowly became the reference to be used by most of the researchers. The ratio between the theoretical resistance and stiffness could be used to calculate the yield rotation, but an experimental verification of any design proposal is anyway required. Besides, information about joint rotation capacity and ductility is still missing or insufficient. Therefore, experimental data on beam-to-column end-plate

joints were collected from the available technical literature. The experimental data were stored into an ad hoc digital data management system developed using Microsoft Access. This tool allows organizing and managing in a flexible manner the recorded data. The digital database permits also to retrieve easily any desired information from the experimental data ensemble.

An analytical study of yield rotations was then carried out by means of the component method. The accuracy of the mechanical approach was evaluated by comparing the theoretical moment resistance and rotational stiffness with the experimental data. The comparison showed that the component method provides a good prediction of the resistance and stiffness in case of extended end-plate connections. In fact, the theoretical moment resistance and initial rotational stiffness resulted to underestimate the corresponding experimental values by 2% and 14% on average. This led to an overestimation of the yield rotation by 16% on average. For flush end-plate connections the comparison showed that the component method provides a joint rotational stiffness about 3 times higher than the experimental value. This was presumably due to the large end-plate width of the considered specimens which were not complying with the reference geometry originally used to develop the component method. The theoretical moment resistance resulted to overestimate the corresponding experimental values by about 5%. This produced an underestimation of the yield rotation by about 54%.

Starting from the conventional definition of the yield rotation, analytical manipulations of the ratio between the joint moment resistance and initial stiffness led also to the identification of closed-form equations in case of flush end-plate connections. Since multiple failure modes are possible, a different Equation was derived for each of them. The derived Equations allowed recognizing the non-dimensional geometrical and material parameters influencing the joint rotations. Subsequently, exploiting the results of the analytical study carried out for flush connections and performing a parametric application of the component method for all types of connections led to the development of simplified design/analysis tools. Examples of such tools were provided in the form of design charts, allowing to evaluate the joint structural performance in terms of stiffness, resistance, failure mode and yield rotations. The design charts are easy and quick tools to be used in the first phases of the

design process, in order to identify joint configurations and geometrical properties satisfying specified joint structural performances.

Concerning the study on the rotation capacity of extended end-plate connections, the analysis of experimental data highlighted that full strength connections are generally characterized by larger values of the plastic rotation capacity compared with partial strength connections. However, yielding of the column web panel in shear might provide large rotation capacity, sometimes comparable or even larger than that obtained in case of a beam plastic hinge. For partial strength joints, generally, a larger plastic rotation capacity is measured for the configuration with a weaker end-plate and stronger bolts, because of the larger ductility of the failure mode involving flexural deformations of the end plate. Investigations on the influence of both the end-plate stiffener and continuity plates showed that the removal of the end-plate stiffener produces the increase of the connection contribution to the plastic rotation capacity because of the greater deformability of the end-plate. The opposite trend was observed in case of removal of the continuity plates.

One main conclusion derived from observation of experimental data is that strain hardening might be responsible for the ultimate failure mode being different from the main (initial) plastic mechanism. The most frequent case is represented by the column web panel in shear, where strain hardening of the shear mechanism can ultimately produce either connection failure or the development of a beam plastic hinge. In these cases, it is difficult to associate a plastic rotation capacity to the whole joint response because of the various potential ultimate failure modes and the small quantity of available experimental data. Therefore, further work should be addressed to a proper characterization of strain hardening of joint components, in view of a possible rational extension of the current component method to evaluate also the joint rotation capacity.



## REFERENCES

- ANSI/AISC 341-10 (2010). Seismic Provisions for Structural Steel Buildings.
- Broderick, B.M. and Thomson, A.W., (2002). The response of flush end-plate joints under earthquake loading. *Journal of Constructional Steel Research*, 58:5, 1161-1175.
- Broderick, B.M. and Thomson, A.W., (2005). Moment rotation response of flush end-plate joints under cycling loading. *Steel Structures*, 5, 441-451.
- da Silva, L.S., De Lima, L.R.O., da S.Velasco, P.C.G, de Andrade, S.A.L., (2004). Behaviour of flush end-plate beam-to-column joints under bending and axial force, *Steel and Composite structures*, 4:2, 77–94.
- Della Corte G., De Matteis G., Landolfo R. and Mazzolani F.M. (2002). Seismic analysis of MR steel frames based on refined hysteretic models of connections. *Journal of Constructional Steel Research*, 58:10, 1331-1345.
- Díaz, C., Martí, P., Victoria, M., Queri, O. M., (2011). Review on the modelling of joint behaviour in steel frames. *Journal of Constructional Steel Research*, 67:5, 741-758.
- European Committee for Standardisation (CEN) (2005). Eurocode 3. Design of steel structures, part 1–8: design of joints (EN 1993-1-8:2005). Brussels.
- Faella, C., Piluso, V., Rizzano, G., (2000). *Structural Steel Semirigid Connections*, CRC Press, Florida, ISBN 0-8493-7433-2.

- FEMA 350 (2000). Recommended Seismic Design Criteria for New Steel Moment-Frame Buildings.
- Ghobarah, A., Osman, A., Korol, R.M. (1990). Behaviour of extended end-plate connections under cyclic loading, *Engineering Structures*, 12, 15–27.
- Jaspart, J.P., (1997) Contributions to recent advances in the field of steel joints, Column bases and further configurations for beam-to-column joints and beam splices. Aggregation thesis. University of Liege, Liege.
- Jaspart, J.P., (2000) General report: session on connections, *Journal of Constructional Steel Research*, 55, 69-89.
- Mochle, J. P., (1996). Displacement based design criteria. *Proceeding of Eleventh World Conference on Earthquake Engineering*.
- Nogueiro, P., Simões da Silva, L., Bento, R., Simões R., (2006). Experimental behaviour of standardised european end-plate beam-to-column steel joints under arbitrary cyclic loading, *Proceeding of Stability and ductility of steel structures*. Lisbon, Portugal, September 6-8.
- Priestley, M. J. N., (1993). Myth and fallacies in earthquake engineering – conflicts between design and reality. ACI SP 157, 231-254.
- Priestley, M. J. N. and Calvi, G. M., (1997). Concepts and procedures for direct displacement based design in (Fajfar & Krawinkler, eds.) *Seismic design methodologies for the next generation of codes*, 171-181, Balkema, Rotterdam.
- Priestley, M.J.N. (1998). Displacement-Based Approaches to Rational Limit States Design of New Structures. Keynote Address, *Proc. XI European Conference of Earthquake Engineering*, Paris.
- SEAOC (1995). Vision 2000. *Conceptual framework for performance based seismic engineering of buildings*. Structural Engineers Association of California, Sacramento, CA, USA.



- Shibata, A. and Sozen, M. A., (1976). Substitute structure method for seismic design in R/C. *Journal of the Structural Division, ASCE*, 102:ST1, 1-18.
- Shi, G., Shi, Y., Wang, Y., (2007a). Behaviour of end-plate moment connections under earthquake loading, *Engineering Structures*, 29, pp. 703–716.
- Shi, G., Shi, Y., Wang, Y., (2007b). Experimental and theoretical analysis of the moment–rotation behaviour of stiffened extended end-plate connections, *Journal of Constructional Steel Research*, 63, 1279–1293.
- Sullivan, T.J., Priestley, M.J.N., Calvi, G.M., (eds) (2012). *A Model Code for the Displacement-Based Seismic Design of Structures*. IUSS Press, ISBN: 978-88-6198-072-3.
- Sumner, E.A., Mays, TW, Murray, TM., (2000). Cyclic testing of bolted moment end-plate connections. *Research report SAC/BD-00/21. CE/VPI-ST 00/03*. Blacksburg (VA): Department of Civil and Environmental Engineering, Virginia Polytechnic Institute and State University.
- Sumner, E.A., Murray, T.M., (2002). Behavior of Extended End-Plate Moment Connections Subject to Cyclic Loading, *Journal of Structural Engineering*, 128:4, 501-508.
- Sumner, E.A., (2003). Unified Design of Extended End-plate Moment Connection Subject to Cyclic Loading, *PhD dissertation*. Blacksburg (VA), Virginia Polytechnic Institute and State University.
- Terracciano, G., Della Corte, G., Di Lorenzo, G., Landolfo, R., (2011). Displacement based design of Moment Resisting Frame structures with semirigid connections: A preliminary study on connection modeling. (In Italian), *Proceedings of XXII C.T.A.*, Ischia 9-13 October 2011, 759-766, ISBN 978-88-89972-23-6.
- Zoetemeijer, P., (1990). Summary of the research on bolted beam-to-column connections. Report 25-6-90-2. Delft University of

## References

---

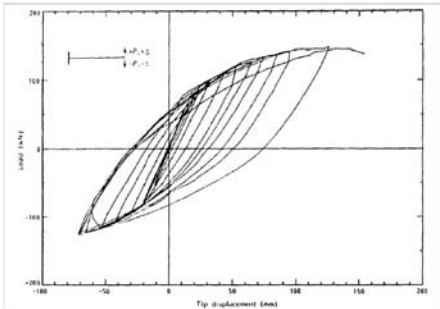

Technology, Technology, Faculty of Civil Engineering, Stevin  
Laboratory—Steel Structures.

## **APPENDIX A**

**DETAILED REPORT ON EXPERIMENTAL TESTS BY THE  
DIGITAL STEEL JOINT DATABASE**



Paper																													
<b>Behaviour of extended end-plate connections under cyclic loading</b>																													
Authors:	Year:																												
Ghobarah A.    Osman A.    Korol R. M.	1990																												
Source: Engineering Structures																													
Test A-1																													
Geometrical properties																													
Scheme: <input type="text" value="Cantilever"/>	Beam length: <input type="text" value="2322"/> Column length: <input type="text" value="1220"/> (mm)																												
	<table border="1"> <thead> <tr> <th colspan="2">Beam</th> </tr> </thead> <tbody> <tr> <td>Section:</td> <td>W360x170x45 (W14x30)</td> </tr> <tr> <td>Height:</td> <td><input type="text" value="352"/></td> </tr> <tr> <td>Width:</td> <td><input type="text" value="171"/></td> </tr> <tr> <td>Fl-thickness:</td> <td><input type="text" value="9.8"/></td> </tr> <tr> <td>W-thickness:</td> <td><input type="text" value="6.9"/></td> </tr> <tr> <td>Root radius:</td> <td><input type="text" value="10"/></td> </tr> <tr> <td>Cross section area:</td> <td><input type="text" value="5710"/></td> </tr> </tbody> </table>	Beam		Section:	W360x170x45 (W14x30)	Height:	<input type="text" value="352"/>	Width:	<input type="text" value="171"/>	Fl-thickness:	<input type="text" value="9.8"/>	W-thickness:	<input type="text" value="6.9"/>	Root radius:	<input type="text" value="10"/>	Cross section area:	<input type="text" value="5710"/>												
	Beam																												
Section:	W360x170x45 (W14x30)																												
Height:	<input type="text" value="352"/>																												
Width:	<input type="text" value="171"/>																												
Fl-thickness:	<input type="text" value="9.8"/>																												
W-thickness:	<input type="text" value="6.9"/>																												
Root radius:	<input type="text" value="10"/>																												
Cross section area:	<input type="text" value="5710"/>																												
	<table border="1"> <thead> <tr> <th colspan="2">Column</th> </tr> </thead> <tbody> <tr> <td>Section:</td> <td>W360x200x64 (W14x43)</td> </tr> <tr> <td>Height:</td> <td><input type="text" value="347"/></td> </tr> <tr> <td>Width:</td> <td><input type="text" value="203"/></td> </tr> <tr> <td>Fl-thickness:</td> <td><input type="text" value="13.5"/></td> </tr> <tr> <td>W-thickness:</td> <td><input type="text" value="7.7"/></td> </tr> <tr> <td>Root radius:</td> <td><input type="text" value="15"/></td> </tr> <tr> <td>Cross section area:</td> <td><input type="text" value="8130"/></td> </tr> <tr> <td><input checked="" type="checkbox"/> Web plate</td> <td>Thickness: <input type="text" value="8"/></td> </tr> <tr> <td><input type="checkbox"/> Continuity plates</td> <td>Thickness: <input type="text"/></td> </tr> </tbody> </table>	Column		Section:	W360x200x64 (W14x43)	Height:	<input type="text" value="347"/>	Width:	<input type="text" value="203"/>	Fl-thickness:	<input type="text" value="13.5"/>	W-thickness:	<input type="text" value="7.7"/>	Root radius:	<input type="text" value="15"/>	Cross section area:	<input type="text" value="8130"/>	<input checked="" type="checkbox"/> Web plate	Thickness: <input type="text" value="8"/>	<input type="checkbox"/> Continuity plates	Thickness: <input type="text"/>								
Column																													
Section:	W360x200x64 (W14x43)																												
Height:	<input type="text" value="347"/>																												
Width:	<input type="text" value="203"/>																												
Fl-thickness:	<input type="text" value="13.5"/>																												
W-thickness:	<input type="text" value="7.7"/>																												
Root radius:	<input type="text" value="15"/>																												
Cross section area:	<input type="text" value="8130"/>																												
<input checked="" type="checkbox"/> Web plate	Thickness: <input type="text" value="8"/>																												
<input type="checkbox"/> Continuity plates	Thickness: <input type="text"/>																												
<table border="1"> <thead> <tr> <th colspan="2">Connection elements</th> </tr> </thead> <tbody> <tr> <td><input type="checkbox"/> Full penetration welds</td> <td></td> </tr> <tr> <td><input checked="" type="checkbox"/> Fillet welds</td> <td>Bolts: <input type="text"/></td> </tr> <tr> <td>Beam flange throat: <input type="text" value="10"/></td> <td>Diameter: <input type="text" value="25"/></td> </tr> <tr> <td>Beam web throat: <input type="text" value="7"/></td> <td>Tensile stress area: <input type="text" value="390.9"/></td> </tr> </tbody> </table>	Connection elements		<input type="checkbox"/> Full penetration welds		<input checked="" type="checkbox"/> Fillet welds	Bolts: <input type="text"/>	Beam flange throat: <input type="text" value="10"/>	Diameter: <input type="text" value="25"/>	Beam web throat: <input type="text" value="7"/>	Tensile stress area: <input type="text" value="390.9"/>	<table border="1"> <thead> <tr> <th colspan="2">End-plate</th> </tr> </thead> <tbody> <tr> <td>Height:</td> <td><input type="text" value="558"/></td> </tr> <tr> <td>Width:</td> <td><input type="text" value="203"/></td> </tr> <tr> <td>Thickness:</td> <td><input type="text" value="25.4"/></td> </tr> <tr> <td>ep:</td> <td><input type="text" value="n.a."/></td> </tr> <tr> <td>ex:</td> <td><input type="text" value="n.a."/></td> </tr> <tr> <td>w:</td> <td><input type="text" value="n.a."/></td> </tr> <tr> <td>mx:</td> <td><input type="text" value="n.a."/></td> </tr> <tr> <td><input type="checkbox"/> Rib stiffener</td> <td>Thickness: <input type="text"/></td> </tr> </tbody> </table>	End-plate		Height:	<input type="text" value="558"/>	Width:	<input type="text" value="203"/>	Thickness:	<input type="text" value="25.4"/>	ep:	<input type="text" value="n.a."/>	ex:	<input type="text" value="n.a."/>	w:	<input type="text" value="n.a."/>	mx:	<input type="text" value="n.a."/>	<input type="checkbox"/> Rib stiffener	Thickness: <input type="text"/>
Connection elements																													
<input type="checkbox"/> Full penetration welds																													
<input checked="" type="checkbox"/> Fillet welds	Bolts: <input type="text"/>																												
Beam flange throat: <input type="text" value="10"/>	Diameter: <input type="text" value="25"/>																												
Beam web throat: <input type="text" value="7"/>	Tensile stress area: <input type="text" value="390.9"/>																												
End-plate																													
Height:	<input type="text" value="558"/>																												
Width:	<input type="text" value="203"/>																												
Thickness:	<input type="text" value="25.4"/>																												
ep:	<input type="text" value="n.a."/>																												
ex:	<input type="text" value="n.a."/>																												
w:	<input type="text" value="n.a."/>																												
mx:	<input type="text" value="n.a."/>																												
<input type="checkbox"/> Rib stiffener	Thickness: <input type="text"/>																												
Notes:	(mm)																												
The beam length provided is the distance between the point of application of the force and the column axis. The paper does not provide any bolts arrangement.																													
Material properties																													
<table border="1"> <thead> <tr> <th colspan="2">Beam</th> </tr> </thead> <tbody> <tr> <td><input type="checkbox"/> Nominal values</td> <td><input type="text"/></td> </tr> <tr> <td><input checked="" type="checkbox"/> Measured values</td> <td></td> </tr> <tr> <td>Fl. yield strength:</td> <td><input type="text" value="310.9"/></td> </tr> <tr> <td>Web yield stress:</td> <td><input type="text" value="315.7"/></td> </tr> </tbody> </table>	Beam		<input type="checkbox"/> Nominal values	<input type="text"/>	<input checked="" type="checkbox"/> Measured values		Fl. yield strength:	<input type="text" value="310.9"/>	Web yield stress:	<input type="text" value="315.7"/>	<table border="1"> <thead> <tr> <th colspan="2">Column</th> </tr> </thead> <tbody> <tr> <td><input checked="" type="checkbox"/> Nominal values</td> <td>G40.21-M300W</td> </tr> <tr> <td><input type="checkbox"/> Measured values</td> <td></td> </tr> <tr> <td>Fl. yield strength:</td> <td><input type="text" value="303.369"/></td> </tr> <tr> <td>Web yield strength:</td> <td><input type="text" value="303.369"/></td> </tr> </tbody> </table>	Column		<input checked="" type="checkbox"/> Nominal values	G40.21-M300W	<input type="checkbox"/> Measured values		Fl. yield strength:	<input type="text" value="303.369"/>	Web yield strength:	<input type="text" value="303.369"/>								
Beam																													
<input type="checkbox"/> Nominal values	<input type="text"/>																												
<input checked="" type="checkbox"/> Measured values																													
Fl. yield strength:	<input type="text" value="310.9"/>																												
Web yield stress:	<input type="text" value="315.7"/>																												
Column																													
<input checked="" type="checkbox"/> Nominal values	G40.21-M300W																												
<input type="checkbox"/> Measured values																													
Fl. yield strength:	<input type="text" value="303.369"/>																												
Web yield strength:	<input type="text" value="303.369"/>																												
	<table border="1"> <thead> <tr> <th colspan="2">End-plate</th> </tr> </thead> <tbody> <tr> <td><input checked="" type="checkbox"/> Nominal value</td> <td>G40.21-M300W</td> </tr> <tr> <td><input type="checkbox"/> Measured value</td> <td></td> </tr> <tr> <td>Yield strength:</td> <td><input type="text" value="303.369"/></td> </tr> </tbody> </table>	End-plate		<input checked="" type="checkbox"/> Nominal value	G40.21-M300W	<input type="checkbox"/> Measured value		Yield strength:	<input type="text" value="303.369"/>																				
End-plate																													
<input checked="" type="checkbox"/> Nominal value	G40.21-M300W																												
<input type="checkbox"/> Measured value																													
Yield strength:	<input type="text" value="303.369"/>																												
(MPa)																													

Test A-1																														
Material properties																														
<table border="1" style="width: 100%; border-collapse: collapse;"> <thead> <tr style="background-color: #cccccc;"> <th style="text-align: left; padding: 2px;">Bolts</th> </tr> </thead> <tbody> <tr> <td style="padding: 2px;"><input checked="" type="checkbox"/> Nominal value</td> <td style="padding: 2px;">A490M</td> </tr> <tr> <td style="padding: 2px;"><input type="checkbox"/> Measured value</td> <td style="padding: 2px;"></td> </tr> <tr> <td style="padding: 2px;">Ultimate strength:</td> <td style="padding: 2px;">1040</td> </tr> </tbody> </table>	Bolts	<input checked="" type="checkbox"/> Nominal value	A490M	<input type="checkbox"/> Measured value		Ultimate strength:	1040	<table border="1" style="width: 100%; border-collapse: collapse;"> <thead> <tr style="background-color: #cccccc;"> <th style="text-align: left; padding: 2px;">Continuity plate</th> </tr> </thead> <tbody> <tr> <td style="padding: 2px;"><input type="checkbox"/> Nominal value</td> <td style="padding: 2px;"></td> </tr> <tr> <td style="padding: 2px;"><input type="checkbox"/> Measured value</td> <td style="padding: 2px;"></td> </tr> <tr> <td style="padding: 2px;">Yield strength:</td> <td style="padding: 2px;"></td> </tr> </tbody> </table>	Continuity plate	<input type="checkbox"/> Nominal value		<input type="checkbox"/> Measured value		Yield strength:		<table border="1" style="width: 100%; border-collapse: collapse;"> <thead> <tr style="background-color: #cccccc;"> <th style="text-align: left; padding: 2px;">Web plate</th> </tr> </thead> <tbody> <tr> <td style="padding: 2px;"><input checked="" type="checkbox"/> Nominal value</td> <td style="padding: 2px;">G40.21-</td> </tr> <tr> <td style="padding: 2px;"><input type="checkbox"/> Measured value</td> <td style="padding: 2px;">M300W</td> </tr> <tr> <td style="padding: 2px;">Yield strength:</td> <td style="padding: 2px;">303.369</td> </tr> </tbody> </table> <table border="1" style="width: 100%; border-collapse: collapse;"> <thead> <tr style="background-color: #cccccc;"> <th style="text-align: left; padding: 2px;">End-plate rib stiffener</th> </tr> </thead> <tbody> <tr> <td style="padding: 2px;"><input type="checkbox"/> Nominal value</td> <td style="padding: 2px;"></td> </tr> <tr> <td style="padding: 2px;"><input type="checkbox"/> Measured value</td> <td style="padding: 2px;"></td> </tr> <tr> <td style="padding: 2px;">Yield strength:</td> <td style="padding: 2px;"></td> </tr> </tbody> </table> <p style="text-align: right; font-size: small;">(MPa)</p>	Web plate	<input checked="" type="checkbox"/> Nominal value	G40.21-	<input type="checkbox"/> Measured value	M300W	Yield strength:	303.369	End-plate rib stiffener	<input type="checkbox"/> Nominal value		<input type="checkbox"/> Measured value		Yield strength:	
Bolts																														
<input checked="" type="checkbox"/> Nominal value	A490M																													
<input type="checkbox"/> Measured value																														
Ultimate strength:	1040																													
Continuity plate																														
<input type="checkbox"/> Nominal value																														
<input type="checkbox"/> Measured value																														
Yield strength:																														
Web plate																														
<input checked="" type="checkbox"/> Nominal value	G40.21-																													
<input type="checkbox"/> Measured value	M300W																													
Yield strength:	303.369																													
End-plate rib stiffener																														
<input type="checkbox"/> Nominal value																														
<input type="checkbox"/> Measured value																														
Yield strength:																														
<p>Notes:</p> <div style="border: 1px solid #ccc; height: 20px; width: 100%;"></div>																														
Experimental results																														
<p>Type of test: <input type="text" value="Cyclic"/></p> <p>Loading sequence: <input type="text" value="Tailor made protocol"/></p> <p>Partial ductility: <input type="text" value="0.5-1-1.5-2-2.5-3-3.5-4-5-6"/></p> <p>Number of cycles: <input type="text" value="4-2-1-1-1-1-1-1-1"/></p> <p>Type of curve: <input type="text" value="Load-Displacement"/></p> <p>Force measured: <input type="text" value="Applied to the beam tip"/></p> <p>Displacement measured: <input type="text" value="Beam tip due to the elastic and inelastic beam rotation"/></p>																														
Failure mode and joint capacity																														
 <p style="font-size: small;">Failure mode: Column flange failure</p>	<table style="width: 100%;"> <tr> <td style="padding: 2px;">Maximum moment:</td> <td style="padding: 2px;"><input type="text"/></td> </tr> <tr> <td style="padding: 2px;">Maximum load:</td> <td style="padding: 2px;">147.7 (kN)</td> </tr> <tr> <td style="padding: 2px;">Maximum rotation:</td> <td style="padding: 2px;"><input type="text"/></td> </tr> <tr> <td style="padding: 2px;">Maximum displacement:</td> <td style="padding: 2px;">158 (mm)</td> </tr> </table>	Maximum moment:	<input type="text"/>	Maximum load:	147.7 (kN)	Maximum rotation:	<input type="text"/>	Maximum displacement:	158 (mm)																					
Maximum moment:	<input type="text"/>																													
Maximum load:	147.7 (kN)																													
Maximum rotation:	<input type="text"/>																													
Maximum displacement:	158 (mm)																													

Paper																																			
<b>Behaviour of extended end-plate connections under cyclic loading</b>																																			
Authors:	Year:																																		
Ghobarah A.    Osman A.    Korol R. M.	1990																																		
Source: Engineering Structures																																			
Test A-2																																			
Geometrical properties																																			
Scheme: <input type="text" value="Cantilever"/>	Beam length: <input type="text" value="2322"/> Column length: <input type="text" value="1220"/> (mm)																																		
	<table border="1"> <thead> <tr> <th colspan="2">Beam</th> </tr> </thead> <tbody> <tr> <td>Section:</td> <td>W360x170x45 (W14x30)</td> </tr> <tr> <td>Height:</td> <td><input type="text" value="352"/></td> </tr> <tr> <td>Width:</td> <td><input type="text" value="171"/></td> </tr> <tr> <td>Fl-thickness:</td> <td><input type="text" value="9.8"/></td> </tr> <tr> <td>W-thickness:</td> <td><input type="text" value="6.9"/></td> </tr> <tr> <td>Root radius:</td> <td><input type="text" value="10"/></td> </tr> <tr> <td>Cross section area:</td> <td><input type="text" value="5710"/></td> </tr> </tbody> </table>	Beam		Section:	W360x170x45 (W14x30)	Height:	<input type="text" value="352"/>	Width:	<input type="text" value="171"/>	Fl-thickness:	<input type="text" value="9.8"/>	W-thickness:	<input type="text" value="6.9"/>	Root radius:	<input type="text" value="10"/>	Cross section area:	<input type="text" value="5710"/>																		
	Beam																																		
Section:	W360x170x45 (W14x30)																																		
Height:	<input type="text" value="352"/>																																		
Width:	<input type="text" value="171"/>																																		
Fl-thickness:	<input type="text" value="9.8"/>																																		
W-thickness:	<input type="text" value="6.9"/>																																		
Root radius:	<input type="text" value="10"/>																																		
Cross section area:	<input type="text" value="5710"/>																																		
	<table border="1"> <thead> <tr> <th colspan="2">Column</th> </tr> </thead> <tbody> <tr> <td>Section:</td> <td>W360x200x64 (W14x43)</td> </tr> <tr> <td>Height:</td> <td><input type="text" value="347"/></td> </tr> <tr> <td>Width:</td> <td><input type="text" value="203"/></td> </tr> <tr> <td>Fl-thickness:</td> <td><input type="text" value="13.5"/></td> </tr> <tr> <td>W-thickness:</td> <td><input type="text" value="7.7"/></td> </tr> <tr> <td>Root radius:</td> <td><input type="text" value="15"/></td> </tr> <tr> <td>Cross section area:</td> <td><input type="text" value="8130"/></td> </tr> <tr> <td><input checked="" type="checkbox"/> Web plate</td> <td>Thickness: <input type="text" value="8"/></td> </tr> <tr> <td><input checked="" type="checkbox"/> Continuity plates</td> <td>Thickness: <input type="text" value="9"/></td> </tr> </tbody> </table>	Column		Section:	W360x200x64 (W14x43)	Height:	<input type="text" value="347"/>	Width:	<input type="text" value="203"/>	Fl-thickness:	<input type="text" value="13.5"/>	W-thickness:	<input type="text" value="7.7"/>	Root radius:	<input type="text" value="15"/>	Cross section area:	<input type="text" value="8130"/>	<input checked="" type="checkbox"/> Web plate	Thickness: <input type="text" value="8"/>	<input checked="" type="checkbox"/> Continuity plates	Thickness: <input type="text" value="9"/>														
Column																																			
Section:	W360x200x64 (W14x43)																																		
Height:	<input type="text" value="347"/>																																		
Width:	<input type="text" value="203"/>																																		
Fl-thickness:	<input type="text" value="13.5"/>																																		
W-thickness:	<input type="text" value="7.7"/>																																		
Root radius:	<input type="text" value="15"/>																																		
Cross section area:	<input type="text" value="8130"/>																																		
<input checked="" type="checkbox"/> Web plate	Thickness: <input type="text" value="8"/>																																		
<input checked="" type="checkbox"/> Continuity plates	Thickness: <input type="text" value="9"/>																																		
<table border="1"> <thead> <tr> <th colspan="2">Connection elements</th> </tr> </thead> <tbody> <tr> <td><input type="checkbox"/> Full penetration welds</td> <td></td> </tr> <tr> <td><input checked="" type="checkbox"/> Fillet welds</td> <td></td> </tr> <tr> <td>Beam flange throat:</td> <td><input type="text" value="10"/></td> </tr> <tr> <td>Beam web throat:</td> <td><input type="text" value="7"/></td> </tr> <tr> <td>Bolts:</td> <td><input type="text"/></td> </tr> <tr> <td>Diameter:</td> <td><input type="text" value="25"/></td> </tr> <tr> <td>Tensile stress area:</td> <td><input type="text" value="390.9"/></td> </tr> </tbody> </table>	Connection elements		<input type="checkbox"/> Full penetration welds		<input checked="" type="checkbox"/> Fillet welds		Beam flange throat:	<input type="text" value="10"/>	Beam web throat:	<input type="text" value="7"/>	Bolts:	<input type="text"/>	Diameter:	<input type="text" value="25"/>	Tensile stress area:	<input type="text" value="390.9"/>	<table border="1"> <thead> <tr> <th colspan="2">End-plate</th> </tr> </thead> <tbody> <tr> <td>Height:</td> <td><input type="text" value="558"/></td> </tr> <tr> <td>Width:</td> <td><input type="text" value="203"/></td> </tr> <tr> <td>Thickness:</td> <td><input type="text" value="25.4"/></td> </tr> <tr> <td>ep:</td> <td><input type="text" value="n.a."/></td> </tr> <tr> <td>ex:</td> <td><input type="text" value="n.a."/></td> </tr> <tr> <td>w:</td> <td><input type="text" value="n.a."/></td> </tr> <tr> <td>mx:</td> <td><input type="text" value="n.a."/></td> </tr> <tr> <td><input type="checkbox"/> Rib stiffener</td> <td>Thickness: <input type="text"/></td> </tr> </tbody> </table>	End-plate		Height:	<input type="text" value="558"/>	Width:	<input type="text" value="203"/>	Thickness:	<input type="text" value="25.4"/>	ep:	<input type="text" value="n.a."/>	ex:	<input type="text" value="n.a."/>	w:	<input type="text" value="n.a."/>	mx:	<input type="text" value="n.a."/>	<input type="checkbox"/> Rib stiffener	Thickness: <input type="text"/>
Connection elements																																			
<input type="checkbox"/> Full penetration welds																																			
<input checked="" type="checkbox"/> Fillet welds																																			
Beam flange throat:	<input type="text" value="10"/>																																		
Beam web throat:	<input type="text" value="7"/>																																		
Bolts:	<input type="text"/>																																		
Diameter:	<input type="text" value="25"/>																																		
Tensile stress area:	<input type="text" value="390.9"/>																																		
End-plate																																			
Height:	<input type="text" value="558"/>																																		
Width:	<input type="text" value="203"/>																																		
Thickness:	<input type="text" value="25.4"/>																																		
ep:	<input type="text" value="n.a."/>																																		
ex:	<input type="text" value="n.a."/>																																		
w:	<input type="text" value="n.a."/>																																		
mx:	<input type="text" value="n.a."/>																																		
<input type="checkbox"/> Rib stiffener	Thickness: <input type="text"/>																																		
Notes:	(mm)																																		
The beam length provided is the distance between the point of application of the force and the column axis. The paper does not provide any bolts arrangement.																																			
Material properties																																			
<table border="1"> <thead> <tr> <th colspan="2">Beam</th> </tr> </thead> <tbody> <tr> <td><input type="checkbox"/> Nominal values</td> <td><input type="text"/></td> </tr> <tr> <td><input checked="" type="checkbox"/> Measured values</td> <td></td> </tr> <tr> <td>Fl. yield strength:</td> <td><input type="text" value="316.1"/></td> </tr> <tr> <td>Web yield stress:</td> <td><input type="text" value="322.1"/></td> </tr> </tbody> </table>	Beam		<input type="checkbox"/> Nominal values	<input type="text"/>	<input checked="" type="checkbox"/> Measured values		Fl. yield strength:	<input type="text" value="316.1"/>	Web yield stress:	<input type="text" value="322.1"/>	<table border="1"> <thead> <tr> <th colspan="2">Column</th> </tr> </thead> <tbody> <tr> <td><input checked="" type="checkbox"/> Nominal values</td> <td>G40.21-M300W</td> </tr> <tr> <td><input type="checkbox"/> Measured values</td> <td></td> </tr> <tr> <td>Fl. yield strength:</td> <td><input type="text" value="303.369"/></td> </tr> <tr> <td>Web yield strength:</td> <td><input type="text" value="303.369"/></td> </tr> </tbody> </table>	Column		<input checked="" type="checkbox"/> Nominal values	G40.21-M300W	<input type="checkbox"/> Measured values		Fl. yield strength:	<input type="text" value="303.369"/>	Web yield strength:	<input type="text" value="303.369"/>														
Beam																																			
<input type="checkbox"/> Nominal values	<input type="text"/>																																		
<input checked="" type="checkbox"/> Measured values																																			
Fl. yield strength:	<input type="text" value="316.1"/>																																		
Web yield stress:	<input type="text" value="322.1"/>																																		
Column																																			
<input checked="" type="checkbox"/> Nominal values	G40.21-M300W																																		
<input type="checkbox"/> Measured values																																			
Fl. yield strength:	<input type="text" value="303.369"/>																																		
Web yield strength:	<input type="text" value="303.369"/>																																		
	<table border="1"> <thead> <tr> <th colspan="2">End-plate</th> </tr> </thead> <tbody> <tr> <td><input checked="" type="checkbox"/> Nominal value</td> <td>G40.21-M300W</td> </tr> <tr> <td><input type="checkbox"/> Measured value</td> <td></td> </tr> <tr> <td>Yield strength:</td> <td><input type="text" value="303.369"/></td> </tr> </tbody> </table>	End-plate		<input checked="" type="checkbox"/> Nominal value	G40.21-M300W	<input type="checkbox"/> Measured value		Yield strength:	<input type="text" value="303.369"/>																										
End-plate																																			
<input checked="" type="checkbox"/> Nominal value	G40.21-M300W																																		
<input type="checkbox"/> Measured value																																			
Yield strength:	<input type="text" value="303.369"/>																																		
(MPa)																																			

Test A-2																	
<b>Material properties</b>																	
<table border="1"> <thead> <tr> <th colspan="2">Bolts</th> </tr> </thead> <tbody> <tr> <td><input checked="" type="checkbox"/> Nominal value</td> <td>A490M</td> </tr> <tr> <td><input type="checkbox"/> Measured value</td> <td></td> </tr> <tr> <td>Ultimate strength:</td> <td>1040</td> </tr> </tbody> </table>	Bolts		<input checked="" type="checkbox"/> Nominal value	A490M	<input type="checkbox"/> Measured value		Ultimate strength:	1040	<table border="1"> <thead> <tr> <th colspan="2">Continuity plate</th> </tr> </thead> <tbody> <tr> <td><input checked="" type="checkbox"/> Nominal value</td> <td>G40.21-M300W</td> </tr> <tr> <td><input type="checkbox"/> Measured value</td> <td></td> </tr> <tr> <td>Yield strength:</td> <td>303.369</td> </tr> </tbody> </table>	Continuity plate		<input checked="" type="checkbox"/> Nominal value	G40.21-M300W	<input type="checkbox"/> Measured value		Yield strength:	303.369
Bolts																	
<input checked="" type="checkbox"/> Nominal value	A490M																
<input type="checkbox"/> Measured value																	
Ultimate strength:	1040																
Continuity plate																	
<input checked="" type="checkbox"/> Nominal value	G40.21-M300W																
<input type="checkbox"/> Measured value																	
Yield strength:	303.369																
<table border="1"> <thead> <tr> <th colspan="2">Web plate</th> </tr> </thead> <tbody> <tr> <td><input checked="" type="checkbox"/> Nominal value</td> <td>G40.21-M300W</td> </tr> <tr> <td><input type="checkbox"/> Measured value</td> <td></td> </tr> <tr> <td>Yield strength:</td> <td>303.369</td> </tr> </tbody> </table>		Web plate		<input checked="" type="checkbox"/> Nominal value	G40.21-M300W	<input type="checkbox"/> Measured value		Yield strength:	303.369								
Web plate																	
<input checked="" type="checkbox"/> Nominal value	G40.21-M300W																
<input type="checkbox"/> Measured value																	
Yield strength:	303.369																
<table border="1"> <thead> <tr> <th colspan="2">End-plate rib stiffener</th> </tr> </thead> <tbody> <tr> <td><input type="checkbox"/> Nominal value</td> <td></td> </tr> <tr> <td><input type="checkbox"/> Measured value</td> <td></td> </tr> <tr> <td>Yield strength:</td> <td></td> </tr> </tbody> </table>		End-plate rib stiffener		<input type="checkbox"/> Nominal value		<input type="checkbox"/> Measured value		Yield strength:									
End-plate rib stiffener																	
<input type="checkbox"/> Nominal value																	
<input type="checkbox"/> Measured value																	
Yield strength:																	
Notes:																	
<div style="border: 1px solid black; height: 20px;"></div>																	
(MPa)																	
<b>Experimental results</b>																	
<p>Type of test: <input type="text" value="Cyclic"/></p> <p>Loading sequence: <input type="text" value="Tailor made protocol"/></p> <p>Partial ductility: <input type="text" value="0.5-1-1.5-2-2.5-3-3.5-4-5-6"/></p> <p>Number of cycles: <input type="text" value="4-2-1-1-1-1-1-1-1-1"/></p> <p>Type of curve: <input type="text" value="Force-Displacement"/></p> <p>Force measured: <input type="text" value="Applied to beam tip"/></p> <p>Displacement measured: <input type="text" value="Beam tip due to the elastic and inelastic beam rotation"/></p>																	
<b>Failure mode and joint capacity</b>																	
<p>Failure mode: Beam flange and web buckling</p>	<p>Maximum moment: <input type="text"/></p> <p>Maximum load: <input type="text" value="154.5"/> (kN)</p> <p>Maximum rotation: <input type="text"/></p> <p>Maximum displacement: <input type="text" value="155"/> (mm)</p>																

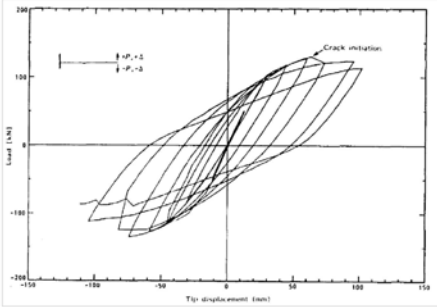



Paper																																			
<b>Behaviour of extended end-plate connections under cyclic loading</b>																																			
Authors:	Year:																																		
Ghobarah A.    Osman A.    Korol R. M.	1990																																		
Source: Engineering Structures																																			
Test A-3																																			
Geometrical properties																																			
Scheme: <input type="text" value="Cantilever"/>	Beam length: <input type="text" value="2325"/> Column length: <input type="text" value="1220"/> (mm)																																		
	<table border="1"> <thead> <tr> <th colspan="2">Beam</th> </tr> </thead> <tbody> <tr> <td>Section:</td> <td>W360x170x45 (W14x30)</td> </tr> <tr> <td>Height:</td> <td><input type="text" value="352"/></td> </tr> <tr> <td>Width:</td> <td><input type="text" value="171"/></td> </tr> <tr> <td>Fl-thickness:</td> <td><input type="text" value="9.8"/></td> </tr> <tr> <td>W-thickness:</td> <td><input type="text" value="6.9"/></td> </tr> <tr> <td>Root radius:</td> <td><input type="text" value="10"/></td> </tr> <tr> <td>Cross section area:</td> <td><input type="text" value="5710"/></td> </tr> </tbody> </table>	Beam		Section:	W360x170x45 (W14x30)	Height:	<input type="text" value="352"/>	Width:	<input type="text" value="171"/>	Fl-thickness:	<input type="text" value="9.8"/>	W-thickness:	<input type="text" value="6.9"/>	Root radius:	<input type="text" value="10"/>	Cross section area:	<input type="text" value="5710"/>																		
	Beam																																		
Section:	W360x170x45 (W14x30)																																		
Height:	<input type="text" value="352"/>																																		
Width:	<input type="text" value="171"/>																																		
Fl-thickness:	<input type="text" value="9.8"/>																																		
W-thickness:	<input type="text" value="6.9"/>																																		
Root radius:	<input type="text" value="10"/>																																		
Cross section area:	<input type="text" value="5710"/>																																		
	<table border="1"> <thead> <tr> <th colspan="2">Column</th> </tr> </thead> <tbody> <tr> <td>Section:</td> <td>W360x200x79 (W14x53)</td> </tr> <tr> <td>Height:</td> <td><input type="text" value="354"/></td> </tr> <tr> <td>Width:</td> <td><input type="text" value="205"/></td> </tr> <tr> <td>Fl-thickness:</td> <td><input type="text" value="16.8"/></td> </tr> <tr> <td>W-thickness:</td> <td><input type="text" value="9.4"/></td> </tr> <tr> <td>Root radius:</td> <td><input type="text" value="15"/></td> </tr> <tr> <td>Cross section area:</td> <td><input type="text" value="10100"/></td> </tr> <tr> <td><input checked="" type="checkbox"/> Web plate</td> <td>Thickness: <input type="text" value="8"/></td> </tr> <tr> <td><input checked="" type="checkbox"/> Continuity plates</td> <td>Thickness: <input type="text" value="9"/></td> </tr> </tbody> </table>	Column		Section:	W360x200x79 (W14x53)	Height:	<input type="text" value="354"/>	Width:	<input type="text" value="205"/>	Fl-thickness:	<input type="text" value="16.8"/>	W-thickness:	<input type="text" value="9.4"/>	Root radius:	<input type="text" value="15"/>	Cross section area:	<input type="text" value="10100"/>	<input checked="" type="checkbox"/> Web plate	Thickness: <input type="text" value="8"/>	<input checked="" type="checkbox"/> Continuity plates	Thickness: <input type="text" value="9"/>														
Column																																			
Section:	W360x200x79 (W14x53)																																		
Height:	<input type="text" value="354"/>																																		
Width:	<input type="text" value="205"/>																																		
Fl-thickness:	<input type="text" value="16.8"/>																																		
W-thickness:	<input type="text" value="9.4"/>																																		
Root radius:	<input type="text" value="15"/>																																		
Cross section area:	<input type="text" value="10100"/>																																		
<input checked="" type="checkbox"/> Web plate	Thickness: <input type="text" value="8"/>																																		
<input checked="" type="checkbox"/> Continuity plates	Thickness: <input type="text" value="9"/>																																		
<table border="1"> <thead> <tr> <th colspan="2">Connection elements</th> </tr> </thead> <tbody> <tr> <td><input type="checkbox"/> Full penetration welds</td> <td></td> </tr> <tr> <td><input checked="" type="checkbox"/> Fillet welds</td> <td></td> </tr> <tr> <td>Beam flange throat:</td> <td><input type="text" value="10"/></td> </tr> <tr> <td>Beam web throat:</td> <td><input type="text" value="7"/></td> </tr> <tr> <td>Bolts:</td> <td><input type="text"/></td> </tr> <tr> <td>Diameter:</td> <td><input type="text" value="25"/></td> </tr> <tr> <td>Tensile stress area:</td> <td><input type="text" value="390.9"/></td> </tr> </tbody> </table>	Connection elements		<input type="checkbox"/> Full penetration welds		<input checked="" type="checkbox"/> Fillet welds		Beam flange throat:	<input type="text" value="10"/>	Beam web throat:	<input type="text" value="7"/>	Bolts:	<input type="text"/>	Diameter:	<input type="text" value="25"/>	Tensile stress area:	<input type="text" value="390.9"/>	<table border="1"> <thead> <tr> <th colspan="2">End-plate</th> </tr> </thead> <tbody> <tr> <td>Height:</td> <td><input type="text" value="558"/></td> </tr> <tr> <td>Width:</td> <td><input type="text" value="203"/></td> </tr> <tr> <td>Thickness:</td> <td><input type="text" value="19"/></td> </tr> <tr> <td>ep:</td> <td><input type="text" value="n.a."/></td> </tr> <tr> <td>ex:</td> <td><input type="text" value="n.a."/></td> </tr> <tr> <td>w:</td> <td><input type="text" value="n.a."/></td> </tr> <tr> <td>mx:</td> <td><input type="text" value="n.a."/></td> </tr> <tr> <td><input checked="" type="checkbox"/> Rib stiffener</td> <td>Thickness: <input type="text" value="9"/></td> </tr> </tbody> </table>	End-plate		Height:	<input type="text" value="558"/>	Width:	<input type="text" value="203"/>	Thickness:	<input type="text" value="19"/>	ep:	<input type="text" value="n.a."/>	ex:	<input type="text" value="n.a."/>	w:	<input type="text" value="n.a."/>	mx:	<input type="text" value="n.a."/>	<input checked="" type="checkbox"/> Rib stiffener	Thickness: <input type="text" value="9"/>
Connection elements																																			
<input type="checkbox"/> Full penetration welds																																			
<input checked="" type="checkbox"/> Fillet welds																																			
Beam flange throat:	<input type="text" value="10"/>																																		
Beam web throat:	<input type="text" value="7"/>																																		
Bolts:	<input type="text"/>																																		
Diameter:	<input type="text" value="25"/>																																		
Tensile stress area:	<input type="text" value="390.9"/>																																		
End-plate																																			
Height:	<input type="text" value="558"/>																																		
Width:	<input type="text" value="203"/>																																		
Thickness:	<input type="text" value="19"/>																																		
ep:	<input type="text" value="n.a."/>																																		
ex:	<input type="text" value="n.a."/>																																		
w:	<input type="text" value="n.a."/>																																		
mx:	<input type="text" value="n.a."/>																																		
<input checked="" type="checkbox"/> Rib stiffener	Thickness: <input type="text" value="9"/>																																		
Notes:																																			
The beam length provided is the distance between the point of application of the force and the column axis. The paper does not provide any bolts arrangement.																																			
Material properties																																			
<table border="1"> <thead> <tr> <th colspan="2">Beam</th> </tr> </thead> <tbody> <tr> <td><input type="checkbox"/> Nominal values</td> <td></td> </tr> <tr> <td><input checked="" type="checkbox"/> Measured values</td> <td></td> </tr> <tr> <td>Fl. yield strength:</td> <td><input type="text" value="310.9"/></td> </tr> <tr> <td>Web yield stress:</td> <td><input type="text" value="315.7"/></td> </tr> </tbody> </table>	Beam		<input type="checkbox"/> Nominal values		<input checked="" type="checkbox"/> Measured values		Fl. yield strength:	<input type="text" value="310.9"/>	Web yield stress:	<input type="text" value="315.7"/>	<table border="1"> <thead> <tr> <th colspan="2">Column</th> </tr> </thead> <tbody> <tr> <td><input checked="" type="checkbox"/> Nominal values</td> <td>G40.21-M300W</td> </tr> <tr> <td><input type="checkbox"/> Measured values</td> <td></td> </tr> <tr> <td>Fl. yield strength:</td> <td><input type="text" value="303.369"/></td> </tr> <tr> <td>Web yield strength:</td> <td><input type="text" value="303.369"/></td> </tr> </tbody> </table>	Column		<input checked="" type="checkbox"/> Nominal values	G40.21-M300W	<input type="checkbox"/> Measured values		Fl. yield strength:	<input type="text" value="303.369"/>	Web yield strength:	<input type="text" value="303.369"/>														
Beam																																			
<input type="checkbox"/> Nominal values																																			
<input checked="" type="checkbox"/> Measured values																																			
Fl. yield strength:	<input type="text" value="310.9"/>																																		
Web yield stress:	<input type="text" value="315.7"/>																																		
Column																																			
<input checked="" type="checkbox"/> Nominal values	G40.21-M300W																																		
<input type="checkbox"/> Measured values																																			
Fl. yield strength:	<input type="text" value="303.369"/>																																		
Web yield strength:	<input type="text" value="303.369"/>																																		
	<table border="1"> <thead> <tr> <th colspan="2">End-plate</th> </tr> </thead> <tbody> <tr> <td><input type="checkbox"/> Nominal value</td> <td>G40.21-M300W</td> </tr> <tr> <td><input type="checkbox"/> Measured value</td> <td></td> </tr> <tr> <td>Yield strength:</td> <td><input type="text" value="303.369"/></td> </tr> </tbody> </table>	End-plate		<input type="checkbox"/> Nominal value	G40.21-M300W	<input type="checkbox"/> Measured value		Yield strength:	<input type="text" value="303.369"/>																										
End-plate																																			
<input type="checkbox"/> Nominal value	G40.21-M300W																																		
<input type="checkbox"/> Measured value																																			
Yield strength:	<input type="text" value="303.369"/>																																		
(MPa)																																			

Appendix A

Test A-3																	
<b>Material properties</b>																	
<table border="1"> <thead> <tr> <th colspan="2">Bolts</th> </tr> </thead> <tbody> <tr> <td><input checked="" type="checkbox"/> Nominal value</td> <td>A490M</td> </tr> <tr> <td><input type="checkbox"/> Measured value</td> <td></td> </tr> <tr> <td>Ultimate strength:</td> <td>1040</td> </tr> </tbody> </table>	Bolts		<input checked="" type="checkbox"/> Nominal value	A490M	<input type="checkbox"/> Measured value		Ultimate strength:	1040	<table border="1"> <thead> <tr> <th colspan="2">Continuity plate</th> </tr> </thead> <tbody> <tr> <td><input checked="" type="checkbox"/> Nominal value</td> <td>G40.21-M300W</td> </tr> <tr> <td><input type="checkbox"/> Measured value</td> <td></td> </tr> <tr> <td>Yield strength:</td> <td>303.369</td> </tr> </tbody> </table>	Continuity plate		<input checked="" type="checkbox"/> Nominal value	G40.21-M300W	<input type="checkbox"/> Measured value		Yield strength:	303.369
Bolts																	
<input checked="" type="checkbox"/> Nominal value	A490M																
<input type="checkbox"/> Measured value																	
Ultimate strength:	1040																
Continuity plate																	
<input checked="" type="checkbox"/> Nominal value	G40.21-M300W																
<input type="checkbox"/> Measured value																	
Yield strength:	303.369																
<table border="1"> <thead> <tr> <th colspan="2">Web plate</th> </tr> </thead> <tbody> <tr> <td><input checked="" type="checkbox"/> Nominal value</td> <td>G40.21-M300W</td> </tr> <tr> <td><input type="checkbox"/> Measured value</td> <td></td> </tr> <tr> <td>Yield strength:</td> <td>303.369</td> </tr> </tbody> </table>		Web plate		<input checked="" type="checkbox"/> Nominal value	G40.21-M300W	<input type="checkbox"/> Measured value		Yield strength:	303.369								
Web plate																	
<input checked="" type="checkbox"/> Nominal value	G40.21-M300W																
<input type="checkbox"/> Measured value																	
Yield strength:	303.369																
<table border="1"> <thead> <tr> <th colspan="2">End-plate rib stiffener</th> </tr> </thead> <tbody> <tr> <td><input checked="" type="checkbox"/> Nominal value</td> <td>G40.21-M300W</td> </tr> <tr> <td><input type="checkbox"/> Measured value</td> <td></td> </tr> <tr> <td>Yield strength:</td> <td>303.369</td> </tr> </tbody> </table>		End-plate rib stiffener		<input checked="" type="checkbox"/> Nominal value	G40.21-M300W	<input type="checkbox"/> Measured value		Yield strength:	303.369								
End-plate rib stiffener																	
<input checked="" type="checkbox"/> Nominal value	G40.21-M300W																
<input type="checkbox"/> Measured value																	
Yield strength:	303.369																
Notes:																	
(MPa)																	
<b>Experimental results</b>																	
<p>Type of test: <input type="text" value="Cyclic"/></p> <p>Loading sequence: <input type="text" value="Tailor made protocol"/></p> <p>Partial ductility: <input type="text" value="0.5-1-1.5-2-2.5-3-3.5-4-5-6"/></p> <p>Number of cycles: <input type="text" value="4-2-1-1-1-1-1-1-1"/></p> <p>Type of curve: <input type="text" value="Force-Displacement"/></p> <p>Force measured: <input type="text" value="Applied to beam tip"/></p> <p>Displacement measured: <input type="text" value="Beam tip due to the elastic and inelastic beam rotation"/></p>																	
<b>Failure mode and joint capacity</b>																	
<p>Failure mode: Beam flange and web buckling</p>	<p>Maximum moment: <input type="text"/></p> <p>Maximum load: <input type="text" value="156.4"/> (kN)</p> <p>Maximum rotation: <input type="text"/></p> <p>Maximum displacement: <input type="text" value="140"/> (mm)</p>																

Paper																													
<b>Behaviour of extended end-plate connections under cyclic loading</b>																													
Authors:	Year:																												
Ghobarah A.    Osman A.    Korol R. M.	1990																												
Source: Engineering Structures																													
Test A-4																													
Geometrical properties																													
Scheme: <input type="text" value="Cantilever"/>	Beam length: <input type="text" value="2325"/> Column length: <input type="text" value="1220"/> (mm)																												
	<table border="1"> <thead> <tr> <th colspan="2">Beam</th> </tr> </thead> <tbody> <tr> <td>Section:</td> <td>W360x170x45 (W14x30)</td> </tr> <tr> <td>Height:</td> <td>352</td> </tr> <tr> <td>Width:</td> <td>171</td> </tr> <tr> <td>Fl-thickness:</td> <td>9.8</td> </tr> <tr> <td>W-thickness:</td> <td>6.9</td> </tr> <tr> <td>Root radius:</td> <td>10</td> </tr> <tr> <td>Cross section area:</td> <td>57.10</td> </tr> </tbody> </table>	Beam		Section:	W360x170x45 (W14x30)	Height:	352	Width:	171	Fl-thickness:	9.8	W-thickness:	6.9	Root radius:	10	Cross section area:	57.10												
	Beam																												
Section:	W360x170x45 (W14x30)																												
Height:	352																												
Width:	171																												
Fl-thickness:	9.8																												
W-thickness:	6.9																												
Root radius:	10																												
Cross section area:	57.10																												
	<table border="1"> <thead> <tr> <th colspan="2">Column</th> </tr> </thead> <tbody> <tr> <td>Section:</td> <td>W360x200x79 (W14x53)</td> </tr> <tr> <td>Height:</td> <td>354</td> </tr> <tr> <td>Width:</td> <td>205</td> </tr> <tr> <td>Fl-thickness:</td> <td>16.8</td> </tr> <tr> <td>W-thickness:</td> <td>9.4</td> </tr> <tr> <td>Root radius:</td> <td>15</td> </tr> <tr> <td>Cross section area:</td> <td>10100</td> </tr> <tr> <td><input checked="" type="checkbox"/> Web plate</td> <td>Thickness: 8</td> </tr> <tr> <td><input type="checkbox"/> Continuity plates</td> <td>Thickness: <input type="text"/></td> </tr> </tbody> </table>	Column		Section:	W360x200x79 (W14x53)	Height:	354	Width:	205	Fl-thickness:	16.8	W-thickness:	9.4	Root radius:	15	Cross section area:	10100	<input checked="" type="checkbox"/> Web plate	Thickness: 8	<input type="checkbox"/> Continuity plates	Thickness: <input type="text"/>								
Column																													
Section:	W360x200x79 (W14x53)																												
Height:	354																												
Width:	205																												
Fl-thickness:	16.8																												
W-thickness:	9.4																												
Root radius:	15																												
Cross section area:	10100																												
<input checked="" type="checkbox"/> Web plate	Thickness: 8																												
<input type="checkbox"/> Continuity plates	Thickness: <input type="text"/>																												
<table border="1"> <thead> <tr> <th colspan="2">Connection elements</th> </tr> </thead> <tbody> <tr> <td><input type="checkbox"/> Full penetration welds</td> <td></td> </tr> <tr> <td><input checked="" type="checkbox"/> Fillet welds</td> <td>Bolts: <input type="text"/></td> </tr> <tr> <td>Beam flange throat: <input type="text" value="10"/></td> <td>Diameter: <input type="text" value="25"/></td> </tr> <tr> <td>Beam web throat: <input type="text" value="7"/></td> <td>Tensile stress area: <input type="text" value="390.9"/></td> </tr> </tbody> </table>	Connection elements		<input type="checkbox"/> Full penetration welds		<input checked="" type="checkbox"/> Fillet welds	Bolts: <input type="text"/>	Beam flange throat: <input type="text" value="10"/>	Diameter: <input type="text" value="25"/>	Beam web throat: <input type="text" value="7"/>	Tensile stress area: <input type="text" value="390.9"/>	<table border="1"> <thead> <tr> <th colspan="2">End-plate</th> </tr> </thead> <tbody> <tr> <td>Height:</td> <td><input type="text" value="558"/></td> </tr> <tr> <td>Width:</td> <td><input type="text" value="203"/></td> </tr> <tr> <td>Thickness:</td> <td><input type="text" value="19"/></td> </tr> <tr> <td>ep:</td> <td><input type="text" value="n.a."/></td> </tr> <tr> <td>ex:</td> <td><input type="text" value="n.a."/></td> </tr> <tr> <td>w:</td> <td><input type="text" value="n.a."/></td> </tr> <tr> <td>mx:</td> <td><input type="text" value="n.a."/></td> </tr> <tr> <td><input type="checkbox"/> Rib stiffener</td> <td>Thickness: <input type="text"/></td> </tr> </tbody> </table>	End-plate		Height:	<input type="text" value="558"/>	Width:	<input type="text" value="203"/>	Thickness:	<input type="text" value="19"/>	ep:	<input type="text" value="n.a."/>	ex:	<input type="text" value="n.a."/>	w:	<input type="text" value="n.a."/>	mx:	<input type="text" value="n.a."/>	<input type="checkbox"/> Rib stiffener	Thickness: <input type="text"/>
Connection elements																													
<input type="checkbox"/> Full penetration welds																													
<input checked="" type="checkbox"/> Fillet welds	Bolts: <input type="text"/>																												
Beam flange throat: <input type="text" value="10"/>	Diameter: <input type="text" value="25"/>																												
Beam web throat: <input type="text" value="7"/>	Tensile stress area: <input type="text" value="390.9"/>																												
End-plate																													
Height:	<input type="text" value="558"/>																												
Width:	<input type="text" value="203"/>																												
Thickness:	<input type="text" value="19"/>																												
ep:	<input type="text" value="n.a."/>																												
ex:	<input type="text" value="n.a."/>																												
w:	<input type="text" value="n.a."/>																												
mx:	<input type="text" value="n.a."/>																												
<input type="checkbox"/> Rib stiffener	Thickness: <input type="text"/>																												
Notes: The beam length provided is the distance between the point of application of the force and the column axis. The paper does not provide any bolts arrangement.																													
Material properties																													
<table border="1"> <thead> <tr> <th colspan="2">Beam</th> </tr> </thead> <tbody> <tr> <td><input type="checkbox"/> Nominal values</td> <td><input type="text"/></td> </tr> <tr> <td><input checked="" type="checkbox"/> Measured values</td> <td><input type="text"/></td> </tr> <tr> <td>Fl. yield strength:</td> <td><input type="text" value="310.9"/></td> </tr> <tr> <td>Web yield stress:</td> <td><input type="text" value="315.7"/></td> </tr> </tbody> </table>	Beam		<input type="checkbox"/> Nominal values	<input type="text"/>	<input checked="" type="checkbox"/> Measured values	<input type="text"/>	Fl. yield strength:	<input type="text" value="310.9"/>	Web yield stress:	<input type="text" value="315.7"/>	<table border="1"> <thead> <tr> <th colspan="2">Column</th> </tr> </thead> <tbody> <tr> <td><input checked="" type="checkbox"/> Nominal values</td> <td>G40.21-M300W</td> </tr> <tr> <td><input type="checkbox"/> Measured values</td> <td><input type="text"/></td> </tr> <tr> <td>Fl. yield strength:</td> <td><input type="text" value="303.369"/></td> </tr> <tr> <td>Web yield strength:</td> <td><input type="text" value="303.369"/></td> </tr> </tbody> </table>	Column		<input checked="" type="checkbox"/> Nominal values	G40.21-M300W	<input type="checkbox"/> Measured values	<input type="text"/>	Fl. yield strength:	<input type="text" value="303.369"/>	Web yield strength:	<input type="text" value="303.369"/>								
Beam																													
<input type="checkbox"/> Nominal values	<input type="text"/>																												
<input checked="" type="checkbox"/> Measured values	<input type="text"/>																												
Fl. yield strength:	<input type="text" value="310.9"/>																												
Web yield stress:	<input type="text" value="315.7"/>																												
Column																													
<input checked="" type="checkbox"/> Nominal values	G40.21-M300W																												
<input type="checkbox"/> Measured values	<input type="text"/>																												
Fl. yield strength:	<input type="text" value="303.369"/>																												
Web yield strength:	<input type="text" value="303.369"/>																												
	<table border="1"> <thead> <tr> <th colspan="2">End-plate</th> </tr> </thead> <tbody> <tr> <td><input checked="" type="checkbox"/> Nominal value</td> <td>G40.21-M300W</td> </tr> <tr> <td><input type="checkbox"/> Measured value</td> <td><input type="text"/></td> </tr> <tr> <td>Yield strength:</td> <td><input type="text" value="303.369"/></td> </tr> </tbody> </table>	End-plate		<input checked="" type="checkbox"/> Nominal value	G40.21-M300W	<input type="checkbox"/> Measured value	<input type="text"/>	Yield strength:	<input type="text" value="303.369"/>																				
End-plate																													
<input checked="" type="checkbox"/> Nominal value	G40.21-M300W																												
<input type="checkbox"/> Measured value	<input type="text"/>																												
Yield strength:	<input type="text" value="303.369"/>																												
(MPa)																													

Test A-4																										
<b>Material properties</b>																										
<table border="1"> <thead> <tr> <th colspan="2">Bolts</th> </tr> </thead> <tbody> <tr> <td><input checked="" type="checkbox"/> Nominal value</td> <td>A490M</td> </tr> <tr> <td><input type="checkbox"/> Measured value</td> <td></td> </tr> <tr> <td>Ultimate strength:</td> <td>1040</td> </tr> </tbody> </table>	Bolts		<input checked="" type="checkbox"/> Nominal value	A490M	<input type="checkbox"/> Measured value		Ultimate strength:	1040	<table border="1"> <thead> <tr> <th colspan="2">Continuity plate</th> </tr> </thead> <tbody> <tr> <td><input type="checkbox"/> Nominal value</td> <td></td> </tr> <tr> <td><input type="checkbox"/> Measured value</td> <td></td> </tr> <tr> <td>Yield strength:</td> <td></td> </tr> </tbody> </table>	Continuity plate		<input type="checkbox"/> Nominal value		<input type="checkbox"/> Measured value		Yield strength:		<table border="1"> <thead> <tr> <th colspan="2">Web plate</th> </tr> </thead> <tbody> <tr> <td><input checked="" type="checkbox"/> Nominal value</td> <td>G40.21-M300W</td> </tr> <tr> <td><input type="checkbox"/> Measured value</td> <td></td> </tr> <tr> <td>Yield strength:</td> <td>303.369</td> </tr> </tbody> </table>	Web plate		<input checked="" type="checkbox"/> Nominal value	G40.21-M300W	<input type="checkbox"/> Measured value		Yield strength:	303.369
Bolts																										
<input checked="" type="checkbox"/> Nominal value	A490M																									
<input type="checkbox"/> Measured value																										
Ultimate strength:	1040																									
Continuity plate																										
<input type="checkbox"/> Nominal value																										
<input type="checkbox"/> Measured value																										
Yield strength:																										
Web plate																										
<input checked="" type="checkbox"/> Nominal value	G40.21-M300W																									
<input type="checkbox"/> Measured value																										
Yield strength:	303.369																									
Notes:		(MPa)																								
<b>Experimental results</b>																										
Type of test:	Cyclic																									
Loading sequence:	Tailor made protocol																									
Partial ductility	0.5-1-1.5-2-2.5-3-3.5-4-5-6																									
Number of cycles:	4-2-1-1-1-1-1-1																									
Type of curve:																										
Force measured:	Applied to beam tip																									
Displacement measured:	Beam tip due to the elastic and inelastic beam rotation																									
																										
<b>Failure mode and joint capacity</b>																										
	Failure mode:	End-plate failure																								
	Maximum moment:																									
	Maximum load:	134.6 (kN)																								
	Maximum rotation:																									
	Maximum displacement:	102 (mm)																								

Paper																															
Behaviour of extended end-plate connections under cyclic loading																															
Authors:			Year:																												
Ghobarah A.	Osman A.	Korol R. M.	1990																												
			Source:																												
			Engineering Structures																												
Test A-5																															
Geometrical properties																															
Scheme: <input type="text" value="Cantilever"/>	Beam length: <input type="text" value="2325"/>																														
	Column length: <input type="text" value="1220"/>	(mm)																													
		<table border="1"> <thead> <tr> <th colspan="2">Beam</th> </tr> </thead> <tbody> <tr> <td>Section:</td> <td>W360x170x45 (W14x30)</td> </tr> <tr> <td>Height:</td> <td>352</td> </tr> <tr> <td>Width:</td> <td>171</td> </tr> <tr> <td>Fl-thickness:</td> <td>9.8</td> </tr> <tr> <td>W-thickness:</td> <td>6.9</td> </tr> <tr> <td>Root radius:</td> <td>10</td> </tr> <tr> <td>Cross section area:</td> <td>5710</td> </tr> </tbody> </table>		Beam		Section:	W360x170x45 (W14x30)	Height:	352	Width:	171	Fl-thickness:	9.8	W-thickness:	6.9	Root radius:	10	Cross section area:	5710												
Beam																															
Section:	W360x170x45 (W14x30)																														
Height:	352																														
Width:	171																														
Fl-thickness:	9.8																														
W-thickness:	6.9																														
Root radius:	10																														
Cross section area:	5710																														
		<table border="1"> <thead> <tr> <th colspan="2">Column</th> </tr> </thead> <tbody> <tr> <td>Section:</td> <td>W360x200x79 (W14x53)</td> </tr> <tr> <td>Height:</td> <td>354</td> </tr> <tr> <td>Width:</td> <td>205</td> </tr> <tr> <td>Fl-thickness:</td> <td>16.8</td> </tr> <tr> <td>W-thickness:</td> <td>9.4</td> </tr> <tr> <td>Root radius:</td> <td>15</td> </tr> <tr> <td>Cross section area:</td> <td>10100</td> </tr> <tr> <td><input checked="" type="checkbox"/> Web plate</td> <td>Thickness: 8</td> </tr> <tr> <td><input checked="" type="checkbox"/> Continuity plates</td> <td>Thickness: 9</td> </tr> </tbody> </table>		Column		Section:	W360x200x79 (W14x53)	Height:	354	Width:	205	Fl-thickness:	16.8	W-thickness:	9.4	Root radius:	15	Cross section area:	10100	<input checked="" type="checkbox"/> Web plate	Thickness: 8	<input checked="" type="checkbox"/> Continuity plates	Thickness: 9								
Column																															
Section:	W360x200x79 (W14x53)																														
Height:	354																														
Width:	205																														
Fl-thickness:	16.8																														
W-thickness:	9.4																														
Root radius:	15																														
Cross section area:	10100																														
<input checked="" type="checkbox"/> Web plate	Thickness: 8																														
<input checked="" type="checkbox"/> Continuity plates	Thickness: 9																														
<table border="1"> <thead> <tr> <th colspan="2">Connection elements</th> </tr> </thead> <tbody> <tr> <td><input type="checkbox"/> Full penetration welds</td> <td></td> </tr> <tr> <td><input checked="" type="checkbox"/> Fillet welds</td> <td>Bolts: <input type="text"/></td> </tr> <tr> <td>Beam flange throat: <input type="text" value="10"/></td> <td>Diameter: <input type="text" value="25"/></td> </tr> <tr> <td>Beam web throat: <input type="text" value="7"/></td> <td>Tensile stress area: <input type="text" value="390.9"/></td> </tr> </tbody> </table>		Connection elements		<input type="checkbox"/> Full penetration welds		<input checked="" type="checkbox"/> Fillet welds	Bolts: <input type="text"/>	Beam flange throat: <input type="text" value="10"/>	Diameter: <input type="text" value="25"/>	Beam web throat: <input type="text" value="7"/>	Tensile stress area: <input type="text" value="390.9"/>	<table border="1"> <thead> <tr> <th colspan="2">End-plate</th> </tr> </thead> <tbody> <tr> <td>Height:</td> <td><input type="text" value="558"/></td> </tr> <tr> <td>Width:</td> <td><input type="text" value="203"/></td> </tr> <tr> <td>Thickness:</td> <td><input type="text" value="16"/></td> </tr> <tr> <td>ep:</td> <td><input type="text" value="n.a."/></td> </tr> <tr> <td>ex:</td> <td><input type="text" value="n.a."/></td> </tr> <tr> <td>w:</td> <td><input type="text" value="n.a."/></td> </tr> <tr> <td>mx:</td> <td><input type="text" value="n.a."/></td> </tr> <tr> <td><input checked="" type="checkbox"/> Rib stiffener</td> <td>Thickness: <input type="text" value="9"/></td> </tr> </tbody> </table>		End-plate		Height:	<input type="text" value="558"/>	Width:	<input type="text" value="203"/>	Thickness:	<input type="text" value="16"/>	ep:	<input type="text" value="n.a."/>	ex:	<input type="text" value="n.a."/>	w:	<input type="text" value="n.a."/>	mx:	<input type="text" value="n.a."/>	<input checked="" type="checkbox"/> Rib stiffener	Thickness: <input type="text" value="9"/>
Connection elements																															
<input type="checkbox"/> Full penetration welds																															
<input checked="" type="checkbox"/> Fillet welds	Bolts: <input type="text"/>																														
Beam flange throat: <input type="text" value="10"/>	Diameter: <input type="text" value="25"/>																														
Beam web throat: <input type="text" value="7"/>	Tensile stress area: <input type="text" value="390.9"/>																														
End-plate																															
Height:	<input type="text" value="558"/>																														
Width:	<input type="text" value="203"/>																														
Thickness:	<input type="text" value="16"/>																														
ep:	<input type="text" value="n.a."/>																														
ex:	<input type="text" value="n.a."/>																														
w:	<input type="text" value="n.a."/>																														
mx:	<input type="text" value="n.a."/>																														
<input checked="" type="checkbox"/> Rib stiffener	Thickness: <input type="text" value="9"/>																														
Notes: <span style="float: right;">(mm)</span>																															
The beam length provided is the distance between the point of application of the force and the column axis. The paper does not provide any bolts arrangement.																															
Material properties																															
<table border="1"> <thead> <tr> <th colspan="2">Beam</th> </tr> </thead> <tbody> <tr> <td><input type="checkbox"/> Nominal values</td> <td><input type="text"/></td> </tr> <tr> <td><input checked="" type="checkbox"/> Measured values</td> <td><input type="text"/></td> </tr> <tr> <td>Fl. yield strength:</td> <td><input type="text" value="316.1"/></td> </tr> <tr> <td>Web yield stress:</td> <td><input type="text" value="322.1"/></td> </tr> </tbody> </table>		Beam		<input type="checkbox"/> Nominal values	<input type="text"/>	<input checked="" type="checkbox"/> Measured values	<input type="text"/>	Fl. yield strength:	<input type="text" value="316.1"/>	Web yield stress:	<input type="text" value="322.1"/>	<table border="1"> <thead> <tr> <th colspan="2">Column</th> </tr> </thead> <tbody> <tr> <td><input checked="" type="checkbox"/> Nominal values</td> <td>G40.21-M300W</td> </tr> <tr> <td><input type="checkbox"/> Measured values</td> <td></td> </tr> <tr> <td>Fl. yield strength:</td> <td><input type="text" value="303.369"/></td> </tr> <tr> <td>Web yield strength:</td> <td><input type="text" value="303.369"/></td> </tr> </tbody> </table>		Column		<input checked="" type="checkbox"/> Nominal values	G40.21-M300W	<input type="checkbox"/> Measured values		Fl. yield strength:	<input type="text" value="303.369"/>	Web yield strength:	<input type="text" value="303.369"/>								
Beam																															
<input type="checkbox"/> Nominal values	<input type="text"/>																														
<input checked="" type="checkbox"/> Measured values	<input type="text"/>																														
Fl. yield strength:	<input type="text" value="316.1"/>																														
Web yield stress:	<input type="text" value="322.1"/>																														
Column																															
<input checked="" type="checkbox"/> Nominal values	G40.21-M300W																														
<input type="checkbox"/> Measured values																															
Fl. yield strength:	<input type="text" value="303.369"/>																														
Web yield strength:	<input type="text" value="303.369"/>																														
		<table border="1"> <thead> <tr> <th colspan="2">End-plate</th> </tr> </thead> <tbody> <tr> <td><input checked="" type="checkbox"/> Nominal value</td> <td>G40.21-M300W</td> </tr> <tr> <td><input type="checkbox"/> Measured value</td> <td></td> </tr> <tr> <td>Yield strength:</td> <td><input type="text" value="303.369"/></td> </tr> </tbody> </table>		End-plate		<input checked="" type="checkbox"/> Nominal value	G40.21-M300W	<input type="checkbox"/> Measured value		Yield strength:	<input type="text" value="303.369"/>																				
End-plate																															
<input checked="" type="checkbox"/> Nominal value	G40.21-M300W																														
<input type="checkbox"/> Measured value																															
Yield strength:	<input type="text" value="303.369"/>																														

Test A-5																	
<b>Material properties</b>																	
<table border="1"> <thead> <tr> <th colspan="2">Bolts</th> </tr> </thead> <tbody> <tr> <td><input checked="" type="checkbox"/> Nominal value</td> <td>A490M</td> </tr> <tr> <td><input type="checkbox"/> Measured value</td> <td></td> </tr> <tr> <td>Ultimate strength:</td> <td>1040</td> </tr> </tbody> </table>	Bolts		<input checked="" type="checkbox"/> Nominal value	A490M	<input type="checkbox"/> Measured value		Ultimate strength:	1040	<table border="1"> <thead> <tr> <th colspan="2">Continuity plate</th> </tr> </thead> <tbody> <tr> <td><input checked="" type="checkbox"/> Nominal value</td> <td>G40.21-M300W</td> </tr> <tr> <td><input type="checkbox"/> Measured value</td> <td></td> </tr> <tr> <td>Yield strength:</td> <td>303.369</td> </tr> </tbody> </table>	Continuity plate		<input checked="" type="checkbox"/> Nominal value	G40.21-M300W	<input type="checkbox"/> Measured value		Yield strength:	303.369
Bolts																	
<input checked="" type="checkbox"/> Nominal value	A490M																
<input type="checkbox"/> Measured value																	
Ultimate strength:	1040																
Continuity plate																	
<input checked="" type="checkbox"/> Nominal value	G40.21-M300W																
<input type="checkbox"/> Measured value																	
Yield strength:	303.369																
<p>Notes:</p> <div style="border: 1px solid black; height: 20px; width: 100%;"></div>	<table border="1"> <thead> <tr> <th colspan="2">Web plate</th> </tr> </thead> <tbody> <tr> <td><input checked="" type="checkbox"/> Nominal value</td> <td>G40.21-M300W</td> </tr> <tr> <td><input type="checkbox"/> Measured value</td> <td></td> </tr> <tr> <td>Yield strength:</td> <td>303.369</td> </tr> </tbody> </table> <table border="1"> <thead> <tr> <th colspan="2">End-plate rib stiffener</th> </tr> </thead> <tbody> <tr> <td><input checked="" type="checkbox"/> Nominal value</td> <td>G40.21-M300W</td> </tr> <tr> <td><input type="checkbox"/> Measured value</td> <td></td> </tr> <tr> <td>Yield strength:</td> <td></td> </tr> </tbody> </table>	Web plate		<input checked="" type="checkbox"/> Nominal value	G40.21-M300W	<input type="checkbox"/> Measured value		Yield strength:	303.369	End-plate rib stiffener		<input checked="" type="checkbox"/> Nominal value	G40.21-M300W	<input type="checkbox"/> Measured value		Yield strength:	
Web plate																	
<input checked="" type="checkbox"/> Nominal value	G40.21-M300W																
<input type="checkbox"/> Measured value																	
Yield strength:	303.369																
End-plate rib stiffener																	
<input checked="" type="checkbox"/> Nominal value	G40.21-M300W																
<input type="checkbox"/> Measured value																	
Yield strength:																	
<b>Experimental results</b>																	
<p>Type of test: <input type="text" value="Cyclic"/></p> <p>Loading sequence: <input type="text" value="Tailor made protocol"/></p> <p>Partial ductility: <input type="text" value="0.5-1-1.5-2-2.5-3-3.5-4-5-6"/></p> <p>Number of cycles: <input type="text" value="4-2-1-1-1-1-1-1-1-1"/></p> <p>Type of curve: <input type="text" value="Force-displacement"/></p> <p>Force measured: <input type="text" value="Applied to beam tip"/></p> <p>Displacement measured: <input type="text" value="Beam tip due to the elastic and inelastic beam rotation"/></p>																	
<b>Failure mode and joint capacity</b>																	
<p>Failure mode: Beam flange and web buckling</p>	<p>Maximum moment: <input type="text"/></p> <p>Maximum load: <input type="text" value="158.9"/> (kN)</p> <p>Maximum rotation: <input type="text"/></p> <p>Maximum displacement: <input type="text" value="145"/> (mm)</p>																

## **APPENDIX B**

### **DESIGN CHARTS**





